Norwegian University of Life Sciences
Faculty of Environmental Sciences
and Natural Resource Management

Philosophiae Doctor (PhD)
Thesis 2023:36

Landscape-scale determinants and dynamics of large carnivore density

Landskapsskala påvirkningsfaktorer og dynamikk i tettheten av store rovdyr

Ehsan Mohammadi Moqanaki

Landscape-scale determinants and dynamics of large carnivore density

Landskapsskala påvirkningsfaktorer og dynamikk i tettheten av store rovdyr

Philosophiae Doctor (PhD) Thesis

Ehsan Moqanaki

Norwegian University of Life Sciences
Faculty of Environmental Sciences and Natural Resource Management

Ås, 2023

Thesis number: 2023:36
ISSN: 1894-6402
ISBN: 978-82-575-2064-9

کو کوزه‌گر و کوزه‌خر و کوزه‌فروش

PhD supervisors

Richard Bischof
Faculty of Environmental Sciences and Natural Resource Management
Norwegian University of Life Sciences
P.O. Box 5003, 1432 Ås
Norway

Cyril Milleret & **Pierre Dupont**
Faculty of Environmental Sciences and Natural Resource Management
Norwegian University of Life Sciences
P.O. Box 5003, 1432 Ås
Norway

Evaluation committee

John D. C. Linnell
Department of Forestry and Wildlife Management
Inland Norway University of Applied Sciences
Anne Evenstads vei 80, Koppang
&
Norwegian Institute for Nature Research
PO Box 5685 Torgarden, Trondheim
Norway

Dana J. Morin
Department of Wildlife, Fisheries and Aquaculture
Mississippi State University
MS 39762, Mississippi
USA

Torbjørn Haugaasen
Faculty of Environmental Sciences and Natural Resource Management
Norwegian University of Life Sciences
P.O. Box 5003, 1432 Ås
Norway

Acknowledgments

About ⅔ of my PhD time was during a global pandemic. I spent more time in my home "office", next to my bed, than in my spacious office at NMBU's MINA. I was fortunate though, to survive the pandemic, stay motivated, and be able to work remotely as part of a larger project with a strong analytical focus and a supportive team of my main supervisor and co-advisors.

Mahdieh – I was lucky to have you during my PhD time and beyond, not only as my predecessor with trustworthy advice, but also as my partner for life. We followed more or less similar PhD paths, but I was luckier than you! I'd like to thank you for your invaluable support and I am excited about our future adventures in the Big Sky Country.

Richard – I am grateful for all you did for me before and during my PhD. I learned a lot from you and you are my role model in academia in many ways. Thank you also for introducing me to jiu-jitsu; few people get the chance to literally wrestle with their PhD supervisor, and I needed that. I hope you will remember me as one of your PhD students who finished on time and moved on proudly.

Cyril & Pierre – I appreciate your contributions to this PhD. I shared an office with Pierre and probably worked more with Cyril virtually. I learned from both of you, through brainstorming, scavenging your codes (eagerly or tearfully), and your feedback on different aspects of my PhD.

Soumen – It was great working with you on two chapters of my PhD, learning from you and your way of looking into problems raised while analyzing wildlife monitoring data. I also admire your overly-complex mathematical notations, gigantic Overleaf documents, and stay-out-of-trouble style of work.

My PhD was done as part of the project WildMap, where I benefited from several external collaborators: Henrik Brøseth, Daniel Turek, Wei Zhang, Perry de Valpine, J. Andrew Royle, Olivier Gimenez, and Jonas Kinberg. In articles III and IV of this dissertation, I had the opportunity to collaborate with Henrik Brøseth, Jenny Mattisson, Malin Aronsson, Jens Persson, Petter Wabakken, and Øystein Flagstad – thank you for your contributions and fruitful

discussions regarding the wolverine ecology, monitoring, and management in Scandinavia. Jon Swenson and Andrés Ordiz read and commented on my Synopsis – I appreciate your thorough reviews and helpful suggestions. Thanks to Anders Gunnar Helle, Katrine Eldegard, and Lisa Fagerli Lunde for polishing the Norwegian summary and title of this PhD dissertation. The names and contributions of other individuals are given in each of the articles that comprise this dissertation.

During my PhD, I received administrative support from the MINA staff, specifically by Kari Margrete Thue, Jan Vermaat, Stein Moe, and Brage Monsen. The "opponents" during my PhD transition process were Katrine Eldegard, Jonathan Coleman, and Stefaniya Kamenova – I appreciate your feedback. Thanks to fellow lab mates, colleagues, and co-workers at the Ecology Group, AQEG, EcoLunch, EcoFika, the so-called PhD cake gatherings, Thursday waffles, and folks from the norskkurs for organizing social events during the past three years. Special thanks to my family, کیانغکیان, for the unconditional support; سپاس فراوان از لطف و محبت شما

My PhD was made possible through funding from the Research Council of Norway to project WildMap (NFR 286886), and from the Swedish Environmental Protection Agency (Naturvårdsverket) to project RovQuant. Staffan Bensch and José Vicente López-Bao were my references when I applied for this position and I thank their support. In three chapters of this PhD dissertation, I used data from the Scandinavian large carnivore monitoring database "Rovbase 3.0", curated by Rovdata at the Norwegian Institute for Nature Research. I also used NMBU's high-performance computing cluster infrastructure "Orion", administered by the Center for Integrative Genetics.

Finally, thank you Norway for all you gave me. There are many things to like about you and I benefited a lot from being "with" you. Sorry for those few times I teased you about your weather and what you call food – no one is perfect, but you are great as you are and I wish you all the best.

Table of Contents

List of articles

Article I

Moqanaki E, Milleret C, Tourani M, Dupont P, and Bischof R (2021) Consequences of ignoring variable and spatially autocorrelated detection probability in spatial capture-recapture. *Landscape Ecology* 36, 2879–2895: https://doi.org/10.1007/s10980-021-01283-x

Article II

Dey S, **Moqanaki E**, Milleret C, Dupont P, Tourani M, and Bischof R (2023) Modelling spatially autocorrelated detection probabilities in spatial capture-recapture using random effects. *Ecological Modelling* 479, 110324: https://doi.org/10.1016/j.ecolmodel.2023.110324

Article III

Moqanaki E, Milleret C, Dupont P, Brøseth H, and Bischof R (2023) Wolverine density distribution reflects past persecution and current management in Scandinavia. *Ecography* (accepted).

Article IV

Moqanaki E, Milleret C, Dupont P, Dey S, Mattisson J, Brøseth H, Aronsson M, Persson J, Wabakken P, Flagstad Ø, and Bischof R. Environmental variability across space and time drives recolonization pattern of a historically persecuted large carnivore population. Manuscript.

The following publications and unpublished manuscripts supported this PhD dissertation, but they were not part of the core dissertation and are therefore not included in this document:

- Milleret C, Dupont P, **Moqanaki E**, Brøseth H, Flagstad Ø, Kleven O, Kinberg J, and Bischof R (2022) Estimates of wolverine density, abundance, and population dynamics in Scandinavia, 2014–2022. *MINA fagrapport 79*: `http://dx.doi.org/10.13140/RG.2.2.18083.32803`

- **Moqanaki E** and Samelius G (2022) *Monitoring the manul: guidelines for practitioners*. The Pallas's cat International Conservation Alliance (PICA), 187 pp.

- **Moqanaki E**, Tourani M, Taktehrani A, Enger KB, Karimi MH, and Bischof R. Scent of a cheetah: selection of marking sites by a critically endangered large carnivore. Manuscript.

- **Moqanaki E**, Tourani M, and Bischof R. Community observations of large mammals reveal conservation priority areas across a global biodiversity hotspot. Manuscript.

- Dey S, Milleret C, Dupont P, **Moqanaki E**, and Bischof R. Model adequacy of movement kernels in open-population spatial capture-recapture. Manuscript.

Summary

1. Wildlife populations live in increasingly human-altered landscapes. Either because of their intrinsic values or due to instrumental values to humans, wildlife populations are monitored to inform about their current status and population trends and to forecast their future status in response to possible changes in their environment. Monitoring wildlife across spatial units and over time is a first step towards adaptive and evidence-based management.

2. This PhD dissertation consists of four articles that are centered on developing new methods, enhancing concepts, and showcasing applications of novel analytical approaches for quantifying landscape-level wildlife population density using noninvasive monitoring data. At the core of this PhD dissertation lie spatially explicit analytical models, namely spatial capture-recapture (SCR), with the ability to yield scale-transcending estimates of population parameters, while accounting for imperfect detection. This PhD dissertation is motivated by applied questions raised during noninvasive genetic monitoring of large carnivores in the Scandinavian Peninsula. However, the methodology and findings have broader implications.

3. The first two articles focus on understanding and mitigating the consequences of spatially variable and autocorrelated detection probability when analyzing wildlife monitoring data. Detection probability – the probability of detecting an individual from the target population, can vary across the study area, because of, for example, certain landscape characteristics or the specifics of the sampling design. Spatial autocorrelation in detection probability occurs when detectability is more similar among neighboring than distant sampling locations or devices. Both articles I and II use simulations to create and test many scenarios that may occur during real-life sampling of wildlife in monitoring studies. **Article I** evaluates the consequences of not accounting for spatial variation in detectability when analyzing monitoring data with SCR, with a specific focus on the impact on estimates of population size. This study shows that a misspecified SCR model performs reasonably well in many situations, from low to even intermediate levels of spatial variation in detectability. However, **Article I** identifies problematic cases of highly

spatially variable and autocorrelated detection, which can lead to pronounced negative bias in population size estimates. Some of these extreme scenarios are expected in the large-scale monitoring of large carnivores in Scandinavia, which led to a follow-up study in the next chapter of this PhD.

4. **Article II** describes and tests three novel modeling approaches to account for spatially variable and autocorrelated detection probability in SCR with random effects. This study extends SCR with generalized linear mixed models (GLMMs) and compares the performance of the SCR-GLMMs that do and do not specifically account for spatial autocorrelation in detection probability. **Article II** then applies the new modeling approaches to Scandinavian brown bear *Ursus arctos* monitoring data from central Sweden, where the majority of the DNA data was collected opportunistically by volunteers and no reliable measure of sampling effort was available to infer spatially variable detectability. This empirical case study demonstrates the application of the proposed modeling approaches and suggests considerable spatial heterogeneity in the detection of bears, where detectability decreases in an east-to-west direction towards the Swedish-Norwegian border. Further, **Article II** discusses solutions to identify potential sampling gaps, where variation in the effort is not fully known and highlights computation trade-offs in using such novel SCR analyses in wildlife monitoring studies.

5. The next two articles demonstrate empirical applications of quantifying variation in wildlife population density and its determinants at the population level. Our current understanding of wildlife space use and habitat selection is dominated by geographically limited studies that often make inferences from a few instrumented individuals. Both articles III and IV use noninvasive genetic monitoring data of the wolverine *Gulo gulo* across the species' entire range in the Scandinavian Peninsula and assess sex-specific responses of the wolverine density to a suit of historical and present-day environmental covariates. Both these articles predict the Scandinavian wolverine density distribution and provide estimates of population size. **Article III**, as a prelude to the next chapter, identifies the factors influencing the current density distribution of the wolverine, with a focus on the role of the relict range along the Swedish-Norwegian border, where the wolverine survived intense human persecution by early 1970s. **Article III** reveals that distance from this

transboundary alpine region is still one of the most important determinants of wolverine density and the highest female and male wolverine densities are expected closer to the relict range. However, current management conditions to limit wolverine expansion, especially in southern Norway, interact with distance from the relict range, and together with other topographic, climatic, and prey-related factors, have shaped the current density distribution of the wolverine in Scandinavia. This study is the first to look into the density determinants of the Scandinavian wolverine population across its entire geographic range.

6. **Article IV** builds on the findings from Article III and quantifies the dynamics of density determinants of the Scandinavian wolverine over a nine-year monitoring period. This study quantified the change in the impact of the environmental covariates over the past decade, as the wolverine has successfully expanded from the alpine relict range into the boreal forest. **Article IV** uses recently developed open-population SCR models that provide not only estimates of annual density and its determinants, but also estimates of the demographic parameters (i.e., recruitment and survival) needed to predict changes in the population dynamics. This study reveals that, on the one hand, whereas the role of the relict range is still important for determining the wolverine's density distribution, its significance is diminishing over time. On the other hand, forest is appearing more and more as a significant predictor of today's wolverine density. **Article IV** tracks temporal trends in the main determinants of male and female wolverine densities and it discusses the results in relation to the population recovery of the wolverine in Scandinavia in the presence of ongoing human pressure.

Norsk sammendrag

1. Viltbestander lever i stadig mer menneskepåvirkedelandskap. Enten på grunn av deres iboende verdier eller på grunn av instrumentelle verdier for mennesker, overvåkes viltpopulasjoner for å informere om deres status og populasjonstrender og for å forutsi deres fremtidige status som respons på mulige miljøendringer. Overvåking av vilt på tvers av romlige enheter og over tid er et første skritt mot adaptiv og kunnskapsbasert forvaltning.

2. Denne doktorgradsavhandlingen består av fire artikler som er sentrert rundt det å utvikle nye metoder, forbedre konsepter og synliggjøre mulige anvendelser av nye analytiske tilnærminger for å kvantifisere bestandstetthet av vilt på landskapsnivå ved bruk av ikke-invasive overvåkingsdata. I kjernen av denne doktorgradsavhandlingen ligger romlig eksplisitte analytiske modeller, nemlig romlig fangst-gjenfangst (SCR), med evnen til å gi skalaoverskridende estimater av populasjonsparametere, samtidig som de tar hensyn til ufullkommen deteksjon. Denne doktorgradsavhandlingen er motivert av anvendte spørsmål reist under ikke-invasiv genetisk overvåking av store rovdyr på den skandinaviske halvøya. Metoden og funnene har imidlertid bredere implikasjoner.

3. De to første artiklene fokuserer på å forstå og forebyggekonsekvensene av romlig variabel og autokorrelert deteksjonssannsynlighet når man analyserer viltovervåkingsdata. Deteksjonssannsynlighet - sannsynligheten for å oppdage et individ fra målpopulasjonen kan variere på tvers av studieområdet på grunn av, for eksempel, visse landskapskarakteristikker eller spesifikasjonene til prøvetakingsdesignet. Romlig autokorrelasjon i deteksjonssannsynlighet oppstår når deteksjonsevnen er mer lik blant nærliggende enn fjerne prøvetakingssteder eller enheter. Både artikkel I og II bruker simuleringer for å lage og teste mange scenarier som kan oppstå under virkelig prøvetaking av vilti overvåkingsstudier. **Artikkel I** evaluerer konsekvensene av å ikke ta hensyn til romlig variasjon i deteksjonsevnen når man analyserer overvåkingsdata med SCR, med et særlig fokus på innvirkningen på estimater av populasjonsstørrelse. Denne studien viser at en feilspesifisert SCR-modell fungerer rimelig godt i mange situasjoner, fra lavt og opp til et middels nivå av romlig variasjon i

deteksjonsevnen. **Artikkel I** identifiserer imidlertid problematiske tilfeller av svært romlig variabel og autokorrelert deteksjon, som kan føre til en særs negativ skjevhet i populasjonsstørrelsesestimater. Noen av disse ekstreme scenariene forventes i den storskala overvåkingen av store rovdyr i Skandinavia, noe som førte til en oppfølgingsstudie i neste kapittel av denne doktorgraden.

4. **Artikkel II** beskriver og tester tre nye modelleringsmetoder for å ta hensyn til romlig variabel og autokorrelert deteksjonssannsynlighet i SCR med tilfeldige effekter. Denne studien utvider SCR med generaliserte lineære blandede modeller (GLMM) og sammenligner ytelsen til SCR-GLMM-er som tar og ikke tar spesifikke hensyn til romlig autokorrelasjon i deteksjonssannsynlighet. **Artikkel II** anvender deretter de nye modelleringstilnærmingene på overvåkingsdata av brunbjørn *Ursus arctos* fra Sentral-Sverige, hvor majoriteten av DNA-dataene ble samlet inn opportunistisk av frivillige og ingen pålitelige mål for prøvetakingsinnsats var tilgjengelig for å konkludere med romlig detektsjonsevne. Denne empiriske casestudien demonstrerer anvendbarheten av de foreslåtte modelleringstilnærmingene og antyder betydelig romlig heterogenitet i påvisningen av bjørn, hvor deteksjonsevnen avtar i øst–vest retning mot den svensk-norske grensen. **Artikkel II** diskuterer videre løsninger for å identifisere potensielle mangler i prøvetaking, der variasjonen i innsatsen ikke er fullt kjent, og fremhever beregningsavveininger ved bruk av slike nye SCR-analyser i viltovervåkingsstudier.

5. De to neste artiklene viser empiriske anvendelser av kvantifisering av variasjon i bestandstetthet hos viltog dets determinanter på populasjonsnivå. Vår nåværende forståelse av viltets arealbruk og habitatvalg består i hovedsak av geografisk begrensede studier som ofte trekker slutninger fra noen få instrumenterte individer. Både artikkel III og IV bruker ikke-invasive genetiske overvåkingsdata for jerven *Gulo gulo* over hele artens utbredelsesområde på den skandinaviske halvøya, og vurderer kjønnsspesifikke responser av jervetettheten til en rekke historiske og nåværende miljøkovariater. Begge disse artiklene forutsier den skandinaviske jervtetthetsfordelingen og gir estimater av bestandsstørrelse. **Artikkel III**, som et frempek til neste kapittel, identifiserer faktorene som påvirker dagens tetthetsfordeling av jerven, med fokus på rollen til reliktområdet langs den svensk-norske grensen, der jerven overlevde intens menneskelig forfølgelse tidlig på 1970-tallet. **Artikkel III**

avslører at avstand fra denne grenseoverskridende alpine regionen fortsatt er en av de viktigste determinantene for jervetetthet, og den høyeste tettheten av hunn- og hannjerv forventes nærmere relikviene. Dagens forvaltningsforhold for å begrense ekspansjon av jerven, spesielt i Sør-Norge, samhandler med avstand fra reliktområdet, og sammen med andre topografiske, klimatiske og byttedyrrelaterte faktorer, har formet dagens tetthetsfordeling av jerven i Skandinavia. Denne studien er den første som ser på tetthetsdeterminantene for den skandinaviske jervebestanden over hele dens geografiske utstrekning.

6. **Artikkel IV** bygger på funnene fra artikkel III og kvantifiserer dynamikken i tetthetsdeterminanter for den skandinaviske jerven over en ni-års overvåkingsperiode. Denne studien kvantifiserte endringen i virkningen av miljøkovariatene i løpet av det siste tiåret ettersom jerven har ekspandert fra det alpine reliktområdet til den boreale skogen. **Artikkel IV** bruker nylig utviklede SCR-modeller for åpen populasjon som ikke bare gir realistiske estimater av årlig tetthet og dens determinanter, men også estimater av de demografiske parameterne (dvs. rekruttering og overlevelse) som trengs for å forutsi endringer i populasjonsdynamikken. Denne studien avslører at på den ene siden, mens rollen til reliktområdet fortsatt er viktig for å bestemme jervens tetthetsfordeling, avtar dens betydning over tid. På den annen side fremstår skog mer og mer som en betydelig prediktor for dagens jervetetthet. **Artikkel IV** sporer tidsmessige trender i hoveddeterminantene for tetthet av hann- og hunnjerv, og den diskuterer resultatene i forhold til bestandsgjenoppretting av jerven i Skandinavia i nærværet av pågående menneskelig press.

Synopsis

Variation in detectability and density of wildlife populations: causes and consequences

You are trying to capture the fog, and no one can do that.
Patrick D. Smith, A Land Remembered

1 Introduction

Wildlife management emerged as a movement led by "sport hunters" in North America, who witnessed devastating wildlife losses during the nineteenth century. These sport hunters, as opposed to the traditional "market hunters", started developing codes of conduct and ethics to protect lands and take responsibility for wildlife therein (Leopold 1933, Meine 2010, Brown et al. 2013). As time went on, these wildlifers realized that they needed reliable up-to-date information about the status of wildlife populations to sustainably harvest them and achieve conservation goals. Such quantities are key to understanding population dynamics – the change in the size and composition of a population over time.

To learn about the status and trends of wildlife populations, researchers and managers typically sample the population. The size of the sample is always less than the size of the population of interest. This is because the entire population is practically impossible to count (as in a census); many wildlife populations are distributed across hundreds to thousands of square kilometers of heterogeneous landscape, and they often occur in low densities, are mobile, and avoid humans (Thompson 2013, Kellner and Swihart 2014). Logistically and economically efficient sampling is therefore a common goal in wildlife population ecology and management. Traditionally, sampling has been done by hunting, trapping and tagging, or tracking some individuals from the target population (Krebs 1999, Buckland et al. 2000, Williams et al. 2002). Besides being logistically challenging for studying large mammals, there are ethical, welfare, and safety considerations in using such invasive approaches. For sampling rare, elusive, or threatened wildlife, "noninvasive" data collection methods that do not require physical capture or handling of animals have been

developed during the past decades (Thompson 2013, Zemanova 2020). The most popular noninvasive data collection methods are genetic sampling from naturally shed biological material in the environment (e.g., feces; Lefort et al. 2022) and camera trapping (Burton et al. 2015). Noninvasive data collection methods are promising tools for wildlife population monitoring by providing a wealth of data over a long time and across large spatial extents (Lamb et al. 2019, Tourani 2022).

The goal of wildlife monitoring is not only to collect ecological data, but also to provide reliable estimates of some population quantities across space and time (Yoccoz et al. 2001, Pollock et al. 2002, Nichols and Williams 2006, Jones et al. 2013). To derive estimates of wildlife population status from a sample of the population, we use ecological modeling to provide quantitative information about population processes and attempt to identify the underlying drivers of population change (Krebs 1991, Buckland et al. 2000, Gimenez et al. 2014, Kéry and Royle 2015, van de Schoot et al. 2021). By taking a quantitative approach to understanding the population's size and dynamics, wildlife monitoring provides valuable insights into the ecology of the focal population and could inform management efforts.

Despite the benefits of long-term wildlife monitoring, analyzing the resulting data to draw reliable inferences is challenging. On the one hand, the analyst has to deal with an incomplete and imperfect picture of the reality – when species are elusive, mobile, and sparsely distributed across large areas, their detection (e.g., confirming their presence) during the sampling is difficult (Kellner and Swihart 2014, Gimenez et al. 2018). Yet, the data collection process is not always fully known to the analyst. On the other hand, logistical constraints, equipment inefficiency, and pooling data across multiple study areas or sampling methods are common examples that cause survey error and variability in wildlife monitoring data (Efford et al. 2013, Moqanaki et al. 2021, Howe et al. 2022). These sources of variation, which can happen across space, over time, or among individuals from the focal population, must be identified, quantified, and accounted for during the analysis of wildlife monitoring data. Failure to address variation in the sampling process may result in erroneous results and misleading conclusions (Cubaynes et al. 2010, Kellner and Swihart 2014, Gimenez et al. 2018, Dupont et al. 2023).

In this PhD dissertation, I studied two main sources of variation in wildlife monitoring data: (i) imperfect and variable detectability of individuals from the target population during the sampling; and (ii) factors and ecological processes leading to spatial and temporal variation in the distribution of individuals that form a population. Hierarchical models offer solutions to address these issues by disentangling observation and ecological processes (Royle and Dorazio 2008, Lele and Dennis 2009, Kéry and Royle 2015, van de Schoot et al. 2021). I used simulations and the comprehensive multinational database of large carnivores in Scandinavia (`rovbase.no` and `rovbase.se`), which is composed of individual identities and locations that have been collected over the past decades using noninvasive DNA sampling. I modeled large-scale variation in animal detectability and density, and quantified their determinants using a hierarchical analytical framework, namely spatial capture-recapture (SCR; Efford 2004, Borchers and Efford 2008, Royle et al. 2014, 2018). In this Synopsis, first, I argue for the importance of wildlife monitoring to learn about wildlife populations (i.e., research) and inform management decisions (i.e., action). Here, I also briefly describe the current system of monitoring and management of large carnivores in Scandinavia. Second, I expand on the two main sources of variation in wildlife monitoring data at the landscape level; heterogeneous detectability and spatial distribution. I describe different situations where such variation exists in wildlife monitoring and discuss some of the solutions to identify and account for variability in the data. This is the core of this PhD dissertation. For the modeling solutions, I focus on SCR as the analytical framework on which this PhD is built. Finally, I discuss quantitative approaches to provide reliable and spatially explicit estimates of wildlife population density. Throughout this Synopsis, I summarize the main findings of this PhD dissertation and identify remaining gaps and future directions.

2 Monitoring for management

2.1 Why, what, and how?

Wildlife monitoring is the process of collecting and analyzing information about a population, often at different points in time, to assess population

status and draw inferences about changes over time (Krebs 1991, Yoccoz et al. 2001, Jones et al. 2013). Sampling depends on the objectives of monitoring (what to measure?) and the resources available. The main metrics of interest are: (i) population size – abundance and density: How many of a given species exist in this study area and how they are distributed in relation to certain features of the area?; (ii) vital rates – e.g., reproduction, survival: Is this population declining, stable, or increasing? How many of the yearlings are expected to live until adulthood?; (iii) characteristics of the population – e.g., age and sex structure, behavior: what proportion of the population is breeding females? In case of a disease outbreak, which individuals in what areas are more susceptible?

Although wildlife monitoring appears as a critical tool for understanding wildlife populations, it is a controversial endeavor. More information is always welcome. However, in a real world of limited resources and changing priorities, there is always a trade-off between allocating available resources to collecting more information and increasing the effectiveness and efficiency of actions, which are supposed to be based on the lessons learned from the monitoring (Legg and Nagy 2006, Chadès et al. 2008, Jones et al. 2013, Maxwell et al. 2015). Monitoring purely for science is therefore not a priority in many situations and, instead, monitoring for adaptive management is favored (Nichols and Williams 2006, Williams 2011, Rist et al. 2013). Adaptive monitoring offers solutions to reduce uncertainty and improve predictions drawn from wildlife monitoring, so that the outcomes of interventions can be continuously improved.

To draw actionable inferences from wildlife monitoring, we either propose a hypothesis and evaluate it or conduct retrospective analysis (Yoccoz et al. 2001, Nichols and Williams 2006, Betts et al. 2021). The former needs an experimental design, where there are competing *a priori* hypotheses to develop some predictions about the expected results of a change in the system. A controlled experiment is subsequently developed to manipulate the system and collect data before and after, or with and without, the manipulation. We would then compare our predictions with estimates derived from the experiment to draw causal inferences. Nevertheless, experimentation is not always possible when dealing with applied questions and retrospective analysis is more common in wildlife monitoring efforts. In this approach, we perform statistical analysis

of the variable of interest, yet the observed pattern can be explained by more than one hypothesis (Yoccoz et al. 2001, Legg and Nagy 2006, Nichols and Williams 2006). For example, if we observed a declining trend in the population size of a given carnivore population after trophy hunting, the decrease could be either a result of hunting or an outcome of other factors, such as an increase in juvenile mortality after a harsh winter or even survey errors. In other words, although we have observed a significant negative correlation between population size and hunting, such associations do not necessarily mean strong evidence of the underlying cause. Thus, the observation of a correlation is usually not sufficient to unambiguously disentangle the cause and the effect of multiple, and sometimes confounding, factors. As a result, retrospective analyses only permit weak inferences (Yoccoz et al. 2001, Legg and Nagy 2006, Stephens et al. 2015). However, hypothesis testing is also possible in retrospective analysis, where *a priori* hypothesis is developed to make predictions, which are then compared with the monitoring data (Betts et al. 2021). Comparable conclusions can be repeatedly obtained across multiple systems or species, which can be a sign of strong support. The empirical studies in articles II-IV of this PhD dissertation should be therefore seen as retrospective analyses that test hypotheses and discuss results regarding the association between population size and sampling design (Article II) or some environmental features of the Scandinavia Peninsula (Articles III and IV), and not causal inferences.

2.2 Of wolverines and bears: Large carnivore monitoring and management in Scandinavia

2.2.1 Background

This PhD was motivated by issues faced during the analysis of noninvasive genetic monitoring data of large carnivores in Scandinavia. Specifically, the empirical case studies in articles II-IV concern different aspects of how to account for variation in detectability and spatial distribution, when quantifying the population density of Scandinavian large carnivores. In this PhD, I use "Scandinavia" and "Scandinavian Peninsula" to refer to the two Nordic countries of Norway and Sweden (Fig. 1). The guild of large carnivores in Scandinavia, which are members of the mammalian order Carnivora with an adult body

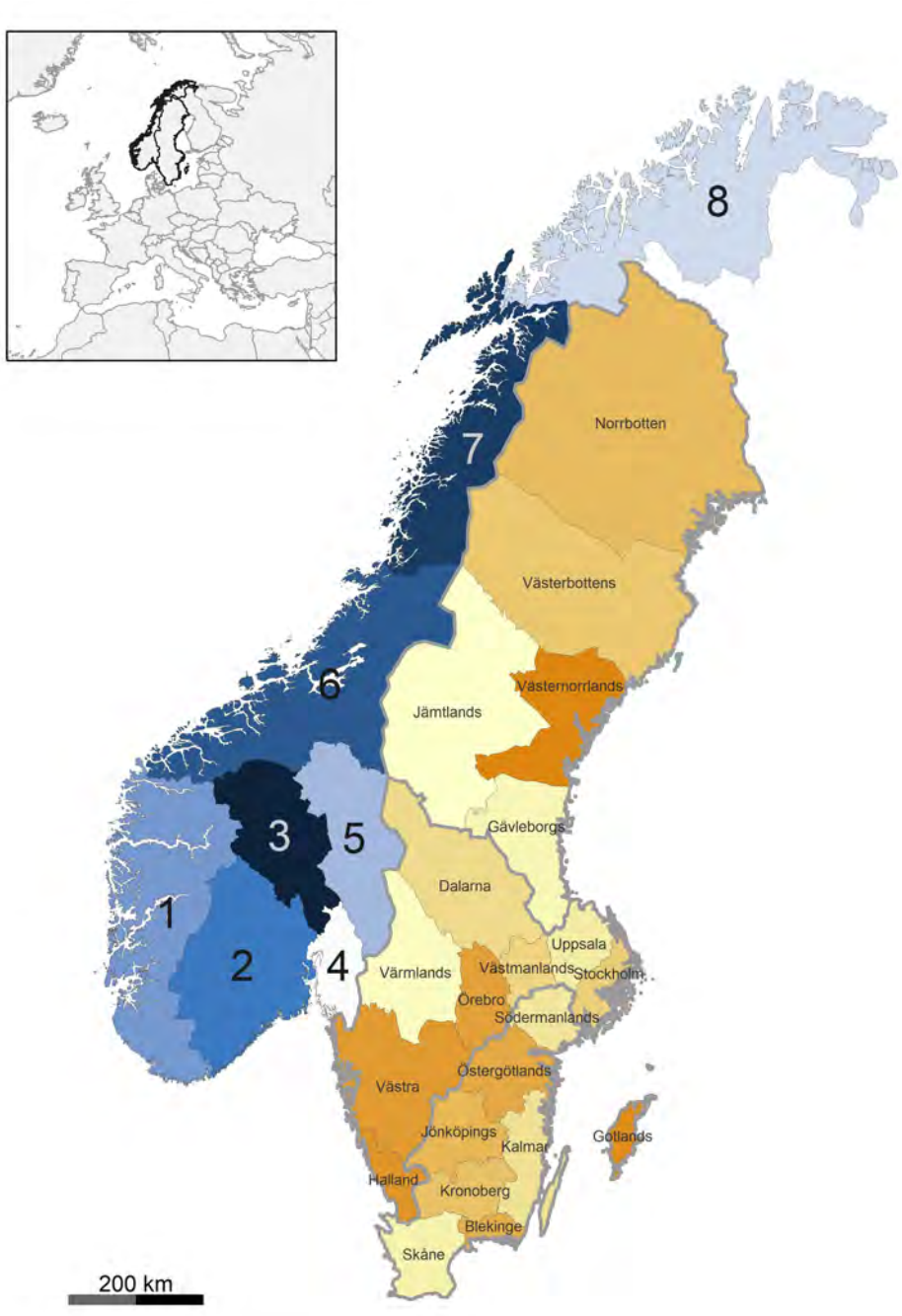

Figure 1: Map of the Scandinavian Peninsula, where noninvasive genetic monitoring and management of large carnivores are coordinated across different jurisdictions. In Norway (left), eight carnivore management regions are color-coded in shades of blue and labeled with numbers. In Sweden (right), counties are labeled with county names and three management regions (Rovdjursförvaltningsområden) are shown with thick borders.

mass greater than or equal to 15 kg (Wolf et al. 2018), consists of brown bear *Ursus arctos*, gray wolf *Canis lupus*, wolverine *Gulo gulo*, and the Eurasian lynx *Lynx lynx* (Swenson and Andrén 2005, Chapron et al. 2014; Fig. 2). In articles III and IV, I analyze monitoring data of the wolverine from Norway and Sweden. Article II involves a case study from the Scandinavian brown bear monitoring in central Sweden.

Norway and Sweden are among the European countries that have witnessed a partial recovery of their large carnivore community (Chapron et al. 2014, Boitani and Linnell 2015, Lindsey et al. 2017; Fig. 2). Despite cultural and socioeconomic similarities, Norway and Sweden differ considerably in how they monitor and manage large carnivores (Swenson and Andrén 2005, Sandström et al. 2009, Linnell et al. 2017, Sjölander-Lindqvist et al. 2020). Here, I summarize important aspects of large carnivore monitoring and the management systems in Norway and Sweden, from the past to the present.

2.2.2 From near extinction to recovery

Both the landscape and national policy regarding large carnivores have changed greatly in Scandinavia through the past centuries (Linnell et al. 2000, Swenson and Andrén 2005). Large carnivores were common almost throughout the Peninsula by the mid-eighteenth century. From this time, government-supported bounties were introduced as an official policy to exterminate large carnivores, which continued until the late nineteenth century (Wabakken et al. 2001, Flagstad et al. 2004, Swenson and Andrén 2005). Besides an intensive eradication of large carnivores and overhunting of their ungulate prey, the landscape in Scandinavia also changed substantially. By the end of this period, almost no true wilderness had remained in Norway and Sweden and the sharp decline of large carnivores was evident (Linnell et al. 2000). Wolves were functionally extinct, relict bear and lynx populations only persisted in parts of Sweden, and the wolverine was restricted to alpine areas along the Swedish-Norwegian border (Swenson et al. 1995, Wabakken et al. 2001, Spong and Hellborg 2002, Flagstad et al. 2004; Fig. 2). Subsequently, public opinion about the large carnivores started to change, which eventually resulted in the abolishment of bounties, restricting carnivore killing to fewer areas and certain

seasons, and making large carnivores the property of the State (Swenson and Andrén 2005). The national policy and responses of large carnivores to the paradigm shift varied among the carnivores. However, subsequent protection measures after the Second World War eventually resulted in partial recovery of large carnivore populations in Scandinavia in the post-1990s (Chapron et al. 2014; Fig. 2).

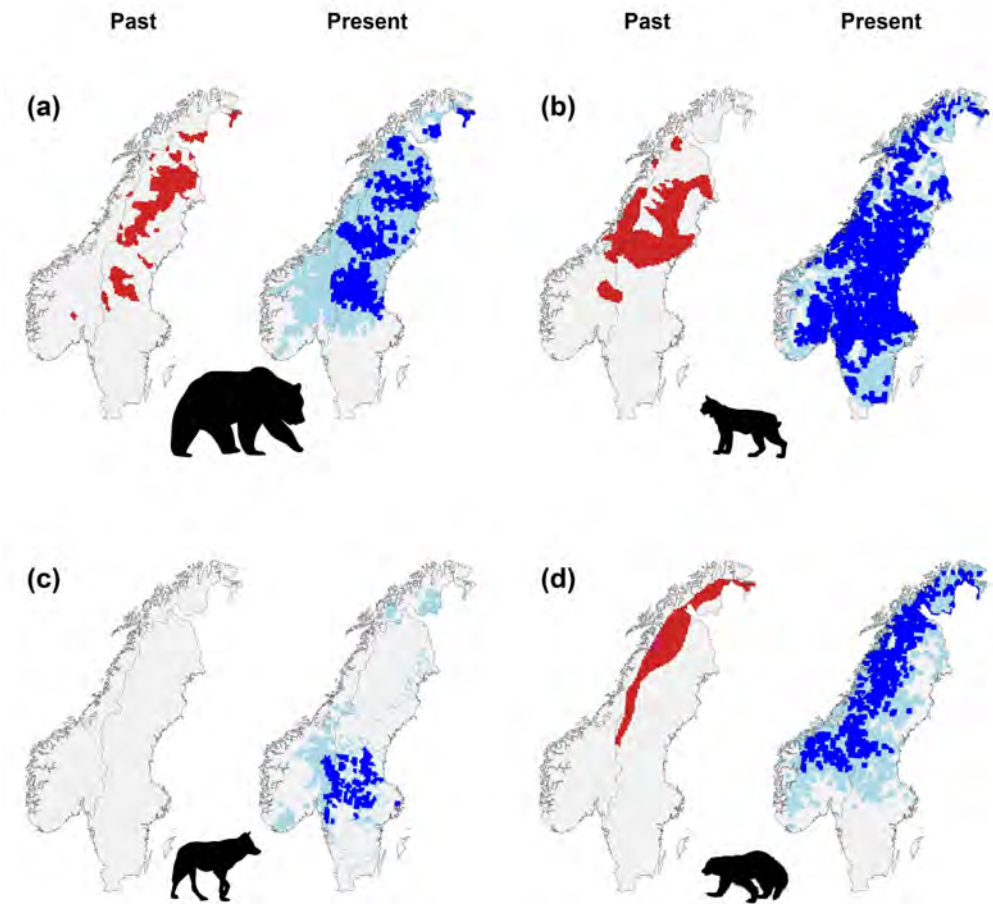

Figure 2: Past (≈ 1970s) and present distribution of large carnivores in the Scandinavian Peninsula after Chapron et al. (2014): (a) Brown bear *Ursus arctos*; (b) Eurasian lynx *Lynx lynx*; (c) Gray wolf *Canis lupus*; and (d) Wolverine *Gulo gulo*. The present distribution maps show approximate areas of permanent (dark blue) and sporadic occurrence (light blue) of each large carnivore species. Animal silhouettes are downloaded from public sources (e.g., `phylopic.org`). This PhD dissertation involves case studies of the wolverine (Articles III and IV) and brown bear (Article II).

2.2.3 Struggle on a modern landscape

Today, public opinion about the Scandinavian large carnivores is polarized (Gangaas et al. 2013, Linnell et al. 2017). Although the majority of the urban public either supports or is neutral towards large carnivores, it is the rural stakeholders who are most affected by the population recovery and demand active interventions (Røskaft et al. 2003, Hobbs et al. 2012, Widman and Elofsson 2018). Wolves and bears are generally less tolerated than lynx and wolverines (Ericsson et al. 2004, Kleiven et al. 2004, Gangaas et al. 2013, Dressel et al. 2014, Rauset et al. 2016). Large carnivore populations in Scandinavia are therefore subject to different management regimes to limit their population size and distribution. The goal is to maintain viable populations, while minimizing conflicts with farmers, livestock breeders, and hunters (Sandström et al. 2009, Strand et al. 2019). As the recovery of the Scandinavian large carnivores has resulted in increasing conflict with human interests, both countries have considered monitoring of population size and its trends to be important for informing management decisions (Liberg et al. 2012, Gervasi et al. 2016, Aronsson and Persson 2017, Bischof et al. 2020). However, the monitoring methods and implementation of the results have changed over time and may also vary at the regional levels for different species (Fig. 1). To highlight these differences, a closer look into each country's general landscape and policy regarding large carnivores is necessary.

2.2.4 No more wilderness

Contrary to the general perception of pristine, human-free, mountains and forests, there is virtually no such wilderness across the Scandinavian Peninsula (Linnell et al. 2000, Watson et al. 2016). Today, the landscape in Norway and Sweden is primarily multiuse, and protected areas are often small and restricted to unproductive mountain regions; thus, large carnivores are forced to share the habitat with humans (Linnell et al. 2001b, Swenson and Andrén 2005, Rauset et al. 2016). Although the size of land areas in Norway and Sweden are comparable ($\approx$ 385 000 vs. 450 000 km^2, respectively; Fig. 1), the human population size of Sweden is almost twice Norway's (10.5 vs. 5.4 million people). Human density and associated disturbances track the climate

suitability and increase from north to south. Human areas are the highest in the south, where the countries' capitals and most of the major cities are located.

The management of large carnivores in Scandinavia is largely influenced by their acceptance by the livestock farming industry and hunters (Sandström et al. 2009, Gangaas et al. 2013, Widman and Elofsson 2018, Strand et al. 2019). Almost the entire northern half of both countries contain semidomesticated reindeer *Rangifer tarandus* husbandry areas, where the indigenous Sámi pastoralists have herding rights under different management units and seasonal grazing schemes (Jernsletten and Klokov 2002, Axelsson-Linkowski et al. 2020). The share of Norway and Sweden in the global reindeer population and production is considerable, which is the leading industry, culturally important, and the traditional area of employment of the indigenous people in Scandinavia (Jernsletten and Klokov 2002, Tveraa et al. 2007, Axelsson-Linkowski et al. 2020). By law, predation losses of semidomesticated reindeer should be fully compensated, which annually exceeds tens of millions of US dollars in each country (Mattisson et al. 2011, Persson et al. 2015, Bautista et al. 2019, Støen et al. 2022). In addition, over two million free-ranging sheep *Ovis aries* graze Norway's forests and mountains, mostly in the southern areas (Strand et al. 2019). Although the pastures are fenced in Sweden, predation of sheep is an issue of growing concern for the stakeholders in both countries (Karlsson and Johansson 2010, Mabille et al. 2015, Widman and Elofsson 2018). Large carnivores also compete with hunters for several species of economically important ungulates, such as moose *Alces alces* and roe deer *Capreolus capreolus* (Jonzén et al. 2013, Andrén and Liberg 2015, Wikenros et al. 2020).

2.2.5 Carnivore management at multiple levels

In Norway and Sweden, the parliaments decide on reference areas and population size goals for the favorable conservation status of large carnivores (Linnell et al. 2017, Strand et al. 2019, Sjölander-Lindqvist et al. 2020). The number of large carnivores allowed to exist in each country and in different regions is therefore largely affected by political decisions, which consider the national reference values in relation to international conventions that each of

the countries is bound by (Sandström et al. 2009, Epstein 2014, Trouwborst et al. 2017). The majority of current disagreements regarding large carnivore management in Scandinavia concerns the wolf (Liberg et al. 2020, Linnell et al. 2017, Trouwborst et al. 2017), which is not the focus of this PhD dissertation.

Norway and Sweden have chosen different paths in large carnivore monitoring and management (Swenson and Andrén 2005, Sjölander-Lindqvist et al. 2020). These differences are specifically related to the Convention on the Conservation of European Wildlife and Natural Habitats (the Bern Convention) and, for Sweden, the European Directive on the Conservation of Natural Habitats and of Wild Fauna and Flora (Habitats Directive 1992). Both Norway and Sweden have signed the Bern Convention, but they implement their large carnivore governance differently, in particular since 2000 (Sandström et al. 2009, Linnell et al. 2017, Sjölander-Lindqvist et al. 2020). The Bern Convention obliges the signatories to take appropriate measures to maintain viable populations of wild flora and fauna based on ecological, scientific, and cultural criteria. However, signatories may make exceptions to the conservation measures to prevent significant damage to forest and agricultural properties, unless the exception is detrimental to the survival of the fauna or flora population (Epstein 2014, Trouwborst et al. 2017). In addition to the Bern Convention, Sweden, as an EU member, also follows the Habitats Directive, which requires each Member State of the European Union to take measures to reach and maintain minimum levels of natural habitats and wild plants and animals, while taking into account the economic, social, cultural, and regional dimensions (Habitats Directive 1992). This includes the "minimum levels of large carnivores", which is much debated, particularly regarding the mitigation methods to address human-carnivore conflicts (Epstein 2014, Linnell et al. 2017, Widman and Elofsson 2018).

In Sweden, the Swedish Environmental Protection Agency (Naturvårdsverket) has received the overall responsibility from the government to implement the international conventions, which include large carnivore management practices. However, there is a decentralized policy in place to increase regional and local influence over large carnivore management through wildlife management delegations, led by the governor of each county (län, the next level of administration below the state; Fig. 1) and including representatives of different

stakeholders (e.g., political parties, farmers, local businesses, hunters, nature conservation groups). This delegation plays an advisory role in deciding on guidelines and management plans for large carnivores, including recommending minimum and interim levels of large carnivore populations in the given county. In the northern areas, the Sámi Parliament also takes some responsibility for the implementation of large carnivore management decisions. Meanwhile, in parallel to the county-level management, three councils have been established to coordinate the monitoring and management of large carnivores among the counties in three northern, middle, and southern regions, known as Rovdjursförvaltningsområden (Fig. 1). If designated large carnivores numbers are not met, the power to take management decisions is re-centralized to the Swedish Environmental Protection Agency (Sjölander-Lindqvist et al. 2020).

Large carnivores are strictly protected under the European Union's Bern Convention and Habitat Directive, but there is also room for management flexibility (Linnell et al. 2017, Trouwborst and Fleurke 2019). As a signatory to both conventions, the legal removal of large carnivores in Sweden is expected to be in accordance with the designated criteria, which requires such decisions to be made if there is no other alternative solution to address serious damages to agricultural or other properties effectively (Epstein 2014). The definition of what constitutes serious wildlife damage to human properties may vary. For example, in reindeer grazing areas, 10% reindeer loss of a herding community to large carnivore predation is defined as the maximum acceptable level of annual losses (Mattisson et al. 2011, Hobbs et al. 2012, Persson et al. 2015).

In Norway, the national policy regarding large carnivores is decided by the Norwegian Parliament, including measures to secure the survival of large carnivores and the persistence of their habitats. Population goals for each of the large carnivore species are decided for each of the eight carnivore management regions (Fig. 1). Currently, the Ministry of Climate and Environment is given the responsibility to implement the international conventions and national interests in large carnivore governance, with delegated authority to the Norwegian Environment Agency (Miljødirektoratet). The Ministry has appointed regional large carnivore committees to make management decisions that take into account the differences in human interests in different areas and for different carnivore species. As a result, the population goals for large

carnivores vary greatly across the different Norwegian carnivore management regions (Fig. 1). Such decisions should also allow for local engagement. The final authority regarding the regional management plans remains at the national level. The regional government-appointed committees usually consist of regionally elected politicians and, if applicable, members nominated by the Sámi Parliament. This committee must comply with the national policies regarding carnivores and may be also instructed by the Norwegian Environment Agency. The committee's decisions may include license, quota, or protective hunting of large carnivores, but the population goals must be reached. At the same time, the Ministry of Local Government and Modernization has also received the responsibility to report on progress, and the Ministry of Agriculture has the overall responsibility for semidomesticated reindeer (Sjölander-Lindqvist et al. 2020).

Norway follows a specific interpretation of the Bern Convention criteria to be more flexible regarding large carnivore management (Linnell et al. 2017, Trouwborst et al. 2017). Subsequently, Norway has developed a zonal management system for each large carnivore species, with eight carnivore management regions (Fig. 1). In a zone that is considered, for example, for the wolverine, livestock must be protected against the wolverine only. Other large carnivores (bear, wolf, and lynx) are not expected therein and will be removed. No zone is considered entirely for all four large carnivores, and the southern zones ($\approx$ 45% of Norway's land area) are prioritized for livestock (Strand et al. 2019). The carnivore management zone for each species is considered to be large enough to sustain a viable population, but "viable" is defined by the Norwegian Parliament. Currently, the largest zone is designated for the lynx, followed by the wolverine, and only small borderline zones are considered for the bear and wolf (Strand et al. 2019; Fig. 2). The latest population target is 65 annual reproductions for the lynx, 39 for the wolverine, 13 for the bear, and four for the wolf. The population targets include part of the population that occurs in Sweden. For the case of wolves, the latest population target allows for two additional annual litters by wolf packs that have part of their territory in Sweden (Strand et al. 2019). If population targets set by the Parliament are met, lethal population control of large carnivores will be then practiced inside the designated carnivore management regions.

Box 1. Wolverine *Gulo gulo* as a study species

The wolverine's global range (Abramov 2016)

© Kjetil Schjølberg/Rovdata

The wolverine is the largest terrestrial species of the carnivoran family Mustelidae, which also includes weasels, badgers, otters, ferrets, martens, and minks. The wolverine's geographic distribution range is primarily associated with the boreal zone of the Northern Hemisphere, from northern Canada, Alaska and some of the western lower states in the US, and in the mainland Fennoscandia towards western Russia and Siberia, and parts of Central Asia to Mongolia and northern China (Landa et al. 2000, Abramov 2016). Globally, the wolverine conservation status is currently considered as "Least Concern", but regionally, populations are considered to be threatened and declining in both numbers and distribution (Abramov 2016). The main threats to the wolverine are human-caused, from overharvesting and retribution killing, because of their predation of livestock to habitat fragmentation and a changing climate (Abramov 2016, Fisher et al. 2022).

The wolverine population in Norway and Sweden is an example of a successful recovery of a historically persecuted species in modern multiuse landscapes (Chapron et al. 2014, Boitani and Linnell 2015). Following centuries of intense persecution, the wolverine was eradicated from most of the Scandinavian Peninsula by the 1970s and was restricted to the alpine region between Norway and Sweden (Flagstad et al. 2004). After introducing conservation interventions, today the Scandinavian wolverine population has recolonized a major part of its historical range (Chapron et al. 2014, Bischof et al. 2020). However, because there is no wilderness without human influence in Scandinavia, the population expansion has caused conflict with sheep *Ovis aries* owners and semidomesticated reindeer *Rangifer tarandus* herders (Hobbs et al. 2012, Rauset et al. 2016). The wolverine population is therefore managed at the regional level to balance the human interests and needs of an ecologically viable wolverine population (Aronsson and Persson 2017, Gervasi et al. 2019).

Noninvasive monitoring of the wolverine population is an integral part of species management in Scandinavia. Annually, authorities and volunteers collect and submit putative wolverine DNA samples (e.g., scat, hair) to be genetically analyzed (Gervasi et al. 2016, Ekblom et al. 2018). Samples are then identified to species and, if possible, individual level, where many of them contain the date and location information. Because the monitoring is done by hundreds of people across almost the entire Scandinavia, there are many sources of variation in the monitoring data that must be accounted for to estimate population-related variables of interest (Bischof et al. 2020, Milleret et al. 2022b). Articles III and IV of this PhD dissertation focus on quantifying density determinants and some other aspects of variation in the monitoring data of the wolverine.

2.2.6 Carnivore monitoring: from invasive to noninvasive, and from indices to estimates

Since the late 1970s, Norway and Sweden have implemented different monitoring and research programs to better understand the population size, dynamics, and habitat requirements of large carnivores in Scandinavia (Swenson et al. 1998, Andrén et al. 2002, Solberg et al. 2006, Kindberg et al. 2009, Liberg et al. 2012, Gervasi et al. 2016, Åkesson et al. 2022). Besides research and monitoring, both countries are also implementing population management measures, including legal removal, which are expected to be informed by the monitoring. Both countries believe that the success of the current management efforts for large carnivores depends on the integration of different management measures, research, and monitoring (Liberg et al. 2012, Gervasi et al. 2016, Bischof et al. 2020). As discussed earlier, both countries are using a zonal management system for large carnivores (Fig. 1), where county administration representatives make regional management plans and conduct populating monitoring (Strand et al. 2019, Sjölander-Lindqvist et al. 2020). Despite sharing transboundary populations of large carnivores and the efforts to unify the monitoring data through a shared database (`rovbase.no` and `rovbase.se`), the population monitoring is still not fully coordinated, mainly because of the differences in national and regional policy and each country's international obligations regarding the large carnivores (Bischof et al. 2016, 2020, Gervasi et al. 2016, 2019, Aronsson and Persson 2017, Åkesson et al. 2022).

The population monitoring of large carnivores in Scandinavia has evolved during the past decades and different methods have been used for different species and in different carnivore management regions. The main objectives of the monitoring programs for large carnivores are to locate and count individuals or family groups, record reproduction events, identify the breeding pairs, and estimate population size and genetic structure and inbreeding (Linnell et al. 2001a, Andrén et al. 2002, Liberg et al. 2005, 2012, Gervasi et al. 2016, Åkesson et al. 2022). The goal is to maintain minimum viable populations of large carnivores that are genetically connected with the neighboring populations (within the Scandinavian Peninsula and, ideally, over Fennoscandina and Karelian), while minimizing human-carnivore conflicts (Liberg et al. 2012, Gervasi et al. 2016, Kopatz et al. 2021, Åkesson et al. 2022).

Box 2. Brown bear *Ursus arctos* as a study species

The approximate extant range of the brown bear

© Staffan Widstrand

The brown bear *Ursus arctos* is a member of the carnivoran family Ursidae, which includes eight extant bear species. Despite the human-caused extirpation in North Africa and substantial declines in distribution and population size in the remaining continents (McLellan et al. 2017), the brown bear is still one of the most widely distributed large carnivores.

Globally, the population status of brown bears is considered "Least Concern" with a stable trend (McLellan et al. 2017). However, outside Russia and parts of North America, many bear populations are small, isolated, and threatened with extinction, because of human killing, habitat loss and fragmentation, and trades in body parts (Can et al. 2014, McLellan et al. 2017).

The Scandinavian brown bear population is shared by Sweden and Norway. Like other large carnivores of Scandinavia, the brown bear has experienced near extinction in modern times (Swenson et al. 1995). The extermination efforts peaked in the nineteenth century in both countries, where the historical bear population was larger in Norway, and at first, Sweden was more successful in the population extirpation (Swenson et al. 1995, 2017). By the 1930s, the bear population in both countries was close to extinction. Whereas Sweden changed its policy, which eventually led to the recovery of the bear population, bears were virtually extinct in Norway by the 1970s (Swenson et al. 1995, Chapron et al. 2014). Today, although the Swedish population of bears has partially recovered and reoccupied parts of its historical range, the Norwegian population is managed intensively to be limited to the designated carnivore management zones along the border with Sweden (Chapron et al. 2014, Swenson et al. 2017, Strand et al. 2019).

The Scandinavian brown bear monitoring is a leading example of noninvasive genetic sampling of wildlife (Swenson et al. 2011). Sampling of putative bear scats and hair is conducted mostly opportunistically by authorities in Norway, as well as hundreds of volunteers (e.g., hunters) during the hunting season in Sweden. Although Norway samples its bear population every year, in Sweden a given region is sampled every five years (Bischof et al. 2020). Because of the unstructured sampling design that also varies at the county level and over time, especially in Sweden, substantial variation in the monitoring data is expected. However, almost no unambiguous measures of sampling effort are available to aid reliable population estimates of the Scandinavian bear population (Bischof et al. 2020). In Article II, noninvasive genetic monitoring data of female bears from central Sweden is used to demonstrate novel modeling approaches for quantifying and accounting for spatially heterogeneous detectability during large-scale wildlife monitoring to improve density estimates.

In the early years of the Scandinavian large carnivore population monitoring, mainly proxies of population size were obtained from snow-tracking surveys (Liberg et al. 2012, Åkesson et al. 2022), direct observations of family groups (Andrén et al. 2002, Kindberg et al. 2009), or other indirect measures such as counts of active dens (Landa et al. 1998b). The resulting data often did not allow for reliable population estimation of large carnivores using conventional analytical frameworks; thus, different approaches to convert the minimum observation counts to indices of abundance, density, or reproduction metrics were used (Andrén et al. 2002, Kindberg et al. 2009, 2011, Liberg et al. 2012). These count-based methods have the advantages of (i) being relatively cheap to conduct; (ii) having a high potential to engage the public; and (iii) minimally impacting the fitness, behavior, or welfare of the study wildlife populations (Mech and Boitani 2007, Kojola et al. 2018, Moqanaki and Samelius 2022). The main assumption is that the obtained indices correlate with abundance or density; thus, they can indicate a change in the status of the population. However, it has been shown that such indices can only be trusted under certain conditions and if properly calibrated to provide inferences about population size and dynamics (Gopalaswamy et al. 2015, Morin et al. 2022). The main disadvantage of these methods is that they do not necessarily reflect abundance; indices often fail to account for different sources of sampling errors and confounding factors, which makes the comparison of results between different areas or over time unreliable (Sollmann et al. 2013, Kellner and Swihart 2014, Stephens et al. 2015). For example, snow conditions during the tracking period may change over time and in different regions, manpower may vary and different personnel with varying experience and skills may be involved in each monitoring season in different management regions, and certain individuals from the target carnivore population are more likely to be sampled more often (e.g., scent-marking males). All of these examples can cause spatial, temporal, or individual heterogeneity in wildlife monitoring data and bias the results (Krebs 1999, Pollock et al. 2002, Efford et al. 2013, Gimenez et al. 2018).

By the late 1990s, radio telemetry (and later, GPS-telemetry) of individuals became an important additional source of information in the Scandinavian large carnivore monitoring (Bjärvall et al. 1990, Landa et al. 1998a, Linnell

et al. 2001a, Wabakken et al. 2001, Liberg et al. 2012). Every population-level monitoring of wildlife aims to provide information on where the species are, how many of them and where they are, and what could affect where they are. Wildlife telemetry appears to be an ideal research tool to answer these questions, as it provides fine-scale individual data about space use and movement of the tagged individuals that are otherwise too rare and too elusive to observe in the wild (Cochran and Lord 1963, White and Garrott 1990, Cagnacci et al. 2010, Fuller and Fuller 2012). The general approach has been to track a few individuals from each carnivore management region. In the case of territorial carnivores (e.g., wolves), usually one "alpha" individual from each pair or pack has been tagged with radio or GPS-telemetry devices to collect information about their territory sizes and reproduction (Wabakken et al. 2001, Liberg et al. 2012). The main disadvantages of wildlife tagging for large-scale wildlife population monitoring are (i) the need to physically capture and handle animals, which in the case of large carnivores, can be risky for both the animal and investigators; (ii) telemetry devices are expensive and come with considerable failures; (iii) trained wildlife veterinarians and highly skilled personnel are required; and (iv) the resulting data may not be a representative sample of the population, especially when few individuals are tagged with collars (Powell and Boyce 2010, Kelly et al. 2012, Moqanaki and Samelius 2022).

Since the 2000s, genetic sampling of DNA material has been increasingly used to monitor large carnivore populations in Scandinavia (e.g., Flagstad et al. 2004, Hedmark et al. 2004, Bellemain et al. 2005, Liberg et al. 2005, 2012, Brøseth et al. 2010, Åkesson et al. 2016, 2022, Bischof et al. 2016, 2020, Gervasi et al. 2016, 2019). Specifically, noninvasive DNA sampling of naturally shed biological material, such as feces (or scats), hair, urine, saliva, and secretion, can be combined with snow tracking, which provides a wealth of data to study species occurrences, individual identification and sex, genetic structure and relatedness, and hormones and diseases (Schwartz et al. 1998, Taberlet et al. 1999, Waits and Paetkau 2005, Lamb et al. 2019, Beng and Corlett 2020). Although there are disagreements about the terminology (e.g., Lefort et al. 2022), I use noninvasive genetic sampling here as it is commonly used in the literature: obtaining target DNA from naturally shed

samples, without capturing or even observing the animals (Taberlet et al. 1999). Noninvasive genetic sampling provides a unique opportunity to repeatedly sample a significant proportion of the population across large spatial extents (Lukacs and Burnham 2005, Kelly et al. 2012, Moqanaki and Samelius 2022). There is also potential to engage the public in the sampling with little survey costs (Bellemain et al. 2005, Cretois et al. 2020). DNA sampling can be, however, limited by the associated costs of optimal sample collection, preservation, storage, and genetic analysis (Taberlet et al. 1999, Waits and Paetkau 2005, Schwartz et al. 2007, Beng and Corlett 2020). The quality and quantity of target DNA in noninvasive samples, such as scats and hair, are also low, which means a significant portion of the samples may fail in providing the expected data resolution in the presence of high genotyping errors (Taberlet et al. 1999, Waits and Paetkau 2005, Schwartz et al. 2007, Lampa et al. 2013, Moqanaki and Samelius 2022).

Another DNA-based source of information in the large carnivore population monitoring in Scandinavia arises from the genetic sampling of dead carnivores. These dead recoveries are made after legal removal of individual carnivores, licensed hunting, and other mortality causes discovered by or reported to the authorities (Spong and Hellborg 2002, Flagstad et al. 2004, Hedmark et al. 2004, Tallmon et al. 2004, Liberg et al. 2005, Åkesson et al. 2016, Kopatz et al. 2021). The integration of this type of data with noninvasive genetic sampling provides additional information about the fate and, often, age class of individuals that can be used to improve ecological inferences (Sandercock 2006, Bischof et al. 2020, Dupont et al. 2021, Hostetter et al. 2021).

2.2.7 Rovbase

All large carnivore monitoring data in Scandinavia are recorded in a unified database called Rovbase (`www.robase.se` and `www.rovbase.no`). The goal is to maintain a common monitoring program with shared protocols for the transboundary wildlife populations, to improve the quality and quantity of the monitoring data (Liberg et al. 2012, Gervasi et al. 2016). This shared database also facilitates communication and collaboration between the authorities and responsible organizations in Sweden and Norway. Rovbase is curated by

Rovdata at the Norwegian Institute for Nature Research (NINA) through funding provided by the Norwegian and Swedish governments. The database is partly open to the public as soon as the data is ready. Different levels of access to the data are defined, because some level of precaution is required in providing fine-scale location data of large carnivores, as well as the personal information of data contributors.

Rovbase offers different features for different large carnivore stakeholders. For example, the database contains and shows geographical locations of observations of any damages caused by predators in Norway and Sweden. These records mostly concern the four large mammalian carnivores (wolf, bear, lynx, and wolverine; Fig. 2). Rovbase also contains records of damages caused by golden eagles *Aquila chrysaetos* and occasionally other wildlife. A considerable proportion of the data stored in Rovbase is based on information provided by local sources and individuals. Thus, the integration of local knowledge and community science into the monitoring is an important aspect of Rovbase. Besides the opportunistic data recorded by the public, Rovbase also contains official monitoring data collected in a structured manner by management authorities in each country. The main categories of official monitoring data are (i) Official investigations of livestock losses and semidomesticated reindeer predation; (ii) Carnivore signs and tracks, including active dens, examined and verified by authorities; (iii) DNA samples, such as tissue, scat, hair, and saliva from bite marks, collected by field personnel of management authorities or as part of research projects. As of January 2023, Rovbase contained approximately 188 000 observation records of large predators, 71 000 sheep predation events, 35 000 predator attacks of semidomesticated reindeer, 14 000 dead recoveries of large predators, and 151 000 processed DNA samples (`rovbase.no/om`).

Rovbase also provides an overview of government-sponsored compensations paid for livestock predation by predators. There are differences between the resolution of the data available from Norway and Sweden. For example in Sweden, currently, only records of damages to semidomesticated reindeer are registered. This is in part because compensations are paid based on carnivore existence and not based on damage or loss (Mattisson et al. 2011, Tveraa et al. 2014, Persson et al. 2015, Swenson et al. 2017).

In this PhD dissertation, I used the genetic monitoring data of the wolverine (Box 1) and brown bears (Box 2) that are maintained by Rovbase. In Articles III and IV, I used the noninvasive genetic monitoring data of the wolverine from Norway and Sweden over multiple sampling months in years 2019 (Article III) and 2014 - 2022 (Article IV). In Article II, noninvasive genetic monitoring data of female brown bears from central Sweden were used. Below, I summarize the wolverine and brown bear data in Scandinavia.

2.2.8 Wolverine genetic monitoring in Scandinavia

Since the mid-1990s, total counts of reproductive units at wolverine natal dens are used to assess the minimum size of the Scandinavian wolverine population (Landa et al. 1998b, Brøseth et al. 2010). The main assumption is that the proportion of reproducing female wolverines remains more or less unchanged in the population over years; thus, a minimum population size estimate can be obtained by averaging every three years of den count data and using extrapolation (see Landa et al. 1998b, Brøseth et al. 2010). Using this approach, however, no analytical method is used to account for those natal dens that are not detected during the sampling and the uncertainty in registering successful reproduction events (i.e., imperfect and variable detection; Gervasi et al. 2014, Kellner and Swihart 2014). Nonetheless, the authorities had to base their decisions on these proxies as representatives of the wolverine population, despite the uncertainties and potential sources of errors (Brøseth et al. 2010, Gervasi et al. 2014, 2016). By the early 2000s, noninvasive genetic monitoring of wolverines was introduced to improve the estimates of population trends, which is used together with the minimum population size based on the den counts (Flagstad et al. 2004, Hedmark et al. 2004, Brøseth et al. 2010, Gervasi et al. 2016, Bischof et al. 2020, Milleret et al. 2022b).

Norway and Sweden follow comparable sampling protocols for the genetic monitoring of the wolverine. The protocol was first developed in 2002 for the southern part of the Scandinavian Peninsula, which was then eventually employed in the northern part as well since 2008 (Gervasi et al. 2016). There has been variation in the monitoring intensity between the countries, as Sweden tends to sample the northern areas of the country less structured

compared to Norway (Gervasi et al. 2016, Bischof et al. 2020, Milleret et al. 2022b). Consequently, there is substantial spatiotemporal heterogeneity in the wolverine monitoring data, specifically during the first decade of noninvasive genetic sampling. In recent years, Norrbotten County in northern Sweden has not been searched comprehensively, which led to substantial spatiotemporal variation in the structured genetic sampling of the wolverine (Bischof et al. 2020, Milleret et al. 2022b). Article IV analyzes the wolverine monitoring data across Scandinavia and how it is affected by this issue.

Two main sources of wolverine DNA are: (i) noninvasive genetic samples, such as scat, hair, and secretion, that are naturally shed in the environment and collected without physically handling or capturing wolverines (Gervasi et al. 2016); and (ii) Muscle tissue samples obtained from legally shot wolverines or those with other causes of death that are registered in Rovbase (i.e., dead recoveries; Gervasi et al. 2016, Dupont et al. 2021). Dead recoveries often contain age information, which is obtained from a method using the upper premolar of the dead wolverines (i.e., counting cementum annuli; Landa and Skogland 1995, Gervasi et al. 2016).

Wolverine noninvasive DNA is collected annually through two main sampling processes (Milleret et al. 2022b); structured and unstructured. First, in "structured" searches conducted by authorities, where most samples are collected on snow and during visits to natal dens, search tracks are recorded by GPS as a measure of sampling effort. To minimize the inclusion of samples from cubs or juveniles that are less than one-year-old, samples are collected in different periods, when yearlings have not emerged from their dens (Gervasi et al. 2016). In the structured sampling between 2014 and 2022, the total effort was on average about 264 686 km of search tracks per year (range: 197 673 to 316 839 km). In articles III and IV of this PhD dissertation, the wolverine DNA samples and, in turn, the estimates, are restricted to the primary monitoring period between December 1 and June 30 each year. Second, DNA sampling is also conducted in an "unstructured" manner both by authorities and the public. No direct measure of effort during the unstructured sampling is available. The unstructured sampling contributes considerably to the sample quantity and spatial coverage over Scandinavia for the wolverine (Milleret et al. 2022b).

In Norway, the collection of putative wolverine noninvasive DNA samples is coordinated at the level of counties by the governmental organization Statens Naturoppsyn (SNO). Noninvasive genetic sampling is conducted by field personnel of SNO, wardens at Statskog Fjelltjenesten (statskog.no) and Fjellstyrene (fjellstyrene.no), local predator contacts, hunters, and other volunteers. In Sweden, DNA sampling is coordinated by the County Administrative Boards (Länsstyrelserna) at subnational levels and is carried out by field officers from Länsstyrelserna.

The laboratory processing of DNA samples has evolved throughout the past decades and has been done by more than one lab (Flagstad et al. 2004, 2019, Hedmark et al. 2004, Brøseth et al. 2010, Gervasi et al. 2016, Ekblom et al. 2018). The process, from DNA extraction to genotyping, is now largely automated to increase efficacy and minimize human errors. Genus-specific and microsatellite nuclear markers, as well as Y-chromosome specific markers for sex determination, are also accompanied by a Single Nucleotide Polymorphism (SNP) chip. After DNA extraction and identification of target DNA segments in each sample using polymerase chain reaction (PCR) techniques, DNA profiles are generated from as many nuclear markers as possible. Samples with identical DNA profiles are classified as one individual. Multiple reliability criteria are used to ensure high sample quality and negligible genotyping error rates (Gervasi et al. 2016, Ekblom et al. 2018, Flagstad et al. 2019).

2.2.9 Bear genetic monitoring in Scandinavia

Traditionally, the population monitoring of brown bears in Scandinavia was based on proxies derived from observation counts of females with cubs of the year (Swenson et al. 1994, 1995, Solberg et al. 2006, Ordiz et al. 2007, Kindberg et al. 2009). The main assumption is that in relatively small bear populations, demographic parameters, such as age structure and proportion of reproducing females, are reasonably stable over time and, because female bears with accompanying cubs are more easily recognizable, trends in their numbers are correlated with the total population trends (Swenson et al. 1994, 1995, Ordiz et al. 2007, Kindberg et al. 2009). The main advantage of such a proxy was the relatively low cost of collecting low-tech observation counts,

although observations of bears from a helicopter, as a superior method that increases the chance of observing the bears, is significantly more expensive (Solberg et al. 2006, Ordiz et al. 2007). The disadvantages are similar to those described for the wolverine count-based proxies; bear family groups are not always individually identifiable, total observation counts do not account for those bear families that were missed during the sampling (i.e., imperfect detection), substantial variation in effort may occur between years and across different spatial units, demographic characteristics of a hunted population can vary considerably from year to year, and, as the Scandinavian brown bear forms a transboundary population, there is a risk of violation of geographical closure assumption, i.e., double counts of family groups that live in the border areas (Solberg et al. 2006, Bischof and Swenson 2012, Bischof et al. 2016, Moqanaki et al. 2018). Subsequently, attempts were made to correct for these observation errors and convert the observation counts to more reliable abundance indices or even total population size estimates (e.g., Ordiz et al. 2007, Kindberg et al. 2009, 2011).

Because the potential errors and uncertainties surrounding the count-based indices were known, this method eventually received little trust from the management authorities. Specifically in Norway, the bear zones are limited to four small areas next to the border with Sweden and the uncorrected double-counting of bears could lead to substantial overestimation of the bear population (Bischof and Swenson 2012, Bischof et al. 2016, Swenson et al. 2017). In the mid-2000s, noninvasive genetic sampling of the Scandinavian brown bear revolutionized the field of wildlife monitoring by using noninvasive DNA samples and became the main source of information regarding the population status of bears (Tallmon et al. 2004, Bellemain et al. 2005, Solberg et al. 2006, Swenson et al. 2011, Bischof and Swenson 2012).

Norway and Sweden differ considerably in their sampling protocols for the noninvasive genetic monitoring of the brown bear population. Norway samples the same five regions every year. Norway's SNO has primary responsibility for the collection of putative bear samples (e.g., scat and hair) in Norway. To do so, often a targeted sampling design is followed to collect bear DNA during snow tracking, visits to known active dens, and during official investigations related to livestock loss and observation reports from the public. In addition,

putative bear samples are collected opportunistically by hunters during the hunting season in the fall, as well as by hikers, landowners, and other volunteers throughout the year (Bischof et al. 2020).

In Sweden, bear scats are predominantly collected by volunteers, mainly hunters, between August 21 and October 31 each year (Bellemain et al. 2005). The collection is coordinated by the Swedish Museum of Natural History at the national level, and at the county or regional level by Länsstyrelserna. The main difference from the bear sampling in Norway is that Sweden samples different regions in different years and that the country did not conduct any noninvasive genetic sampling in 2013 and 2018 (Bischof et al. 2020). Such interruptions and spatiotemporal variations in sampling effort pose considerable challenges in combined analyses of the monitoring data throughout Scandinavia.

The lab protocols have been constantly optimized throughout the past years (Tallmon et al. 2004, Bellemain et al. 2005, Swenson et al. 2011, Andreassen et al. 2012, Kopatz et al. 2021). All putative bear DNA samples are analyzed with as many nuclear markers as possible and at least a marker for sex determination. Genetically identified bear samples are then assigned to a unique bear individual based on a reliability threshold described in detail elsewhere (e.g., Andreassen et al. 2012, Kopatz et al. 2021).

In Article II, bear noninvasive DNA samples from the Swedish counties of Jämtland and Västernorrland (Fig. 1) that were genetically assigned to female bears, for which coordinates, collection date, and individual identity were available, were used in the analysis. Because of the opportunistic nature of the sampling design and engagement of volunteers, substantial spatial heterogeneity in bear detectability is expected. Article II, as a follow-up of Article I, uses bear monitoring data from central Sweden as a case study to show a rather extreme scenario of spatial variation in detectability and how analysts can account for such variations, when there is no direct measure of sampling effort.

3 Drawing population-level inferences

3.1 Hierarchical models

Because of spatial variation in detectability and distribution of individuals, a corresponding change in the resulting data is expected (e.g., number of detections). Such variations do not necessarily reflect a change in the population and, therefore, should be accounted for when analyzing the data. Otherwise, we would be unable to disentangle between sampling effort and variation in the animal distribution or density in space or time (McCarthy et al. 2013, Guillera-Arroita et al. 2014). To address these issues, methods have been developed to estimate and account for detection probability in the estimates of ecological parameters. These methods include hierarchical models, such as capture-recapture, distance sampling, and occupancy models (Kellner and Swihart 2014, Buckland et al. 2023). These models describe the data as the result of two (or more) conditionally linked processes (Royle and Dorazio 2008, Kéry and Royle 2015): (i) the ecological (or state) process: e.g., where the species or individuals from the population occur; and (ii) the observation process: how the species or individuals are detected at sampling sites where they are present. In other words, separate assumptions are used to describe variability in observed quantities from the variability in unobserved (i.e., latent) quantities of parameters of interest (Dorazio 2016). This multilevel statistical modeling structure is typically known as hierarchical models (Royle and Dorazio 2008, Kéry and Royle 2015). These models are called hierarchical as they model multiple levels of variation in the data, making them ideal tools to account for imperfect detectability and variation in large-scale and long-term wildlife monitoring data.

In a hierarchical model, different types of monitoring data can be modeled statistically by considering multiple sources of variation in the processes that resulted in the data, including variations in both sampling and the ecological metrics, such as occupancy, habitat use, species richness, or population size and vital rates (Royle and Dorazio 2008, Kéry and Royle 2015). The key to the estimation of the detection probability of wildlife is to collect data through repeated sampling (Otis et al. 1978, Krebs 1999, MacKenzie et al. 2005). For example, if observations of a species community are recorded, multiple visits

to the study sites or independent observations by multiple observers within a single visit would allow the estimation of detection probability and its potential variation in the study sites. The higher the detectability during a survey (e.g., using more efficient sampling methods) and the more the number of surveys (e.g., more visits or more independent surveyors), the higher the overall probability of detecting species or individuals. If the overall detectability is high and correlated with the spatial variation in the population size, then imperfect detection would not be a major problem in estimating population inferences (McCarthy et al. 2013, Guillera-Arroita et al. 2014, Moqanaki et al. 2021). Nonetheless, such high sampling efforts, if ever possible, come with a substantial cost and many studies attempt to quantify the trade-offs (Caughlan and Oakley 2001, Nichols and Williams 2006, Maxwell et al. 2015).

As noted above, one of the main advantages of hierarchical models as tools for analyzing wildlife monitoring data is that they allow for the incorporation of uncertainty and variation in the data at multiple levels (Royle and Dorazio 2008, Cressie et al. 2009, Kéry and Royle 2015, van de Schoot et al. 2021). When estimating population size, which is the focus of this PhD dissertation, a hierarchical model can account for the uncertainty in the detection probability of individuals from the population, as well as the spatial or temporal variation in population density across different regions. This makes the estimates more robust and reliable compared to alternative models that ignore these sources of variation (Royle et al. 2014, Schofield and Barker 2014). Hierarchical models also allow for the incorporation of multiple sources of data, such as data from different monitoring methods. Multiple types of monitoring data are actively used in the large-scale monitoring of large carnivores in Scandinavia (Solberg et al. 2006, Liberg et al. 2012, Gervasi et al. 2016, Åkesson et al. 2022). This can provide a more complete picture of population dynamics and can improve the population estimates by reducing uncertainty (Bischof et al. 2020, Dupont et al. 2021).

3.2 Spatial capture-recapture

Capture-recapture models are ubiquitous tools in the estimation of population size and dynamics in ecology (Otis et al. 1978, Krebs 1991, Lukacs and

Burnham 2005, Buckland et al. 2023). These models boil down to the estimation of detection probability from repeated encounters of, often, individually-identified animals, which provides a link between the observation of individuals and the population parameters (Nichols 1992, Royle et al. 2014). Conventional capture-recapture methods model detection probabilities as time- or occasion-specific and, therefore, detections are not linked to the detection locations and characteristics of the detection locations. Spatial capture-recapture (also referred to as spatially explicit capture-recapture) extends capture-recapture models by incorporating this readily available spatial information, and makes a powerful analytical tool for estimating wildlife population size and vital rates (Efford 2004, Borchers 2012, Royle et al. 2014, 2018). The framework is based on the assumption that individuals in a population have a probability of being detected that varies with their location in space, and that this probability can be modeled using statistical methods (Borchers and Efford 2008, Royle et al. 2018). Since the introductory paper by Efford (2004), spatial capture-recapture has been widely used in ecology to estimate the population size and dynamics of a range of species at various temporal and spatial scales, from insects to large terrestrial mammals and even marine megafauna (Tourani 2022).

As a hierarchical model, the most basic spatial capture-recapture model has two primary components (Borchers 2012, Royle et al. 2014): (i) a model of the detection process that led to the observed spatial patterns in individual detections (e.g., noninvasively collected DNA samples) – the probability of detecting an individual from the population at a given location in space; (ii) a model of the ecological process, whereby individuals are distributed in space – the mechanism by which population density is realized across the study landscape. Thus, spatial capture-recapture models use the spatially referenced individual detection histories to estimate different population parameters, while accounting for imperfect detection (Efford 2004, Borchers 2012, Royle et al. 2014).

The choice of the spatial detection probability model is one of the key steps in spatial capture-recapture, which is used to estimate the probability of detecting an individual from the target population at a given location (Borchers and Efford 2008, Royle et al. 2014). A standard spatial capture-recapture framework assumes every individual from the population of interest has a

home-range location that is fixed during the sampling season. The detectability changes with distance from individual's home-range center ("activity center"), while this location is unknown to the analyst (Efford 2004, Borchers and Efford 2008, Royle et al. 2014). In other words, the location of individuals in space is represented by their activity centers within the spatial domain of interest. Individuals may be detected at a fixed grid of detectors that represent observation and search locations or devices (e.g., physical traps, camera traps), or can be discretized to the nearest grid cell center, where individuals can be detected continuously in space (Borchers 2012, Royle et al. 2014).

Spatial capture-recapture models account for spatial variation in detection probability that is linked to how far the individual locations are in relation to detectors. To do so, the spatial information contained in the patterns of individual detections and non-detections are used through an explicit model for detection probability as a function of the distance from individuals' activity center (such as the half-normal form; Royle et al. 2014, Dey et al. 2022). Spatial capture-recapture is therefore a powerful analytical tool to estimate density and derive spatially explicit information on the ecology of wild populations (Borchers 2012, Royle et al. 2018).

A conventional spatial capture-recapture model can estimate density, the effect of spatial, temporal, and individual covariates on detection, and the effect of spatial covariates on density, with the assumption that the target population was demographically closed during sampling (i.e., no births, mortality, immigration or emigration; Royle et al. 2014). However, monitoring data across multiple years (i.e., detection of individuals in more than one year) can be used to study temporal variation in density and its determinants by reconstructing individual detection histories over the sampling years (Gardner et al. 2010, Royle et al. 2014). By extending the single-season model to an open-population model, we can also estimate interannual movement and vital rates (e.g., survival and recruitment; Ergon and Gardner 2014, Chandler et al. 2018, Efford and Schofield 2022). Subsequently, spatial capture-recapture models have been used recently to estimate large-scale and long-term population density and vital rates of different species of large carnivores in Scandinavia (Bischof et al. 2016, 2020, Milleret et al. 2022a).

3.3 A Bayesian approach

In this PhD, I built on custom spatial capture-recapture models using the open-source software R (R Core Team 2022) and software-package NIMBLE (de Valpine et al. 2017, 2022). These models use the Markov chain Monte Carlo (MCMC) method in a Bayesian framework (Bischof et al. 2021, Turek et al. 2021). Bayesian inference is different from the frequentist inference in several ways, but for this PhD, the main benefits were those outlined for Bayesian hierarchical models in ecology (Ellison 2004, Royle and Dorazio 2008, Lele and Dennis 2009, Kéry and Royle 2015, Dorazio 2016, van de Schoot et al. 2021): (i) increasing availability and flexibility of efficient open-access tools for ecologists; (ii) access to posterior distributions of all parameter estimates, which facilitates their reporting and interpretation (e.g., Bayesian credible interval); (iii) using prior knowledge along with the sample data; and (iv) providing a quantitative measure of the probability of a hypothesis being true, given the available data.

MCMC is a customizable approach that is widely used in ecological modeling (Ellison 2004, Hobbs and Hooten 2015, Kéry and Royle 2015). MCMC algorithms explore the range of plausible values that may explain the data. More technically, MCMC is a method to sample from the posterior distribution of latent (i.e., unknown or partially known) ecological parameters, given the observed quantities and assumptions about the prior distribution of parameters. One of the main limitations of MCMC in Bayesian hierarchical modeling is computation; when a model has many latent states and parameters, such as the large-scale spatial capture-recapture models used in this dissertation, MCMC may require several hours to even weeks to run (Ponisio et al. 2020, Turek et al. 2021, McCrea et al. 2023). For the modeling framework of this PhD, a number of methods have been used to dramatically improve MCMC estimation and efficiency, making large-scale estimation of density and detectability possible (Bischof et al. 2021). More details can be found in the studies cited in each chapter of this PhD.

3.4 The power of simulations

We almost never know the true values of ecological parameters of interest, let alone validate different analytical methods and their estimates of the truth.

Simulation studies have greatly assisted scientists in developing analytical tools, as well as evaluating the uncertainty and potential biases of ecological models. Simulations are transforming the way monitoring data are collected and used to infer and understand complex ecological processes (Kéry and Royle 2015, Gomes et al. 2019). Regardless of the analytical approach, frequentist, Bayesian, and machine learning modelers use and benefit from simulation studies. The main advantage of simulations is that the "truth" is known by the analyst. Thus, it is possible to test and validate the performance of ecological models under different scenarios of data realization and violation of model assumptions. Simulation studies allow flexible parameterization of processes of interest, where assumptions are known to be met (or violated) and, therefore, realistic modeling at different stages of a study can be performed (Kéry and Royle 2015, Murr et al. 2022, DiRenzo et al. 2023). In addition, simulations can advance theoretical understanding of problems raised during wildlife monitoring and quantify the performance of different data collection and analytical methods in real-world conditions, as well as probabilistically inform potential future outcomes of changes in the environment or management actions (Hoban 2014, DiRenzo et al. 2023): how many samples are required to answer this question? which model is superior to use to analyze the resulting data? How has the model performed in the analysis?

Simulation studies are not intended to replace, but rather to assist empirical studies. Simulations are indeed limited by their realism, flexibility, and accessibility. In recent years, advances in computational science and engineering have resulted in increasing processor power, access to cluster computing facilities, and increasingly open-access software tools (Hoban 2014, Gomes et al. 2019, DiRenzo et al. 2023, McCrea et al. 2023). All these recent advances strongly favored large simulation studies. Articles I and II of this PhD dissertation involve extensive simulations to create and test many scenarios of spatially variable detectability in wildlife sampling using spatial capture-recapture.

4 This PhD dissertation

This PhD dissertation aims at answering the question; how do spatial variations in detectability and density influence population estimates of large

carnivores in Scandinavia? Articles I and II provide novel insights about spatially variable and autocorrelated detectability in monitoring data. Articles III and IV account for such variable detectability during large-scale noninvasive monitoring of the wolverine in Scandinavia, while focusing on variation in the spatial distribution of individuals (i.e., density). Some aspects of this PhD are specific to the monitoring of large carnivores in Scandinavia, whereas others involve technical issues that are commonly encountered in large-scale wildlife monitoring studies. Here, I argue that ignoring these sources of variation in the monitoring data can lead to substantial biases in the estimates of population size and, in turn, erroneous conclusions about the status of target populations. I highlight the advantages of using hierarchical models for accounting for variation in detectability and quantifying variation in density, when analyzing large-scale wildlife monitoring data, especially using spatial capture-recapture models of population density.

4.1 Coping with imperfect and variable detection

Sampling wildlife populations for an estimate of population size typically involves recording the presence of some individuals from the target population. We then make ecological inferences about the status of the population (or other metrics) based on this sample from the population (Krebs 1999, Thompson 2013). This is contrary to complete counts (i.e., censuses); many factors, from species elusiveness to observer errors and confounding environmental conditions, prevent almost all wildlife censuses in real life. In other words, the probability to detect and record all the required information from every single individual in the population is less than one. Thus, there is virtually no "perfect" sampling and there is always a chance that we miss some information that is crucial for making inferences about the target population (Williams et al. 2002, Kellner and Swihart 2014, Gimenez et al. 2018). We, therefore, define detectability on a probabilistic scale – the probability to detect a species or an individual during a survey, given that it occupies the sampling site (Gu and Swihart 2004, McCarthy et al. 2013). Imagine we have searched an area for a species, but we did not find it (Fig. 3). This means either the species did not occur therein (i.e., true absence) or we did not find it (i.e., missed detection). Here I do not discuss false-positive detections (i.e., species or individual misidentifications), which

are also important to be accounted for when there is such a risk (Royle and Link 2006, McClintock et al. 2010, Augustine et al. 2020). The fact that there are always individuals or events that remain undetected during the sampling means that conclusions drawn from the data may provide an incomplete picture of the true state of the population, unless appropriate methods are used to disentangle the state variable from imperfect detection (Royle and Dorazio 2008, Guillera-Arroita et al. 2014, Kéry and Royle 2015).

Ignoring detectability might not be a major problem in some situations, if the biasing effect is consistent across space and time (Guillera-Arroita et al. 2014). However, in many situations detectability is not only imperfect, but also variable. This variability refers to the fact that the probability of detecting an individual or target species can vary depending on various factors, such as the species' ecology and behavior, the monitoring method, different environmental features in the study area, or phenotypic differences (e.g., age, sex, body size) among the individuals. Detection probability is imperfect and variable, due to several factors that are collectively considered as sampling error, which is a common challenge in population monitoring and estimation (Guillera-Arroita et al. 2014, Kellner and Swihart 2014; Fig. 3).

Imperfect and variable detection can lead to biased estimates of population size, as well as incorrect conclusions about population trends and dynamics. For example, if detectability is lower for certain groups (e.g., females; Fig. 3), population estimates based on the heterogeneous monitoring data will be unrepresentative of this variation, leading to an underestimation of the actual population size (Gimenez et al. 2018). Likewise, if detectability varies across different regions or habitats (Fig. 4), but we mistakenly assume spatially homogeneous detectability, population estimates will be biased (Link 2003, MacKenzie et al. 2005, Royle 2006, Efford et al. 2013). Spatially heterogeneous detectability is the focus of articles I and II of this PhD dissertation that I discuss in more detail below. Nevertheless, imperfect and variable detection is almost impossible to avoid during the sampling of wildlife populations, because, by definition, a fraction of the total population is sampled at one point in time (Williams et al. 2002, Royle and Dorazio 2008, Kellner and Swihart 2014). When sampling is conducted at large spatial extents over thousands of km^2, such as the noninvasive genetic monitoring of large carnivores in Scandinavia,

imperfect and variable detection is expected to be a major issue to deal with when collecting and analyzing wildlife monitoring data.

(a) (b)

(c) (d)

Figure 3: Examples of different sources of variation in detectability during wildlife monitoring: **(a,b) Spatial heterogeneity:** (a) During a sign survey in an alpine habitat, the more rugged the area and the denser the vegetation, the more likely that some signs of animal presence are missed. It is also likely that investigators tend to search lower elevations more intensively than higher elevation areas because of the accessibility. (b) In drive counts, animals closer to the road, like this Cape buffalo *Syncerus caffer*, are more likely to be detected than those farther away. **(c) Temporal heterogeneity:** During the breeding season, rock wrens *Salpinctes obsoletus* (red circle) move to dry rocky locations, where their calling and displays peak, which altogether makes the bird easier to spot. **(d) Individual heterogeneity:** Coalitions of male Asiatic cheetahs *Acinonyx jubatus venaticus* had higher detectability than females during a camera-trap survey in central Iran, because adult males were moving together and were frequently visiting scent-marking locations, where several of the camera traps were installed (Photos a-c: E. Moqanaki, d: ICS/DoE/CACP).

4.2 Articles I and II: Unknown spatial heterogeneity in detectability

The first two articles of this dissertation study the consequences of unknown and unmodeled spatial heterogeneity in detectability for population size estimation using spatial capture-recapture analysis (Article I) and propose model-based solutions to accommodate the heterogeneity to improve the estimates (Article II). The research question was guided by the analysis of large carnivore monitoring from Scandinavia, where different sampling designs and varying efforts were incorporated across two countries in which for a considerable portion of the data, no direct measure of sampling effort was available (Bischof et al. 2020).

Detection probability varies across space and time and among individuals. Common examples in wildlife monitoring are differences in the local environment that cause variable detectability, varying sampling effort and designs across a landscape, and variation in exposure of individuals to detection (Moqanaki et al. 2021, Stevenson et al. 2022, Howe et al. 2022; Fig. 4). Besides the amount of variation in detection probability that may have biasing effects on population estimates, the spatial structure of the variation in detection probability may also have a substantial impact on the inferences. Spatial autocorrelation (Dormann et al. 2007, Guélat and Kéry 2018, Gaspard et al. 2019) in detection indicates a situation where baseline detection probability at

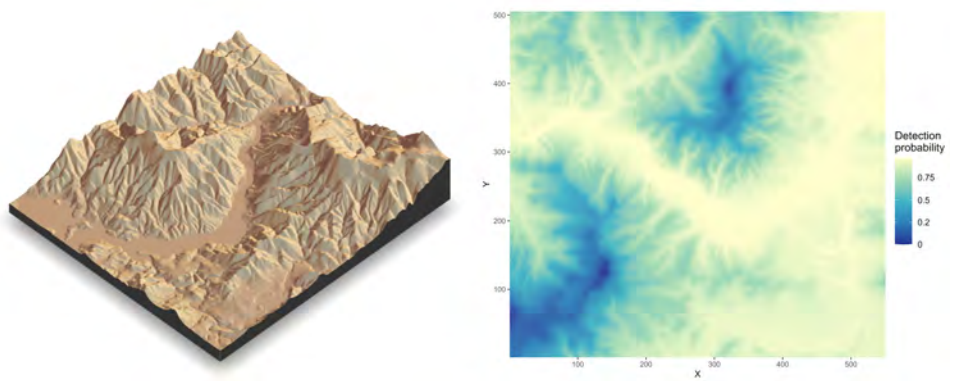

Figure 4: A schematic representation of a scenario of spatially heterogeneous detectability, where detection probability is decreasing with increasing ruggedness.

a detector is correlated with neighboring detectors. Consequently, the residuals of a spatial capture-recapture model for predicting the values of detectability will be spatially structured. There are many realistic scenarios that may induce spatial autocorrelation among detections, such as selection of certain habitats by the species or habitat connectivity that would make some individuals more exposed to detection than the others (Royle et al. 2013, Morin et al. 2017, Stevenson et al. 2022; Fig. 4). These would violate the assumption of independence between detectors, conditional on the activity center location, in spatial capture-recapture analysis (Efford et al. 2009).

Model-based approaches to accommodate the effect of spatial heterogeneity in detection probability are implemented in spatial capture-recapture when the source of heterogeneity is known (Efford et al. 2013, Royle et al. 2013, Sutherland et al. 2015). One of the advantages of spatial capture-recapture models over the non-spatial capture-recapture is indeed the ability to address the effects of known spatial variation in the effort, thus providing a more realistic model of the observation process (Borchers and Efford 2008, Royle et al. 2014, 2018). Further, previous studies have found that random spatial variation in detection probability does not have to be a major cause for concern for inferences drawn from spatial capture-recapture studies, at least in terms of biased parameter estimates (e.g., Bischof et al. 2017, Clark 2019, Paterson et al. 2019), because, contrary to the conventional capture-recapture, individuals can be detected by multiple detectors (Borchers 2012, Royle et al. 2014).

Many unknown or unrecorded factors may cause additional heterogeneity in detection probability. For example, it is common that during sampling, surveyors do not search randomly, because of their prior knowledge or accessibility (Gervasi et al. 2014), or where a camera trapping or DNA search effort was conducted more intensively in a specific habitat type, inducing some forms of undocumented preferential sampling (Conn et al. 2017). Likewise, equipment failure and human errors can cause detectors to perform in clusters of varying effectiveness unbeknownst to the analyst. As a result, there will be groups of detectors whose detectability is spatially correlated, and the intensity of effort also varies across the study area (Fig. 4). Thus, one can expect that combinations of different search intensities and spatial autocorrelation may result in different biasing effects in spatial capture-recapture analysis.

Articles I and II use extensive simulations to quantify the consequences of ignoring variation in detectability in a wide range of situations of spatially variable and autocorrelated detectability that can occur during wildlife monitoring (Figs. 3 and 4). The general approach is: (i) create different scenarios of spatially heterogeneous detectability based on real-life examples from the literature, especially the noninvasive genetic monitoring of large carnivores in Scandinavia; (ii) generate spatial capture-recapture data from a population with predefined characteristics, so that the data are deliberately affected by different levels of spatially heterogeneity detectability; (iii) fit a conventional, single-season, spatial capture-recapture model that does not account for the spatially heterogeneous detectability (i.e., a model with a misspecified observation submodel), to mimic situations where the variability in detection remains unknown and, in turn, unmodeled; (iv) evaluate the performance of the model. Knowing the true (simulated) values, we can quantify the model performance in different scenarios and evaluate bias – the systematic difference between the true parameters and their estimates; precision – how close the estimates are to the true simulated value as a measure of observation error; and coverage – the proportion of the times that the estimated credible interval covered the true value (Walther and Moore 2005, DiRenzo et al. 2023).

Article I describes two broad cases of spatially varying detectability (and, thus, baseline detection probability or magnitude of the detection function), and includes simulation scenarios with different levels of spatial autocorrelation among detectors – i.e., when detection locations close to each other exhibit similar sampling effort than those further apart: (i) continuous spatial variation in detectability, such as when elevation gradient (Fig. 4), distance from the road, or the number of camera-trap days affect the detection probability; and (ii) discrete spatial variation in detectability, because of two regions of high and low detectability across the study area, the underlying habitat (e.g., forest vs. agricultural fields), different sampling designs, or personnel with varying skills. In these simulations, there was no variation in population density and individuals had equal home range sizes. Such simplistic assumptions help to isolate and monitor the components of interest in simulations, even though they are not realistic in the wild. Fitting the conventional spatial capture-recapture model with a misspecified observation submodel to the

simulated data sets revealed that spatial autocorrelation in detectability can be a greater source of concern for population size estimation than spatial variation alone. This is good news that conventional spatial capture-recapture with a misspecified observation submodel that does not account for spatial variation in detectability can perform reasonably well in situations of low to intermediate spatial heterogeneity in detectability. However, the estimates of population size were negatively biased, precision decreased, and the coverage probability declined to near zero when the level of spatial autocorrelation was high, particularly when there were considerable patches with very little sampling effort. These scenarios are specifically expected when citizen-science (i.e., participatory) data or some form of opportunistic data collection in certain regions across the study area are integrated with the structured sampling, but these clusters remain unknown to analysts, because there is no unambiguous measure of sampling effort (Bird et al. 2014, Altwegg and Nichols 2019, Sicacha-Parada et al. 2021).

Solutions are discussed in Article I to avoid such scenarios when designing and collecting spatial capture-recapture data, from aiming for more structured and balanced sampling designs to encouraging the volunteers to record their effort or at least more evenly search for animal detections. A partial solution to account for unknown varying effort is to proxy the knowledge of possible sources of non-randomization in sampling (e.g., accessibility) by using a spatial covariate as a fixed effect on detection probability (Bischof et al. 2020). However, there are many situations in which some sources of spatial heterogeneity remain unmodeled. Thus, the development of methods to test and correct for unknown spatial heterogeneity in detection probability is required in spatial capture-recapture studies to deal with situations where the data, in part or as a whole, inherently lacks information on the observation process. This study paved the road for Article II.

Article II builds on the simulation set-up from Article I, to recreate the problematic scenarios of spatially heterogeneous detectability to test and evaluate novel modeling approaches to account for the variability. Specifically, three new extensions of spatial capture-recapture models are introduced that use the information from the detection data to describe the underlying spatial structure in detectability and improve the estimates of population size using random

effects. Article II shows that all the proposed models perform reasonably well in different scenarios of spatially autocorrelated detectability that were considered, but the models that use the spatial information in the detections to explicitly account for spatial autocorrelation between detectors outperform the rest of the models. Furthermore, noninvasive genetic monitoring data of female brown bears from two counties in central Sweden are used to demonstrate the real-life applications of these models, where such substantial spatial variation in the effort is suspected but there is no direct measure to account for it. In addition, Article II shows how mapping the detection probability surface and model evaluation metrics can help the investigator to locate potential areas of varying sampling effort. The trade-offs in using such new extensions of spatial capture-recapture are discussed in Article II. A limitation is that currently, goodness-of-fit tests are lacking for spatial capture-recapture to inform the analyst about the fit, because by definition the sources of heterogeneity in detectability are unknown or only partially known, so the model assumptions (e.g., the conditional independence assumption; Efford et al. 2009) may be violated without obvious hints in the results.

4.3 Articles III and IV: Explaining variation in density

Many fundamental questions in ecology and wildlife management are about population size and factors leading to variation in population size (abundance and density) and structure (e.g., sex-age ratio): how many of a given species exist in a protected area and where are they distributed? Why are there more breeding females of a species in one locality compared to another locality? What has caused a decline in the numbers of conservation-dependent species? All these questions have a strong spatial component; the distribution of individuals in a specific geographical area (Fig. 5). Even if there are traditionally well-established analytical frameworks to estimate animal abundance (Otis et al. 1978, Krebs 1999, Buckland et al. 2000, 2023, Pollock et al. 2002, Lukacs and Burnham 2005), it is challenging to convert these numbers to density, because of spatial variation in distribution of individuals (Efford 2004, Borchers 2012, Royle et al. 2014). Many factors lead some individuals to aggregate in, avoid, or specifically select for specific locations, causing variation in density. This spatial variation in animal abundance, combined with the logistical challenges of

sampling large spatial extents, has most likely plagued most wildlife monitoring data (Yoccoz et al. 2001, Pollock et al. 2002, Williams et al. 2002). For example, because resources are distributed unevenly in a landscape, more individuals are expected to gather near the habitats with more water, food, and cover (Fig. 5). Therefore, sampling near these localities would likely result in more data compared to other areas. Likewise, individuals from the population

(a) (b) (c) (d)

Figure 5: An even distribution of individuals from a population in space or time is unlikely (a). Spatial heterogeneity in the environment induces substantial variation in population density. (b) California mussel *Mytilus californianus* beds can be found on open rocky coasts with high salinity and low sediment conditions. However, the mortality rate in such intertidal open coastal environments is high. (c) Diving birds, such as these gregarious cormorants of the family Phalacrocoracidae, aggregate on bare rocks offshore for resting. (d) Water sources in arid environments are rare and proximity to them is an important determinant of variation in wildlife density, particularly during the hot season for the Persian gazelles *Gazella subgutturosa* (Photos a-c: E. Moqanaki, d: ICS/DoE/CACP).

(intraspecific) and also between species (interspecific) constantly interact and compete with each other over resources, which has consequences on how species and individuals are distributed in space. Humans are also one of the main drivers of variation in animal density, by directly or indirectly competing with wildlife by hunting or killing them and changing the distribution and availability of resources in a given landscape (Nyhus 2016). A representative sample of the population should account for such spatial variations. However, in addition to the design-based solutions, such as conducting spatially balanced sampling, model-based approaches that explicitly account for the heterogeneous spatial distribution of individuals from the population have many advantages (Royle et al. 2018, Buckland et al. 2023).

Spatial distribution can be modeled as a function of spatial covariates; for example, the availability or percentage of a certain habitat type or human disturbances. By modeling the relationship between species abundance and spatial covariates using appropriate models, one can estimate variation in density and density-dependent processes (e.g., dispersal, growth rate). Articles III and IV of this PhD dissertation study variation in the Scandinavian wolverine density at the landscape level, where the population has successfully recovered in recent decades.

Wildlife populations vary in size and composition across their natural habitats. Variations in population size and dynamics are both natural and a consequence of human pressure. For example, part of the habitat that is more productive may support a larger proportion of the population, or individuals from the target population may actively select some habitat types that are disproportionately distributed across the landscape. In addition, human disturbances may cause local extinctions or force the wildlife population to avoid certain areas for some periods of time.

Although estimates of abundance, density, and trends of wildlife populations are highly sought after by scientists and wildlife managers for the reasons discussed above, many studies fail to provide such metrics at ecologically meaningful extents. First, long-term monitoring data of wildlife over the entire population is lacking for many species (Krebs 1991, Hayes and Schradin 2017). Especially for large carnivores that use very large areas, persist in low

density, and move over long distances, effectively sampling a large enough proportion of the population over several generations is extremely challenging (Kelly et al. 2012, Smith et al. 2017, Morin et al. 2022). Second, even if such comprehensive monitoring data is available, appropriate analytical tools are required to address different sources of variability in the data to provide reliable and robust estimates of population parameters. Despite the recent advances, these models are usually very complex to build, and fitting them to the empirical data is challenging (Royle and Dorazio 2008, Newman et al. 2014, Royle et al. 2014, Kéry and Royle 2015). Particularly for Bayesian inferences, computation limits wider applications (Hobbs and Hooten 2015, Ponisio et al. 2020, Turek et al. 2021). Articles III and IV of this PhD dissertation overcame these challenges by using (i) a comprehensive monitoring data set of genetically identified wolverine individuals across the entire Scandinavian population; and (ii) efficient Bayesian spatial capture-recapture models that are able to provide spatially explicit estimates of population size at this substantially large spatial extent with reasonable run times, while accounting for variable and imperfect detection (Bischof et al. 2020, Turek et al. 2021).

Besides the technical novelty and contribution to the analytical framework, the story of wolverines in Scandinavia, from near extinction by the 1970s to recovery (Flagstad et al. 2004, Chapron et al. 2014), provides an exciting opportunity to explore some fundamental ecological questions about species-habitat relationships in heterogeneous landscapes. How animals use space at different scales is an important topic in many questions raised in large carnivore monitoring and management. Spatial capture-recapture models in Articles III and IV quantify animal space use at the home-range level, also known as the second-order habitat selection (Johnson 1980, Royle et al. 2014), with the added benefit of modeling detectability to estimate population density (Royle et al. 2013). Both these articles include several explicit landscape covariates that are believed to have influenced how individual wolverines distribute their home ranges, thus explaining variation in population density. Articles III and IV pay special attention to mapping density surfaces, as abundance and density values alone have limited use for addressing increasing challenges on multi-use landscapes where humans and wildlife have to share resources. By estimating locations of activity centers for both detected and undetected individuals from

the population, abundance and density can be extracted at any spatial unit of interest using spatial capture-recapture, which is not easily possible for many other statistical models of population size (Royle et al. 2018, Buckland et al. 2023). Both these studies account for possible differences in the responses of female and male wolverines to the spatial determinants of density. Wolverines, like many other mammals, exhibit sexual dimorphism – i.e., adult males and females differ in size and some ecological and behavioral traits (Shine 1989, Isaac 2005). Because there are sex differences in energy requirements and variability in fitness and survival, both these studies hypothesize that there are differences between the density and effect of spatial determinants of density at the population level between female and male wolverines. Articles III and IV are among the first attempts to quantify wolverine density variation across the species' entire range in the Scandinavian Peninsula, and both improve our understanding of wolverine population size and dynamics that are otherwise often studied at comparatively much smaller extents (Fisher et al. 2022).

Article III is focused on the role of "relict range" in determining the current density of the wolverine in Scandinavia. As discussed earlier (Box 1), the wolverine population has recovered from centuries of direct persecution by humans (Landa et al. 2000, Flagstad et al. 2004, Chapron et al. 2014). At some point by the 1970s, the population size and distribution range was limited to a narrow alpine area along the Norwegian-Swedish border (i.e., the relict range; Fig. 2). Previous studies have shown the importance of this border area as a source landscape for the wolverine population (e.g., Gervasi et al. 2019). Article III hypothesizes that distance from this alpine transboundary area is still an important determinant of wolverine density, but this effect interacts and varies at different coarse management zones considered for the wolverine in Scandinavia. Article III finds strong evidence to support this hypothesis and shows that the highest wolverine densities for both sexes are expected closer to the relict range. Further, higher wolverine densities near the relict range are more pronounced in the northern areas, where not only the environmental conditions for the wolverine are probably more favorable, but also more wolverine reproductions are tolerated based on the current management goals. In contrast, in southern areas, lower wolverine densities were estimated, where management pressure is higher and farther distance from

the relict range has to be traveled to recolonize the historical range. Article III suggests sex-specific differences in the density distribution of the wolverine, and that the current Scandinavian population is likely to be highly skewed towards females.

Article IV builds on the findings from Article III, and advances our understanding of wolverine density distribution in Scandinavia by specifically looking into the temporal trends in the effect of spatial determinants of density. To approach the research question in this article, cutting-edge open-population spatial capture-recapture models are used. Article IV has two main ecological hypothesizes: as the wolverine has successfully recolonized many areas of its historical range in Scandinavia, (i) the negative effect of distance from the relict range on wolverine density that was observed in Article III has not been static; as wolverines started their recovery, the expansion frontline was the relict range and thus the effect of this covariate has been very strong. As the wolverine successfully established itself farther away from the relict range, this effect has become weaker over the years. (ii) Because the wolverine population has been limited to the Norwegian-Swedish border for a long time, the species has been mainly associated with lower productive alpine areas with low human disturbances. This has possibly created an incomplete picture of wolverine ecology, that the species does not select the boreal forest (but see Glass et al. 2022). However, after about three decades of expansion, there are now wolverines in both alpine areas and boreal forests. Thus, it is likely that the effect of boreal forest has been less significant in the early years of recovery, but it is now becoming more strongly positive. Although Article IV is limited by the availability of monitoring data from the last decade, two decades after the start of the recovery in the 1970s, this study shows temporal changes in the effects of the spatial determinants of density for the wolverine. These results are particularly interesting, given the relatively short period to study the density dynamics of a long-living carnivore species. Article IV discusses the implications of the findings for such a recovering population on a landscape that no longer holds any intact wilderness areas to separate large carnivores from humans. Further, potential confounding factors and future directions to incorporate these findings into wolverine monitoring and management in Scandinavia are discussed.

5 Concluding remarks

This PhD dissertation focuses on cases of spatial variation in detectability and density when analyzing large-scale wildlife monitoring data and develops approaches in spatial capture-recapture to address them. The spatial capture-recapture framework is increasingly popular for analyzing wildlife monitoring data to estimate population parameters and detectability (Royle et al. 2018, Tourani 2022). The benefits of using spatial capture-recapture models for explicitly estimating abundance, density, and population trends of large carnivores in Scandinavia have already been demonstrated (Bischof et al. 2016, 2017, 2020). This PhD dissertation contributes to the ongoing efforts to provide reliable population estimates for applied questions faced by large carnivore monitoring and management in Scandinavia. Nonetheless, by demonstrating usefulness and applicability, these studies can also motivate similar efforts at the landscape level for other rare, elusive, threatened, or socially and economically important species, where conservation scientists and managers require reliable information to guide their actions.

References

Abramov, A. (2016). *Gulo gulo*. The IUCN Red List of Threatened Species, 2016: e. t9561a45198537.

Åkesson, M., Liberg, O., Sand, H., Wabakken, P., Bensch, S., and Flagstad, Ø. (2016). Genetic rescue in a severely inbred wolf population. *Molecular Ecology*, 25(19):4745–4756.

Åkesson, M., Svensson, L., Flagstad, Ø., Wabakken, P., and Frank, J. (2022). Wolf monitoring in Scandinavia: evaluating counts of packs and reproduction events. *The Journal of Wildlife Management*, page e22206.

Altwegg, R. and Nichols, J. D. (2019). Occupancy models for citizen-science data. *Methods in Ecology and Evolution*, 10(1):8–21.

Andreassen, R., Schregel, J., Kopatz, A., Tobiassen, C., Knappskog, P., Hagen, S., Kleven, O., Schneider, M., Kojola, I., Aspi, J., et al. (2012). A forensic DNA profiling system for Northern European brown bears (*Ursus arctos*). *Forensic Science International: Genetics*, 6(6):798–809.

Andrén, H. and Liberg, O. (2015). Large impact of Eurasian lynx predation on roe deer population dynamics. *PLoS ONE*, 10(3):e0120570.

Andrén, H., Linnell, J. D., Liberg, O., Ahlqvist, P., Andersen, R., Danell, A., Franzén, R., Kvam, T., Odden, J., and Segerström, P. (2002). Estimating total lynx *Lynx lynx* population size from censuses of family groups. *Wildlife Biology*, 8(4):299–306.

Aronsson, M. and Persson, J. (2017). Mismatch between goals and the scale of actions constrains adaptive carnivore management: the case of the wolverine in Sweden. *Animal Conservation*, 20(3):261–269.

Augustine, B. C., Royle, J. A., Linden, D. W., and Fuller, A. K. (2020). Spatial proximity moderates genotype uncertainty in genetic tagging studies. *Proceedings of the National Academy of Sciences*, 117(30):17903–17912.

Axelsson-Linkowski, W., Fjellström, A.-M., Sandström, C., Westin, A., Östlund, L., and Moen, J. (2020). Shifting strategies between generations in Sami

reindeer husbandry: The challenges of maintaining traditions while adapting to a changing context. *Human Ecology*, 48(4):481–490.

Bautista, C., Revilla, E., Naves, J., Albrecht, J., Fernández, N., Olszańska, A., Adamec, M., Berezowska-Cnota, T., Ciucci, P., Groff, C., et al. (2019). Large carnivore damage in Europe: Analysis of compensation and prevention programs. *Biological Conservation*, 235:308–316.

Bellemain, E., Swenson, J. E., Tallmon, D., Brunberg, S., and Taberlet, P. (2005). Estimating population size of elusive animals with DNA from hunter-collected feces: four methods for brown bears. *Conservation Biology*, 19(1):150–161.

Beng, K. C. and Corlett, R. T. (2020). Applications of environmental DNA (eDNA) in ecology and conservation: opportunities, challenges and prospects. *Biodiversity and Conservation*, 29:2089–2121.

Betts, M. G., Hadley, A. S., Frey, D. W., Frey, S. J., Gannon, D., Harris, S. H., Kim, H., Kormann, U. G., Leimberger, K., Moriarty, K., et al. (2021). When are hypotheses useful in ecology and evolution? *Ecology and Evolution*, 11(11):5762–5776.

Bird, T. J., Bates, A. E., Lefcheck, J. S., Hill, N. A., Thomson, R. J., Edgar, G. J., Stuart-Smith, R. D., Wotherspoon, S., Krkosek, M., Stuart-Smith, J. F., et al. (2014). Statistical solutions for error and bias in global citizen science datasets. *Biological Conservation*, 173:144–154.

Bischof, R., Brøseth, H., and Gimenez, O. (2016). Wildlife in a politically divided world: insularism inflates estimates of brown bear abundance. *Conservation Letters*, 9(2):122–130.

Bischof, R., Milleret, C., Dupont, P., Chipperfield, J., Tourani, M., Ordiz, A., de Valpine, P., Turek, D., Royle, J. A., Gimenez, O., et al. (2020). Estimating and forecasting spatial population dynamics of apex predators using transnational genetic monitoring. *Proceedings of the National Academy of Sciences*, 117(48):30531–30538.

Bischof, R., Steyaert, S. M., and Kindberg, J. (2017). Caught in the mesh: Roads and their network-scale impediment to animal movement. *Ecography*, 40(12):1369–1380.

Bischof, R. and Swenson, J. E. (2012). Linking noninvasive genetic sampling and traditional monitoring to aid management of a trans-border carnivore population. *Ecological Applications*, 22(1):361–373.

Bischof, R., Turek, D., Milleret, C., Ergon, T., Dupont, P., Dey, S., Zhang, W., and de Valpine, P. (2021). *nimbleSCR: Spatial Capture-Recapture (SCR) Methods Using 'nimble'*.

Bjärvall, A., Sandegren, F., and Wabakken, P. (1990). Large home ranges and possible early sexual maturity in Scandinavian bears. *Bears: Their Biology and Management*, pages 237–241.

Boitani, L. and Linnell, J. D. (2015). Bringing large mammals back: large carnivores in Europe. In Pereira, H. M. and Navarro, L. M., editors, *Rewilding European Landscapes*, pages 67–84. Springer.

Borchers, D. (2012). A non-technical overview of spatially explicit capture–recapture models. *Journal of Ornithology*, 152(2):435–444.

Borchers, D. L. and Efford, M. (2008). Spatially explicit maximum likelihood methods for capture–recapture studies. *Biometrics*, 64(2):377–385.

Brøseth, H., Flagstad, Ø., Wärdig, C., Johansson, M., and Ellegren, H. (2010). Large-scale noninvasive genetic monitoring of wolverines using scats reveals density dependent adult survival. *Biological Conservation*, 143(1):113–120.

Brown, R., Krausman, P., and Cain, J. (2013). The history of wildlife conservation in North America. In Krausman, P. R. and Cain, J. W., editors, *Wildlife management and conservation: contemporary principles and practices*, pages 6–23. Johns Hopkins University Press.

Buckland, S., Borchers, D., Marques, T., and Fewster, R. (2023). Wildlife population assessment: Changing priorities driven by technological advances. *Journal of Statistical Theory and Practice*, 17(20).

Buckland, S., Goudie, I., and Borchers, D. (2000). Wildlife population assessment: past developments and future directions. *Biometrics*, 56(1):1–12.

Burton, A. C., Neilson, E., Moreira, D., Ladle, A., Steenweg, R., Fisher, J. T., Bayne, E., and Boutin, S. (2015). Wildlife camera trapping: a review and recommendations for linking surveys to ecological processes. *Journal of Applied Ecology*, 52(3):675–685.

Cagnacci, F., Boitani, L., Powell, R. A., and Boyce, M. S. (2010). Animal ecology meets GPS-based radiotelemetry: a perfect storm of opportunities and challenges. *Philosophical Transactions of the Royal Society B: Biological Sciences*, 365(1550):2157–2162.

Can, Ö. E., D'Cruze, N., Garshelis, D. L., Beecham, J., and Macdonald, D. W. (2014). Resolving human-bear conflict: A global survey of countries, experts, and key factors. *Conservation Letters*, 7(6):501–513.

Caughlan, L. and Oakley, K. L. (2001). Cost considerations for long-term ecological monitoring. *Ecological Indicators*, 1(2):123–134.

Chadès, I., McDonald-Madden, E., McCarthy, M. A., Wintle, B., Linkie, M., and Possingham, H. P. (2008). When to stop managing or surveying cryptic threatened species. *Proceedings of the National Academy of Sciences*, 105(37):13936–13940.

Chandler, R. B., Hepinstall-Cymerman, J., Merker, S., Abernathy-Conners, H., and Cooper, R. J. (2018). Characterizing spatio-temporal variation in survival and recruitment with integrated population models. *The Auk: Ornithological Advances*, 135(3):409–426.

Chapron, G., Kaczensky, P., Linnell, J. D., von Arx, M., Huber, D., Andrén, H., López-Bao, J. V., Adamec, M., Álvares, F., Anders, O., et al. (2014). Recovery of large carnivores in Europe's modern human-dominated landscapes. *Science*, 346(6216):1517–1519.

Clark, J. D. (2019). Comparing clustered sampling designs for spatially explicit estimation of population density. *Population Ecology*, 61(1):93–101.

Cochran, W. W. and Lord, R. D. (1963). A radio-tracking system for wild animals. *The Journal of Wildlife Management*, pages 9–24.

Conn, P. B., Thorson, J. T., and Johnson, D. S. (2017). Confronting preferential sampling when analysing population distributions: diagnosis and model-based triage. *Methods in Ecology and Evolution*, 8(11):1535–1546.

Cressie, N., Calder, C. A., Clark, J. S., Hoef, J. M. V., and Wikle, C. K. (2009). Accounting for uncertainty in ecological analysis: the strengths and limitations of hierarchical statistical modeling. *Ecological Applications*, 19(3):553–570.

Cretois, B., Linnell, J. D., Grainger, M., Nilsen, E. B., and Rød, J. K. (2020). Hunters as citizen scientists: Contributions to biodiversity monitoring in Europe. *Global Ecology and Conservation*, 23:e01077.

Cubaynes, S., Pradel, R., Choquet, R., Duchamp, C., Gaillard, J.-M., Lebreton, J.-D., Marboutin, E., Miquel, C., Reboulet, A.-M., Poillot, C., et al. (2010). Importance of accounting for detection heterogeneity when estimating abundance: the case of French wolves. *Conservation Biology*, 24(2):621–626.

de Valpine, P., Paciorek, C., Turek, D., Michaud, N., Anderson-Bergman, C., Obermeyer, F., Wehrhahn Cortes, C., Rodrìguez, A., Temple Lang, D., and S., P. (2022). *NIMBLE User Manual*. R package manual version 0.12.2.

de Valpine, P., Turek, D., Paciorek, C. J., Anderson-Bergman, C., Lang, D. T., and Bodik, R. (2017). Programming with models: writing statistical algorithms for general model structures with NIMBLE. *Journal of Computational and Graphical Statistics*, 26(2):403–413.

Dey, S., Bischof, R., Dupont, P. P., and Milleret, C. (2022). Does the punishment fit the crime? consequences and diagnosis of misspecified detection functions in Bayesian spatial capture–recapture modeling. *Ecology and Evolution*, 12(2):e8600.

DiRenzo, G. V., Hanks, E., and Miller, D. A. (2023). A practical guide to understanding and validating complex models using data simulations. *Methods in Ecology and Evolution*, 14(1):203–217.

Dorazio, R. M. (2016). Bayesian data analysis in population ecology: motivations, methods, and benefits. *Population Ecology*, 58(1):31–44.

Dormann, C., McPherson, J., Araújo, M., Bivand, R., Bolliger, J., Carl, G., Davies, R., Hirzel, A., Jetz, W., Daniel Kissling, W., et al. (2007). Methods to account for spatial autocorrelation in the analysis of species distributional data: a review. *Ecography*, 30(5):609–628.

Dressel, S., Sandström, C., and Ericsson, G. (2014). A meta-analysis of studies on attitudes toward bears and wolves across Europe 1976–2012. *Conservation Biology*, 29(2):565–574.

Dupont, P., Milleret, C., Tourani, M., Brøseth, H., and Bischof, R. (2021). Integrating dead recoveries in open-population spatial capture–recapture models. *Ecosphere*, 12(7):e03571.

Dupont, P. P., Bischof, R., Milleret, C., Peters, W., Edelhoff, H., Ebert, C., Klamm, A., and Hohmann, U. (2023). An evaluation of spatial capture-recapture models applied to ungulate non-invasive genetic sampling data. *The Journal of Wildlife Management*, page e22373.

Efford, M. (2004). Density estimation in live-trapping studies. *Oikos*, 106(3):598–610.

Efford, M. G., Borchers, D. L., and Mowat, G. (2013). Varying effort in capture–recapture studies. *Methods in Ecology and Evolution*, 4(7):629–636.

Efford, M. G., Dawson, D. K., and Borchers, D. L. (2009). Population density estimated from locations of individuals on a passive detector array. *Ecology*, 90(10):2676–2682.

Efford, M. G. and Schofield, M. R. (2022). A review of movement models in open population capture–recapture. *Methods in Ecology and Evolution*, 13(10):2106–2118.

Ekblom, R., Brechlin, B., Persson, J., Smeds, L., Johansson, M., Magnusson, J., Flagstad, Ø., and Ellegren, H. (2018). Genome sequencing and conservation genomics in the Scandinavian wolverine population. *Conservation Biology*, 32(6):1301–1312.

Ellison, A. M. (2004). Bayesian inference in ecology. *Ecology Letters*, 7(6):509–520.

Epstein, Y. (2014). The Habitats Directive and Bern Convention: synergy and dysfunction in public international and EU law. *Georgetown International Environmental Law Review*, 26:139.

Ergon, T. and Gardner, B. (2014). Separating mortality and emigration: modelling space use, dispersal and survival with robust-design spatial capture–recapture data. *Methods in Ecology and Evolution*, 5(12):1327–1336.

Ericsson, G., Heberlein, T. A., Karlsson, J., Bjärvall, A., and Lundvall, A. (2004). Support for hunting as a means of wolf *Canis lupus* population control in Sweden. *Wildlife Biology*, 10(4):269–276.

Fisher, J. T., Murray, S., Barrueto, M., Carroll, K., Clevenger, A. P., Hausleitner, D., Harrower, W., Heim, N., Heinemeyer, K., Jacob, A. L., et al. (2022). Wolverines (*Gulo gulo*) in a changing landscape and warming climate: a decadal synthesis of global conservation ecology research. *Global Ecology and Conservation*, page e02019.

Flagstad, Ø., Hedmark, E., Landa, A., Brøseth, H., Persson, J., Andersen, R., Segerström, P., and Ellegren, H. (2004). Colonization history and noninvasive monitoring of a reestablished wolverine population. *Conservation Biology*, 18(3):676–688.

Flagstad, Ø., Kleven, O., Erlandsen, S. E., Brandsegg, H., Spets, M. H., Spets, M. H., Eriksen, L. B., Andersskog, I. P. Ø., Johansson, M., Ekblom, R., Ellegren, H., and Brøseth, H. (2019). DNA-based monitoring of the Scandinavian wolverine population 2019: Nina report 1762. Technical report, Norwegian Institute for Nature Research (NINA).

Fuller, M. R. and Fuller, T. K. (2012). Radio-telemetry equipment and applications for carnivores. In Boitani, L. and Powell, R., editors, *Carnivore ecology and conservation: A handbook of techniques*, pages 152–68. Oxford University Press, Oxford, UK.

Gangaas, K. E., Kaltenborn, B. P., and Andreassen, H. P. (2013). Geo-spatial aspects of acceptance of illegal hunting of large carnivores in Scandinavia. *PLoS ONE*, 8(7):e68849.

Gardner, B., Reppucci, J., Lucherini, M., and Royle, J. A. (2010). Spatially explicit inference for open populations: estimating demographic parameters from camera-trap studies. *Ecology*, 91(11):3376–3383.

Gaspard, G., Kim, D., and Chun, Y. (2019). Residual spatial autocorrelation in macroecological and biogeographical modeling: a review. *Journal of Ecology and Environment*, 43(1):1–11.

Gervasi, V., Brøseth, H., Gimenez, O., Nilsen, E. B., and Linnell, J. D. (2014). The risks of learning: confounding detection and demographic trend when using count-based indices for population monitoring. *Ecology and Evolution*, 4(24):4637–4648.

Gervasi, V., Brøseth, H., Gimenez, O., Nilsen, E. B., Odden, J., Flagstad, Ø., and Linnell, J. D. (2016). Sharing data improves monitoring of transboundary populations: The case of wolverines in central Scandinavia. *Wildlife Biology*, 22(3):95–106.

Gervasi, V., Linnell, J. D., Brøseth, H., and Gimenez, O. (2019). Failure to coordinate management in transboundary populations hinders the achievement of national management goals: the case of wolverines in Scandinavia. *Journal of Applied Ecology*, 56(8):1905–1915.

Gimenez, O., Buckland, S. T., Morgan, B. J., Bez, N., Bertrand, S., Choquet, R., Dray, S., Etienne, M.-P., Fewster, R., Gosselin, F., et al. (2014). Statistical ecology comes of age. *Biology Letters*, 10(12):20140698.

Gimenez, O., Cam, E., and Gaillard, J.-M. (2018). Individual heterogeneity and capture–recapture models: what, why and how? *Oikos*, 127(5):664–686.

Glass, T. W., Magoun, A. J., Robards, M. D., and Kielland, K. (2022). Wolverines (*Gulo gulo*) in the Arctic: Revisiting distribution and identifying research and conservation priorities amid rapid environmental change. *Polar Biology*, 45(9):1465–1482.

Gomes, C., Dietterich, T., Barrett, C., Conrad, J., Dilkina, B., Ermon, S., Fang, F., Farnsworth, A., Fern, A., Fern, X., et al. (2019). Computational sustainability: Computing for a better world and a sustainable future. *Communications of the ACM*, 62(9):56–65.

Gopalaswamy, A. M., Delampady, M., Karanth, K. U., Kumar, N. S., and Macdonald, D. W. (2015). An examination of index-calibration experiments: counting tigers at macroecological scales. *Methods in Ecology and Evolution*, 6(9):1055–1066.

Gu, W. and Swihart, R. K. (2004). Absent or undetected? effects of non-detection of species occurrence on wildlife–habitat models. *Biological conservation*, 116(2):195–203.

Guélat, J. and Kéry, M. (2018). Effects of spatial autocorrelation and imperfect detection on species distribution models. *Methods in Ecology and Evolution*, 9(6):1614–1625.

Guillera-Arroita, G., Lahoz-Monfort, J. J., MacKenzie, D. I., Wintle, B. A., and McCarthy, M. A. (2014). Ignoring imperfect detection in biological surveys is dangerous: A response to 'fitting and interpreting occupancy models'. *PLoS ONE*, 9(7):e99571.

Habitats Directive (1992). Council Directive 92/43/eec of 21 May 1992 on the conservation of natural habitats and of wild fauna and flora. *Official Journal of the European Union*, 206:7–50.

Hayes, L. D. and Schradin, C. (2017). Long-term field studies of mammals: what the short-term study cannot tell us. *Journal of Mammalogy*, 98(3):600–602.

Hedmark, E., Flagstad, Ø., Segerström, P., Persson, J., Landa, A., and Ellegren, H. (2004). DNA-based individual and sex identification from wolverine (*Gulo gulo*) faeces and urine. *Conservation Genetics*, 5:405–410.

Hoban, S. (2014). An overview of the utility of population simulation software in molecular ecology. *Molecular Ecology*, 23(10):2383–2401.

Hobbs, N. T., Andrén, H., Persson, J., Aronsson, M., and Chapron, G. (2012). Native predators reduce harvest of reindeer by Sámi pastoralists. *Ecological Applications*, 22(5):1640–1654.

Hobbs, N. T. and Hooten, M. B. (2015). *Bayesian models: A Statistical Primer for Ecologists*. Princeton University Press.

Hostetter, N. J., Lunn, N. J., Richardson, E. S., Regehr, E. V., and Converse, S. J. (2021). Age-structured Jolly-Seber model expands inference and improves parameter estimation from capture-recapture data. *PLoS ONE*, 16(6):e0252748.

Howe, E. J., Potter, D., Beauclerc, K. B., Jackson, K. E., and Northrup, J. M. (2022). Estimating animal abundance at multiple scales by spatially explicit capture–recapture. *Ecological Applications*, 32(7):e2638.

Isaac, J. L. (2005). Potential causes and life-history consequences of sexual size dimorphism in mammals. *Mammal Review*, 35(1):101–115.

Jernsletten, J.-L. L. and Klokov, K. B. (2002). Sustainable reindeer husbandry.

Johnson, D. H. (1980). The comparison of usage and availability measurements for evaluating resource preference. *Ecology*, 61(1):65–71.

Jones, J. P., Asner, G. P., Butchart, S. H., and Karanth, K. U. (2013). The 'why', 'what' and 'how' of monitoring for conservation. In Macdonald, D. W. and Willis, K. J., editors, *Key topics in conservation biology 2*, pages 327–343. Wiley Online Library.

Jonzén, N., Sand, H., Wabakken, P., Swenson, J. E., Kindberg, J., Liberg, O., and Chapron, G. (2013). Sharing the bounty—adjusting harvest to predator return in the Scandinavian human–wolf–bear–moose system. *Ecological Modelling*, 265:140–148.

Karlsson, J. and Johansson, Ö. (2010). Predictability of repeated carnivore attacks on livestock favours reactive use of mitigation measures. *Journal of Applied Ecology*, 47(1):166–171.

Kellner, K. F. and Swihart, R. K. (2014). Accounting for imperfect detection in ecology: a quantitative review. *PLoS ONE*, 9(10):e111436.

Kelly, M. J., Betsch, J., Wultsch, C., Mesa, B., and Mills, L. S. (2012). Noninvasive sampling for carnivores. In Boitani, L. and Powell, R., editors, *Carnivore ecology and conservation: a handbook of techniques*, pages 47–69. Oxford University Press, New York.

Kéry, M. and Royle, J. A. (2015). Applied hierarchical modeling in ecology: Analysis of distribution, abundance and species richness in R and BUGS.

Kindberg, J., Ericsson, G., and Swenson, J. E. (2009). Monitoring rare or elusive large mammals using effort-corrected voluntary observers. *Biological Conservation*, 142(1):159–165.

Kindberg, J., Swenson, J. E., Ericsson, G., Bellemain, E., Miquel, C., and Taberlet, P. (2011). Estimating population size and trends of the Swedish brown bear *Ursus arctos* population. *Wildlife Biology*, 17(2):114–123.

Kleiven, J., Bjerke, T., and Kaltenborn, B. P. (2004). Factors influencing the social acceptability of large carnivore behaviours. *Biodiversity & Conservation*, 13:1647–1658.

Kojola, I., Heikkinen, S., and Holmala, K. (2018). Balancing costs and confidence: volunteer-provided point observations, GPS telemetry and the genetic monitoring of Finland's wolves. *Mammal Research*, 63(4):415–423.

Kopatz, A., Kleven, O., Kojola, I., Aspi, J., Norman, A. J., Spong, G., Gyllenstrand, N., Dalén, L., Fløystad, I., Hagen, S. B., et al. (2021). Restoration of transborder connectivity for Fennoscandian brown bears (*Ursus arctos*). *Biological Conservation*, 253:108936.

Krebs, C. (1999). *Ecological Methodology*. Addison-Wesley Longman, California, USA.

Krebs, C. J. (1991). The experimental paradigm and long-term population studies. *Ibis*, 133:3–8.

Lamb, C. T., Ford, A. T., Proctor, M. F., Royle, J. A., Mowat, G., and Boutin, S. (2019). Genetic tagging in the Anthropocene: scaling ecology from alleles to ecosystems. *Ecological Applications*, 29(4):e01876.

Lampa, S., Henle, K., Klenke, R., Hoehn, M., and Gruber, B. (2013). How to overcome genotyping errors in non-invasive genetic mark-recapture population size estimation—a review of available methods illustrated by a case study. *The Journal of Wildlife Management*, 77(8):1490–1511.

Landa, A., Lindén, M., Kojola, I., et al. (2000). *Action plan for the conservation of wolverines in Europe (Gulo gulo)*. Number 18-115. Council of Europe.

Landa, A. and Skogland, T. (1995). The relationship between population density and body size of wolverines *Gulo gulo* in Scandinavia. *Wildlife Biology*, 1(3):165–175.

Landa, A., Strand, O., Linnell, J. D., and Skogland, T. (1998a). Home-range sizes and altitude selection for arctic foxes and wolverines in an alpine environment. *Canadian Journal of Zoology*, 76(3):448–457.

Landa, A., Tufto, J., Franzén, R., Bø, T., Lindén, M., and Swenson, J. E. (1998b). Active wolverine *Gulo gulo* dens as a minimum population estimator in Scandinavia. *Wildlife Biology*, 4(3):159–168.

Lefort, M.-C., Cruickshank, R. H., Descovich, K., Adams, N. J., Barun, A., Emami-Khoyi, A., Ridden, J., Smith, V. R., Sprague, R., Waterhouse, B., et al. (2022). Blood, sweat and tears: a review of non-invasive DNA sampling. *Peer Community Journal*, 2.

Legg, C. J. and Nagy, L. (2006). Why most conservation monitoring is, but need not be, a waste of time. *Journal of Environmental Management*, 78(2):194–199.

Lele, S. R. and Dennis, B. (2009). Bayesian methods for hierarchical models: are ecologists making a Faustian bargain? *Ecological Applications*, 19(3):581–584.

Leopold, A. (1933). *Game management*. Scribner's, New York.

Liberg, O., Andrén, H., Pedersen, H.-C., Sand, H., Sejberg, D., Wabakken, P., Åkesson, M., and Bensch, S. (2005). Severe inbreeding depression in a wild wolf *Canis lupus* population. *Biology Letters*, 1(1):17–20.

Liberg, O., Aronson, Å., Sand, H., Wabakken, P., Maartmann, E., Svensson, L., and Åkesson, M. (2012). Monitoring of wolves in Scandinavia. *Hystrix, the Italian Journal of Mammalogy*, 23(1):29–34.

Liberg, O., Suutarinen, J., Åkesson, M., Andrén, H., Wabakken, P., Wikenros, C., and Sand, H. (2020). Poaching-related disappearance rate of wolves in Sweden was positively related to population size and negatively to legal culling. *Biological Conservation*, 243:108456.

Lindsey, P. A., Chapron, G., Petracca, L. S., Burnham, D., Hayward, M. W., Henschel, P., Hinks, A. E., Garnett, S. T., Macdonald, D. W., Macdonald, E. A., et al. (2017). Relative efforts of countries to conserve world's megafauna. *Global Ecology and Conservation*, 10:243–252.

Link, W. A. (2003). Nonidentifiability of population size from capture-recapture data with heterogeneous detection probabilities. *Biometrics*, 59(4):1123–1130.

Linnell, J., Trouwborst, A., and Fleurke, F. (2017). When is it acceptable to kill a strictly protected carnivore? exploring the legal constraints on wildlife management within Europe's Bern Convention. 12(21):129–157.

Linnell, J. D., Andersen, R., Kvam, T., Andren, H., Liberg, O., Odden, J., and Moa, P. (2001a). Home range size and choice of management strategy for lynx in Scandinavia. *Environmental Management*, 27(6):869–879.

Linnell, J. D., Swenson, J. E., and Andersen, R. (2000). Conservation of biodiversity in Scandinavian boreal forests: large carnivores as flagships, umbrellas, indicators, or keystones? *Biodiversity & Conservation*, 9(7):857–868.

Linnell, J. D., Swenson, J. E., and Anderson, R. (2001b). Predators and people: conservation of large carnivores is possible at high human densities if management policy is favourable. *Animal Conservation*, 4(4):345–349.

Lukacs, P. M. and Burnham, K. P. (2005). Review of capture–recapture methods applicable to noninvasive genetic sampling. *Molecular Ecology*, 14(13):3909–3919.

Mabille, G., Stien, A., Tveraa, T., Mysterud, A., Brøseth, H., and Linnell, J. D. (2015). Sheep farming and large carnivores: what are the factors influencing claimed losses? *Ecosphere*, 6(5):1–17.

MacKenzie, D. I., Nichols, J. D., Sutton, N., Kawanishi, K., and Bailey, L. L. (2005). Improving inferences in population studies of rare species that are detected imperfectly. *Ecology*, 86(5):1101–1113.

Mattisson, J., Odden, J., Nilsen, E. B., Linnell, J. D., Persson, J., and Andrén, H. (2011). Factors affecting Eurasian lynx kill rates on semi-domestic reindeer in northern Scandinavia: Can ecological research contribute to the development of a fair compensation system? *Biological Conservation*, 144(12):3009–3017.

Maxwell, S. L., Rhodes, J. R., Runge, M. C., Possingham, H. P., Ng, C. F., and McDonald-Madden, E. (2015). How much is new information worth? evaluating the financial benefit of resolving management uncertainty. *Journal of Applied Ecology*, 52(1):12–20.

McCarthy, M. A., Moore, J. L., Morris, W. K., Parris, K. M., Garrard, G. E., Vesk, P. A., Rumpff, L., Giljohann, K. M., Camac, J. S., Bau, S. S., et al. (2013). The influence of abundance on detectability. *Oikos*, 122(5):717–726.

McClintock, B. T., Bailey, L. L., Pollock, K. H., and Simons, T. R. (2010). Unmodeled observation error induces bias when inferring patterns and dynamics of species occurrence via aural detections. *Ecology*, 91(8):2446–2454.

McCrea, R., King, R., Graham, L., and Börger, L. (2023). Realising the promise of large data and complex models. *Methods in Ecology and Evolution*, 14(1):4–11.

McLellan, B., Proctor, M., Huber, D., and Michel, S. (2017). *Ursus arctos*. The IUCN Red List of Threatened Species, 2017: e.t41688a121229971.

Mech, L. D. and Boitani, L. (2007). *Wolves: behavior, ecology, and conservation*. University of Chicago Press.

Meine, C. (2010). Conservation biology: past and present. In Sodhi, N. S. and Ehrlich, P. R., editors, *Conservation Biology for All*, volume 1, pages 7–26. Oxford University Press, Oxford.

Milleret, C., Dey, S., Dupont, P., Brøseth, H., Turek, D., de Valpine, P., and Bischof, R. (2022a). Estimating spatially variable and density-dependent survival using open-population spatial capture–recapture models. *Ecology*, page e3934.

Milleret, C., Dupont, P., Moqanaki, E., Brøseth, H., Flagstad, Ø., Kleven, O., Kindberg, J., and Bischof, R. (2022b). *Estimates of wolverine density, abundance, and population dynamics in Scandinavia, 2014–2022*. The Faculty of Environmental Sciences and Natural Resource Management (MINA), Norwegian University of Life Sciences.

Moqanaki, E. and Samelius, G. (2022). *Monitoring the manul: guidelines for practitioners*. The Pallas's cat International Conservation Alliance (PICA), Sweden.

Moqanaki, E. M., Jiménez, J., Bensch, S., and López-Bao, J. V. (2018). Counting bears in the Iranian Caucasus: remarkable mismatch between scientifically-sound population estimates and perceptions. *Biological Conservation*, 220:182–191.

Moqanaki, E. M., Milleret, C., Tourani, M., Dupont, P., and Bischof, R. (2021). Consequences of ignoring variable and spatially autocorrelated detection probability in spatial capture-recapture. *Landscape Ecology*, 36(10):2879–2895.

Morin, D. J., Boulanger, J., Bischof, R., Lee, D. C., Ngoprasert, D., Fuller, A. K., McLellan, B., Steinmetz, R., Sharma, S., Garshelis, D., et al. (2022). Comparison of methods for estimating density and population trends for low-density Asian bears. *Global Ecology and Conservation*, 35:e02058.

Morin, D. J., Fuller, A. K., Royle, J. A., and Sutherland, C. (2017). Model-based estimators of density and connectivity to inform conservation of spatially structured populations. *Ecosphere*, 8(1):e01623.

Murr, A., Traunmüller, R., and Gill, J. (2022). Computing quantities of interest and their uncertainty using Bayesian simulation. *Political Science Research and Methods*, pages 1–10.

Newman, K., Buckland, S., Morgan, B. J., King, R., Borchers, D., Cole, D. J., Besbeas, P., Gimenez, O., and Thomas, L. (2014). *Modelling Population Dynamics: Model Formulation, Fitting and Assessment using State-Space Methods*. Springer, New York, USA.

Nichols, J. D. (1992). Capture-recapture models. *BioScience*, 42(2):94–102.

Nichols, J. D. and Williams, B. K. (2006). Monitoring for conservation. *Trends in Ecology & Evolution*, 21(12):668–673.

Nyhus, P. J. (2016). Human–wildlife conflict and coexistence. *Annual Review of Environment and Resources*, 41:143–171.

Ordiz, A., Rodríguez, C., Naves, J., Fernandez, A., Huber, D., Kaczensky, P., Mertens, A., Mertzanis, Y., Mustoni, A., Palazon, S., et al. (2007). Distance-based criteria to identify minimum number of brown bear females with cubs in Europe. *Ursus*, pages 158–167.

Otis, D. L., Burnham, K. P., White, G. C., and Anderson, D. R. (1978). Statistical inference from capture data on closed animal populations. *Wildlife Monographs*, (62):3–135.

Paterson, J. T., Proffitt, K., Jimenez, B., Rotella, J., and Garrott, R. (2019). Simulation-based validation of spatial capture-recapture models: A case study using mountain lions. *PLoS ONE*, 14(4):e0215458.

Persson, J., Rauset, G. R., and Chapron, G. (2015). Paying for an endangered predator leads to population recovery. *Conservation Letters*, 8(5):345–350.

Pollock, K. H., Nichols, J. D., Simons, T. R., Farnsworth, G. L., Bailey, L. L., and Sauer, J. R. (2002). Large scale wildlife monitoring studies: statistical methods for design and analysis. *Environmetrics*, 13(2):105–119.

Ponisio, L. C., de Valpine, P., Michaud, N., and Turek, D. (2020). One size does not fit all: Customizing MCMC methods for hierarchical models using NIMBLE. *Ecology and Evolution*, 10(5):2385–2416.

Powell, R. A. and Boyce, M. S. (2010). Challenges and opportunities of using GPS-based location data in animal ecology. *Philosophical Transactions of the Royal Society B: Biological Sciences*, 365(1550):2153–2312.

R Core Team (2022). *R: A Language and Environment for Statistical Computing*. R Foundation for Statistical Computing, Vienna, Austria.

Rauset, G. R., Andrén, H., Swenson, J. E., Samelius, G., Segerström, P., Zedrosser, A., and Persson, J. (2016). National parks in northern Sweden as refuges for illegal killing of large carnivores. *Conservation Letters*, 9(5):334–341.

Rist, L., Campbell, B. M., and Frost, P. (2013). Adaptive management: where are we now? *Environmental Conservation*, 40(1):5–18.

Røskaft, E., Bjerke, T., Kaltenborn, B., Linnell, J. D., and Andersen, R. (2003). Patterns of self-reported fear towards large carnivores among the Norwegian public. *Evolution and Human Behavior*, 24(3):184–198.

Royle, J. A. (2006). Site occupancy models with heterogeneous detection probabilities. *Biometrics*, 62(1):97–102.

Royle, J. A., Chandler, R. B., Sollmann, R., and Gardner, B. (2014). *Spatial Capture-Recapture*. Academic Press, Waltham.

Royle, J. A., Chandler, R. B., Sun, C. C., and Fuller, A. K. (2013). Integrating resource selection information with spatial capture–recapture. *Methods in Ecology and Evolution*, 4(6):520–530.

Royle, J. A. and Dorazio, R. M. (2008). *Hierarchical modeling and inference in ecology: the analysis of data from populations, metapopulations and communities*. Elsevier.

Royle, J. A., Fuller, A. K., and Sutherland, C. (2018). Unifying population and landscape ecology with spatial capture–recapture. *Ecography*, 41(3):444–456.

Royle, J. A. and Link, W. A. (2006). Generalized site occupancy models allowing for false positive and false negative errors. *Ecology*, 87(4):835–841.

Sandercock, B. K. (2006). Estimation of demographic parameters from live-encounter data: a summary review. *The Journal of Wildlife Management*, 70(6):1504–1520.

Sandström, C., Pellikka, J., Ratamäki, O., and Sande, A. (2009). Management of large carnivores in Fennoscandia: new patterns of regional participation. *Human Dimensions of Wildlife*, 14(1):37–50.

Schofield, M. R. and Barker, R. J. (2014). Hierarchical modeling of abundance in closed population capture–recapture models under heterogeneity. *Environmental and Ecological Statistics*, 21:435–451.

Schwartz, M. K., Luikart, G., and Waples, R. S. (2007). Genetic monitoring as a promising tool for conservation and management. *Trends in Ecology & Evolution*, 22(1):25–33.

Schwartz, M. K., Tallmon, D. A., and Luikart, G. (1998). Review of DNA-based census and effective population size estimators. *Animal Conservation*, 1(4):293–299.

Shine, R. (1989). Ecological causes for the evolution of sexual dimorphism: a review of the evidence. *The Quarterly Review of Biology*, 64(4):419–461.

Sicacha-Parada, J., Steinsland, I., Cretois, B., and Borgelt, J. (2021). Accounting for spatial varying sampling effort due to accessibility in citizen science data: A case study of moose in Norway. *Spatial Statistics*, 42:100446.

Sjölander-Lindqvist, A., Risvoll, C., Kaarhus, R., Lundberg, A. K., and Sandström, C. (2020). Knowledge claims and struggles in decentralized large carnivore governance: Insights from Norway and Sweden. *Frontiers in Ecology and Evolution*, 8:120.

Smith, J. E., Lehmann, K. D., Montgomery, T. M., Strauss, E. D., and Holekamp, K. E. (2017). Insights from long-term field studies of mammalian carnivores. *Journal of Mammalogy*, 98(3):631–641.

Solberg, K. H., Bellemain, E., Drageset, O.-M., Taberlet, P., and Swenson, J. E. (2006). An evaluation of field and non-invasive genetic methods to

estimate brown bear (*Ursus arctos*) population size. *Biological Conservation*, 128(2):158–168.

Sollmann, R., Mohamed, A., Samejima, H., and Wilting, A. (2013). Risky business or simple solution–relative abundance indices from camera-trapping. *Biological Conservation*, 159:405–412.

Spong, G. and Hellborg, L. (2002). A near-extinction event in lynx: do microsatellite data tell the tale? *Conservation Ecology*, 6(1).

Stephens, P. A., Pettorelli, N., Barlow, J., Whittingham, M. J., and Cadotte, M. W. (2015). Management by proxy? the use of indices in applied ecology. *Journal of Applied Ecology*, 52(1):1–6.

Stevenson, B. C., Fewster, R. M., and Sharma, K. (2022). Spatial correlation structures for detections of individuals in spatial capture–recapture models. *Biometrics*, 78(3):963–973.

Støen, O.-G., Sivertsen, T. R., Tallian, A., Rauset, G. R., Kindberg, J., Persson, L.-T., Stokke, R., Skarin, A., Segerström, P., and Frank, J. (2022). Brown bear predation on semi-domesticated reindeer and depredation compensations. *Global Ecology and Conservation*, 37:e02168.

Strand, G.-H., Hansen, I., de Boon, A., and Sandström, C. (2019). Carnivore management zones and their impact on sheep farming in Norway. *Environmental Management*, 64(5):537–552.

Sutherland, C., Fuller, A. K., and Royle, J. A. (2015). Modelling non-Euclidean movement and landscape connectivity in highly structured ecological networks. *Methods in Ecology and Evolution*, 6(2):169–177.

Swenson, J. and Andrén, H. (2005). A tale of two countries: large carnivore depredation and compensation schemes. In Woodroffe, R., Thirgood, S., and Rabinowitz, A., editors, *People and wildlife, conflict or co-existence?*, pages 323–339. Cambridge University Press, Cambridge.

Swenson, J. E., Sandegren, F., Bjärvall, A., Söderberg, A., Wabakken, P., and Franzén, R. (1994). Size, trend, distribution and conservation of the

brown bear *Ursus arctos* population in Sweden. *Biological Conservation*, 70(1):9–17.

Swenson, J. E., Sandegren, F., Bjärvall, A., and Wabakken, P. (1998). Living with success: research needs for an expanding brown bear population. *Ursus*, pages 17–23.

Swenson, J. E., Schneider, M., Zedrosser, A., Söderberg, A., Franzén, R., and Kindberg, J. (2017). Challenges of managing a European brown bear population; lessons from Sweden, 1943–2013. *Wildlife Biology*, 2017(1):1–13.

Swenson, J. E., Taberlet, P., and Bellemain, E. (2011). Genetics and conservation of European brown bears *Ursus arctos*. *Mammal Review*, 41(2):87–98.

Swenson, J. E., Wabakken, P., Sandegren, F., Bjärvall, A., Franzén, R., and Söderberg, A. (1995). The near extinction and recovery of brown bears in Scandinavia in relation to the bear management policies of Norway and Sweden. *Wildlife Biology*, 1(1):11–25.

Taberlet, P., Waits, L. P., and Luikart, G. (1999). Noninvasive genetic sampling: look before you leap. *Trends in Ecology & Evolution*, 14(8):323–327.

Tallmon, D. A., Bellemain, E., Swenson, J. E., and Taberlet, P. (2004). Genetic monitoring of Scandinavian brown bear effective population size and immigration. *The Journal of wildlife Management*, 68(4):960–965.

Thompson, W. (2013). *Sampling rare or elusive species: concepts, designs, and techniques for estimating population parameters*. Island Press.

Tourani, M. (2022). A review of spatial capture–recapture: Ecological insights, limitations, and prospects. *Ecology and Evolution*, 12(1):e8468.

Trouwborst, A. and Fleurke, F. M. (2019). Killing wolves legally: Exploring the scope for lethal wolf management under European nature conservation law. *Journal of International Wildlife Law & Policy*, 22(3):231–273.

Trouwborst, A., Fleurke, F. M., and Linnell, J. D. (2017). Norway's wolf policy and the Bern Convention on European Wildlife: avoiding the "manifestly absurd". *Journal of International Wildlife Law & Policy*, 20(2):155–167.

Turek, D., Milleret, C., Ergon, T., Brøseth, H., Dupont, P., Bischof, R., and De Valpine, P. (2021). Efficient estimation of large-scale spatial capture–recapture models. *Ecosphere*, 12(2):e03385.

Tveraa, T., Fauchald, P., Gilles Yoccoz, N., Anker Ims, R., Aanes, R., and Arild Høgda, K. (2007). What regulate and limit reindeer populations in Norway? *Oikos*, 116(4):706–715.

Tveraa, T., Stien, A., Brøseth, H., and Yoccoz, N. G. (2014). The role of predation and food limitation on claims for compensation, reindeer demography and population dynamics. *Journal of Applied Ecology*, 51(5):1264–1272.

van de Schoot, R., Depaoli, S., King, R., Kramer, B., Märtens, K., Tadesse, M. G., Vannucci, M., Gelman, A., Veen, D., Willemsen, J., et al. (2021). Bayesian statistics and modelling. *Nature Reviews Methods Primers*, 1(1):1–26.

Wabakken, P., Sand, H., Liberg, O., and Bjärvall, A. (2001). The recovery, distribution, and population dynamics of wolves on the Scandinavian Peninsula, 1978-1998. *Canadian Journal of Zoology*, 79(4):710–725.

Waits, L. P. and Paetkau, D. (2005). Noninvasive genetic sampling tools for wildlife biologists: a review of applications and recommendations for accurate data collection. *The Journal of Wildlife Management*, 69(4):1419–1433.

Walther, B. A. and Moore, J. L. (2005). The concepts of bias, precision and accuracy, and their use in testing the performance of species richness estimators, with a literature review of estimator performance. *Ecography*, 28(6):815–829.

Watson, J. E., Shanahan, D. F., Di Marco, M., Allan, J., Laurance, W. F., Sanderson, E. W., Mackey, B., and Venter, O. (2016). Catastrophic declines in wilderness areas undermine global environment targets. *Current Biology*, 26(21):2929–2934.

White, G. C. and Garrott, R. A. (1990). *Analysis of wildlife radio-tracking data*. Elsevier.

Widman, M. and Elofsson, K. (2018). Costs of livestock depredation by large carnivores in Sweden 2001 to 2013. *Ecological Economics*, 143:188–198.

Wikenros, C., Sand, H., Månsson, J., Maartmann, E., Eriksen, A., Wabakken, P., and Zimmermann, B. (2020). Impact of a recolonizing, cross-border carnivore population on ungulate harvest in Scandinavia. *Scientific Reports*, 10(1):1–11.

Williams, B. K. (2011). Passive and active adaptive management: approaches and an example. *Journal of Environmental Management*, 92(5):1371–1378.

Williams, B. K., Nichols, J. D., and Conroy, M. J. (2002). *Analysis and management of animal populations*. Academic Press.

Wolf, C., Betts, M. G., Levi, T., Newsome, T. M., and Ripple, W. J. (2018). Large species within carnivora are large carnivores. *Royal Society Open Science*, 5(9):181228.

Yoccoz, N. G., Nichols, J. D., and Boulinier, T. (2001). Monitoring of biological diversity in space and time. *Trends in Ecology & Evolution*, 16(8):446–453.

Zemanova, M. A. (2020). Towards more compassionate wildlife research through the 3rs principles: moving from invasive to non-invasive methods. *Wildlife Biology*, 2020(1):1–17.

Article I

Landscape Ecol (2021) 36:2879–2895
https://doi.org/10.1007/s10980-021-01283-x

RESEARCH ARTICLE

Consequences of ignoring variable and spatially autocorrelated detection probability in spatial capture-recapture

Ehsan M. Moqanaki · Cyril Milleret · Mahdieh Tourani · Pierre Dupont · Richard Bischof

Received: 24 December 2020 / Accepted: 11 June 2021 / Published online: 26 June 2021

Abstract

Context Spatial capture-recapture (SCR) models are increasingly popular for analyzing wildlife monitoring data. SCR can account for spatial heterogeneity in detection that arises from individual space use (detection kernel), variation in the sampling process, and the distribution of individuals (density). However, unexplained and unmodeled spatial heterogeneity in detectability may remain due to cryptic factors, both intrinsic and extrinsic to the study system. This is the case, for example, when covariates coding for variable effort and detection probability in general are incomplete or entirely lacking.

Objectives We identify how the magnitude and configuration of unmodeled, spatially variable detection probability influence SCR parameter estimates.

Methods We simulated SCR data with spatially variable and autocorrelated detection probability. We then fitted an SCR model ignoring this variation to the simulated data and assessed the impact of model misspecification on inferences.

Results Highly-autocorrelated spatial heterogeneity in detection probability (Moran's I = 0.85–0.96), modulated by the magnitude of the unmodeled heterogeneity, can lead to pronounced negative bias (up to 65%, or about 44-fold decrease compared to the reference scenario), reduction in precision (249% or 2.5-fold) and coverage probability of the 95% credible intervals associated with abundance estimates to 0. Conversely, at low levels of spatial autocorrelation (median Moran's I = 0), even severe unmodeled heterogeneity in detection probability did not lead to pronounced bias and only caused slight reductions in precision and coverage of abundance estimates.

Conclusions Unknown and unmodeled variation in detection probability is liable to be the norm, rather than the exception, in SCR studies. We encourage practitioners to consider the impact that spatial autocorrelation in detectability has on their inferences and urge the development of SCR methods that can take structured, unknown or partially unknown spatial variability in detection probability into account.

Keywords Capture-recapture · Detection probability · Heterogeneity · Spatial autocorrelation · Varying effort · Wildlife monitoring

Supplementary Information The online version contains supplementary material available at https://doi.org/10.1007/s10980-021-01283-x.

E. M. Moqanaki (✉) · C. Milleret · M. Tourani · P. Dupont · R. Bischof
Faculty of Environmental Sciences and Natural Resource Management, Norwegian University of Life Sciences, P.O. Box 5003, 1432 Ås, Norway
e-mail: ehsan.moqanaki@gmail.com

M. Tourani
Department of Wildlife, Fish, and Conservation Biology, University of California Davis, Davis, USA

Introduction

Imperfect detection is one of the primary challenges to the estimation of the size of wild populations. Regardless of the data collection method employed, rarely, if ever, are all individuals in a population detected. This challenge is amplified with the increasingly widespread application of non-invasive sampling methods for making landscape-level assessments across time and space, such as camera trapping and non-invasive DNA sampling (Burton et al. 2015; Beng and Corlett 2020), which often trade off local sampling intensity for extent of spatial coverage (grain vs. extent; Chandler and Hepinstall-Cymerman 2016; Steenweg et al. 2018). Capture-recapture and, more recently, spatial capture-recapture (SCR) models estimate and account for imperfect detection, thereby producing robust estimates of the focal ecological parameters (Chao 2001; Efford 2004; Lukacs and Burnham 2005; Borchers and Efford 2008; Royle et al. 2014). SCR has become particularly popular as it exploits the information contained in the spatial configuration of detections and non-detections across the study area to produce spatially explicit estimates of abundance (i.e., density; Borchers and Efford 2008; Royle and Young 2008; Royle et al. 2018).

In most field studies, detection probability—the probability of detecting a species or individual when it is present—is not only imperfect but also variable. Detection probability can vary across individuals, time, and space (Gimenez et al. 2008; Kellner and Swihart 2014; Conn et al. 2017; Guélat and Kéry 2018). The implications and treatment of individual and temporal variability in detection probability have been extensively documented in the non-spatial capture-recapture literature (Chao 2001; Link 2003; Borchers et al. 2006; Gimenez et al. 2018a). SCR models are particularly well-suited to account for spatially variable detectability, as studies are usually configured into discrete detection locations referred to as detectors (or traps) that are distributed across the study area (Efford et al. 2013; Royle et al. 2014). Spatial variation in detection probability resulting from individual space use relative to detector locations, i.e. the declining probability of detection with increasing distance from an individual's activity center (AC), is in fact exploited by SCR models to estimate the distribution of individual ACs (Borchers and Efford 2008; Royle and Young 2008). Other potential sources of spatial heterogeneity in detectability include those caused by the study itself, such as variable search effort, and local intrinsic and extrinsic factors that influence the detectability of animals. Known sources of variation in detection probability can be modeled and accounted for in SCR (Efford et al. 2013; Efford and Mowat 2014; Royle et al. 2014). This is the case when variable sampling effort is recorded, for example, during camera trapping or non-invasive DNA sampling (Royle et al. 2009; Efford et al. 2013), or when spatial covariates, such as habitat proxies for vulnerability to detection, are used (Bischof et al. 2017; Kendall et al. 2019).

In many wildlife monitoring studies, spatial heterogeneity in detection probability remains partially unknown. Unaccounted environmental factors may impact exposure to detectors; for example, site-specific characteristics may affect visibility, or local climate can influence genotyping success rate of non-invasively collected DNA samples (Efford et al. 2013; Kendall et al. 2019). Survey effort may also vary across the study area unbeknownst to the investigator. For example, many large-scale monitoring programs combine structured sampling with unstructured data collection methods to increase the spatial extent and sampling intensity, and involve members of the public in the process (Thompson et al. 2012; Conn et al. 2017; Altwegg and Nichols 2019; Bischof et al. 2020a; Sicacha-Parada et al. 2021). Data from unstructured sources introduce unknown spatial heterogeneity in detection probability in SCR studies. In the analysis of monitoring data, ignoring the variability in detection can seriously degrade population inferences (Nichols and Williams 2006; Gimenez et al. 2008; Gerber and Parmenter 2015). However, it has also been previously shown that spatially random variation in detection probability does not seem to be a major source of bias in parameter estimates from SCR analysis (Bischof et al. 2017). In such situations, most individuals in the sampling grid will be detected by at least one detector, if detectors are spaced closely enough (high grain) and cover a large enough area (large extent) relative to home range sizes in the study population (Sollman et al. 2012; Efford and Fewster 2013).

Spatial autocorrelation in detection probability—when detectability is more similar among neighboring than distant detectors—is common in ecological studies (Guélat and Kéry 2018). Observed and

unobserved spatially autocorrelated variation in detection probability could have many causes (Gaspard et al. 2019), divided into two broad categories. On the one hand is the nature of the data collection; for example, regional differences in the mobilization of volunteers for non-invasive DNA collections, variation in camera trap efficiency due to inadvertent scent contamination at a cluster of sites, or reduced physical capture success in traps installed by a less-experienced operator in their designated area (Kristensen and Kovach 2018; Bischof et al. 2020a; Tourani et al. 2020a). On the other hand are characteristics of the study species and its environment, such as spatial variation in site attractiveness or individual behaviors (e.g., shyness) that lead to variable detectability (Efford et al. 2013; Howe et al. 2013; Stevenson et al. 2021). Variable detection probability that is highly autocorrelated may disproportionately affect the overall detectability of certain individuals in the population based on the location of their ACs. When areas with virtually zero probability of detection are known, for example in clustered sampling designs, they can be specified as detector-free regions (or holes) in the sampling grid and be treated like the unsampled habitat buffer in SCR (Efford and Fewster 2013; Royle et al. 2014). In extreme cases, however, large swaths of the study area, and the individuals inhabiting them, may be left unsampled, unbeknownst to the investigator. This can occur when, for example, SCR data are obtained opportunistically (e.g., contributed by citizen scientists), where the incomplete information about the detection process makes it unclear whether areas without detections were sampled or not (i.e., true vs. false negatives; Thompson et al. 2012; Bird et al. 2014; Bischof et al. 2020a). We expect flawed inferences from SCR studies if autocorrelated heterogeneity in detection probability remains cryptic, and thus unaccounted for. Specifically, when detection probability is not correlated with animal density (Clark 2019; Paterson et al. 2019), we predict that an SCR model ignoring contiguous areas with low or zero detection probability would produce positively biased estimates of average detection probability as it is inferred from areas with detections, and therefore negatively biased estimates of density (Royle et al. 2013; Guélat and Kéry 2018).

Most, if not all, SCR analyses of empirical data that are collected across large spatial extents, ignore some sources of spatial variation in detection probability. The extent to which the misspecification of the detection process in the presence of variable and spatially autocorrelated detection probability may affect the estimates of focal parameters in SCR studies has not yet been systematically investigated. Using simulations with an envelope that includes scenarios encountered during wildlife monitoring, we quantify how unmodeled, spatially variable detection probability influences parameter estimates obtained via SCR. Specifically, our objective in this study is to identify scenarios where unmodeled heterogeneity in detection probability can lead to problematic inferences in SCR analysis. We do so with a focus on both the magnitude of variability in detection probability and the autocorrelation therein.

Methods

Spatial capture-recapture model

For the purpose of this study, we used a standard, single-session SCR model in a Bayesian framework (Royle et al. 2014; see the model code in Online Appendix 1). Our model is composed of two hierarchical levels:

1. *The ecological sub-model* reflects the underlying ecological process of interest and describes the distribution of individuals in space, i.e. density. Following a homogeneous point process (Royle et al. 2014), we assume every individual i in the population has a fixed AC (or home range center; s_i) and that these individual ACs are randomly distributed across the habitat S according to a uniform distribution:

$$s_i \sim Uniform(S) \quad (1)$$

We used a data augmentation approach to account for those individuals in the population that are not detected (Royle et al. 2007). Detected and augmented individuals make up the super-population of size M (see below). A latent state variable z_i describes inclusion of individual i in the population, governed by the inclusion probability ψ:

$$z_i \sim Bernoulli(\psi) \quad (2)$$

where z_i takes value 1 if individual i is a member of the true population and 0 otherwise. Population size N is therefore:

$$N = \sum_{i=1}^{M} z_i \quad (3)$$

2. *The observation sub-model* describes the individual and detector-specific probability of detection p_{ij} as a function of Euclidean distance d_{ij} between the location of an individual AC and a given detector j. We used the half-normal detection function to model p_{ij} (Borchers and Efford 2008; Royle et al. 2014):

$$p_{ij} = p_0 \exp\left(-d_{ij}^2 \Big/ 2\sigma^2\right) \quad (4)$$

where p_0 is the baseline detection probability (or magnitude of the detection function). In the half-normal model, the detection probability p_{ij} decreases monotonically with distance d_{ij} from s_i (Borchers and Efford 2008; Royle et al. 2014). The spatial scale parameter σ defines the rate of decline in p_{ij} with distance d_{ij} from detector j to the s_i. By including the spatial information through an explicit model for detection, SCR accounts for one important source of spatial variation in detection probability: the location of an individual's AC relative to the detectors (Borchers and Efford 2008; Royle et al. 2014).

We considered the observations of individuals at detectors as the outcome of a Bernoulli process (detections [$y_{ij} = 1$] and non-detections [$y_{ij} = 0$]) with probability p_{ij} and conditional on the state z_i of individual i:

$$y_{ij} \sim Bernoulli\left(p_{ij} z_i\right) \quad (5)$$

Importantly, this observation model assumes constant baseline detection probability among detectors, and thus does not account for additional detector-specific variation in detectability.

Simulation

General approach

To evaluate the consequences of unmodeled spatial heterogeneity in detectability, we generated SCR data sets with varying patterns of spatial heterogeneity in the baseline detection probability (i.e., detector-specific $p_0 = p_{0_j}$), before fitting SCR models assuming constant baseline detection probability across detectors. We considered two types of scenarios: continuous and categorical spatial variation in detectability. For each scenario, we varied both the level of spatial autocorrelation and the magnitude of the spatial variation to resemble sampling configurations and intensities that may occur in real-life studies (Fig. 1). We also included a reference scenario without spatial heterogeneity in detection probability; thus, the observation sub-model was not misspecified.

Set up

For all simulations, we used a 20 × 20-distance unit (du) square grid of 400 detectors with 1 du inter-detector spacing. The habitat S included the region covered by detectors and a 4.5-du wide buffer around it (i.e., three times the simulated value for σ; Efford 2011) for a total area of 29 × 29 du^2 (Fig. 1). The buffer allows individuals with ACs located outside but near the detector area to be detected within. We fixed the values for the true population size to $N = 250$ and the spatial scale parameter of the half-normal detection function to $\sigma = 1.5$ du across all simulation scenarios for simplicity. We set the size of the augmented population size to be 2.5 times the simulated number of ACs ($M = 625$). With this set up, we detected, on average, about 40% (range = 15–60%) of the true population size N under any given scenario (Table S2.1, Online Appendix 2).

Detector-level covariates

We generated spatially autocorrelated covariates of the baseline detection probability encompassing the extent of the 20 × 20 du^2 detector grid with the same spatial resolution (1 du) using a function developed by Guélat (2013), with minor modifications (Online Appendix 1). The detector-specific, spatial covariate $\mathbf{X}$ was generated using a multivariate normal distribution:

$$\mathbf{X} \sim MVN(0, \Sigma) \quad (6)$$

where the covariance matrix Σ determines the spatial association between detectors. Σ is calculated using a

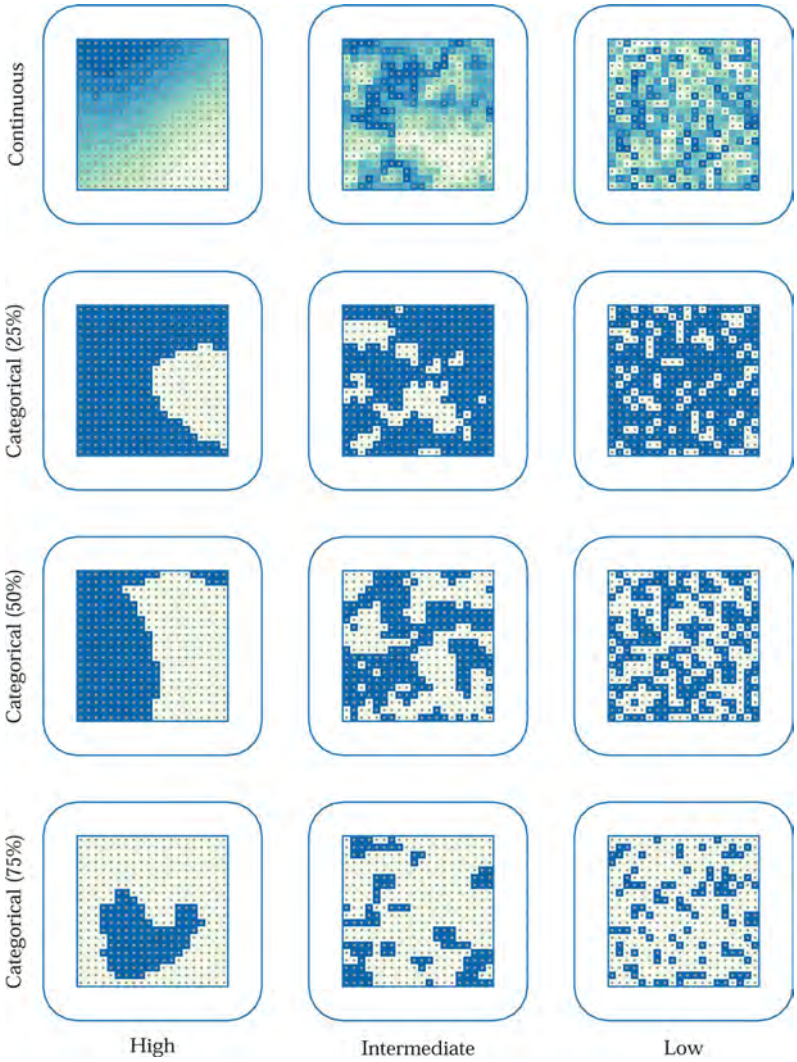

Fig. 1 Examples of spatially variable and autocorrelated baseline detection probability (higher = darker blue shading) in grid of detectors (gray dots) centered in a habitat (entire area surrounded by the blue line with rounded corners). Shown in rows, spatial variation may be continuous or categorical (with different proportion of area in the lower detectability category). Shown in columns, spatial autocorration may vary from high (Moran's $I \approx 1$) to low (Moran's $I \approx 0$). For a detailed description of each scenario, see the main text.

function D representing the decay in correlation between pairs of detectors with distance. We followed Guélat (2013) and modeled the covariance of $\mathbf{X}$ at two detectors j and j' as an exponential decay with distance:

$$D(\delta_{jj'}) = \exp(-\phi\delta_{jj'}) \quad (7)$$

where $\delta_{jj'}$ is the distance between detectors j and j', and ϕ is the rate determining how rapidly correlation declines with distance. We varied ϕ to simulate covariates with low ($\phi = 1000$), intermediate ($\phi = 1$), or high ($\phi = 0.001$) spatial autocorrelation (Fig. 1). We randomly generated 100 covariate

surfaces for each simulation scenario and scaled the resulting values. We then extracted the spatial covariate values for each detector grid cell $\mathbf{X}_j$ (but see below the extra step for simulating continuous spatial variation in detectability). We quantified the realized spatial autocorrelation using the Moran's index of global spatial autocorrelation, Moran's *I* (Moran 1950; Sokal and Oden 1978; Lichstein et al. 2002) for each simulated spatial covariate with the R package 'raster' (Hijmans 2019). *I* ranges from −1 (perfectly negatively correlated) to 0 (no correlation) and 1 (perfectly positively correlated).

Simulation scenarios

1. *Continuous, detector-level variation in detectability*—Continuous spatial variation in detection probability may arise in situations where an underlying habitat covariate, such as elevation, forest cover, or distance from a feature (e.g., roads or human settlements) linearly affects baseline detection probability at detectors (Fig. 1) but remains unmodeled. We modeled the detector-specific baseline detection probability p_{0_j} as a linear function of the simulated spatial covariate $\mathbf{X}$:

$$logit(p_{0_j}) = \beta_0 + \beta_{\mathbf{X}}\mathbf{X}_j \quad (8)$$

where β_0 is the intercept value of the simulated baseline detection probability p_0 on the logit scale and $\beta_{\mathbf{X}}$ is the regression coefficient of the covariate effect. We kept β_0 constant across simulations, which corresponds to an intercept value of 0.15 for p_0. We used two values of $\beta_{\mathbf{X}}$ to generate low ($\beta_{\mathbf{X}} = -0.5$) or high ($\beta_{\mathbf{X}} = -2.0$) amounts of spatial variation in detection probability. Generating spatial covariates directly as spatially autocorrelated rasters as described above, leads to less tractable outcomes as the level of spatial autocorrelation ϕ influences not only the spatial distribution, but also the density distribution of the covariate. To ensure that the density distribution of spatial covariates on detection probability remained comparable across simulations, regardless of the level of autocorrelation, we mapped a uniformly-distributed spatial covariate with values in the range between −1.96 and 1.96 onto the spatially autocorrelated similarity raster created as described above (see the code in Online Appendix 1). As a result, the mean covariate value and variance were constant across simulations, regardless of the level of spatial autocorrelation. In other words, we sought stationarity when all simulations of a given scenario are considered jointly, but not within a given simulated detector grid. Following Eq. 8, the detector-specific baseline detection probability p_{0_j} was between 0.06 and 0.32 (median = 0.15) when the variation in detectability was low ($\beta_{\mathbf{X}} = -0.5$). By increasing $\beta_{\mathbf{X}}$ to −2.0, p_{0_j} was between 0.003 and 0.9 (median = 0.15; Table S2.1, Online Appendix 2). p_{ij} was then calculated by reformulating Eq. 4:

$$p_{ij} = p_{0_j} \exp\left(-d_{ij}^2 \Big/ 2\sigma^2\right) \quad (9)$$

Finally, the SCR data y_{ij} was generated by realizing the detection process following Eq. 5. Note that such large differences in p_{0_j} do not translate into a correspondingly large differences in overall detectability. The probability of detecting any given individual at least once, depends not only on p_{0_j}, but also on the scale parameter of the detection function σ, and the position of its AC relative to the entire detector grid. Comparatively extensive spatial differences in baseline detection probabilities have been reported for three large carnivore species in Scandinavia (Bischof et al. 2020a). For example, p_0 estimates (after conversion from binomial to Bernoulli) for wolves *Canis lupus* ranged from near 0 to 0.8, depending on administrative region.

2. *Categorical, detector-level variation in detectability*—In real-world monitoring studies, this situation arises when there are at least two regions with different sampling intensity across the study area; for example, two regions with varying sampling effort (or different sampling protocols that lead to varying sampling intensity), or two contrasting landscapes (e.g., forest vs. grassland) or detector types (e.g., camera traps on and off trails) across the study area that influence the detection probability (Fig. 1). To represent this situation, we transformed the underlying continuous spatial covariate into a binary one ($\mathbf{X}_j = 0$ or 1) before simulating scenarios with two classes of

detector-specific baseline detection probability p_{0_j} using Eq. 8. The R code in Online Appendix 1 shows the method used to define the cut-off value to discretize the spatial covariates. We used the same values of $\beta_{\mathbf{X}}$ to generate low or high amount of spatial variation in detectability between the discrete classes of detectors. With this set-up, the baseline detection probability at a group of detectors ($\mathbf{X}_j = 0$) was equal to the intercept value ($p_{0_j} = \beta_0 = 0.15$), and p_{0_j} for the remaining detectors with lower detectability ($\mathbf{X}_j = 1$) was either 0.1 (when $\beta_{\mathbf{X}} = -0.5$) or 0.02 ($\beta_{\mathbf{X}} = -2.0$) depending on the simulated amount of spatial variation in detectability (Table S2.1, Online Appendix 2). In addition, we considered an extreme case, where a portion of the study area remained entirely unsampled unbeknownst to the investigator, and therefore unaccounted for in the model. This situation could be encountered in, for example, volunteer-based monitoring programs, where SCR data are collected opportunistically but no or only limited spatial information exists about the spatial configuration of sampling. Logistic issues, such as systematic equipment failure (e.g., trap malfunction or damage) or human error, if unreported, may also result in clusters of detectors that remain inactive without the investigator's knowledge. We set $\beta_{\mathbf{X}}$ to -10000, so that $p_{0_j} \approx 0$ for detectors with a covariate value of $\mathbf{X}_j = 1$, and therefore no detection could occur at these inactive detectors.
To evaluate the potential effect of the proportion of detectors with a different baseline detection probability, we varied the proportion of detectors assigned to each class of the discrete covariate simulated (Fig. 1). We simulated SCR data sets with 25% (n = 100 detectors), 50% (n = 200), or 75% (n = 300) of the detectors assigned to the lower detectability class ($\mathbf{X}_j = 1$).

Simulation realization—In total, we generated six simulation scenarios of continuous spatial variation in baseline detection probability with the combinations of two values of $\beta_{\mathbf{X}}$ and three levels of spatial autocorrelation ϕ. For the discrete categorical variation in baseline detection probability, we simulated 27 scenarios from all possible combinations of the three values of $\beta_{\mathbf{X}}$, three different proportions of detectors with lower detectability, and three levels of spatial autocorrelation. Finally, we included a scenario of constant detection probability across detectors for reference, i.e. the observation sub-model was correctly specified. We repeated the data simulation procedure 100 times for each combination of parameters, resulting in a total of 3400 simulated SCR data sets (Table S2.1, Online Appendix 2).

Additional simulations—Another common formulation of the detection process in SCR is the Poisson distribution. This models count-based data arising from sampling methods in which individuals can be detected multiple times at a detector during a single occasion, such as in camera trapping studies (Royle et al. 2014). To evaluate the consequences of similar model misspecification in SCR models with a Poisson detection process, we simulated additional count-based SCR data sets and repeated the analysis. We simulated SCR data with counts as observations and fitted a standard, single-session, Poisson-distributed SCR model assuming homogeneous baseline detection rate. A description of the data simulation procedure and fitting of the misspecified Poisson SCR model is provided in Online Appendix 3.

SCR model fitting and evaluation of model performance

We fitted the SCR model described earlier, which does not account for spatial variability in baseline detection probability, to the simulated data sets using NIMBLE (version 0.8.0; de Valpine et al. 2017), nimbleSCR (Bischof et al. 2020b), and R 3.6.1 (R Core Team 2019). We chose vague priors for all primary parameters (ψ, σ, p_0, and λ_0 as the baseline detection rate in the Poisson SCR model; Table S1.1, Online Appendix 1). We used a local evaluation approach to reduce computation time (Turek et al. 2021). We drew from 3 chains, 15000 Markov chain Monte Carlo (MCMC) samples each, and discarded the initial 5000 samples as burn-in. We visually inspected the mixing of the chains using trace-plots and considered models as converged when all parameters had a potential scale reduction value (Rhat) < 1.10 (Brooks and Gelman 1998). We removed from further analysis simulation runs that had failed to reach convergence. R code exemplifying the SCR data simulation for each scenario and model fitting are provided in Online Appendix 1.

To quantify the consequences of unaccounted spatial heterogeneity in detection probability for SCR models, we calculated the relative bias (RB), coefficient of variation (CV), and coverage probability of the 95% credible intervals (hereafter, coverage; Walther and Moore 2005) of the estimates of population size ($\hat{N}$) and spatial scale parameter ($\hat{\sigma}$). RB was calculated as:

$$\widehat{RB}(\theta) = \left(\hat{\theta} - \theta_0\right) \Big/ \theta_0 \quad (10)$$

where $\hat{\theta}$ is the posterior mean estimate for the parameter of interest and θ_0 is the true (simulated) value of that parameter. CV was calculated to assess the precision of each parameter estimate as:

$$\widehat{CV}(\theta) = \widehat{SD}(\theta) \Big/ \hat{\theta} \quad (11)$$

where $\widehat{SD}(\theta)$ is the standard deviation of the MCMC posterior samples of that parameter. Further, we calculated the coverage as a metric of model fit, which was computed as the proportion of simulation runs in which the 95% credible interval of the parameter estimate included the simulated value of that parameter (Walther and Moore 2005).

Results

Overview

Of the 3400 simulation runs, 3384 (99.5%) reached convergence and were retained: 599 (99.8%) and 2685 (99.4%) for the continuous and categorical scenarios of spatial variation in detectability, respectively (Table S2.2, Online Appendix 2). Our results indicate that the misspecified SCR model was robust to unmodelled spatial heterogeneity in detection probability for most of the scenarios explored. Population size ($\hat{N}$) and spatial scale parameter ($\hat{\sigma}$) estimators exhibited pronounced bias only in the presence of high spatial autocorrelation and high amount of variation in detectability among detectors (Fig. 2). Precision (Fig. 3) and coverage (Fig. 4) were also affected in our extreme scenarios when the detector-specific variation in detection probability remained unmodeled. The consequences of spatial autocorrelation were amplified with increasing proportions of detectors with lower detectability in the categorical scenarios and, in certain situations, when the amount of variation in detection probability was high (Table S2.2, Online Appendix 2). Qualitatively, misspecification of the observation sub-model for Bernoulli- and Poisson-distributed data had comparable consequences. Results for the simulations with the Poisson SCR model are provided in Online Appendix 3.

Fig. 2 Relative bias (RB) for population size ($\hat{N}$) and the spatial scale parameter of the half-normal detection function ($\hat{\sigma}$) estimated by a spatial capture-recapture model fitted to simulated data sets. Spatial variation in detection was simulated but not accounted for in the estimation model. Numbers provided on the x-axes refer to the unique ID of the simulation scenario and link with the more detailed information provided for each simulation in Online Appendix 2. Violins show the biasing effects of spatial autocorrelation at the detector-level covariates simulated (decreasing from dark [High] to light colors [Low]) in different scenarios of continuous (top row) and discrete categorical (bottom three rows) variation in baseline detection probability. For the categorical scenarios, the proportions of detectors that belong to a group of detectors with lower detectability increases from top (25%) to bottom (75%). Background colors correspond to three different sets of simulation scenarios with similar values of the magnitude of the covariate effect: Low ($\beta_{\mathbf{X}} = -0.5$; light gray), High ($\beta_{\mathbf{X}} = -2.0$; white), and Extreme ($\beta_{\mathbf{X}} = -10000$; dark gray). Yellow violins labeled as Reference in the top row show the results for a baseline scenario without heterogeneity in detection probability

Continuous, detector-level variation in detectability

We observed increasingly negative bias in $\hat{N}$ with increasing spatial autocorrelation (Fig. 2; Table S2.2, Online Appendix 2). The magnitude of RB in $\hat{N}$ obtained with high spatial autocorrelation (simulation scenarios 1 and 4: median Moran's $I = 0.96$; median RB($\hat{N}$) = 16%) was substantially greater than that for scenarios with low spatial autocorrelation (scenarios 3 and 6: median Moran's $I = 0$; median RB($\hat{N}$) = 0.2%). This pattern was amplified when the amount of variation in detectability was high (scenario 4: median RB($\hat{N}$) = 30%). In contrast, we detected no noticeable bias in $\hat{\sigma}$ (Fig. 2), even when the amount of variation in detectability was high and spatial autocorrelation was high or intermediate (scenarios 4 and 5: median RB($\hat{\sigma}$) = 4% and 7%, respectively).

The pattern in precision of $\hat{N}$ and $\hat{\sigma}$ were almost identical across the scenarios considered (Fig. 3).

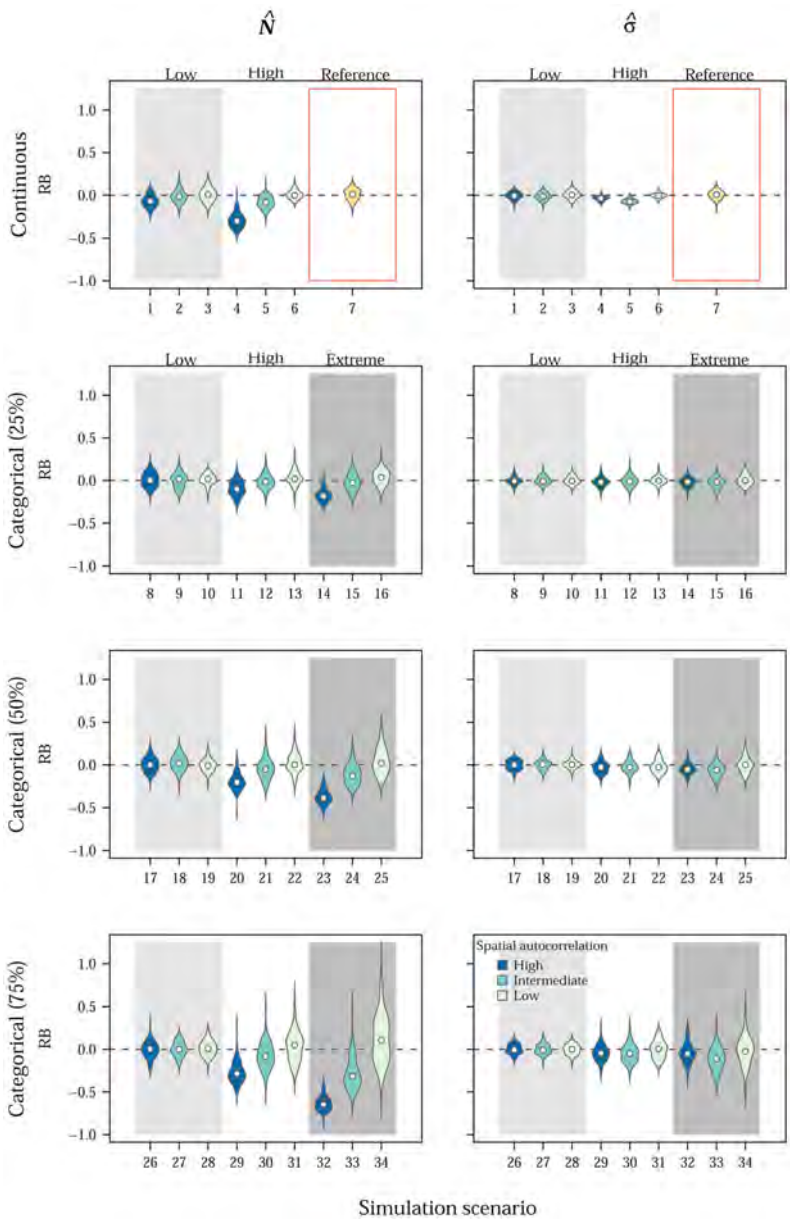

When the amount of variation in detectability was low (scenarios 1–3), precision of the parameter estimates were comparable to those of the reference scenario without spatial heterogeneity in detection probability (scenario 7: median CV($\hat{N}$) = 7% and median CV($\hat{\sigma}$) = 5%). Precision of $\hat{N}$ and $\hat{\sigma}$ were inflated when the magnitude of variation in detectability was high (scenarios 4–6: median CV($\hat{N}$) = 5% and median CV($\hat{\sigma}$) = 3%), where increasing the spatial

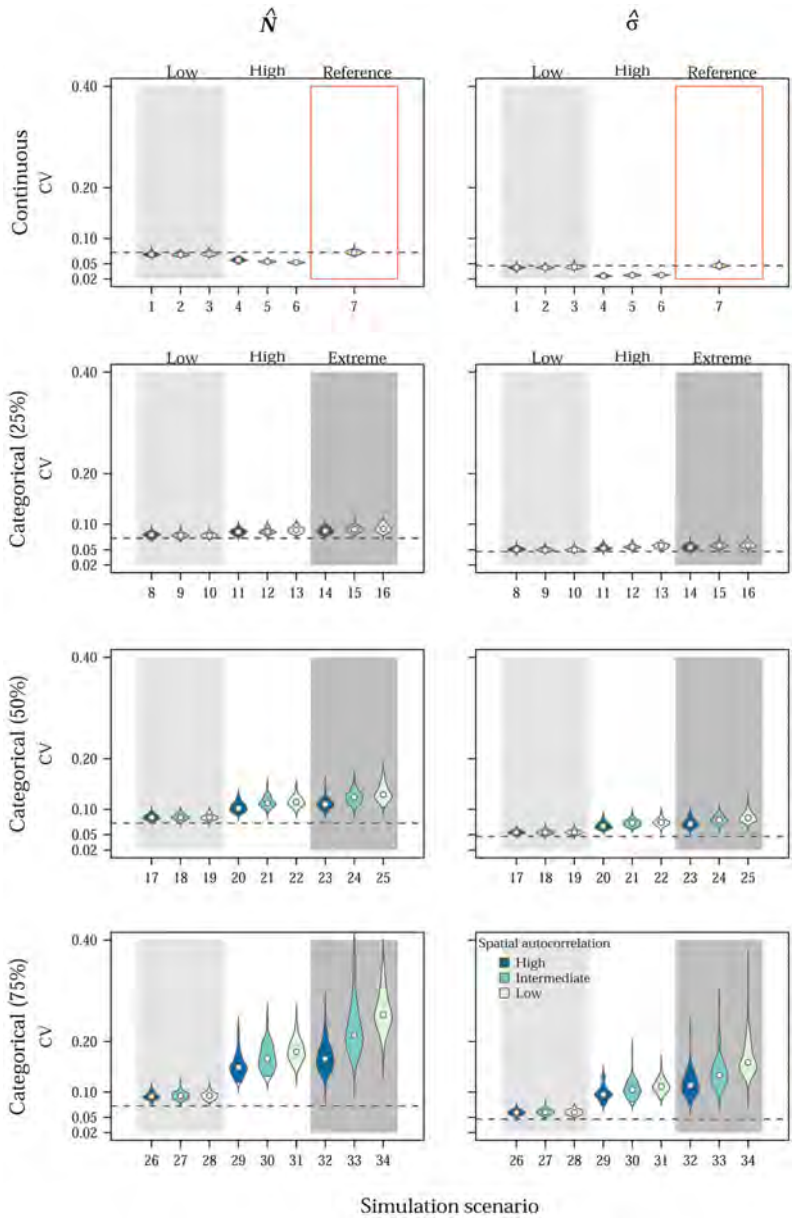

autocorrelation slightly decreased the precision of $\hat{N}$ (scenario 4; Table S2.2, Online Appendix 2).

Coverage of both $\hat{N}$ and, to a lesser extent, $\hat{\sigma}$ were drastically impacted by spatial autocorrelation (Fig. 4; Table S2.2, Online Appendix 2). In situations of high spatial autocorrelation and low variability in detection probability, we observed a 14% reduction in coverage of $\hat{N}$, compared to low spatial autocorrelation (from Coverage($\hat{N}$) = 93% in scenario 3 to Coverage($\hat{N}$) = 80% in scenario 1). The combination of high spatial

◀**Fig. 3** Coefficient of variation (CV) for population size ($\hat{N}$) and the spatial scale parameter of the half-normal detection function ($\hat{\sigma}$) estimated by a spatial capture-recapture model fitted to simulated data sets. Spatial variation in detection was simulated but not accounted for in the estimation model. Numbers provided on the x-axes refer to the unique ID of the simulation scenario and link with the more detailed information provided for each simulation in Online Appendix 2. Violins show the effects of spatial autocorrelation in the detector-level covariates simulated (decreasing from dark [High] to light colors [Low]) in different scenarios of continuous (top row) and discrete categorical (bottom three rows) variation in baseline detection probability. For the categorical scenarios, the proportions of detectors that belong to a group of detectors with lower detectability increases from top (25%) to bottom (75%). Background colors correspond to three different sets of simulation scenarios with similar values of the magnitude of the covariate effect: Low ($\beta_{\mathbf{X}} = -0.5$; light gray), High ($\beta_{\mathbf{X}} = -2.0$; white), and Extreme ($\beta_{\mathbf{X}} = -10000$; dark gray). Yellow violins labaled as Reference in the top row show the results for a baseline scenario without heterogeneity in detection probability, which was included for reference. The dashed lines show median CV for the parameter estimates achieved in the reference scenario

autocorrelation and high variation in detectability led to coverage of $\hat{N}$ as low as 3% (scenario 4; Fig. 4). The pattern was less pronounced for $\hat{\sigma}$ (scenario 4: Coverage($\hat{\sigma}$) = 70%). However, we detected a drastic decrease in the coverage of $\hat{\sigma}$ for the scenario of intermediate spatial autocorrelation and high amount of variation in detectability (scenario 5: median Moran's $I = 0.63$, Coverage($\hat{\sigma}$) = 26%; Fig. 4).

Categorical, detector-level variation in detectability

We observed increasing negative bias in $\hat{N}$ with increasing spatial autocorrelation and increasing proportion of detectors with lower detectability (Fig. 2; Table S2.2, Online Appendix 2). The bias was particularly pronounced in scenarios of extreme, spatially autocorrelated variation in detectability (median Moran's I = 0.86), where 50% or more of detectors were inactive, ultimately leading to an entire region with little or no sampling (scenarios 23 and 32: median RB($\hat{N}$) = 49%). However, when the variation in detectability was low (scenarios 8–10, 17–19, and 26–28), $\hat{N}$ was minimally affected in terms of bias regardless of the spatial autocorrelation and proportions of detectors with lower detectability (Table S2.2, Online Appendix 2). Similarly, when spatial autocorrelation in detectability was low, $\hat{N}$ remained relatively unbiased even in the extreme scenarios of a portion of detectors being inactive. We observed no systematic bias in $\hat{\sigma}$ under any of the scenarios tested (Fig. 2; Table S2.2, Online Appendix 2).

Precision of $\hat{N}$ and $\hat{\sigma}$ decreased with increasing proportions of detectors with lower detectability and increasing variation in detectability (Fig. 3; Table S2.2, Online Appendix 2). However, precision increased with spatial autocorrelation. For the extreme scenario of a partially-sampled area, when 75% of the detectors were inactive and spatial autocorrelation was low (scenario 34; Fig. 3), median CV($\hat{N}$) and median CV($\hat{\sigma}$) increased by 249% and 242%, respectively, compared to the reference scenario. In contrast, the increase in median CV($\hat{N}$) and median CV($\hat{\sigma}$) was 129% and 145%, respectively, for the scenario of high spatial autocorrelation (scenario 32; Table S2.2, Online Appendix 2).

The coverage of $\hat{N}$ drastically decreased with increasing spatial autocorrelation (Fig. 4). With high spatial autocorrelation, the coverage of $\hat{N}$ dropped to between 39% and 44% in the presence of high variation in detectability and higher proportions of detectors with lower detectability (scenarios 29 and 20). When more than 50% of the detectors were inactive, coverage of $\hat{N}$ was near 0 (scenarios 23 and 32; Fig. 4). Coverage was nominal for $\hat{\sigma}$ under low and high levels of spatial autocorrelation, and only decreased to between 79% and 87% when spatial autocorrelation was intermediate (scenarios 15, 24, and 33: median Moran's I = 0.42; Table S2.2, Online Appendix 2).

Discussion

Our study revealed that unmodeled spatial variation in detection probability, which is ubiquitous in wildlife monitoring studies, can have pronounced consequences for inferences from SCR analyses. The critical factor is spatial autocorrelation in detection probability: highly autocorrelated and highly variable detectability leads to pronounced bias and reduction in precision and coverage of SCR estimates of population size, the main parameter of interest in such studies (Royle et al. 2014, 2018). Conversely, at low levels of spatial autocorrelation, SCR model estimates

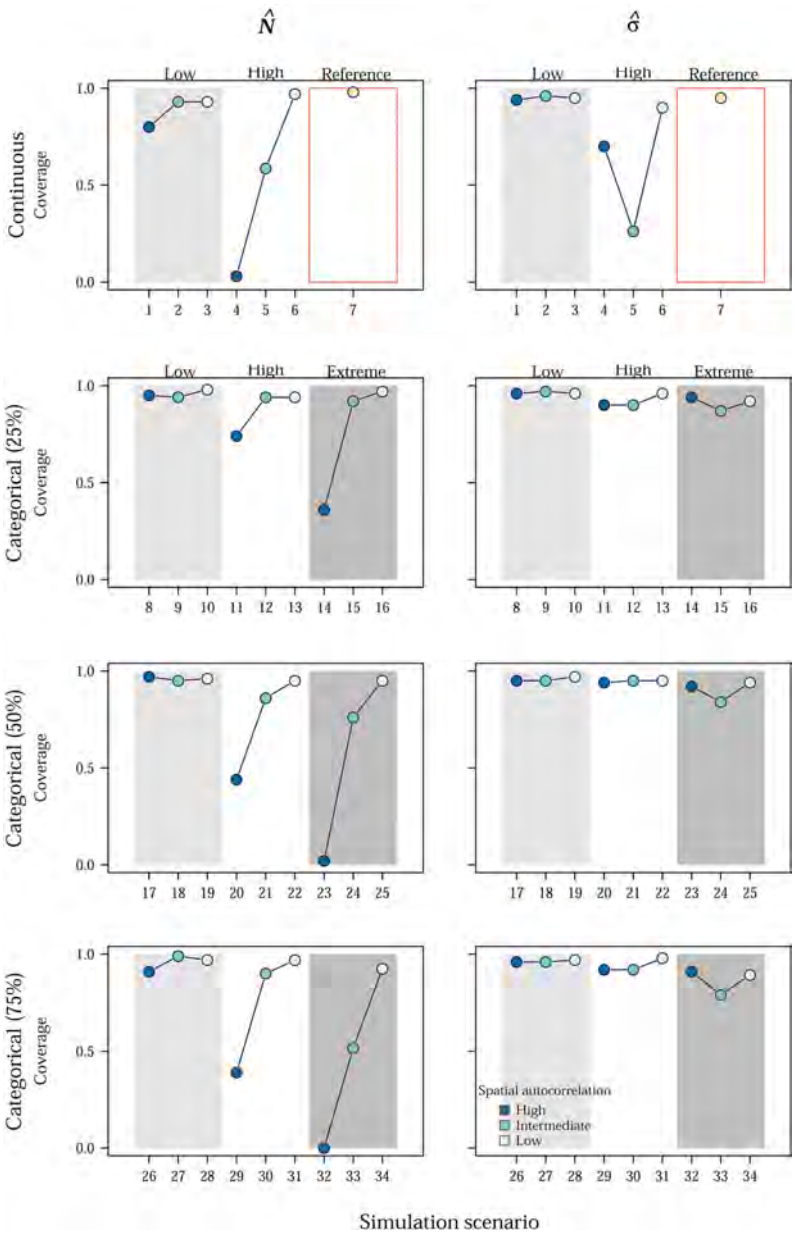

remained robust even to extremely high levels of unmodeled spatial heterogeneity in detection probability. Estimates of the spatial scale parameter of the half-normal detection function were, however, unbiased and coverage remained comparatively high for most scenarios of spatially autocorrelated detection probability. Nonetheless, the pattern of reduction

◀**Fig. 4** Coverage probability of the 95% credible intervals of population size ($\hat{N}$) and the spatial scale parameter of the half-normal detection function ($\hat{\sigma}$) estimated by a spatial capture-recapture model fitted to simulated data sets. Spatial variation in detection was simulated but not accounted for in the estimation model. Numbers provided on the x-axes refer to the unique ID of the simulation scenario and link with the more detailed information provided for each simulation in Online Appendix 2. Points show the effects of spatial autocorrelation of continuous (top row) or discrete categorical (bottom three rows) baseline detection probabilities (decreasing from dark [High] to light colors [Low]). For the categorical scenarios, the proportions of detectors that belong to a group of detectors with lower detectability increases from top (25%) to bottom (75%). Background colors correspond to three different levels of variation in the baseline detection probability: Low ($\beta_{\mathbf{X}} = -0.5$; light gray), High ($\beta_{\mathbf{X}} = -2.0$; white), and Extreme ($\beta_{\mathbf{X}} = -10000$; dark gray). Yellow points labeled as Reference in the top row show results for a baseline scenario without heterogeneity in detection probability

in precision of the estimates of the scale parameter was similar to those in the estimates of population size.

SCR is a powerful analytical tool for spatially explicit inference on the ecology of wild populations while accounting for imperfect detection (Royle et al. 2018). One of the advantages of SCR models over non-spatial capture-recapture models is the ability to address the effects of known spatial variation in detectability as a result of the spatial configuration of ACs relative to detectors and detector-specific characteristics; thus, providing a more realistic model of the detection process (Efford et al. 2013; Royle et al. 2014). Yet, despite the spatially explicit nature of SCR data collection and analysis, it is liable to be afflicted by unknown or undocumented variation in detection probability; for example, due to inadvertent (e.g., equipment failure, within-individual variations) or design-induced factors (e.g., non-random or preferential sampling), or as the result of pooling or integrating data across multiple survey methods or detectors (Efford et al. 2013; Howe et al. 2013; Efford and Mowat 2014; Royle et al. 2013, 2014; Gerber and Parmenter 2015). Consistent with our predictions, failure to adequately account for variable and spatially autocorrelated detection probability may bias SCR parameter estimates, impact estimates of precision, and generally lead to erroneous inferences. In extreme cases among the ones we considered, this led to up to 65% bias and to virtually zero probability that the credible interval contains the true value of population size (Table S2.2, Online Appendix 2). Comparable results are reported when individual heterogeneity remains unaccounted for in both spatial and non-spatial capture-recapture (Royle et al. 2013; Gimenez et al. 2018a, Stevenson et al. 2021). Thus, a misspecified detection model may not only impact inferences, but also reduce the chance of meeting the management and conservation objectives that often motivate these studies.

We observed the strongest systematic bias in cases where a substantial and distinct region of the detector space was unsampled, essentially leaving a hole in the detector grid that remained unaccounted for in the model. The pronounced negative bias in $\hat{N}$ that arises in these situations can be explained if we consider that individuals with ACs within such a hole have a high chance of being missed entirely during sampling, essentially creating a latent class of individuals with very low or zero detectability. This is the case when a portion of detectors are assumed to be active or searched when they are not. As a consequence, detection probability estimates are biased high as they are based primarily on recaptures of individuals detected in active regions of the detector grid, and estimates of abundance and density are consequently biased low. This pattern is amplified by the magnitude of variation in detection probability between regions of lower and higher detectability, and by the size of the region with lower detection probability (Table S2.2, Online Appendix 2).

Situations where entire regions of the study area remain unsampled are fairly common in monitoring studies, where the data are gathered opportunistically, either in part or as a whole (Conn et al. 2017; Altwegg and Nichols 2019; Sicacha-Parada et al. 2021). Unstructured sampling can augment information, and thus improve population inferences about rare or elusive species (Thompson et al. 2012; Tenan et al. 2017; Sun et al. 2019; Bischof et al. 2020a). Opportunistically-collected data obtained as part of public surveys (e.g., citizen-science data) are sometimes integrated into monitoring programs as this allows investigators to sample areas at unprecedented scales with lower costs and the added benefit of public involvement in management and conservation practices (Altwegg and Nichols 2019; Bischof et al. 2020a; Sicacha-Parada et al. 2021). To minimize and account for variation in detection probability in such sampling

schemes, volunteers should be encouraged to visit all habitats within the study area, reduce variability in observer proficiency by providing standardized training, and collect data on potentially relevant covariates (Altwegg and Nichols 2019).

We considered a wide range of scenarios in terms of the magnitude and spatial configuration of variability in detection probability. Our extreme scenarios of unknown and unmodeled, high spatial variation and high autocorrelation in p_0 are probably less common, but plausible, in real-life SCR monitoring studies. These scenarios were specifically motivated by our previous work on landscape-scale monitoring of large carnivores, where spatial variation in effort can be challenging to quantify because the data are collected in a structured fashion by field personnel associated with multiple jurisdictions and opportunistically by volunteer members of the public (Bischof et al. 2016, 2017, 2020a; Milleret et al. 2020). These SCR studies revealed significant differences in baseline detection probability across administrative units (i.e., counties in Sweden and large carnivore management regions in Norway). Even after controlling for spatio-temporal variations in sampling effort by including detector-level and individual covariates on the baseline detection probability, spatial variation in detectability remained substantial, presumably linked with unmeasured regional differences in search effort by volunteers and sampling configuration implemented by the authorities (Bischof et al. 2020a). Nevertheless, we expect the consequences of such an unmodeled spatial heterogeneity to be relaxed when detection probability is relatively high. In such situations, unknown and unmodeled variation in detectability is likely to be less problematic as individuals from the population are more likely to be detected at multiple detectors (i.e., increase in both the proportion of detected individuals from the population and spatial recaptures). The effects of spatial heterogeneity in detectability may also be mediated by species space-use characteristics. Here, we simulated a target population with intermediate home-range overlap ($k = \sigma\sqrt{Density} = 0.83$; Efford et al. 2016) with a density of 0.3 AC/du^2, which was constant across simulation scenarios. For species with small home-range sizes, where the spatial scale parameter is small relative to the distance between detectors, unmodeled spatially autocorrelated detection probability may lead to more problematic inferences due to the increased risk of individuals going completely undetected in the resulting "holes" in the detector grid. In addition, we assumed homogeneous population density across the study area, which is rarely, if ever, the case in wild populations. Previous studies have suggested that the consequences of unmodeled heterogeneity in detection probability could be amplified when detectability is correlated with density (e.g., Clark 2019; Paterson et al. 2019). As a positive correlation between animal density and detection probability results in a positive bias in estimates of population size, we expect that the biasing effects we detected would be comparatively less pronounced when the unmodeled detection probability is spatially autocorrelated but the effects of unmodeled spatial heterogeneity would not be mitigated. The misspecification of the observation sub-model may also lead to confounding effects between variation in detection probability and animal density that must be accounted for in order to avoid flawed inferences (Efford et al. 2013).

When the drivers of spatial variation in detection probability are known or suspected, the variation can be accounted for by, for example, including relevant covariates (e.g., transect length, camera trap nights, habitat or line-of-sight visibility) in the observation sub-model of SCR models (Royle et al. 2009, 2014; Efford et al. 2013; Efford and Mowat 2014; Bischof et al. 2017, 2020a). In the absence of proxies that can serve as fixed or random effects, how should investigators deal with unknown spatial heterogeneity in detectability in SCR analyses? One solution would be to discard affected data, such as observations contributed by members of the public without corresponding measures of search effort. This, however, would lead to a loss of potentially valuable information, both in terms of number of individuals detected and spatial recaptures (Marques et al. 2011; Sollmann et al. 2012; Tourani et al. 2020b). Explicitly modeling spatially autocorrelated detectability, for example using mixture methods (e.g., by drawing baseline detection probability at each detector from a finite mixture of distributions; Royle 2006) or conditional autoregressive (CAR) models, may offer a solution. CAR models have been implemented in other hierarchical modeling frameworks, such as non-spatial capture-recapture and spatial distribution modeling (e.g., Johnson et al. 2013; Chen and Ficetola 2019;

Nicolau et al. 2020), but we are not aware of similar extensions in SCR studies. The added complexity resulting from the inclusion of an autoregressive component on a latent variable like detection probability could pose a significant computation barrier to implementation in Bayesian SCR at large spatial scales. However, recent advances in both software (de Valpine et al. 2017; Bischof et al. 2020b) and Bayesian SCR model formulations (Milleret et al. 2018; Turek et al. 2021) have improved model fitting efficiency, allowing fitting SCR models of unprecedented complexity and spatial scales (Bischof et al. 2020a); thus, opening new possibilities.

Goodness-of-fit tests could help practitioners diagnose potential violations of model assumptions, including unmodeled spatial variation in detection probability, and determine whether there is a need to account for it in the model in the first place. Such diagnostics should be an integral part of any ecological modeling exercise (Conn et al. 2018), and Bayesian p-values (Gelman et al. 1996) have been proposed as a general framework for goodness-of-fit testing of Bayesian SCR models (Royle et al. 2014). However, goodness-of-fit diagnostics for SCR is a developing field of research and specific tests and recommendations, such as those that were developed for non-spatial capture-recapture models (e.g., Gimenez et al. 2018b) are still lacking. Thus, testing and accounting for possible violations, as well as correcting model estimates, is still challenging in SCR.

Conclusions

Unmodeled spatially autocorrelated variation in detection probability can noticeably impact the reliability of inferences derived using SCR, when variability in detection and spatial autocorrelation is high. This specifically affects estimates of abundance and density, primary parameters in wildlife monitoring studies, and can therefore have severe consequences for wildlife management and conservation. Unobserved spatial variability in detection probability is likely ubiquitous in real-life SCR studies, and we encourage research to develop approaches that help practitioners diagnose and account for it.

Acknowledgements This study received funding from the Norwegian Research Council grant 286886 (project WildMap). We thank two anonymous reviewers and S. Dey for their comments on the manuscript.

Author contributions Conceptualization: RB; Design and methodology: EM, RB, MT, CM, PD; Analysis: EM; Writing - original draft preparation: EM; Writing - review and editing: EM, RB, CM, MT, PD.

Funding Open access funding provided by Norwegian University of Life Sciences.

Declarations

Conflict of interest The authors have no interests which might be perceived as posing a conflict or bias.

References

Altwegg R, Nichols JD (2019) Occupancy models for citizen-science data. Methods Ecol Evol 10(1):8–21

Beng KC, Corlett RT (2020) Applications of environmental dna (edna) in ecology and conservation: opportunities, challenges and prospects. Biodivers Conserv 29(7):2089–2121

Bird TJ, Bates AE, Lefcheck JS, Hill NA, Thomson RJ, Edgar GJ, Stuart-Smith RD, Wotherspoon S, Krkosek M, Stuart-Smith JF (2014) Statistical solutions for error and bias in global citizen science datasets. Biol Conserv 173:144–154

Bischof R, Brøseth H, Gimenez O (2016) Wildlife in a politically divided world: insularism inflates estimates of brown bear abundance. Conserv Lett 9(2):122–130

Bischof R, Steyaert SM, Kindberg J (2017) Caught in the mesh: roads and their network-scale impediment to animal movement. Ecography 40(12):1369–1380

Bischof R, Milleret C, Dupont P, Chipperfield J, Tourani M, Ordiz A, de Valpine P, Turek D, Royle JA, Gimenez O, Flagstad Ø, Åkesson M, Svensson L, Brøseth H, Kindberg J (2020a) Estimating and forecasting spatial population dynamics of apex predators using transnational genetic monitoring. Proc Natl Acad Sci USA 117(48):30531–30538

Bischof R, Turek D, Milleret C, Ergon T, Dupont P, de Valpine, P (2020b) nimbleSCR: Spatial Capture-Recapture (SCR)

methods using 'nimble'. https://cran.r-project.org/web/packages/nimbleSCR/index.html
Borchers DL, Efford MG (2008) Spatially explicit maximum likelihood methods for capture-recapture studies. Biometrics 64(2):377–385
Borchers DL, Laake JL, Southwell C, Paxton CG (2006) Accommodating unmodeled heterogeneity in double-observer distance sampling surveys. Biometrics 62(2):372–378
Brooks SP, Gelman A (1998) General methods for monitoring convergence of iterative simulations. J Comput Graph Stat 7(4):434–455
Burton AC, Neilson E, Moreira D, Ladle A, Steenweg R, Fisher JT, Bayne E, Boutin S (2015) Wildlife camera trapping: a review and recommendations for linking surveys to ecological processes. J Appl Ecol 52(3):675–685
Chandler R, Hepinstall-Cymerman J (2016) Estimating the spatial scales of landscape effects on abundance. Landsc Ecol 31(6):1383–1394
Chao A (2001) An overview of closed capture-recapture models. J Agric Biol Environ Stat 6(2):158–175
Chen W, Ficetola GF (2019) Conditionally autoregressive models improve occupancy analyses of autocorrelated data: an example with environmental DNA. Mol Ecol Resour 19(1):163–175
Clark JD (2019) Comparing clustered sampling designs for spatially explicit estimation of population density. Popul Ecol 61(1):93–101
Conn PB, Thorson JT, Johnson DS (2017) Confronting preferential sampling when analysing population distributions: diagnosis and model-based triage. Methods Ecol Evol 8(11):1535–1546
Conn PB, Johnson DS, Williams PJ, Melin SR, Hooten MB (2018) A guide to Bayesian model checking for ecologists. Ecol Monogr 88(4):526–542
de Valpine P, Turek D, Paciorek CJ, Anderson-Bergman C, Lang DT, Bodik R (2017) Programming with models: writing statistical algorithms for general model structures with NIMBLE. J Comput Graph Stat 26(2):403–413
Efford M (2004) Density estimation in live-trapping studies. Oikos 106(3):598–610
Efford MG (2011) Estimation of population density by spatially explicit capture-recapture analysis of data from area searches. Ecology 92(12):2202–2207
Efford MG, Fewster RM (2013) Estimating population size by spatially explicit capture-recapture. Oikos 122(6):918–928
Efford MG, Mowat G (2014) Compensatory heterogeneity in spatially explicit capture-recapture data. Ecology 95(5):1341–1348
Efford MG, Borchers DL, Mowat G (2013) Varying effort in capture-recapture studies. Methods Ecol Evol 4(7):629–636
Efford M, Dawson DK, Jhala Y, Qureshi Q (2016) Density-dependent home-range size revealed by spatially explicit capture-recapture. Ecography 39(7):676–688
Gaspard G, Kim D, Chun Y (2019) Residual spatial autocorrelation in macroecological and biogeographical modeling: a review. J Ecol Environ 43(1):1–11
Gelman A, Meng X-L, Stern H (1996) Posterior predictive assessment of model fitness via realized discrepancies. Stat Sin 6(4):733–760
Gerber BD, Parmenter RR (2015) Spatial capture-recapture model performance with known small-mammal densities. Ecol Appl 25(3):695–705
Gimenez O, Viallefont A, Charmantier A, Pradel R, Cam E, Brown CR, Anderson MD, Brown MB, Covas R, Gaillard J-M (2008) The risk of flawed inference in evolutionary studies when detectability is less than one. Am Nat 172(3):441–448
Gimenez O, Cam E, Gaillard J-M (2018a) Individual heterogeneity and capture-recapture models: what, why and how? Oikos 127(5):664–686
Gimenez O, Lebreton JD, Choquet R, Pradel R (2018b) R2ucare: an R package to perform goodness-of-fit tests for capture-recapture models. Methods Ecol Evol 9(7):1749–1754
Guélat J (2013) Spatial autocorrelation (introduction). https://rpubs.com/jguelat/autocorr
Guélat J, Kéry M (2018) Effects of spatial autocorrelation and imperfect detection on species distribution models. Methods Ecol Evol 9(6):1614–1625
Hijmans RJ (2019) raster: Geographic data analysis and modeling. https://cran.r-project.org/package=raster
Howe EJ, Obbard ME, Kyle CJ (2013) Combining data from 43 standardized surveys to estimate densities of female American black bears by spatially explicit capture-recapture. Popul Ecol 55(4):595–607
Johnson DS, Conn PB, Hooten MB, Ray JC, Pond BA (2013) Spatial occupancy models for large data sets. Ecology 94(4):801–808
Kellner KF, Swihart RK (2014) Accounting for imperfect detection in ecology: a quantitative review. PLoS ONE 9:e111436. https://doi.org/10.1371/journal.pone.0111436
Kendall KC, Graves TA, Royle JA, Macleod AC, McKelvey KS, Boulanger J, Waller JS (2019) Using bear rub data and spatial capture-recapture models to estimate trend in a brown bear population. Sci Rep 9(1):1–11
Kristensen TV, Kovach AI (2018) Spatially explicit abundance estimation of a rare habitat specialist: implications for SECR study design. Ecosphere 9(5):e02217
Lichstein JW, Simons TR, Shriner SA, Franzreb KE (2002) Spatial autocorrelation and autoregressive models in ecology. Ecol Monogr 72(3):445–463
Link WA (2003) Nonidentifiability of population size from capture-recapture data with heterogeneous detection probabilities. Biometrics 59(4):1123–1130
Lukacs PM, Burnham KP (2005) Review of capture-recapture methods applicable to noninvasive genetic sampling. Mol Ecol 14(13):3909–3919
Marques TA, Thoma L, Royle JA (2011) A hierarchical model for spatial capture-recapture data: comment. Ecology 92(2):526–528
Milleret C, Dupont P, Brøseth H, Kindberg J, Royle JA, Bischof R (2018) Using partial aggregation in spatial capture recapture. Methods Ecol Evol 9(8):1896–1907
Milleret C, Dupont P, Akesson M, Svensson L, Brøseth H, Bischof R (2020) Consequences of reduced sampling intensity for estimating population size of wolves in Scandinavia with spatial capture-recapture models. Technical report. https://hdl.handle.net/11250/2650153
Moran P (1950) Notes on continuous stochastic phenomena. Biometrika 37(1):17–23

Nichols JD, Williams BK (2006) Monitoring for conservation. Trends Ecol Evol 21(12):668–673
Nicolau PG, Sørbye SH, Yoccoz NG (2020) Incorporating capture heterogeneity in the estimation of autoregressive coefficients of animal population dynamics using capture-recapture data. Ecol Evol 10(23):12710–12726
Paterson JT, Proffitt K, Jimenez B, Rotella J, Garrott R (2019) Simulation-based validation of spatial capture-recapture models: a case study using mountain lions. PLoS ONE 14(4):1–20
R Core Team (2019) R: a language and environment for statistical computing. R Foundation for Statistical Computing, Vienna, Austria. https://www.R-project.org/
Royle JA (2006) Site occupancy models with heterogeneous detection probabilities. Biometrics 62(1):97–102
Royle JA, Young KV (2008) A hierarchical model for spatial capture-recapture data. Ecology 89(8):2281–2289
Royle JA, Dorazio RM, Link WA (2007) Analysis of multinomial models with unknown index using data augmentation. J Comput Graph Stat 16(1):67–85
Royle JA, Nichols JD, Karanth KU, Gopalaswamy AM (2009) A hierarchical model for estimating density in camera-trap studies. J Appl Ecol 46(1):118–127
Royle JA, Chandler RB, Gazenski KD, Graves TA (2013) Spatial capture-recapture models for jointly estimating population density and landscape connectivity. Ecology 94(2):287–294
Royle JA, Chandler RB, Sollmann R, Gardner B (2014) Spatial capture-recapture. Academic Press, Waltham
Royle JA, Fuller AK, Sutherland C (2018) Unifying population and landscape ecology with spatial capture-recapture. Ecography 41(3):444–456
Sicacha-Parada J, Steinsland I, Cretois B, Borgelt J (2021) Accounting for spatial varying sampling effort due to accessibility in citizen science data: a case study of moose in Norway. Spat Stat 42:100446. https://doi.org/10.1016/j.spasta.2020.100446
Sokal RR, Oden NL (1978) Spatial autocorrelation in biology. 1. Methodology. Biol J Linn Soc 10(2):199–228
Sollmann R, Gardner B, Belant JL (2012) How does spatial study design influence density estimates from spatial capture-recapture models? PLoS ONE 7(4):1–8
Steenweg R, Hebblewhite M, Whittington J, Lukacs P, McKelvey K (2018) Sampling scales define occupancy and underlying occupancy-abundance relationships in animals. Ecology 99(1):172–183
Stevenson BC, Fewster RM, Sharma K (2021) Spatial correlation structures for detections of individuals in spatial capture–recapture models. Biometrics. https://doi.org/10.1111/biom.13502
Sun CC, Royle JA, Fuller AK (2019) Incorporating citizen science data in spatially explicit integrated population models. Ecology 100(9):1–12
Tenan S, Pedrini P, Bragalanti N, Groff C, Sutherland C (2017) Data integration for inference about spatial processes: a model-based approach to test and account for data inconsistency. PLoS ONE 12(10):e0185588
Thompson CM, Royle JA, Garner JD (2012) A framework for inference about carnivore density from unstructured spatial sampling of scat using detector dogs. J Wildl Manag 76(4):863–871
Tourani M, Brøste EN, Bakken S, Odden J, Bischof R (2020a) Sooner, closer, or longer: detectability of mesocarnivores at camera traps. J Zool 312:259–270
Tourani M, Dupont P, Nawaz MA, Bischof R (2020b) Multiple observation processes in spatial capture-recapture models: how much do we gain? Ecology 101(7):1–8
Turek D, Milleret C, Ergon T, Brøseth H, Dupont P, Bischof R, de Valpine P (2021) Efficient estimation of large-scale spatial capture-recapture models. Ecosphere 12(2):e03385
Walther BA, Moore JL (2005) The concepts of bias, precision and accuracy, and their use in testing the performance of species richness estimators, with a literature review of estimator performance. Ecography 28(6):815–829

Supplementary Information Moqanaki EM, Milleret C, Tourani M, Dupont P, Bischof R. Consequences of ignoring variable and spatially autocorrelated detection probability in spatial capture-recapture. *Landscape Ecology*, https://doi.org/10.1007/s10980-021-01283-x

Appendix 1: R scripts and model parameters

R scripts for simulating spatially autocorrelated detector-specific covariates and single-session spatial capture-recapture analysis in NIMBLE can be found here: https://github.com/eMoqanaki/HeterogeneousDetectionSCR

Table S1.1: Description, prior distribution, and initial values for the focal parameters estimated by the spatial capture-recapture model used in this study.

Parameter	Description	Prior	Initial values
ψ	Inclusion probability	Uniform(0,1)	Uniform(0,1)
σ	Scale parameter of the detection function	Uniform(0,50)	Uniform(0,10)
p_0	Baseline detection probability	Uniform(0,1)	Uniform(0,1)
λ_0	Baseline detection rate	Uniform(0,10)	Uniform(0,10)

Appendix 2: Simulation characteristics and results

Table S2.1: Characteristics of the simulation scenarios included in this study. Data were generated from a Bernoulli detection process. N°: the unique scenario ID; $\beta_{\mathbf{X}}$: magnitude of the effect of the spatial, detector-specific covariate for the baseline detection probability (continuous or categorical spatial variation); %Det: percentage of detectors (out of 400) with lower detectability (for categorical variation only); ϕ: parameter defining the rate of decline in correlation with distance; Moran's I: median and range (minimum and maximum values) of Moran's index of global spatial autocorrelation across 100 detector-specific covariates simulated for each scenario; p_{0_j}: range (min, max) of detector-specific, baseline detection probability; Ndetected: number of individuals detected out of 250 (median and range); Ndetections: number of detections or recaptures (median and range) across the 20×20-square distance unit (du^2) detector grid, surrounded by an unsampled 4.5×4.5-du^2 habitat buffer. See the main text for additional information.

N°	$\beta_{\mathbf{X}}$	%Det	ϕ	Moran's I	p_{0_j}	Ndetected	Ndetections
Continuous							
1	−0.5	-	0.001	0.96 (0.93 - 0.98)	0.06 - 0.32	120 (100 - 140)	277 (212 - 342)
2	−0.5	-	1	0.62 (0.48 - 0.76)	0.06 - 0.32	126 (106 - 145)	280 (233 - 326)
3	−0.5	-	1000	0.00 (−0.05 - 0.08)	0.06 - 0.32	128 (107 - 148)	272 (218 - 320)
4	−2.0	-	0.001	0.95 (0.91 - 0.98)	0.003 - 0.9	112 (88 - 156)	498 (380 - 620)
5	−2.0	-	1	0.63 (0.47 - 0.75)	0.003 - 0.9	140 (110 - 173)	492 (385 - 584)
6	−2.0	-	1000	0.00 (−0.08 - 0.07)	0.003 - 0.9	152 (137 - 175)	496 (410 - 595)
None							
7*	-	-	-	-	0.15	124 (106 - 141)	256 (216 - 298)
Categorical							
8	−0.5	25	0.001	0.85 (0.60 - 0.90)	0.1, 0.15	117 (100 - 138)	226 (176 - 278)
9	−0.5	25	1	0.41 (0.29 - 0.58)	0.1, 0.15	118 (100 - 137)	232 (185 - 278)
10	−0.5	25	1000	0.00 (−0.08 - 0.08)	0.1, 0.15	119 (99 - 133)	232 (186 - 265)

* The reference scenario with constant detection probability (i.e., no misspecification of the detection process).

Table S2.1: (continued).

Nº	$\beta_{\mathbf{X}}$	%Det	ϕ	Moran's I	p_{0_j}	Ndetected	Ndetections
Categorical							
11	−2.0	25	0.001	0.86 (0.64 - 0.90)	0.02, 0.15	105 (86 - 128)	198 (165 - 251)
12	−2.0	25	1	0.41 (0.22 - 0.61)	0.02, 0.15	110 (90 - 134)	200 (164 - 242)
13	−2.0	25	1000	0.00 (−0.06 - 0.05)	0.02, 0.15	112 (88 - 130)	200 (161 - 238)
14	−10000	25	0.001	0.86 (0.61 - 0.90)	0, 0.15	96 (78 - 116)	187 (152 - 242)
15	−10000	25	1	0.42 (0.27 - 0.56)	0, 0.15	106 (87 - 125)	188 (157 - 231)
16	−10000	25	1000	0.00 (−0.07 - 0.07)	0, 0.15	110 (92 - 135)	192 (159 - 242)
17	−0.5	50	0.001	0.89 (0.75 - 0.92)	0.1, 0.15	112 (94 - 129)	209 (165 - 246)
18	−0.5	50	1	0.45 (0.30 - 0.59)	0.1, 0.15	114 (91 - 132)	210 (170 - 272)
19	−0.5	50	1000	0.00 (−0.05 - 0.07)	0.1, 0.15	112 (93 - 130)	208 (170 - 262)
20	−2.0	50	0.001	0.89 (0.80 - 0.92)	0.02, 0.15	84 (51 - 102)	150 (92 - 182)
21	−2.0	50	1	0.44 (0.30 - 0.57)	0.02, 0.15	90 (71 - 109)	145 (112 - 178)
22	−2.0	50	1000	0.00 (−0.06 - 0.09)	0.02, 0.15	94 (70 - 115)	148 (106 - 192)
23	−10000	50	0.001	0.89 (0.78 - 0.91)	0, 0.15	68 (43 - 88)	125 (72 - 163)
24	−10000	50	1	0.44 (0.28 - 0.64)	0, 0.15	80 (59 - 104)	125 (90 - 162)
25	−10000	50	1000	0.00 (−0.05 - 0.06)	0, 0.15	86 (68 - 105)	129 (92 - 166)
26	−0.5	75	0.001	0.86 (0.64 - 0.90)	0.1, 0.15	107 (90 - 126)	188 (149 - 234)
27	−0.5	75	1	0.41 (0.22 - 0.56)	0.1, 0.15	106 (87 - 127)	185 (140 - 232)
28	−0.5	75	1000	0.00 (−0.06 - 0.05)	0.1, 0.15	107 (89 - 126)	184 (145 - 226)
29	−2.0	75	0.001	0.86 (0.62 - 0.90)	0.02, 0.15	63 (44 - 77)	94 (62 - 123)
30	−2.0	75	1	0.41 (0.28 - 0.56)	0.02, 0.15	68 (52 - 79)	94 (70 - 119)
31	−2.0	75	1000	0.00 (−0.07 - 0.06)	0.02, 0.15	69 (50 - 89)	93 (68 - 121)
32	−10000	75	0.001	0.85 (0.63 - 0.90)	0, 0.15	37 (15 - 61)	63 (29 - 104)
33	−10000	75	1	0.42 (0.21 - 0.56)	0, 0.15	46 (28 - 62)	62 (34 - 87)
34	−10000	75	1000	−0.01 (−0.06 - 0.11)	0, 0.15	52 (37 - 69)	63 (45 - 90)

Table S2.2: Relative bias (RB, median and 95% quantiles), coefficient of variation (CV, median and 95% quantiles), and coverage probability of the 95% confidence interval around the estimates of population size ($\hat{N}$) and the spatial scale parameter of the half-normal detection function ($\hat{\sigma}$) across each scenario from a standard, single-session, spatial capture-recapture model, where detection probability was erroneously considered to be constant across the 20×20-square distance unit detector grid. N°: the scenario number; Rep: number of successfully fitted, spatial capture-recapture models out of 100 replications of the data simulation procedure.

N°	Rep	$\hat{N}$				$\hat{\sigma}$			
		RB		CV	Coverage	RB		CV	Coverage
Continuous									
1	100	−0.07	(−0.22 - 0.06)	0.07 (0.06 - 0.08)	0.80	−0.01	(−0.09 - 0.07)	0.04 (0.04 - 0.05)	0.94
2	100	−0.01	(−0.16 - 0.15)	0.07 (0.06 - 0.07)	0.93	−0.01	(−0.09 - 0.07)	0.04 (0.04 - 0.05)	0.96
3	100	0.01	(−0.14 - 0.16)	0.07 (0.06 - 0.08)	0.93	0.01	(−0.08 - 0.09)	0.04 (0.04 - 0.05)	0.95
4	100	−0.30	(−0.44 - −0.11)	0.06 (0.05 - 0.06)	0.03	−0.04	(−0.10 - 0.02)	0.03 (0.02 - 0.03)	0.70
5	99	−0.08	(−0.21 - 0.03)	0.05 (0.05 - 0.06)	0.59	−0.07	(−0.13 - −0.01)	0.03 (0.02 - 0.03)	0.26
6	100	0.00	(−0.09 - 0.11)	0.05 (0.05 - 0.06)	0.97	0.00	(−0.06 - 0.06)	0.03 (0.03 - 0.03)	0.90
None									
7*	100	0.01	(−0.11 - 0.13)	0.07 (0.07 - 0.08)	0.98	0.01	(−0.08 - 0.09)	0.05 (0.04 - 0.05)	0.95
Categorical									
8	100	0.00	(−0.15 - 0.17)	0.08 (0.07 - 0.09)	0.95	0.00	(−0.09 - 0.11)	0.05 (0.04 - 0.06)	0.96
9	100	0.02	(−0.15 - 0.15)	0.08 (0.07 - 0.09)	0.94	−0.01	(−0.08 - 0.09)	0.05 (0.04 - 0.06)	0.97
10	100	0.02	(−0.14 - 0.12)	0.08 (0.07 - 0.09)	0.98	0.00	(−0.08 - 0.09)	0.05 (0.04 - 0.06)	0.96
11	100	−0.10	(−0.26 - 0.08)	0.09 (0.08 - 0.10)	0.74	−0.02	(−0.11 - 0.10)	0.05 (0.05 - 0.06)	0.90
12	100	−0.01	(−0.18 - 0.17)	0.09 (0.08 - 0.10)	0.94	−0.01	(−0.12 - 0.13)	0.06 (0.05 - 0.06)	0.90
13	100	0.02	(−0.14 - 0.21)	0.09 (0.08 - 0.10)	0.94	0.00	(−0.09 - 0.11)	0.06 (0.05 - 0.07)	0.96
14	100	−0.18	(−0.29 - 0.00)	0.09 (0.08 - 0.10)	0.36	−0.02	(−0.12 - 0.07)	0.06 (0.05 - 0.06)	0.94
15	100	−0.03	(−0.19 - 0.14)	0.09 (0.08 - 0.10)	0.92	−0.02	(−0.15 - 0.08)	0.06 (0.05 - 0.07)	0.87
16	100	0.04	(−0.13 - 0.20)	0.09 (0.08 - 0.11)	0.97	0.00	(−0.10 - 0.13)	0.05 (0.05 - 0.07)	0.92

* The reference scenario with constant detection probability (i.e., no misspecification of the detection process).

Table S2.2: (continued).

Nº	Rep	$\hat{N}$				$\hat{\sigma}$			
		RB		CV	Coverage	RB		CV	Coverage
Categorical									
17	100	0.00	(−0.14 - 0.17)	0.08 (0.08 - 0.09)	0.97	0.00	(−0.10 - 0.09)	0.05 (0.05 - 0.06)	0.95
18	100	0.02	(−0.16 - 0.20)	0.08 (0.07 - 0.10)	0.95	0.01	(−0.10 - 0.11)	0.05 (0.05 - 0.06)	0.95
19	100	−0.01	(−0.14 - 0.17)	0.08 (0.08 - 0.10)	0.96	0.01	(−0.09 - 0.09)	0.05 (0.05 - 0.06)	0.97
20	100	−0.20	(−0.34 - 0.03)	0.10 (0.09 - 0.13)	0.44	−0.03	(−0.15 - 0.10)	0.07 (0.06 - 0.08)	0.94
21	100	−0.05	(−0.26 - 0.19)	0.11 (0.10 - 0.14)	0.86	−0.03	(−0.17 - 0.13)	0.07 (−0.17 - 0.13)	0.95
22	100	0.00	(−0.21 - 0.26)	0.11 (0.10 - 0.14)	0.95	−0.03	(−0.15 - 0.14)	0.07 (0.06 - 0.09)	0.95
23	100	−0.38	(−0.52 - −0.21)	0.11 (0.09 - 0.14)	0.02	−0.05	(−0.17 - 0.11)	0.07 (0.06 - 0.09)	0.92
24	100	−0.13	(−0.31 - 0.15)	0.12 (0.10 - 0.16)	0.76	−0.06	(−0.20 - 0.09)	0.08 (0.07 - 0.10)	0.84
25	100	0.02	(−0.20 - 0.39)	0.13 (0.11 - 0.17)	0.95	0.00	(−0.16 - 0.19)	0.08 (0.07 - 0.11)	0.94
26	100	0.00	(−0.21 - 0.17)	0.09 (0.08 - 0.11)	0.91	0.00	(−0.11 - 0.11)	0.06 (0.05 - 0.07)	0.96
27	100	0.00	(−0.16 - 0.15)	0.09 (0.08 - 0.11)	0.99	−0.01	(−0.09 - 0.12)	0.06 (0.05 - 0.07)	0.96
28	100	0.01	(−0.14 - 0.20)	0.09 (0.08 - 0.11)	0.97	0.00	(−0.11 - 0.11)	0.06 (0.05 - 0.07)	0.97
29	100	−0.28	(−0.49 - 0.02)	0.15 (0.12 - 0.22)	0.39	−0.05	(−0.24 - 0.14)	0.10 (0.08 - 0.13)	0.92
30	100	−0.08	(−0.36 - 0.19)	0.17 (0.13 - 0.23)	0.90	−0.05	(−0.23 - 0.16)	0.10 (0.08 - 0.13)	0.92
31	97	0.05	(−0.26 - 0.43)	0.18 (0.15 - 0.23)	0.96	0.01	(−0.18 - 0.20)	0.11 (0.09 - 0.14)	0.97
32	100	−0.65	(−0.75 - −0.46)	0.17 (0.13 - 0.23)	0.00	−0.05	(−0.26 - 0.22)	0.11 (0.08 - 0.16)	0.91
33	95	−0.31	(−0.54 - 0.11)	0.21 (0.16 - 0.37)	0.52	−0.11	(−0.36 - 0.13)	0.13 (0.10 - 0.21)	0.79
34	93	0.11	(−0.30 - 0.73)	0.25 (0.19 - 0.35)	0.92	−0.02	(−0.40 - 0.33)	0.16 (0.13 - 0.26)	0.89

Appendix 3: Additional simulations

We performed an additional simulation study by repeating the analysis described in the main text. Here, we simulated count data arising from a Poisson detection process instead of binary data from the Bernoulli process. We then fitted a Poisson spatial capture-recapture (SCR) model, assuming homogeneous baseline detection rate to evaluate the consequences of model misspecification and compare the results with that of the Bernoulli simulations and observation model. The code to simulate data and fit the model is available in Appendix 1. We followed the simulation set up and population characteristics described in the main text. In brief:

1. *Poisson observation process* – We reformulated the observation sub-model of our standard, single-session, SCR model (Equation 5; see the main text), assuming that the detection histories for the observed individuals followed a Poisson distribution:

$$y_{ij} \sim Poisson(\lambda_{ij}\, z_i) \tag{3.1}$$

Here, λ_{ij} is the mean number of detections of individual i at detector j and is described using the half-normal detection function:

$$\lambda_{ij} = \lambda_0\, exp(-d_{ij}^2/2\sigma^2) \tag{3.2}$$

In this formulation, λ_0 is the expected detection rate when $d_{ij} = 0$.

2. *Simulation of Poisson-distributed SCR data* – To simulate scenarios that were comparable to the Bernoulli detection process in terms of number of detected individuals and number of detections (Table S2.1, Appendix 2), we approximated the intercept

value of p_0 ($= 0.15$) in the Bernoulli-distributed simulations to λ_0 by:

$$\lambda_0 = -log(1 - p_0) = 0.1625189 \tag{3.3}$$

We repeated the same procedure described in the main text to simulate the spatial, detector-level covariate $\mathbf{X}_j$ (see Equations 6 and 7). We included only two combinations of $\phi = 0.001$ or high (Moran's $I \approx 1$) vs. $\phi = 1000$ or low (Moran's $I \approx 0$) spatial autocorrelation in the detector-specific baseline detection rate λ_{0_j}.

3. *Simulations* – To model λ_{0_j}, we reformulated Equation 8 in the main text as:

$$\lambda_{0_j} = exp(log(\lambda_0) + \beta_{\mathbf{X}}\, \mathbf{X}_j) \tag{3.4}$$

Note that by approximating p_{0_j} to λ_{0_j} in this fashion, we maintained a comparable baseline detection probability. Thus, the Bernoulli observation sub-model described in the main text can be considered a compressed version of the Poisson model, where detections are compressed into singletons.

We considered the same two types of scenarios of continuous and categorical spatial variation in detectability as described in the main text, where y_{ij} was instead simulated by realizing the Poisson detection process (detections $[y_{ij} = 1, 2, 3, \dots]$ and non-detections $[y_{ij} = 0]$). We considered $\beta_{\mathbf{X}} = -0.5$ or -1 for simulating low and high amount of variation in the detector-specific, baseline detection rate λ_{0_j}, respectively. For the alternative scenarios of continuous spatial variation in detectability ($\mathbf{X}_j = -1.96$ - 1.96), λ_{0_j} then ranged between 0.06 and 0.43 (median $\lambda_{0_j} = 0.16$) when $\beta_{\mathbf{X}} = -0.5$, and between 0.02 and 1.15 (median $\lambda_{0_j} = 0.16$) when $\beta_{\mathbf{X}} = -1$ following Equation 3.4. For the alternative scenarios with categorical spatial variation ($\mathbf{X}_j = 0$ or 1), λ_{0_j} was equal to the intercept value of $\lambda_0 = 0.16$ (Equation 3.3) for a varying percentage of detectors

with higher detectability (25%, 50%, or 75%), and was 0.1 ($\beta_{\mathbf{X}} = -0.5$), 0.06 ($\beta_{\mathbf{X}} = -1$), or 0 ($\beta_{\mathbf{X}} = -10000$) for the group of detectors with lower detectability depending on the simulation scenario (Table S3.1, Appendix 3). Together with a reference scenario of constant detection rate (i.e., no model misspecification), we generated 23 additional simulation scenarios with 25 repetitions each, leading to 575 Poisson-distributed SCR data sets in total (Table S3.1, Appendix 3). See the main text for information on SCR model fitting and the approach to evaluate model performance.

Table S3.1: Characteristics of the additional simulation scenarios included. Here, data were generated from a count-based (Poisson) detection process. N°: the scenario number; $\beta_{\mathbf{X}}$: magnitude of the effect of the spatial, detector-specific covariate for the baseline detection rate (continuous or categorical spatial variation); %Det: percentage of detectors (out of 400) with lower detectability (for categorical variation only); ϕ: parameter defining the rate of decline in correlation with distance; Moran's I: median and range (minimum and maximum values) of Moran's index of global spatial autocorrelation across 25 detector-specific covariates simulated for each scenario; λ_{0_j}: range (min, max) of detector-specific, baseline detection rate; Ndetected: number of individuals detected out of 250 (median and range); Ndetections: number of detections or recaptures (median and range) across the 20×20-square distance unit (du^2) detector grid, surrounded by an unsampled 4.5×4.5-du^2 habitat buffer.

N°	$\beta_{\mathbf{X}}$	%Det	ϕ	Moran's I	λ_{0_j}	Ndetected	Ndetections
Continuous							
1	−0.5	-	1000	0 (−0.06 - 0.05)	0.06 - 0.43	133 (122 - 144)	315 (269 - 358)
2	−0.5	-	0.001	0.95 (0.90 - 0.98)	0.06 - 0.43	123 (113 - 147)	329 (269 - 391)
3	−1	-	1000	−0.01 (−0.06 - 0.09)	0.02 - 1.15	148 (131 - 167)	486 (410 - 567)
4	−1	-	0.001	0.95 (0.92 - 0.97)	0.02 - 1.15	128 (95 - 144)	491 (373 - 564)
None							
5*	-	-	-	-	0.16	117 (104 - 137)	238 (197 - 288)
Categorical							
6	−0.5	25	1000	0 (−0.05 - 0.07)	0.1, 0.16	124 (106 - 136)	262 (221 - 312)
7	−0.5	25	0.001	0.86 (0.74 - 0.90)	0.1, 0.16	117 (102 - 142)	248 (215 - 303)
8	−1	25	1000	−0.01 (−0.06 - 0.06)	0.06, 0.16	117 (104 - 137)	238 (197 - 288)
9	−1	25	0.001	0.85 (0.71 - 0.89)	0.06, 0.16	113 (105 - 129)	222 (195 - 257)
10	−10000	25	1000	0 (−0.04 - 0.04)	0, 0.16	110 (102 - 123)	205 (171 - 235)
11	−10000	25	0.001	0.86 (0.69 - 0.90)	0, 0.16	103 (84 - 111)	205 (185 - 243)
12	−0.5	50	1000	−0.01 (−0.04 - 0.05)	0.1, 0.16	114 (104 - 138)	220 (186 - 271)
13	−0.5	50	0.001	0.89 (0.81 - 0.91)	0.1, 0.16	111 (97 - 129)	225 (175 - 251)

* The reference scenario without model misspecification (i.e., homogeneous baseline detection rate).

Table S3.1: (continued).

Nº	$\beta_{\mathbf{X}}$	%Det	ϕ	Moran's I	λ_{0_j}	Ndetected	Ndetections
Categorical							
14	−1	50	1000	0 (−0.06 - 0.06)	0.06, 0.16	105 (93 - 119)	188 (160 - 223)
15	−1	50	0.001	0.89 (0.78 - 0.91)	0.06, 0.16	104 (83 - 119)	187 (137 - 239)
16	−10000	50	1000	0 (−0.04 - 0.03)	0, 0.16	86 (69 - 104)	138 (112 - 164)
17	−10000	50	0.001	0.88 (0.8 - 0.91)	0, 0.16	70 (53 - 82)	136 (108 - 164)
18	−0.5	75	1000	−0.01 (−0.04 - 0.03)	0.1, 0.16	109 (92 - 131)	195 (176 - 224)
19	−0.5	75	0.001	0.86 (0.78 - 0.90)	0.1, 0.16	108 (91 - 123)	192 (160 - 225)
20	−1	75	1000	−0.01 (−0.08 - 0.05)	0.06, 0.16	92 (63 - 105)	141 (93 - 168)
21	−1	75	0.001	0.86 (0.74 - 0.90)	0.06, 0.16	86 (70 - 96)	139 (117 - 163)
22	−10000	75	1000	0 (−0.07 - 0.04)	0, 0.16	55 (42 - 71)	71 (56 - 95)
23	−10000	75	0.001	0.87 (0.65 - 0.90)	0, 0.16	37 (21 - 60)	67 (44 - 101)

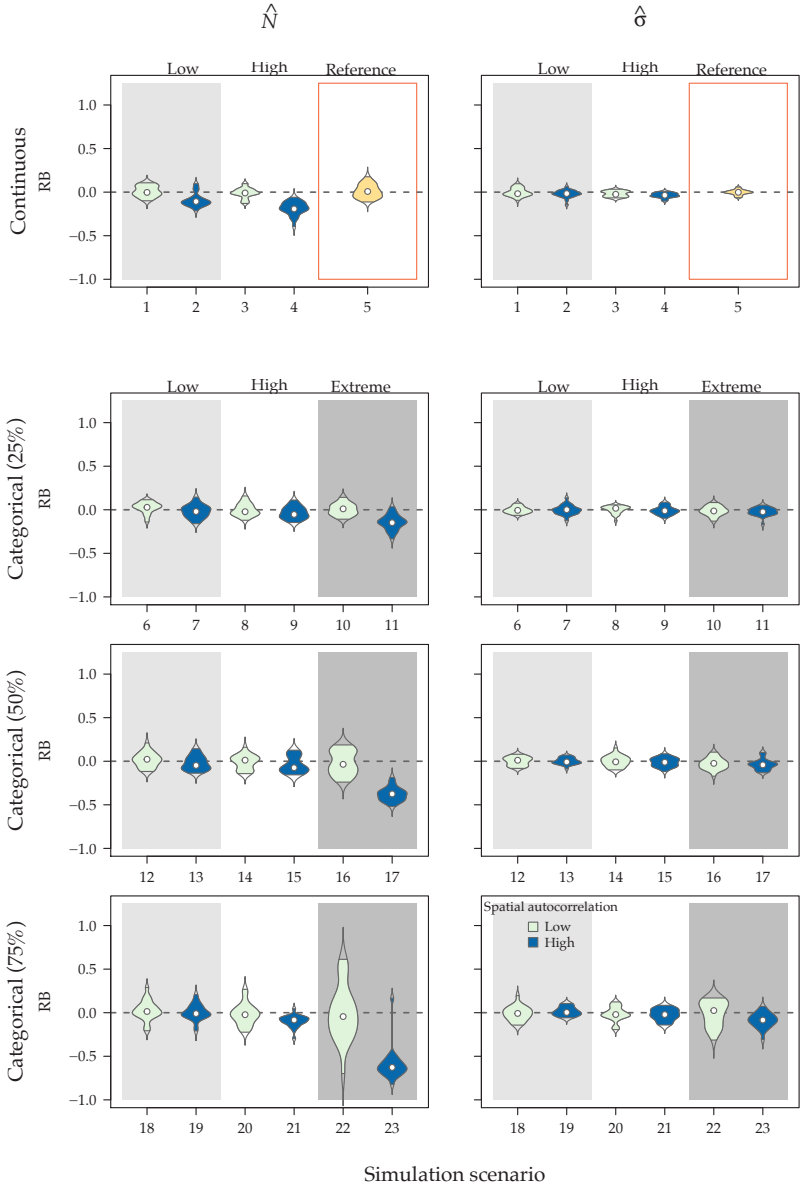

Figure S3.1: Relative bias (RB) for population size ($\hat{N}$) and the spatial scale parameter of the half-normal detection function ($\hat{\sigma}$) estimated by a mis-specified, standard spatial capture-recapture model fitted to Poisson-distributed data sets simulated ($n = 25$). Violins show the effects of spatial autocorrelation in the detector-level covariates simulated in different scenarios of continuous (top row) and categorical (bottom three rows) spatial variation in baseline detection rate. Numbers provided on the x-axes refer to the unique ID of the simulation scenario and link with the more detailed information provided for each simulation in Table S3.1 in Appendix 3.

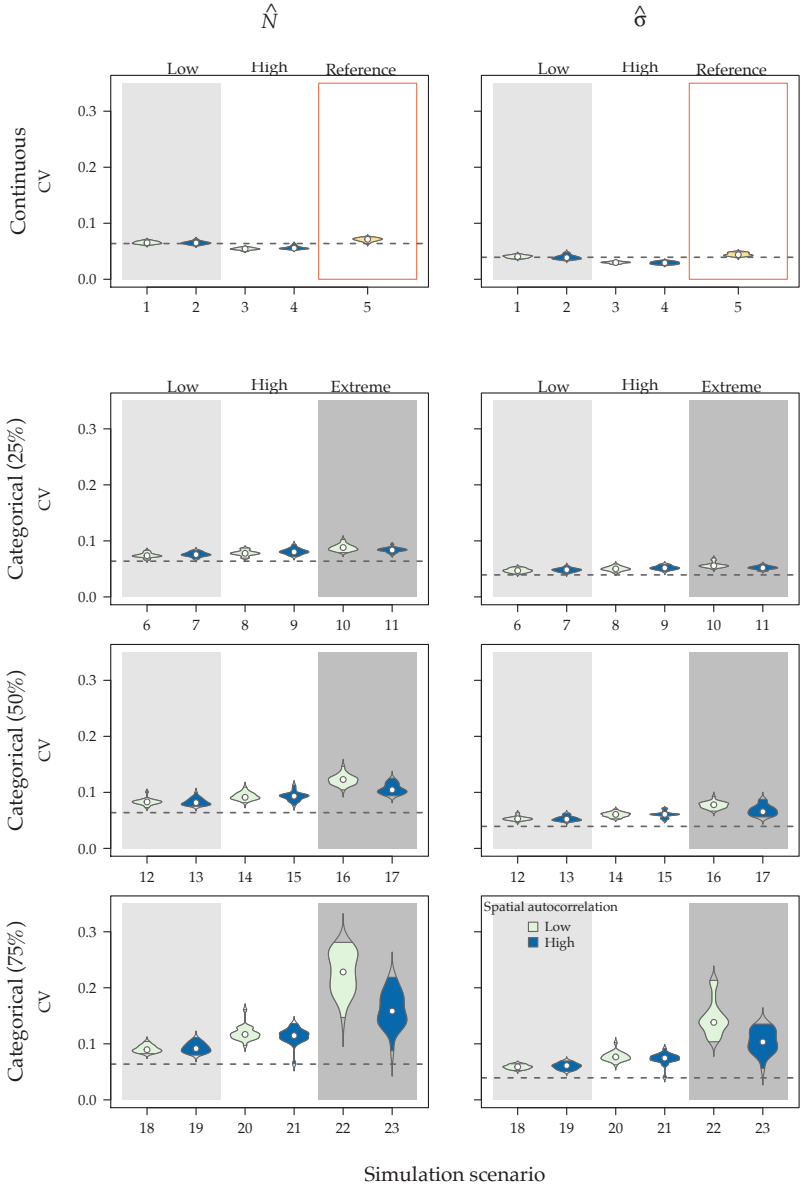

Figure S3.2: Coefficient of variation (CV) for population size ($\hat{N}$) and the spatial scale parameter of the half-normal detection function ($\hat{\sigma}$) estimated by a mis-specified, standard spatial capture-recapture model fitted to Poisson-distributed data sets simulated ($n = 25$). Violins show the effects of spatial autocorrelation in the detector-level covariates simulated in different scenarios of continuous (top row) and categorical (bottom three rows) spatial variation in baseline detection rate. The dashed lines show median CV for the parameter estimates achieved in the reference scenario. Numbers provided on the x-axes refer to the unique ID of the simulation scenario and link with the more detailed information provided for each simulation in Table S3.1 in Appendix 3.

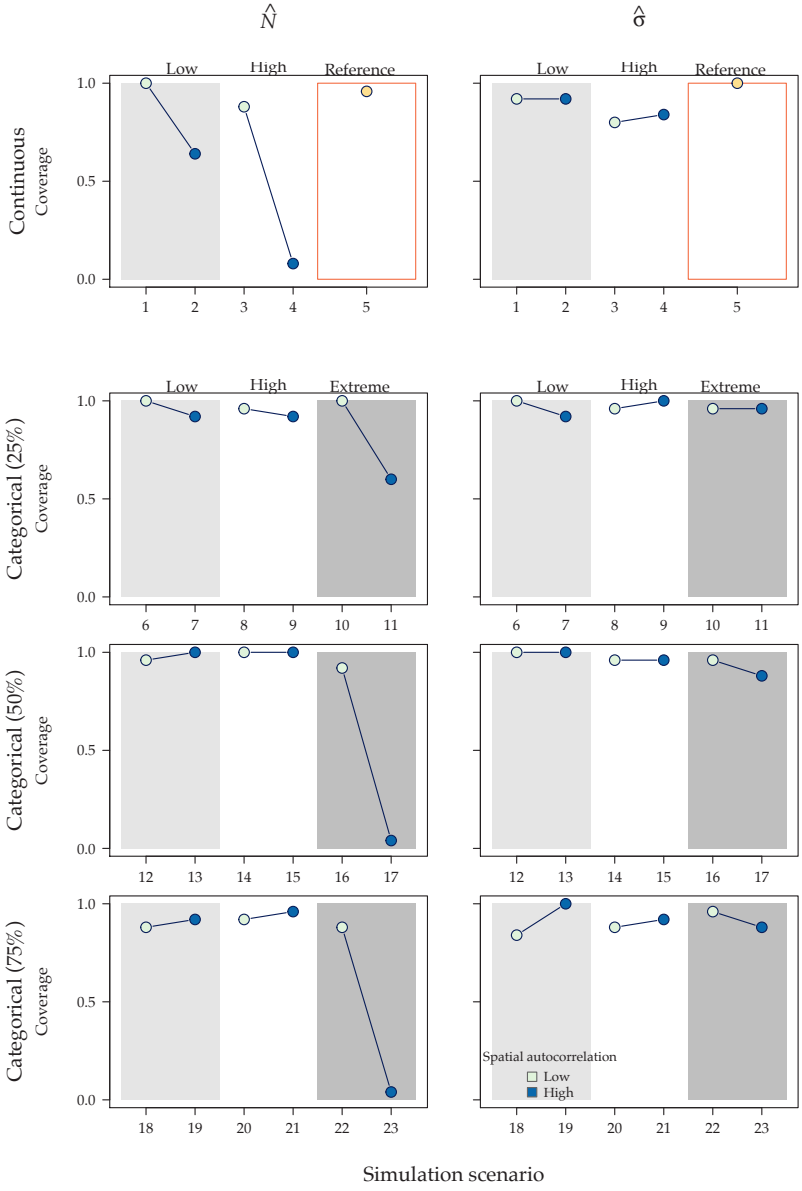

Figure S3.3: Coverage probability of the 95% credible intervals of population size ($\hat{N}$) and the spatial scale parameter of the half-normal detection function ($\hat{\sigma}$) estimated by a mis-specified, standard spatial capture-recapture model fitted to Poisson-distributed data sets simulated ($n = 25$). Violins show the effects of spatial autocorrelation in the detector-level covariates simulated in different scenarios of continuous (top row) and categorical (bottom three rows) spatial variation in baseline detection rate. Numbers provided on the x-axes refer to the unique ID of the simulation scenario and link with the more detailed information provided for each simulation in Table S3.1 in Appendix 3.

Article II

Ecological Modelling 479 (2023) 110324

Contents lists available at ScienceDirect

Ecological Modelling

journal homepage: www.elsevier.com/locate/ecolmodel

Modelling spatially autocorrelated detection probabilities in spatial capture-recapture using random effects

Soumen Dey [a,*], Ehsan Moqanaki [a], Cyril Milleret [a], Pierre Dupont [a], Mahdieh Tourani [a,b], Richard Bischof [a]

[a] Faculty of Environmental Sciences and Natural Resource Management, Norwegian University of Life Sciences, 1432 Ås, Norway
[b] Department of Ecosystem and Conservation Sciences, University of Montana, Missoula, USA

ARTICLE INFO

Dataset link: https://github.com/soumenstat89/HetDetSol

Keywords:
Spatial capture-recapture
Detection probability
Spatial autocorrelation
Generalized linear mixed model
Random effects
Finite mixture model
Population size estimation

ABSTRACT

Spatial capture-recapture (SCR) models are now widely used for estimating density from repeated individual spatial encounters. SCR accounts for the inherent spatial autocorrelation in individual detections by modelling detection probabilities as a function of distance between the detectors and individual activity centres. However, additional spatial heterogeneity in detection probability may still creep in due to environmental or sampling characteristics. if unaccounted for, such variation can lead to pronounced bias in population size estimates.

In this paper, we address this issue by describing three Bayesian SCR models that use generalized linear mixed modelling (GLMM) approach to account for latent heterogeneity in baseline detection probability across detectors with: independent random effects (RE), spatially autocorrelated random effects (SARE) with components of prior covariance matrix modelled as a decreasing function of inter-detector distance, and a two-group finite mixture model (FM) to identify latent detectability classes of each detector. We test these models using a simulation study and an empirical application to a non-invasive genetic monitoring data set of female brown bears (*Ursus arctos*) in central Sweden.

In the simulation study, all three models largely succeeded in mitigating the biasing effect of spatially heterogeneous detection probability on population size estimates. Overall, SARE provided the least biased population size estimates (median RB: -9% – 6%). When spatial autocorrelation in detection probability was high, SARE also performed best at predicting the spatial pattern of heterogeneity in detection probability. At intermediate levels of autocorrelation, spatially-explicit estimates of detection probability obtained with FM were more accurate than those generated by SARE and RE. The empirical example revealed patterns consistent with the results from the simulation study. We found that ignoring spatial heterogeneity in detection probability led to at least 22% lower estimate of bear population size compared to models that accounted for it (i.e., SARE and RE models). When the number of detections per detector is low (≤ 1), the GLMMs considered here may require dimension reduction of the random effects by pooling baseline detection probability parameters across neighbouring detectors ("aggregation") to avoid over-parameterization.

The added complexity and computational overhead associated with SCR-GLMMs may only be justified in extreme cases of spatial heterogeneity, e.g., large clusters of inactive detectors unbeknownst to the investigator. However, even in less extreme cases, detecting and estimating spatially heterogeneous detection probability may assist in planning or adjusting monitoring schemes.

1. Introduction

Spatial capture-recapture (SCR) models are now widely used to estimate demographic parameters, particularly density. SCR data inherently varies across space because animal movements are not completely random and an individual is more likely to be detected close to its centre of activity ('activity centre', AC). SCR models account for and, in fact, exploit such spatial heterogeneity in detection by modelling the detection probability as a decreasing function of distance between a detector - e.g., an observer, a trap, or a search location - and a latent AC (Efford, 2004; Borchers and Efford, 2008). However, the relative distance between a detector and an AC may not be the only cause of variation in detection probability. Spatially variable and autocorrelated detection probability can occur due to various other factors, such

* Corresponding author.
E-mail address: soumenstat89@gmail.com (S. Dey).

https://doi.org/10.1016/j.ecolmodel.2023.110324
Received 6 May 2022; Received in revised form 30 January 2023; Accepted 14 February 2023
Available online 24 February 2023

as local differences in how animals use space and how sampling is performed (Moqanaki et al., 2021; Stevenson et al., 2021).

Known sources of variation in detection probability are readily modelled in SCR using covariates, for example, through proxies or direct measures of sampling effort (Efford et al., 2013), resource selection data obtained from telemetry studies (Royle et al., 2013), or information about landscape connectivity (Sutherland et al., 2015). However, not all sources of variation are known and fully observed. For example, local site-specific characteristics affecting detector exposure, or effect of local atmospheric conditions on the genotyping success rate of non-invasively collected DNA samples may remain unaccounted for during SCR analyses (Efford et al., 2013; Kendall et al., 2019; Moqanaki et al., 2021). Furthermore, large-scale wildlife monitoring programmes sometimes include both structured and unstructured sampling data. The latter may be data collected by the general public to increase the extent and intensity of sampling (Thompson et al., 2012; Bischof et al., 2020a). Unstructured and opportunistic sampling data is likely to be associated with unknown spatial variation in detection probability. Unmodelled spatial variation in detection probability, particularly in the presence of high spatial autocorrelation, can lead to biased and overdispersed population size estimates in SCR analyses (Moqanaki et al., 2021). A worst-case scenario are pockets or clusters of detectors where, unbeknownst to the investigator, detection probability is null.

Adequately accounting for spatial heterogeneity and autocorrelation in detection probability is essential for obtaining reliable statistical inference in SCR analyses (Moqanaki et al., 2021; Howe et al., 2022). In the absence of known covariates, the effect of detector-specific variation in detection probability can be modelled by using a function that explains the true pattern of heterogeneity. This function is always unknown and we approximate it using random effects, i.e., by extending SCR with generalized linear mixed models (GLMM). Bayesian implementation of SCR-GLMMs allows modelling and estimation of heterogeneous detection probability surfaces in SCR models (Hooten et al., 2003). Spatially-explicit estimates of detection probability can in turn reveal problematic areas (e.g., regions with very low detection probability), which are important to wildlife monitoring and conservation.

Using simulations, we describe and test three extensions of Bayesian SCR-GLMMs that aim to account for latent spatial heterogeneity in detection probability via the use of random effects: (1) a simple GLMM extension of the basic single-season SCR model by assigning independent random effects (RE) to detector-specific baseline detection probabilities — with the aim to account for unknown spatial variation in detection probability among detectors; (2) a GLMM extension of the basic single-season SCR model incorporating spatial autocorrelation between detectors by means of spatially autocorrelated random effects (SARE), where covariance is modelled as a function of inter-detector distance, thus implicitly defining an ordered neighbourhood structure; and (3) a two-group finite mixture (FM) model to identify latent detectability classes of detectors.

We assessed and compared these three structurally different models in terms of (i) their ability to produce unbiased abundance estimates, (ii) their capacity to realistically predict detection probability surfaces, (iii) their model complexity, and (iv) their computational overhead. Finally, we considered the role that model comparison could play in selecting the 'best' SCR model under different conditions. Finally, we provide an empirical demonstration of our modelling approaches by applying them to a non-invasive genetic monitoring data set on brown bears (*Ursus arctos*) from central Sweden. We chose this example because a large proportion of the data were collected opportunistically by volunteers without reliable measures of sampling effort or spatial variation therein.

2. Methods

We first describe a basic single-season SCR model, where we assume a homogeneous baseline detection probability across all the detectors. Following that, we describe three extensions of the SCR model, namely: (i) a SCR-GLMM with independent random effects (RE), (ii) a SCR-GLMM with spatially autocorrelated random effect (SARE), and (iii) a SCR-GLMM with two-group mixture to model detector-specific baseline detection probabilities (FM). Lastly, as a reference point for making comparisons, we use a SCR-GLM model where the known true cause of the variation in detection probability is modelled using fixed effects.

2.1. Model 1: Basic single-season SCR model (SCR)

A single-season SCR model typically consists of two submodels: a submodel for the spatial distribution of individual ACs within a given habitat $\mathcal{V} \subset \mathbb{R}^2$, and another submodel for the individual and detector-specific observations, conditional on the location of ACs.

2.1.1. The ecological submodel

We considered N individuals to reside in $\mathcal{V}$, each of whom was assumed to move randomly around its AC (with coordinates $\boldsymbol{s}_i$). Following a homogeneous point process, each individual AC was assumed to be uniformly distributed across the habitat $\mathcal{V}$:

$$\boldsymbol{s}_i \sim \text{Uniform}(\mathcal{V}),\ i = 1, 2, \dots, N. \tag{1}$$

In our analysis, the location $\boldsymbol{s}_i$ of individual ACs and the number of these ACs (N) are both unknown. We used a data augmentation approach to model N (Royle et al., 2007), with a large integer M as an upper bound for N. We introduced a vector of M latent binary variables $\boldsymbol{z} = (z_1, z_2, \dots, z_M)'$ such that $z_i = 1$ if individual i is a member of the population and $z_i = 0$ otherwise. Then we assumed that each z_i follows a Bernoulli distribution with inclusion probability ψ, the probability that an arbitrary individual from the augmented population of M individuals is a member of the population under study:

$$\boldsymbol{z}_i \sim \text{Bernoulli}(\psi). \tag{2}$$

Consequently, population size $N = \sum_{i=1}^{M} z_i$ is a derived parameter, following a binomial distribution with parameters M and ψ.

2.1.2. The observation submodel

We considered one sampling occasion and a set of J detectors located in $\mathcal{V}$. The capture history of the ith individual is denoted as $(y_{i1}, y_{i2}, \dots, y_{iJ})$, where each y_{ij} is binary, i.e., y_{ij} is 1 if individual i is detected at detector j and 0 otherwise. The observed capture-recapture data set, denoted by $\boldsymbol{Y}_{\text{obs}}$, is of dimension $n \times J$, where n is the number of detected individuals during the SCR survey. We augmented this data set $\boldsymbol{Y}_{\text{obs}}$ with $M - n$ "all-zero" capture histories $\boldsymbol{0}_J$ following the data augmentation approach. The zero-augmented data set is denoted by $\boldsymbol{Y}$ and is of dimension $M \times J$. We assumed a Bernoulli model for each y_{ij}, conditional on z_i:

$$y_{ij} \sim \text{Bernoulli}(p_{ij} z_i), \tag{3}$$

where p_{ij} denotes the detection probability of the ith individual at the jth detector. The detection probability p_{ij} is a decreasing function of distance, modelled following a half-normal form (Efford, 2004):

$$p_{ij} = p_0 \exp\left(-\frac{d_{ij}^2}{2\sigma^2}\right), \tag{4}$$

where $d_{ij} = d(\boldsymbol{s}_i, \boldsymbol{x}_j) = \|\boldsymbol{s}_i - \boldsymbol{x}_j\|$ is the Euclidean distance between the detector location $\boldsymbol{x}_j$ and individual AC $\boldsymbol{s}_i$, p_0 is the baseline detection probability, and the scale parameter σ quantifies the rate of decline in detection probability p_{ij} with distance d_{ij}. The full SCR model can thus be written as:

$$\psi \sim \text{Uniform}(0, 1)$$
$$\sigma \sim \text{Uniform}(0, 50)$$
$$\text{logit}(p_0) \sim \mathcal{N}(0, 2^2)$$
$$i = 1, 2, \dots, M\ :$$

$$
\begin{aligned}
&\boldsymbol{s}_i \sim \text{Uniform}(\mathcal{V})\\
&z_i \sim \text{Bernoulli}(\psi)\\
&p_{ij} = p_0 \exp(-d_{ij}^2/(2\sigma^2)) \text{ for } j = 1, 2, \dots, J\\
&y_{ij} \sim \text{Bernoulli}(p_{ij}\, z_i) \text{ for } j = 1, 2, \dots, J
\end{aligned} \tag{5}
$$

By modelling detection probability p_{ij} in terms of individual ACs and fitting a decreasing detection function (as in (4)) using the distance between ACs and detector location, the SCR model accounts for the spatial autocorrelation within individual capture histories. However, under this model, detection probabilities p_{ij} and $p_{ij'}$ are equal at two detectors j and j' when they are located at the same distance from the AC $\boldsymbol{s}_i$ regardless of other potential sources of variation between the two detectors. In other words, this model does not consider the additional variation in detection probability that may be present at different detectors due to their locations in the landscape and other heterogeneous characteristics.

2.2. Model 2: Independent random effects SCR model (RE)

To account for spatial heterogeneity in detection probability, causing detector-specific variation in detection probabilities, we used a simple GLMM extension of the basic single-season SCR model (Model 1). Here, we assigned a logistic-regression type model to baseline detection probability for each detector:

$$\text{logit}(p_{0j}) = \mu + W_j,\ j = 1, 2, \dots, J, \tag{6}$$

where μ denotes the intercept and W_j denotes the random effect for the jth detector. The detection probability p_{ij} for individual i at detector j is expressed as

$$p_{ij} = p_{0j} \exp\Big(-\frac{d_{ij}^2}{2\sigma^2}\Big). \tag{7}$$

We assumed a $\mathcal{N}(0, \sigma_w^2)$ prior for each W_j, $j = 1, 2, \dots, J$ and a $\mathcal{N}(0, 2^2)$ prior for μ. The variance parameter σ_w^2 can be given a weakly informative prior. Note that the RE model does not specifically account for spatial autocorrelation in detection probability across detectors.

2.3. Model 3: Spatially autocorrelated random effects SCR model (SARE)

We extended the basic single-season SCR model (Model 1) to account for spatial autocorrelation among detectors. In particular, we developed a SCR model for situations where detectors at close proximity are more likely to have similar detection probability compared to more distant detectors. We modelled this spatial autocorrelation by introducing an autocorrelated random effect $\boldsymbol{W} = (W_1, W_2, \dots, W_J)'$ of length J. We assumed W to follow a multivariate normal distribution with mean $\mathbf{0}_J$ and covariance matrix $\Gamma = ((\gamma_{jj'}))$, which controls the spatial dependence between detectors. We modelled each element $\gamma_{jj'}$ of this covariance matrix as a decreasing function of distance between detectors j and j' following (Moqanaki et al., 2021),

$$\gamma_{jj'} = \exp(-\phi\, \delta_{jj'}), \tag{8}$$

where $\delta_{jj'} = d(\boldsymbol{x}_j, \boldsymbol{x}_{j'}) = \|\boldsymbol{x}_j - \boldsymbol{x}_{j'}\|$ is the Euclidean distance between the detector locations $\boldsymbol{x}_j$ and $\boldsymbol{x}_{j'}$. This covariance function implicitly defines an ordered neighbourhood for each detector and ϕ controls the rate of distance-dependent decay of spatial autocorrelation between the detectors. In particular, detectors are highly autocorrelated if ϕ is small (e.g., 0.05), and autocorrelation decreases as ϕ increases (Figs. 1 and 4). Similar to the RE model, the detection probability p_{ij} for individual i at detector j is then expressed as

$$p_{ij} = p_{0j} \exp\Big(-\frac{d_{ij}^2}{2\sigma^2}\Big), \tag{9}$$

where

$$\text{logit}(p_{0j}) = \mu + W_j,\ j = 1, 2, \dots, J. \tag{10}$$

Here, we assigned a $\mathcal{N}(0, 2^2)$ prior for μ and a $\mathcal{N}(0, 5^2)$ prior for log-transformed ϕ.

When $\phi = 0$, each component $\gamma_{jj'} = 1$ (for any j and j'), the random effect $\boldsymbol{W}$ becomes a degenerate process, implying exact dependence between the detectors. Hence, the value of each random effect W_j is identical at any location of the detector grid. This is equivalent to the basic single-season SCR model. Conversely, when $\phi \to \infty$, the covariance matrix Γ reduces to an identity matrix, and consequently, the SARE model reduces to a SCR-GLMM with independent random effects (RE).

2.4. Model 4: Two-group finite mixture SCR model (FM)

Variable sampling intensity could be associated with ordered classes of unknown variation in detection probability across the landscape. For our study, we proposed using a two-group finite mixture SCR model (FM) to model heterogeneity in detection probability between detectors (Cubaynes et al., 2010; Turek et al., 2021). Here, we defined two groups of heterogeneity, viz., 1 and 2, and introduced two detection probability parameters η_1 and η_2, where η_k is the detection probability of the bth subgroup, $b = 1, 2$. A constraint is imposed on these parameters $\eta_1 < \eta_2$ to ensure identifiability. Further, we defined binary indicator variables u_j ($j = 1, 2, \dots, J$) to indicate the subgroup that a detector belongs to:

$$p_{0j} = (1 - u_j)\,\eta_1 + u_j\,\eta_2,\ j = 1, 2, \dots, J. \tag{11}$$

MCMC computation allows the binary classification in our two-group mixture model to implicitly account for the group membership probabilities $\Pr(u_j = 1)$ and consequently, allows estimation of each p_{0j} via (11) accounting for the uncertainty in the group membership probabilities of each detector. We assigned a Bernoulli prior to each u_j with probability π of being assigned to second group. We further assumed bounded uniform priors over the $(0, 1)$ interval for the probability parameters η_1, η_2, and π.

2.5. Model 5: SCR model with known fixed effects (FE)

For the sake of assessing and comparing the performance of the above models, we considered a GLM extension of basic single-season SCR model (Model 1) using detector-specific effects (i.e., the true source of variation) to model baseline detection probability. This can be executed by supplying the known simulated effect $\boldsymbol{W}$ as an observed "virtual" covariate and then model the baseline detection probability:

$$\text{logit}(p_{0j}) = \mu + W_j. \tag{12}$$

Consequently, the detection probability p_{ij} is expressed as:

$$p_{ij} = p_{0j} \exp\Big(-\frac{d_{ij}^2}{2\sigma^2}\Big). \tag{13}$$

The rest of this FE model remains the same as the basic SCR (Model 1).

3. Simulation study

For simulations, we used a 32 × 32 detector array (number of traps $J = 1024$) with 1 distance unit (du) of minimum inter-detector spacing. The detector array is centred on a 41 × 41 du habitat, surrounded by a 5-du habitat buffer (Fig. 1). We used a σ value of 1.5 for all the simulations so that the buffer width is larger than 3σ; resulting in negligible detection probability of individuals with ACs near the habitat boundary (Efford, 2011). We simulated SCR data sets for $N = 300$ individuals leading to a population-level home range overlap index $k = \sigma\sqrt{\text{Density}} = 0.63$ (Efford et al., 2016). We set the size of the augmented population M to be 500.

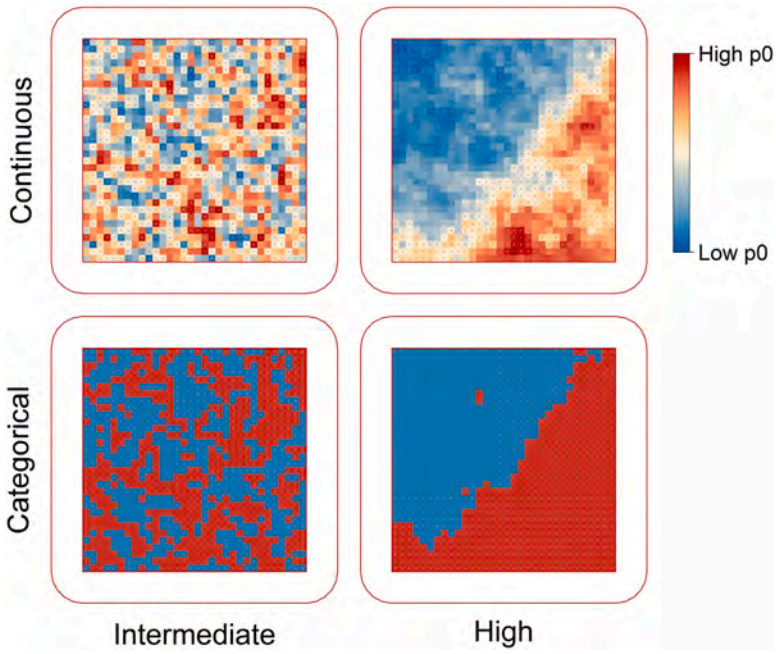

Fig. 1. Examples of spatially variable and autocorrelated baseline detection probability surfaces $\boldsymbol{p_0} = (p_{01}, p_{02}, \ldots, p_{0J})'$. The colour gradient corresponds to different values of baseline detection probability. The surface is overlayed on a grid of detectors (grey dots) centred in a habitat (entire area surrounded by the red line with rounded corners). Shown in rows, spatial variation in detection probability can be either continuous or categorical (with 50% of the detectors remaining inactive while the rest have a constant baseline detection probability). Shown in columns, spatial autocorrelation may vary from intermediate (Moran's $I \approx 0.3$) to high (Moran's $I \approx 1$).

3.1. Simulation scenarios

For each simulation, we used the SARE model (Model 3, Section 2.3) to generate SCR data with spatially autocorrelated detection probability between detectors. We created simulation scenarios by varying spatial autocorrelation rate parameter ϕ with high ($\phi = 0.05$) and intermediate ($\phi = 1$) spatial autocorrelation to simulate spatially varying random effect $\boldsymbol{W} = (W_1, W_2, \ldots, W_J)'$ (Fig. 1).

3.1.1. Continuous detector-specific variation in detection probability

Detection probability may exhibit continuous spatial variation if it is linked with underlying habitat characteristics, such as elevation, forest cover, or distance from roads that influence animal behaviour or detection effort and efficiency (Moqanaki et al., 2021). For simplifying the interpretation of μ in SARE (Model 3), we transformed it into a new variable η via the link $\mu = \text{logit}(\eta)$. Here, η can also be viewed as the average baseline detection probability, providing a clearer interpretation for the readers. In simulations, we used three values of η to generate low ($\eta = 0.1$), intermediate ($\eta = 0.3$), and high ($\eta = 0.6$) baseline detection probability for each detector, subject to spatial autocorrelation infused by $\boldsymbol{W}$ (Fig. 1, row 1).

3.1.2. Categorical detector-specific variation in detection probability

Discrete differences in sampling or environmental characteristics can lead to categorical classes of variation in detection probability between detectors. We considered an extreme case, where 50% of the detectors would remain inactive, and the remaining detectors would have a constant detection probability (Moqanaki et al., 2021). Thus, a portion of the study area would remain entirely unsampled. To simulate such scenarios, we transformed each p_{0j} into a discrete variable taking only one of the two values 0 and logit(η) to create two classes of detector-specific baseline detection probability using (10):

$$p_{0j} = \begin{cases} 0, & \text{if } W_j \leq q_{50} \\ \text{logit}(\eta), & \text{otherwise,} \end{cases} \tag{14}$$

where q_{50} is the 50% quantile of the effect W_j's. We used two values of η to generate low ($\eta = 0.1$) and intermediate ($\eta = 0.3$) levels of baseline detection probability for active detectors (Fig. 1, row 2).

In summary, we divided all simulation scenarios in two broad setups, viz. continuous and categorical, with respect to detector-specific variation in detection probability. In the continuous setup ('CON'), we generated six simulation scenarios by combining two levels of autocorrelation ϕ and three levels of detection η. In the categorical setup ('CAT'), we generated four simulation scenarios by combining two levels of ϕ and two levels of η. Thus, in total, we generated 10 simulation scenarios. For each simulation scenario, we generated 100 independent SCR data sets, resulting in 1000 simulated SCR data sets in total (Table 1).

3.2. Curse of dimensionality

In many SCR studies the majority of detectors are associated with no or very few detections (Gerber and Parmenter, 2015; Tourani, 2022). In such situations, fitting complex models such as SARE, FM, and RE, which involves large number of parameters and latent variables, may lead to poor Markov chain Monte Carlo (MCMC) convergence, below par mixing, and over-fitting. This phenomenon is known as the curse of dimensionality and expected to occur when models are over-parameterized (Wikle and Hooten, 2010).

We mitigated this issue by dimension reduction of the random effects. To do this, we aggregated random effects that are used to model

Table 1
Summary of simulated spatial capture-recapture data sets. The number of detected individuals, the total number of detections, the number of detections per detector, the number of detections per individual and the number of detections per detected individual are calculated over 100 replications for each of the 10 simulation scenarios are tabulated. The last three columns show mean values.

Scenario	η	ϕ	No. of detected individuals			No. of detections			Detections per detector	Detections per individual	Detections per detected individual
			Mean	2.5% Quantile	97.5% Quantile	Mean	2.5% Quantile	97.5% Quantile			
Continuous											
1	0.1	1	179	164	197	372	326	432	0.36	1.24	2.08
2	0.1	0.05	163	92	224	407	127	921	0.40	1.36	2.33
3	0.3	1	229	215	245	926	843	1041	0.90	3.09	4.04
4	0.3	0.05	221	186	250	984	446	1814	0.96	3.28	4.37
5	0.6	1	244	233	255	1610	1495	1753	1.57	5.37	6.59
6	0.6	0.05	243	223	257	1675	1106	2357	1.64	5.58	6.87
Categorical											
7	0.1	1	103	89	119	140	138	162	0.14	0.47	1.37
8	0.1	0.05	93	82	111	144	144	166	0.14	0.48	1.55
9	0.3	1	186	170	205	415	412	468	0.41	1.38	2.23
10	0.3	0.05	150	128	176	422	419	492	0.41	1.41	2.82

baseline detection probability, such that a single random effect value is assigned to a cluster of neighbouring detectors. Note that we are not aggregating detections themselves. For instance, in SARE, if each cluster contains n_c detectors, then each detector belonging to a cluster (say, jth) will share the same random effect value W_j, $j = 1, 2, \ldots, J/n_c$ (J being the total number of detectors). Here, we aggregated the random effects by a factor of 4 (squares of 4×4 detectors = one cluster). When aggregated, the 32×32 detector grid (i.e., 1024 detectors; Fig. 1) forms a grid of 8×8 clusters.

3.3. Model fitting description

We fitted five SCR models to the same simulated datasets: (i) basic single-season SCR model without aggregation (Section 2.1), (ii) RE model, both with and without aggregation (Section 2.2), (iii) SARE model, both with and without aggregation (Section 2.3), (iv) FM model, both with and without aggregation (Section 2.4), and (v) FE model without aggregation (Section 2.5). The models were fitted using MCMC simulation with NIMBLE (de Valpine et al., 2017; NIMBLE Development Team, 2021) in R version 3.6.2 (R Core Team, 2019). We used the R package nimbleSCR (Bischof et al., 2020b; Turek et al., 2021), which implements the local evaluation approach (Milleret et al., 2019) to increase MCMC efficiency. For each simulated data set, we ran three chains of (i) 30,000 iterations for both basic single-season SCR and FE model including burn-in 12,000 iterations, (ii) 100,000 iterations for SARE and RE including burn-in 20,000 iterations (both with and without aggregation), and (iii) 60,000 iterations for FM (without aggregation) including burn-in 12,000 iterations and 20,000 iterations for FM (with aggregation) including 4000 iteration burn-in. MCMC convergence of each model was monitored using the Gelman–Rubin convergence diagnostic $\hat{R}$ (with upper threshold 1.1, Gelman et al., 2014a) and visual inspection of traceplots.

3.4. Model performance measures

We used relative bias, coefficient of variation, and coverage probability to evaluate the performance of each fitted models with respect to estimation of focal parameters (e.g., N, σ). Suppose $\{\theta^{(r)} : r = 1, 2, \ldots, R\}$ denotes a set of MCMC draws from the posterior distribution of a scalar parameter θ.

Relative bias. Relative bias (RB) is calculated as

$$\widehat{\mathrm{RB}}(\theta) = \frac{\hat{\theta} - \theta_0}{\theta_0}, \tag{15}$$

where $\hat{\theta}$ denotes the posterior mean $\frac{1}{R}\sum_{r=1}^{R}\theta^{(r)}$ and θ_0 gives the true value.

Coefficient of variation. Precision was measured by the coefficient of variation (CV):

$$\widehat{\mathrm{CV}}(\theta) = \frac{\widehat{\mathrm{SD}}(\theta)}{\hat{\theta}}, \tag{16}$$

where $\widehat{\mathrm{SD}}(\theta) = \sqrt{\frac{1}{R}\sum_{r=1}^{R-1}(\theta^{(r)} - \hat{\theta})^2}$ is the posterior standard deviation of parameter θ.

Coverage probability. Coverage probability was computed as the proportion of converged model fits for which the estimated 95% credible interval (CI) of the parameter θ contained the true value θ_0.

3.4.1. Effective sample size and MCMC efficiency

To compare the efficiency of the different MCMC algorithms of the fitted models, we computed the effective sample size (ESS) and MCMC efficiency (= ESS/MCMC run time) of each top-level parameter for each of the model runs. We used the 'effectiveSize' function from the R package coda to compute ESS (Plummer et al., 2006). The calculation of ESS is based on the combined samples of the converged MCMC chains after discarding the burn-in period. The MCMC computation time was calculated excluding the burn-in period. To obtain stable estimates of the quantities of interest, it is recommended to have ESS greater than 400 (Vehtari et al., 2021).

Although MCMC algorithms are used to generate sample from posterior distributions, efficiency can vary between different algorithms. There are two primary measures of efficiency of MCMC algorithms — quality of MCMC mixing and speed of MCMC computation. We computed 'MCMC efficiency' as a combined metric to assess both of these characteristics of MCMC algorithms, so that we could compare the efficiency of different MCMC algorithms. We reported the mean MCMC efficiency for each top-level parameters in the model and across all the converged replicates in each scenario.

3.4.2. Spatial accuracy of predicted baseline detection probability surfaces

Baseline detection probability surfaces obtained from SCR analyses are useful in evaluating the performance of our SCR models as they have the potential to reveal spatial patterns in detection probability, such as pockets with very low or very high detection probability, that could be of practical relevance. We compared the accuracy of the detector-specific baseline detection probability surfaces predicted by the different models with the true simulated surface $\boldsymbol{p_0}$ =

Table 2
Percentage of converged replicates with respect to the top-level parameters (e.g., N, σ, η, $\log(\phi)$, π) for the 100 replicated data sets for each of the 10 simulation scenarios and five fitted models. Here, '1 × 1' indicates that the model is fitted without aggregation and '4 × 4' refers to the level to aggregation of the random effects (Section 3.2).

Scenario	η	ϕ	SCR	RE		SARE		FM		FE
				1 × 1	4 × 4	1 × 1	4 × 4	1 × 1	4 × 4	
Continuous										
1	0.1	1	100	34	100	0	18	14	84	100
2	0.1	0.05	100	42	100	0	67	6	86	100
3	0.3	1	100	11	100	0	39	24	97	100
4	0.3	0.05	100	16	100	0	94	11	99	100
5	0.6	1	100	8	100	0	29	6	96	100
6	0.6	0.05	100	6	100	0	87	5	99	100
Categorical										
7	0.1	1	100	78	100	0	5	0	66	100
8	0.1	0.05	100	60	100	0	79	2	86	100
9	0.3	1	100	25	100	0	39	48	80	100
10	0.3	0.05	100	20	100	0	96	24	99	100

Table 3
Mean MCMC efficiency of the fitted models (SCR, RE, SARE, FM, and FE). Here we report 'MCMC efficiency' averaged over each top-level parameters in a model (e.g., N, σ, η) and over each of the converged replicates. MCMC efficiency is calculated as 'ESS/MCMC run time' where the ESS (i.e., effective sample size) is based on the combined samples from the converged MCMC chains after discarding the burn-in period. MCMC run time is calculated excluding the burn-in period. Scenarios without any converged replicates are denoted by '–'. Here, '1 × 1' indicates that the model is fitted without aggregation and '4 × 4' refers to the level to aggregation in the random effects (Section 3.2).

Scenario	η	ϕ	SCR	RE		SARE		FM		FE
				1 × 1	4 × 4	1 × 1	4 × 4	1 × 1	4 × 4	
Continuous										
1	0.1	1	1.22	0.56	0.54	–	1.03	0.07	0.04	1.07
2	0.1	0.05	1.31	0.49	0.52	–	0.81	0.09	0.05	1.06
3	0.3	1	1.85	0.81	0.87	–	1.36	0.09	0.06	1.32
4	0.3	0.05	1.92	0.85	0.83	–	1.26	0.11	0.07	1.31
5	0.6	1	2.10	0.85	1.00	–	1.56	0.11	0.06	1.41
6	0.6	0.05	2.14	0.90	1.00	–	1.41	0.12	0.07	1.42
Categorical										
7	0.1	1	0.41	0.18	0.23	–	0.77	–	0.01	0.88
8	0.1	0.05	0.84	0.36	0.31	–	0.27	0.06	0.04	0.90
9	0.3	1	1.39	0.61	0.59	–	0.70	0.08	0.04	1.18
10	0.3	0.05	2.31	0.90	1.00	–	0.54	0.13	0.09	1.15

$(p_{01}, p_{02}, \ldots, p_{0J})'$. We quantified the accuracy by calculating the expected sum of squared errors (SSE). In practice, we first obtained posterior MCMC sample of baseline detection probability surface $\boldsymbol{p_0} = (p_{01}, p_{02}, \ldots, p_{0J})'$ and computed the mean squared error for detector j: $\text{SSE}_j = \frac{1}{R}\sum_{r=1}^{R}(p_{0j}^{(r)} - p_{0j})^2$, where $\{p_{0j}^{(1)}, p_{0j}^{(2)}, \ldots, p_{0j}^{(R)}\}$ denotes a posterior MCMC sample of p_{0j}, $j = 1, 2, \ldots, J$. Finally, we calculated total error sum of squares $\text{SSE} = \sum_{j=1}^{J}\text{SSE}_j$ as a measure of predictive accuracy of detection probability surface. Smaller SSE implies a more accurate prediction (closer to the truth) of the baseline detection probability surface. We used ΔSSE, relative to the model with the lowest SSE ($\Delta\text{SSE} = \text{SSE} - \min\{\text{SSE}\}$), to compare the accuracy of predicted baseline detection probability surface amongst the different models.

3.4.3. Model comparison using WAIC

We compared the fitted models using Watanabe–Akaike information criterion (WAIC) (Watanabe, 2010), which is computed as

$$\text{WAIC} = -2\sum_{i=1}^{M}\log\Big(\frac{1}{R}\sum_{r=1}^{R} f(\mathbf{Y}_i \mid \boldsymbol{\theta}^{(r)})\Big) + 2\,p_w, \tag{17}$$

where $f(\mathbf{Y}_i \mid \boldsymbol{\theta})$ denotes the likelihood of ith individual capture history $\mathbf{Y}_i = (y_{i1}, y_{i2}, \ldots, y_{iJ})'$ in the model. Here, we adopted the second of the two variants of the penalty term p_w proposed by Gelman et al. (2014b):

$$p_w = \sum_{i=1}^{M}\Big\{\frac{1}{R-1}\sum_{r=1}^{R}\Big(\log f(\mathbf{Y}_i \mid \boldsymbol{\theta}^{(r)}) - \frac{1}{R}\sum_{r=1}^{R}\log f(\mathbf{Y}_i \mid \boldsymbol{\theta}^{(r)})\Big)^2\Big\}. \tag{18}$$

A model with smaller WAIC is preferred. We use ΔWAIC (= WAIC – $\min\{\text{WAIC}\}$) to compare the different models in terms of their model fit and complexity.

4. Empirical example

The brown bear population in Sweden is monitored primarily using non-invasive genetic sampling of scats and hair (Bischof et al., 2016, 2020a). The majority of samples are collected voluntarily by hundreds of hunters. Due to the opportunistic nature of sample collection, there are no direct measures of sampling effort available. Sampling effort, meanwhile, is liable to be both spatially heterogeneous and spatially autocorrelated (Isaac and Pocock, 2015). Thus, this data set offers a good case study to demonstrate the application of our modelling approaches. For this analysis, we considered genetic samples of adult female bears with confirmed individual identity, sex, location, and sampling date from two Swedish counties of Jämtland and Västernorrland during the monitoring from 1 April to 30 November 2020 (Fig. 2) that were stored in the Scandinavian large carnivore monitoring database Rovbase 3.0 (www.rovbase.se). The data set was composed of 2207 successfully genotyped non-invasive genetic samples associated with 731 individual female bears (Fig. 2(b)). Bear detections were assigned to the closest detector in a grid of 3152 detectors at 5 km resolution. On average, there were 0.7 detections per detector (range: 0 – 14, Fig. 2(c)) and 3 detections per detected individual (range: 1 – 31).

For the purpose of demonstration, we fitted five single-season models – SCR, RE, SARE, FM, and FE (as described in Section 2) – to the bear data and compared estimates of baseline detection probability and population size. Because of the low number of detections per detector, we aggregated the random effects to 20 km resolution for models SARE, FM, and RE, so that each random effect value was shared by a maximum of 16 detectors. In an effort to model the spatial heterogeneity in

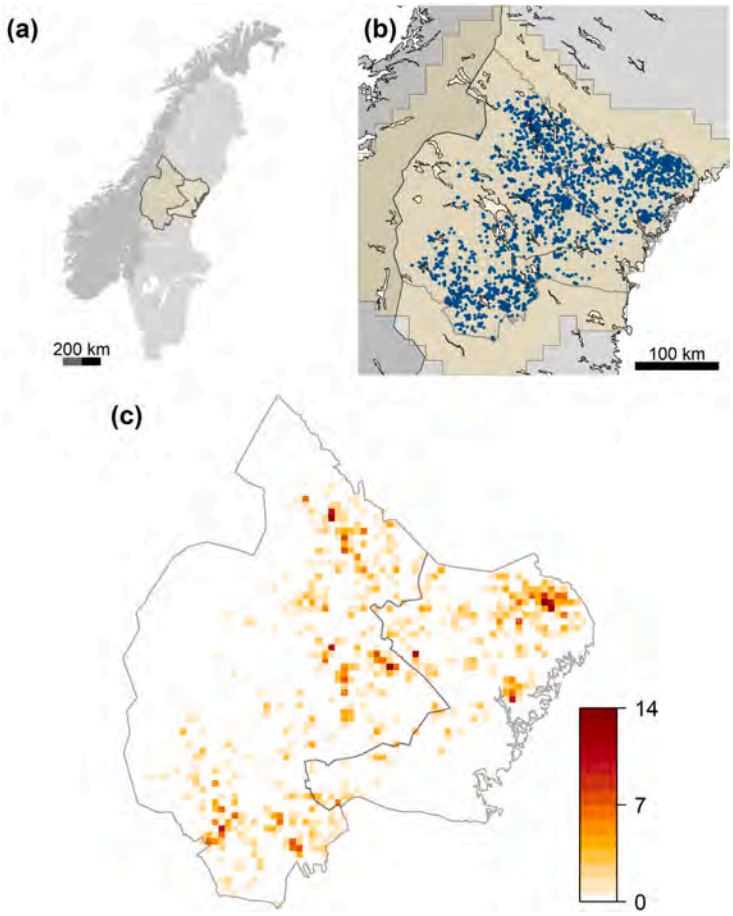

Fig. 2. Illustration of the study area, individual detection locations and detector-specific counts in the non-invasive genetic monitoring data of female brown bears (*Ursus arctos*) from central Sweden, April - November 2020. (a): study area (yellow shaded): the two counties from central Sweden, Jämtland and Västernorrland. (b): detection locations of individual female brown bears during non-invasive genetic monitoring. (c): the number of female bear detections assigned to each detector (at 5 km resolution) across the study area.

detection probability with the FE model, we picked three spatial covariates (Figure S5, Supp. material) that were known to play an important role in detectability (Bischof et al., 2020a): (i) distance (m) from the nearest road, as a measure of site accessibility during sampling, (ii) a binary covariate indicating whether an observation from a large carnivore was recorded by members of the public (www.skandobs.se) or the authorities (www.rovbase.se) during the sampling period. This binary covariate distinguishes areas with very low detectability from those where carnivore DNA samples, if present, could have been detected and submitted for genetic analysis (see Milleret et al., 2022). In addition, (iii) separate intercepts were estimated for the two counties (μ(Jämtland) = μ_1, and μ(Västernorrland) = μ_2):

$$\text{logit}(p_{0j}) = \mu(\text{county}_j) + \boldsymbol{x}_j'\boldsymbol{\beta}, \tag{19}$$

where county_j denotes the county corresponding to the jth detector, $\boldsymbol{\beta} = (\beta_1, \beta_2)'$ denotes the vector of regression coefficients (without intercept) and $\boldsymbol{x}_j = (x_{1j}, x_{2j})'$ denotes the distance to the nearest road and the presence/absence of other observations at the jth detector. We ran four MCMC chains for each of the five models. The chain lengths, burn-in period and thinning rate were as following: (i) SCR: 50,000 iterations, burn-in = 6000, thinning rate = 1, (ii) RE: 13,000 iterations, burn-in = 5000, thinning rate = 1, (iii) SARE: 300,000 iterations, burn-in = 160,000, thinning rate = 2, (iv) FM: 40,000 iterations, burn-in = 2000, thinning rate = 1, and (v) FE: 21,000 iterations, burn-in = 6000, thinning rate = 1. We followed the same procedure to assess model performance as we did in the simulation study, but reported posterior parameter estimates, as RB could not be calculated for the empirical example.

5. Results

5.1. Simulation study

5.1.1. Model convergence, effective sample size and MCMC efficiency

During comparison and interpretation, we only considered models that had reached convergence and exhibited proper mixing of all the top level parameters (e.g., N, σ, ϕ, η), with $\hat{R} \leq 1.1$. While all SCR and FE models converged, convergence of the SARE, RE, and FM models was challenging without aggregating the random effects (Table 2). Only under the extreme categorical scenarios with low baseline detection

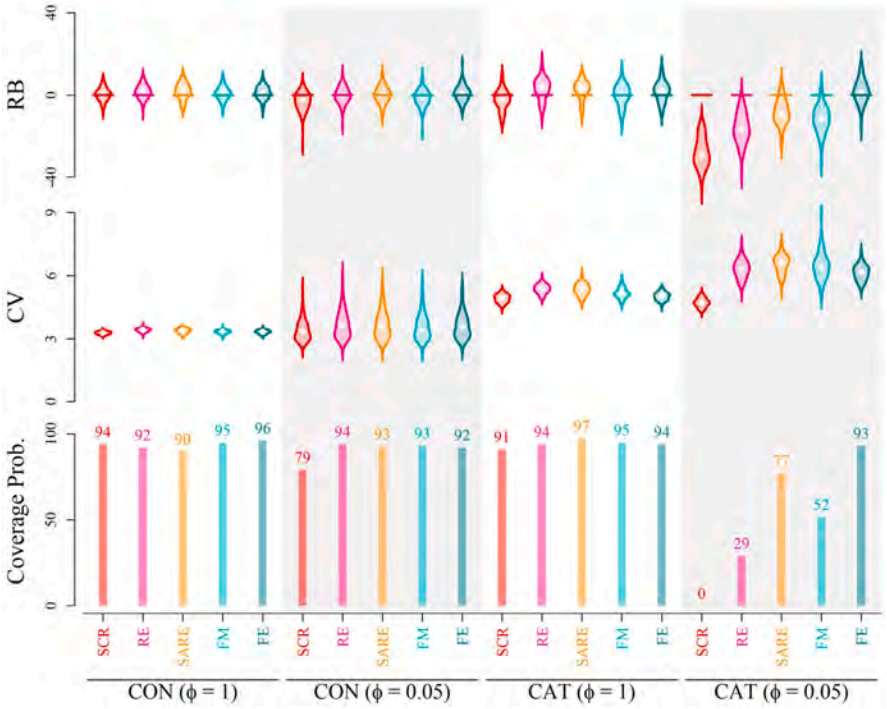

Fig. 3. Performance of the estimator of population size (N) from five models (i) SCR, (ii) RE (aggregation 4 × 4), (iii) SARE (aggregation 4 × 4), (iv) FM (aggregation 4 × 4), and (v) FE. From top to bottom, (1) relative bias (RB, in %), (2) coefficient of variation (CV, in %), and (3) coverage probability of the 95% credible interval (in %) of N for simulation scenarios under average baseline detection probability $\eta = 0.3$. Violins represent the distribution of RB and CV over 100 simulations. (Values above the bars represent the corresponding coverage probability. Labels on the x-axis refer to scenarios with continuous ("CON") and categorical ("CAT") detector-specific variation in baseline detection probability for high autocorrelation ($\phi = 0.05$) and intermediate autocorrelation ($\phi = 1$) scenarios. All results shown are based on models that met convergence criteria.

probability ($\eta = 0.1$), the convergence rates (i.e., the number of converged models out of 100 repetitions) of RE were found to be higher ($\geq 60\%$) than the other two GLMM models. The convergence rate of the RE and FM models improved substantially when random effects were aggregated (66% – 100%). The convergence rate for the SARE model also improved substantially (67% – 96%) after aggregating the random effects under high spatial autocorrelation scenarios ($\phi = 0.05$), whereas the improvement was less pronounced (5% – 39%) under intermediate autocorrelation scenarios ($\phi = 1$).

For all the models that converged, the mean ESS was considerably higher than the suggested threshold of 400, indicating that the MCMC chains were long enough to provide stable estimates (Tables S6 – S9, Supp. material). SCR and FE had the highest MCMC efficiency (mean MCMC eff. > 0.8) under most scenarios except for the extreme categorical scenario with $\eta = 0.1$ and $\phi = 0.05$, where SCR had a relatively lower mean MCMC efficiency 0.41 (see Table 3). MCMC efficiency of both SARE and RE models were 1.5 – 2 times lower than SCR and FE models in these scenarios despite spatial aggregation of the random effects. Among the three GLMM formulations, SARE showed the highest MCMC efficiency in most scenarios (mean: 0.8 – 1.6 in continuous and 0.27 – 0.77 in categorical scenarios). FM model had the lowest MCMC efficiency (mean: 0.01 – 0.1) across all scenarios, primarily due to the higher MCMC computation time (Table S9). Considering the overall poor MCMC convergence of the three GLMMs when fitted without aggregation, we only considered the results with dimension reduction.

5.1.2. Estimates of population size

All five models showed negligible bias in population size N estimates under most simulation scenarios tested here. Both SARE and FE (models that account for spatial autocorrelation) estimated population size with moderate accuracy across all the scenarios (median RB: −9% – 6%) (Tables S3, S5). Although SCR and RE did not specifically model spatial autocorrelation between detectors, population size estimates from these models showed negligible bias (median RB: −10% – 5%) in most scenarios considered (Tables S1 and S2, Supp. material). However, under scenarios with categorical spatial variation in baseline detection probability and high autocorrelation ($\phi = 0.05$), the SCR model showed approximately 30% negative bias in population size (Fig. 3). The RE model produced an elevated negative bias (median RB: −17%) under the categorical scenario with $\eta = 0.3$ and $\phi = 0.05$ (Table S2). The FM model also showed a similar level of accuracy in estimating population size compared to the SARE and FE models for all continuous scenarios (Table S4). Although the FM model seemed to be structurally better suited for the scenarios with categorical variation in detection probability (due to the integration of membership in discrete detectability groups), it showed an 11% negative bias in each of the categorical scenarios with high autocorrelation.

The coefficient of variation (CV) in population size estimated with the five fitted models varied moderately (median CV: 3% – 16%) under $\eta = 0.1$ and was less than 8% for the remaining scenarios with $\eta \geq 0.3$. Coverage probabilities for the SCR model were > 90% for the

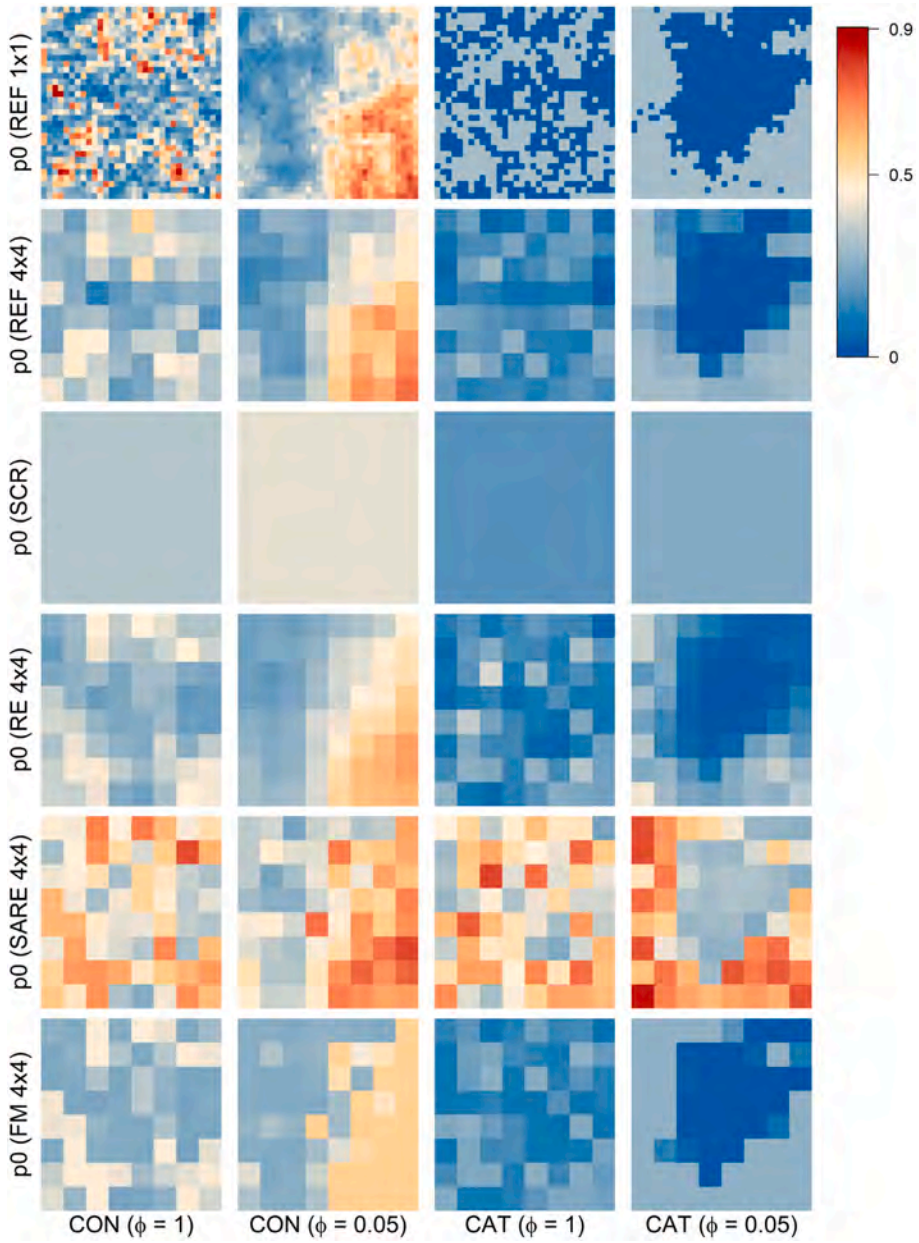

Fig. 4. Illustration of baseline detection probability surfaces for simulation scenarios under average baseline detection probability $\eta = 0.3$. In rows: simulated baseline detection probability surface ('REF 1 × 1'), aggregated simulated baseline detection probability surface (average by clusters of 16 detectors; 'REF 4 × 4'), mean predicted baseline detection probability surfaces from four models: SCR, RE (aggregation 4 × 4), SARE (aggregation 4 × 4) and FM (aggregation 4 × 4). Labels on the x-axis refer to scenarios with continuous ("CON") and categorical ("CAT") variation in baseline detection probability. Second and fourth columns represent high autocorrelation among detectors (i.e., under $\phi = 0.05$), whereas first and the third column represent intermediate autocorrelation (i.e., under $\phi = 1$). Colours correspond to different values of baseline detection probability.

scenarios with intermediate autocorrelation ($\phi = 1$). But when spatial autocorrelation was high ($\phi = 0.05$), coverage declined drastically (65% – 97% coverage) for the continuous scenarios and dropped to less than 20% for the categorical scenarios (Table S1). Coverage probabilities for SARE, RE, and FE were $\geq$ 90% (coverage for FM $\geq$ 81%) for all the scenarios except for the extreme categorical scenario with $\eta = 0.3$ and $\phi = 0.05$, where coverage probabilities were 0.77, 0.29, and 0.51, respectively (Tables S2-S5).

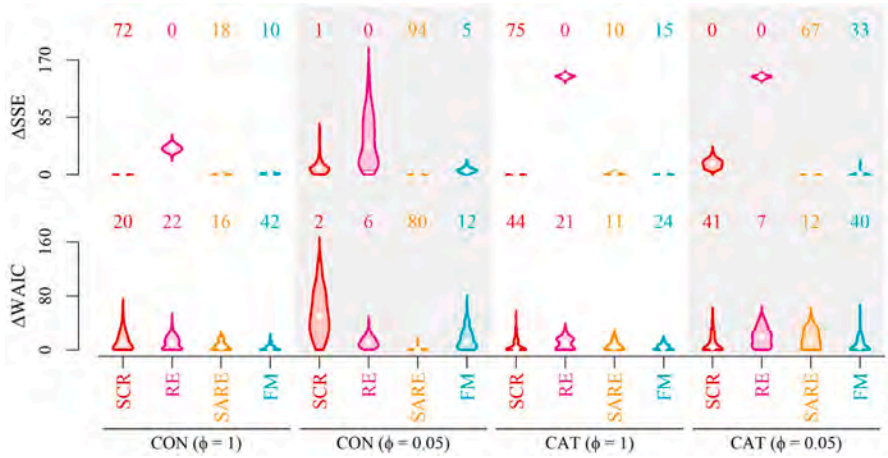

Fig. 5. Model comparison using SSE and WAIC from the simulation study for simulation scenarios under average baseline detection probability $\eta = 0.3$. ΔSSE and ΔWAIC were calculated among four models (SCR, RE (aggregation 4 × 4), SARE (aggregation 4 × 4), and FM (aggregation 4 × 4), but ignoring the FE model). Violins represent the distribution over 100 replicated data sets in each scenario. The number above each violin represents the frequency of times (out of the 100 replicated data sets) when the metric (e.g., ΔSSE, ΔWAIC) of a respective model is minimum among the five models. Labels on the x-axis refer to scenarios with continuous ("CON") and categorical ("CAT") detector-specific variation in detection probability. Grey shaded background indicates scenarios with high autocorrelation among detectors ($\phi = 0.05$), whereas white background indicates scenarios with intermediate autocorrelation ($\phi = 1$). All results shown based on models that met convergence criteria.

5.1.3. Detection probability surfaces and model comparison

Both the SARE and FM models produced reliable detection probability surfaces in the presence of high spatial autocorrelation between detectors (Fig. 4). SARE-generated surfaces were more accurate in estimating surfaces of baseline detection probability, with the lowest SSE in 65% – 94% of the replicates in both continuous and categorical scenarios with high autocorrelation. Although FM was more precise than SARE and RE in scenarios with intermediate autocorrelation, the SCR model (which assumes homogeneous baseline detection probability) had the lowest SSE in 72% – 97% of the replicates in these scenarios (Figs. 5, S2).

Under the scenarios with continuous spatial variation in detectability and high autocorrelation, SARE was selected as the best model 4 – 6 times more frequently than the other models based on WAIC when $\eta \geq 0.3$. With intermediate autocorrelation, FM and RE were selected 1.5 – 2 times more frequently than the other models when η was 0.3 and 0.6, respectively. For all remaining scenarios (including the scenarios with categorical spatial variation), the SCR model was selected.

5.2. Empirical example

All bear models converged and effective sample sizes of all top-level parameters (e.g., N, σ, ϕ, η) were higher than the threshold of 400, which ensured stable estimates (Table 4, Fig. 2). MCMC efficiency of N was highest for the SCR model (≈ 0.114) and lowest for the RE model (≈ 0.0006). Among the three GLMMs, N had the highest MCMC efficiency (≈ 0.0175) under the SARE model.

Based on WAIC values, the best model was SARE followed by RE, FE, FM and finally SCR (Table 4). Estimates of the number of female brown bears (N) were (a) at least 22% lower under the SCR model and (b) at least 18% lower under the FM model compared to the SARE and RE models (Table 4, Figure S6). The 95% CI also showed a similar pattern, with the CI width being larger for the SARE, RE, and FE models (CI width: 213, 234, and 181, respectively) than for the SCR and FM models (CI width: 127 and 141, respectively). However, the CVs of the population size estimates were rather low (2% – 4%) under all five fitted models. The SCR-GLMMs, especially the SARE and RE models, also predicted the largest heterogeneity for the baseline detection probability surface (range: 0.0005 – 0.14; Fig. 6).

6. Discussion

Using a simulation study, we developed and tested three SCR-GLMMs; an independent random effects SCR model (RE), a spatially autocorrelated random effects SCR model (SARE), and a two-group finite mixture SCR model (FM). We assessed and compared the performance of these three models in terms of their ability to account for latent spatial heterogeneity and autocorrelation in detection probability among detectors. The SARE model, the data-generating model in the simulation study, was the most reliable model in estimating population size across all the tested scenarios. When autocorrelation was high ($\phi = 0.05$), the SARE model also performed best in predicting the baseline detection probability surface (as indicated by SSE). Population size estimates from the RE and FM models were largely unbiased in the presence of continuous detector-specific variation in baseline detection probability surface, but subject to a pronounced negative bias when fitted to the extreme scenarios with categorical variation and high autocorrelation. The FM model outperformed the SARE and RE models in terms of SSE for predicted surfaces of baseline detection probability when autocorrelation was at intermediate level ($\phi = 1$).

Unknown latent and autocorrelated variation in detection probability among detectors is common in SCR studies (Stevenson et al., 2021). As shown by Moqanaki et al. (2021), failure to properly account for spatially autocorrelated detection probability may result in biased and overdispersed population size estimates (Fig. 3). In this study, we presented a Bayesian SCR-GLMM (SARE) that specifically accounts for spatial autocorrelation between detectors. The primary advantages of modelling spatial autocorrelation among detectors include the ability to use the information on detector configuration to correctly account for uncertainty in the estimates. In a practical context, this may aid the identification of locations or regions inside the study area with very low or no sampling effort. Fitting the basic SCR model in cases of high autocorrelation produced a 30% RB with approximately zero coverage probability, whereas the SARE model showed less than 10% RB and coverage probability over 77%. Even models that allow variation among detectors but do not explicitly account for spatial autocorrelation (RE and FM models) were able to produce estimates of population size with little bias in most cases.

Table 4
Population size estimates for female brown bears (*Ursus arctos*) in central Sweden. Provided are the posterior mean, coefficient of variation (CV), 2.5%, 50% and 97.5% quantiles, $\hat{R}$, effective sample size (ESS), MCMC efficiency (=ESS/MCMC run time), full MCMC run time of a single chain (in hours) and ΔWAIC for the population size estimate (N) for the five models (SCR, FE, RE, SARE, and FM) fitted to the non-invasive genetic monitoring data of female brown bears collected in Jämtland and Västernorrland counties between 1 April and 30 November 2020. This empirical analysis was conducted with the sole purpose of demonstrating the application of the various models developed here. The model is overly simplistic; for example, it ignores likely spatial heterogeneity in density. For this reason, abundance estimates presented here are neither intended nor suitable for interpretation as an actionable result in terms of population management.

Models	Mean	CV	2.5% Quantile	50% Quantile	97.5% Quantile	$\hat{R}$	ESS	MCMC efficiency	MCMC run time	ΔWAIC
SCR	1290.98	0.025	1229	1290	1356	1.000	14 500	0.1138	10.05	896.02
RE	1653.54	0.036	1545	1651	1779	1.008	835	0.0006	155.89	203.37
SARE	1721.91	0.032	1617	1721	1830	1.011	7 659	0.0175	65.17	0.00
FM	1353.46	0.027	1283	1353	1427	1.008	7 885	0.0057	66.57	505.56
FE	1621.38	0.029	1533	1621	1714	1.004	2 641	0.0132	19.39	371.49

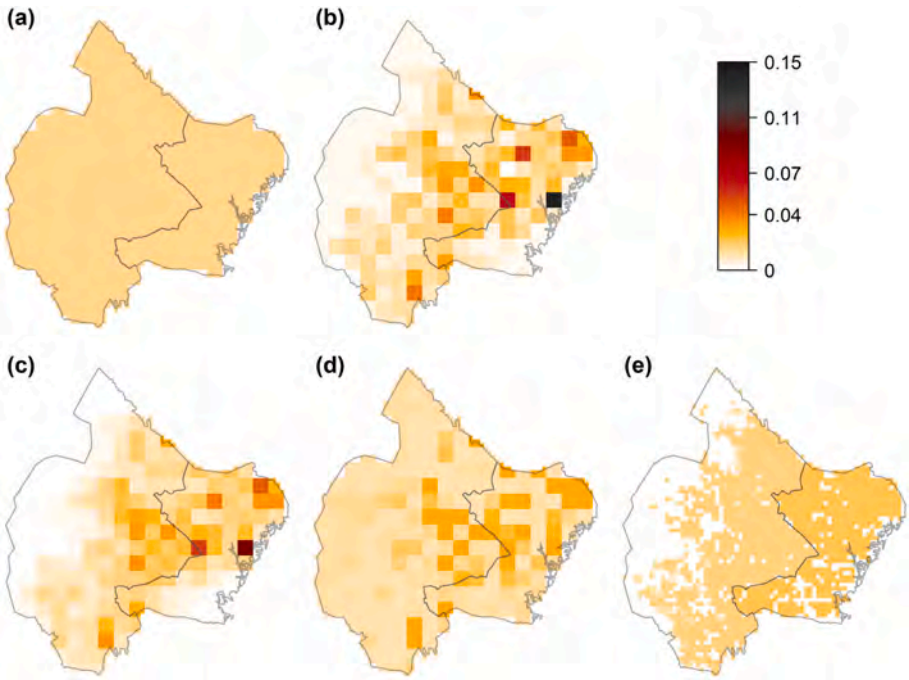

Fig. 6. Illustration of the predicted baseline detection probability surfaces from the five models fitted to non-invasive genetic monitoring data of female brown bears (*Ursus arctos*) from central Sweden, April - November 2020. (a-e): Predicted maps of baseline detection probability (p_0) surfaces from the five models (a) SCR, (b) RE, (c) SARE, (d) FM, and (e) FE fitted to the bear data. For models RE, SARE, and FM, the estimates are obtained after aggregating the random effects to 20 km resolution.

We demonstrated the modelling approaches in a real-life SCR study, non-invasive genetic sampling of brown bear in central Sweden. Therein, members of the public (i.e., hunters) opportunistically collect most of the bear genetic samples with no measure of sampling effort (Bischof et al., 2020a). More than half (56%) of detectors on the east side of the study area had no bear detections compared to 74% on the west along the Swedish–Norwegian border (Fig. 2). This apparent disparity was picked-up by the SCR-GLMMs which suggested a moderately high spatial autocorrelation in detection probability over the study area. This was highlighted in the estimated baseline detection probability surface from the SARE, RE, and FM models which had Moran's I values, a measure of spatial autocorrelation (Lichstein et al., 2002), greater than 0.7.

One major difference between these models was that the estimated baseline detection probability p_0 at one group of aggregated detectors (Figs. 6, black shaded pixel in subplot (b) and dark red shaded pixel in subplot (c), near the eastern boundary) was significantly higher (> 0.1) than the remaining surface with models SARE and RE but not with models SCR, FM, or FE. This is most likely due to one of the female bears that was detected 23 times at this group of detectors, which represents the highest detection rate of any individual at any detector group. This localized apparent hotspot in sampling effort and corresponding large difference in detection probability could neither be accounted for by the SCR model that assumed homogeneous detectability, nor explained by the spatial covariates used in the FE model.

Furthermore, the size of the female brown bear population was estimated to be (a) at least 22% lower with the SCR model and (b) at least 18% lower with the FM model compared to the SARE and RE models. This pattern was consistent with our findings from the simulation study (Scenarios 2 and 8, Figure S2, Tables S1 and S4) and previous results from the literature (Moqanaki et al., 2021; Stevenson et al., 2021) that showed an underestimation of abundance when not accounting for spatially heterogeneous detection probability. Finally, with larger WAIC values, the basic SCR model, FM, and FE seemed

to have poorer predictive ability than the SARE and RE. These results should be interpreted with caution as the models presented here all assume homogeneous density, i.e., uniform placement of individual ACs. When population density varies over space, the number of samples collected in a given location will reflect both the variation in density and sampling effort. For example, if sampling effort is positively correlated with population density, any of the SCR-GLMM models presented here would likely overestimate the heterogeneity in detection and presumably return biased estimates of abundance. Further research is thus needed on the potential confounding effects of simultaneous spatial heterogeneity in density and sampling effort (Clark, 2019; Paterson et al., 2019), and the ability of SCR-GLMMs to account for and quantify such variation.

In large-scale monitoring programmes, like our bear example, data often hail from both structured and unstructured or opportunistic sampling (Altwegg and Nichols, 2019; Bischof et al., 2020a; Isaac et al., 2020). In certain extreme cases (e.g., citizen science data), large portions of the study area may be left unsampled, unbeknownst to the investigator (Bird et al., 2014; Johnston et al., 2022). The three SCR-GLMMs tested here (SARE, RE, and FM) allow modelling and quantifying unknown spatial variation in detection probability in the absence of known fixed effects. Spatially-explicit estimates of detection probability obtained with SCR-GLMMs can be useful in planning and adjusting large-scale surveys, as they help investigators identify regions with high and low detection probability, including apparent holes in sampling. On the flip side, Bayesian SCR-GLMMs involve a large number of unknown parameters, making these models challenging to fit, manifested in slow computation speeds and convergence issues under certain conditions (e.g., SCR data with low number of detections per detector, fitting of GLMM models without aggregating the random effects). For choosing a model, practitioners will need to weigh the benefits of accounting for spatial heterogeneity in detection probability against the costs associated with model complexity.

High dimensional random effects models can easily overfit typical SCR data with few or no detections at the majority of detectors. Dimension reduction of the random effects is a typical strategy to avoid overfitting and to control the number of random effects in a model (Section 3.2) (Hefley et al., 2017; Gelman et al., 2014a). Pooling information allows reliable inference from model fitting that would otherwise be computationally unstable as shown by the improved convergence rates of all SCR-GLMM models when random effects were aggregated (Table 2). The choice of aggregation level implies a trade-off between sample size per detector (high aggregation to achieve dimension reduction) and the resolution of spatially explicit estimates of detectability (low aggregation for more spatial detail). To balance the need for spatial detail and computation, we recommend increasing the aggregation level until the MCMC convergence criteria are met for the key parameters of interest. In empirical analyses, random effects can also be aggregated based on natural groups of detectors, such as administrative units, sub-regions that differ in varying sampling effort, or some other categorical factors.

For the SARE model, we advise caution in choosing an upper bound for the aggregation scale as the spatial autocorrelation is specifically modelled as a decreasing function of inter-detectors distance. It may become computationally intractable to estimate model parameters with low number of random effects since the fitted coarse surface would over-dilute the true scale of variation in the autocorrelated surface. Further, one might introduce negative bias in the estimate of population size under highly autocorrelated scenarios, similar to what we experienced when fitting the basic SCR model to our simulated data with heterogeneous and spatially autocorrelated detection probability.

When the number of detections per detector in SCR data sets is low, multicollinearity can occur between the detector- or cluster-specific random effects and other parameters in the half-normal detection function. For instance, such multicollinearity arises in situations where the SARE model is fitted to SCR data sets that are not sufficiently informative to reveal underlying autocorrelation amongst detectors. Based on SSE values and WAIC in our study, we recommend fitting the SARE model primarily to data from extreme sampling situations, where both detection probability and spatial autocorrelation are high. In all other situations, SARE is expected to give a poorer fit (and poor MCMC convergence), whereas basic SCR can cope with moderate levels of variation present among the detectors even under low detectability (as indicated by SSE and WAIC; Figure S3, Supp. material). Overall, we found WAIC to be useful in selecting the best model in scenarios with different levels of autocorrelation, which holds promise for WAIC application in empirical analyses.

In this study, we focused on three extensions of the SCR model that can account for latent heterogeneous detection probability. Other potential modelling solutions for dealing with this situation include: (i) Bayesian non-parametric models allowing for the possibility of infinite number of subgroups for the detection probability (Turek et al., 2021), (ii) conditionally autoregressive random effects model (CAR) that specifically models spatial autocorrelation between detectors (Nicolau et al., 2020), and (iii) basis function models which use a basis expansion from factorization of a pre-specified correlation matrix (Hefley et al., 2017). Recently, Stevenson et al. (2021) developed a SCR model that models spatially autocorrelated detections based on Gaussian random fields. While the modelling approach can be advantageous in situations where variation in detection probability occurs regularly within individual home ranges, the use of Gaussian random fields requires integrating out the spatially autocorrelated random effects as well as the AC locations, resulting in a significant computational burden. Each of these different classes of models is computationally extensive, overparameterized, and likely to overfit the sparse SCR data sets that are common in ecological studies (Gerber and Parmenter, 2015; Tourani, 2022). Nonetheless, we anticipate future advancements can overcome these computational and modelling barriers to facilitate successful application of these techniques to model heterogeneity in detection probability.

6.1. Conclusions

Accounting for spatial autocorrelation in detection probability can mitigate bias in population size estimates. Dimension reduction of the random effects can help avoid overfitting of such complex models, but caution should be applied when choosing the aggregation scale given the trade-offs between MCMC efficiency and spatial detail. Investigators specifically interested in predicting detection probability surfaces or in identifying sampling holes in their study area, should choose the SARE model in situations where spatial autocorrelation is high and the average number of detections per detector is above one. In situations where either detectability or autocorrelation is low to moderate, we recommend the FM model instead.

CRediT authorship contribution statement

Soumen Dey: Developed the concept, Methodology, Analysis to run the models, Discussed the results, Writing – original draft. **Ehsan Moqanaki:** Developed the concept, Methodology, Help with empirical analysis, Discussed the results, Writing – original draft. **Cyril Milleret:** Discussed the results, Writing – original draft. **Pierre Dupont:** Discussed the results, Writing – original draft. **Mahdieh Tourani:** Discussed the results, Writing – original draft. **Richard Bischof:** Developed the concept, Methodology, Discussed the results, Writing – original draft.

Declaration of competing interest

The authors declare that they have no known competing financial interests or personal relationships that could have appeared to influence the work reported in this paper.

Data availability

R code for generating simulated data and data analysis are provided in the Supplementary material and also can be found on Github (https://github.com/soumenstat89/HetDetSol). Data for the empirical case study can also be accessed from the above Github repository.

Acknowledgements

This work was funded by the Research Council of Norway through project WildMap (NFR 286886) and the Swedish Environmental Protection Agency (Naturvårdsverket). Data for the empirical case study was downloaded from the Scandinavian large carnivore monitoring database Rovbase 3.0 (www.rovbase.se) curated by Rovdata at the Norwegian Institute for Nature Research (NINA), and we thank all contributors, including the Centre for Genetic Identification (CGI) at the Swedish Museum of Natural History.

Appendix A. Supplementary data

Supplementary material related to this article can be found online at https://doi.org/10.1016/j.ecolmodel.2023.110324.

References

Altwegg, R., Nichols, J.D., 2019. Occupancy models for citizen-science data. Methods Ecol. Evol. 10 (1), 8–21.

Bird, T.J., Bates, A.E., Lefcheck, J.S., Hill, N.A., Thomson, R.J., Edgar, G.J., Stuart-Smith, R.D., Wotherspoon, S., Krkosek, M., Stuart-Smith, J.F., Pecl, G.T., Barrett, N., Frusher, S., 2014. Statistical solutions for error and bias in global citizen science datasets. Biol. Cons. 173, 144–154.

Bischof, R., Brøseth, H., Gimenez, O., 2016. Wildlife in a politically divided world: Insularism inflates estimates of brown bear abundance. Conserv. Lett. 9 (2), 122–130.

Bischof, R., Milleret, C., Dupont, P., Chipperfield, J., Tourani, M., Ordiz, A., de Valpine, P., Turek, D., Royle, J.A., Gimenez, O., Flagstad, Ø., Åkesson, M., Svensson, L., Brøseth, H., Kindberg, J., 2020a. Estimating and forecasting spatial population dynamics of apex predators using transnational genetic monitoring. Proc. Natl. Acad. Sci. 117 (48), 30531–30538.

Bischof, R., Turek, D., Milleret, C., Ergon, T., Dupont, P., de Valpine, P., 2020b. nimbleSCR: Spatial capture-recapture (SCR) methods using 'nimble'. R package version 0.1.0.

Borchers, D.L., Efford, M.G., 2008. Spatially explicit maximum likelihood methods for capture–recapture studies. Biometrics 64 (2), 377–385.

Clark, J.D., 2019. Comparing clustered sampling designs for spatially explicit estimation of population density. Popul. Ecol. 61 (1), 93–101.

Cubaynes, S., Pradel, R., Choquet, R., Duchamp, C., Gaillard, J.-M., Lebreton, J.-D., Marboutin, E., Miquel, C., Reboulet, A.-M., Poillot, C., Taberlet, P., Gimenez, O., 2010. Importance of accounting for detection heterogeneity when estimating abundance: the case of French wolves. Conserv. Biol. 24 (2), 621–626.

de Valpine, P., Turek, D., Paciorek, C.J., Anderson-Bergman, C., Lang, D.T., Bodik, R., 2017. Programming with models: writing statistical algorithms for general model structures with NIMBLE. J. Comput. Graph. Statist. 26 (2), 403–413.

Efford, M., 2004. Density estimation in live-trapping studies. Oikos 106 (3), 598–610.

Efford, M.G., 2011. Estimation of population density by spatially explicit capture–recapture analysis of data from area searches. Ecology 92 (12), 2202–2207.

Efford, M.G., Borchers, D.L., Mowat, G., 2013. Varying effort in capture–recapture studies. Methods Ecol. Evol. 4 (7), 629–636.

Efford, M.G., Dawson, D.K., Jhala, Y.V., Qureshi, Q., 2016. Density-dependent home-range size revealed by spatially explicit capture–recapture. Ecography 39 (7), 676–688.

Gelman, A., Carlin, J.B., Stern, H.S., Dunson, D.B., Vehtari, A., Rubin, D.B., 2014a. Bayesian Data Analysis, third ed. CRC Press, Taylor & Francis Group, Boca Raton, FL.

Gelman, A., Hwang, J., Vehtari, A., 2014b. Understanding predictive information criteria for Bayesian models. Stat. Comput. 24 (6), 997–1016.

Gerber, B.D., Parmenter, R.R., 2015. Spatial capture–recapture model performance with known small-mammal densities. Ecol. Appl. 25 (3), 695–705.

Hefley, T.J., Broms, K.M., Brost, B.M., Buderman, F.E., Kay, S.L., Scharf, H.R., Tipton, J.R., Williams, P.J., Hooten, M.B., 2017. The basis function approach for modeling autocorrelation in ecological data. Ecology 98 (3), 632–646.

Hooten, M.B., Larsen, D.R., Wikle, C.K., 2003. Predicting the spatial distribution of ground flora on large domains using a hierarchical Bayesian model. Landsc. Ecol. 18 (5), 487–502.

Howe, E.J., Potter, D., Beauclerc, K.B., Jackson, K.E., Northrup, J.M., 2022. Estimating animal abundance at multiple scales by spatially explicit capture–recapture. Ecol. Appl. e2638.

Isaac, N.J.B., Jarzyna, M.A., Keil, P., Dambly, L.I., Boersch-Supan, P.H., Browning, E., Freeman, S.N., Golding, N., Guillera-Arroita, G., Henrys, P.A., Jarvis, S., Lahoz-Monfort, J., Pagel, J., Pescott, O.L., Schmucki, R., Simmonds, E.G., O'Hara, R.B., 2020. Data integration for large-scale models of species distributions. Trends Ecol. Evol. 35 (1), 56–67.

Isaac, N.J.B., Pocock, M.J.O., 2015. Bias and information in biological records. Biol. J. Linnean Soc. 115 (3), 522–531.

Johnston, A., Matechou, E., Dennis, E.B., 2022. Outstanding challenges and future directions for biodiversity monitoring using citizen science data. Methods Ecol. Evol..

Kendall, K.C., Graves, T.A., Royle, J.A., Macleod, A.C., McKelvey, K.S., Boulanger, J., Waller, J.S., 2019. Using bear rub data and spatial capture–recapture models to estimate trend in a brown bear population. Sci. Rep. 9 (1), 1–11.

Lichstein, J.W., Simons, T.R., Shriner, S.A., Franzreb, K.E., 2002. Spatial autocorrelation and autoregressive models in ecology. Ecol. Monograph 72 (3), 445–463.

Milleret, C., Dupont, P., Bonenfant, C., Brøseth, H., Flagstad, Ø., Sutherland, C., Bischof, R., 2019. A local evaluation of the individual state-space to scale up Bayesian spatial capture–recapture. Ecol. Evol. 9 (1), 352–363.

Milleret, C., Dupont, P., Moqanaki, E., Brøseth, H., Flagstad, Ø., Kleven, O., Kindberg, J., Bischof, R., 2022. Estimates of Wolverine Density, Abundance, and Population Dynamics in Scandinavia, 2014–2022. The Faculty of Environmental Sciences and Natural Resource Management (MINA), Norwegian University of Life Sciences.

Moqanaki, E.M., Milleret, C., Tourani, M., Dupont, P., Bischof, R., 2021. Consequences of ignoring variable and spatially autocorrelated detection probability in spatial capture-recapture. Landsc. Ecol. 36 (10), 2879–2895.

Nicolau, P.G., Sørbye, S.H., Yoccoz, N.G., 2020. Incorporating capture heterogeneity in the estimation of autoregressive coefficients of animal population dynamics using capture–recapture data. Ecol. Evol. 10 (23), 12710–12726.

NIMBLE Development Team, 2021. NIMBLE: MCMC, particle filtering, and programmable hierarchical modeling. http://dx.doi.org/10.5281/zenodo.5562925, Version 0.12.1.

Paterson, J.T., Proffitt, K., Jimenez, B., Rotella, J., Garrott, R., 2019. Simulation-based validation of spatial capture-recapture models: A case study using mountain lions. PLoS One 14 (4), e0215458.

Plummer, M., Best, N., Cowles, K., Vines, K., 2006. CODA: Convergence diagnosis and output analysis for MCMC. R News 6 (1), 7–11.

R Core Team, 2019. R: A Language and Environment for Statistical Computing. R Foundation for Statistical Computing, Vienna, Austria, Version 3.6.2.

Royle, J.A., Chandler, R.B., Sun, C.C., Fuller, A.K., 2013. Integrating resource selection information with spatial capture–recapture. Methods Ecol. Evol. 4 (6), 520–530.

Royle, J.A., Dorazio, R.M., Link, W.A., 2007. Analysis of multinomial models with unknown index using data augmentation. J. Comput. Graph. Statist. 16 (1), 67–85.

Stevenson, B.C., Fewster, R.M., Sharma, K., 2021. Spatial correlation structures for detections of individuals in spatial capture–recapture models. Biometrics.

Sutherland, C., Fuller, A.K., Royle, J.A., 2015. Modelling non-euclidean movement and landscape connectivity in highly structured ecological networks. Methods Ecol. Evol. 6 (2), 169–177.

Thompson, C.M., Royle, J.A., Garner, J.D., 2012. A framework for inference about carnivore density from unstructured spatial sampling of scat using detector dogs. J. Wildlife Manage. 76 (4), 863–871.

Tourani, M., 2022. A review of spatial capture–recapture: Ecological insights, limitations, and prospects. Ecol. Evol. 12 (1), e8468.

Turek, D., Wehrhahn, C., Gimenez, O., 2021. Bayesian non-parametric detection heterogeneity in ecological models. Environ. Ecol. Stat. 28 (2), 355–381.

Vehtari, A., Gelman, A., Simpson, D., Carpenter, B., Bürkner, P.-C., 2021. Rank-normalization, folding, and localization: An improved $\hat{R}$ for assessing convergence of MCMC (with discussion). Bayesian Anal. 16 (2), 667–718.

Watanabe, S., 2010. Asymptotic equivalence of Bayes cross validation and widely applicable information criterion in singular learning theory. J. Mach. Learn. Res. 11 (Dec), 3571–3594.

Wikle, C.K., Hooten, M.B., 2010. A general science-based framework for dynamical spatio-temporal models. Test 19 (3), 417–451.

Supplementary Material

Modelling spatially autocorrelated detection probabilities in spatial capture-recapture using random effects

Soumen Dey*[1], Ehsan Moqanaki[1], Cyril Milleret[1], Pierre Dupont[1], Mahdieh Tourani[1,2], and Richard Bischof[1]

[1]Faculty of Environmental Sciences and Natural Resource Management, Norwegian University of Life Sciences, 1432 Ås, Norway

[2]Department of Ecosystem and Conservation Sciences, University of Montana, Missoula, USA

Running headline: Spatially heterogeneous detectability in SCR

*E-mail: *soumenstat89@gmail.com*

S1 Simulations Study: Tables of posterior estimates and effective sample size (ESS) of different models

Table S1: **SCR**: Relative bias (RB, median and 2.5% and 97.5% quantiles), coefficient of variation (CV, median and 2.5% and 97.5% quantiles), and coverage probability of 95% CI of the population size (N) and the spatial scale parameter of the half-normal detection function (σ) across each scenario.

Scenario	η	ϕ	RB			CV			Coverage prob.
			Median	2.5% Quantile	97.5% Quantile	Median	2.5% Quantile	97.5% Quantile	
N									
Continuous									
1	0.100	1	−0.027	−0.105	0.086	0.054	0.047	0.060	0.96
2	0.100	0.050	−0.095	−0.275	0.048	0.054	0.033	0.143	0.65
3	0.300	1	0.005	−0.060	0.070	0.033	0.031	0.034	0.94
4	0.300	0.050	−0.025	−0.116	0.044	0.033	0.027	0.046	0.79
5	0.600	1	0.006	−0.037	0.055	0.028	0.027	0.029	0.97
6	0.600	0.050	−0.006	−0.061	0.051	0.028	0.026	0.031	0.97
Categorical									
7	0.100	1	−0.032	−0.185	0.271	0.137	0.111	0.166	0.99
8	0.100	0.050	−0.295	−0.438	−0.040	0.113	0.092	0.138	0.20
9	0.300	1	−0.022	−0.125	0.087	0.049	0.045	0.053	0.91
10	0.300	0.050	−0.290	−0.409	−0.142	0.047	0.043	0.051	0
σ									
Continuous									
1	0.100	1	−0.022	−0.094	0.049	0.037	0.033	0.042	0.90
2	0.100	0.050	−0.012	−0.098	0.068	0.037	0.019	0.086	0.94
3	0.300	1	−0.007	−0.042	0.032	0.019	0.017	0.020	0.92
4	0.300	0.050	−0.004	−0.046	0.030	0.019	0.012	0.031	0.93
5	0.600	1	−0.001	−0.031	0.026	0.013	0.012	0.014	0.90
6	0.600	0.050	−0.001	−0.024	0.023	0.013	0.010	0.016	0.95
Categorical									
7	0.100	1	−0.026	−0.195	0.170	0.085	0.073	0.103	0.88
8	0.100	0.050	−0.032	−0.185	0.144	0.073	0.062	0.085	0.82
9	0.300	1	−0.020	−0.103	0.041	0.034	0.031	0.037	0.81
10	0.300	0.050	−0.038	−0.100	0.022	0.031	0.028	0.034	0.72

Table S2: **RE** (4×4): Relative bias (RB, median and 2.5% and 97.5% quantiles), coefficient of variation (CV, median and 2.5% and 97.5% quantiles), and coverage probability of 95% CI of the population size (N) and the spatial scale parameter of the half-normal detection function (σ) across each scenario. Here '4 × 4' refers to the level to aggregation in the random effects (Section 3.2, main text).

Scenario	η	ϕ	RB			CV			Coverage prob.
			Median	2.5% Quantile	97.5% Quantile	Median	2.5% Quantile	97.5% Quantile	
N									
Continuous									
1	0.100	1	0.032	−0.056	0.133	0.058	0.051	0.065	0.96
2	0.100	0.050	−0.017	−0.141	0.152	0.062	0.035	0.149	0.94
3	0.300	1	0.015	−0.048	0.077	0.034	0.032	0.036	0.92
4	0.300	0.050	−0.003	−0.082	0.065	0.036	0.028	0.052	0.94
5	0.600	1	0.010	−0.035	0.065	0.029	0.028	0.030	0.95
6	0.600	0.050	0.002	−0.049	0.053	0.029	0.026	0.033	0.99
Categorical									
7	0.100	1	0.047	−0.118	0.349	0.139	0.115	0.162	0.94
8	0.100	0.050	−0.065	−0.296	0.168	0.133	0.117	0.153	0.90
9	0.300	1	0.037	−0.082	0.131	0.054	0.049	0.057	0.94
10	0.300	0.050	−0.166	−0.291	−0.016	0.063	0.055	0.071	0.29
σ									
Continuous									
1	0.100	1	−0.010	−0.094	0.059	0.038	0.034	0.043	0.93
2	0.100	0.050	−0.008	−0.083	0.080	0.038	0.019	0.090	0.94
3	0.300	1	−0.008	−0.040	0.030	0.019	0.018	0.021	0.93
4	0.300	0.050	−0.003	−0.040	0.035	0.019	0.012	0.033	0.92
5	0.600	1	−0.007	−0.039	0.022	0.013	0.012	0.014	0.86
6	0.600	0.050	−0.005	−0.028	0.019	0.013	0.009	0.016	0.94
Categorical									
7	0.100	1	−0.012	−0.196	0.212	0.087	0.076	0.104	0.89
8	0.100	0.050	−0.007	−0.160	0.186	0.077	0.066	0.091	0.86
9	0.300	1	−0.008	−0.092	0.047	0.035	0.031	0.038	0.89
10	0.300	0.050	−0.015	−0.075	0.044	0.032	0.029	0.036	0.92

Table S3: **SARE** (4×4): Relative bias (RB, median and 2.5% and 97.5% quantiles), coefficient of variation (CV, median and 2.5% and 97.5% quantiles), and coverage probability of 95% CI of the population size (N) and the spatial scale parameter of the half-normal detection function (σ) across each scenario. Here '4×4' refers to the level to aggregation in the random effects (Section 3.2, main text).

Scenario	η	ϕ	RB			CV			Coverage prob.
			Median	2.5% Quantile	97.5% Quantile	Median	2.5% Quantile	97.5% Quantile	
N									
Continuous									
1	0.100	1	−0.014	−0.077	0.096	0.055	0.049	0.064	1
2	0.100	0.050	−0.004	−0.130	0.189	0.055	0.035	0.138	0.94
3	0.300	1	0.020	−0.061	0.079	0.034	0.031	0.035	0.90
4	0.300	0.050	0.001	−0.082	0.071	0.036	0.028	0.051	0.93
5	0.600	1	0.016	−0.024	0.051	0.028	0.028	0.029	0.97
6	0.600	0.050	0.0002	−0.051	0.049	0.029	0.026	0.033	0.99
Categorical									
7	0.100	1	0.064	−0.017	0.242	0.132	0.123	0.142	1
8	0.100	0.050	0.002	−0.235	0.229	0.131	0.117	0.146	0.91
9	0.300	1	0.032	−0.074	0.101	0.053	0.048	0.057	0.97
10	0.300	0.050	−0.091	−0.219	0.035	0.066	0.057	0.074	0.77
σ									
Continuous									
1	0.100	1	−0.006	−0.080	0.049	0.035	0.030	0.039	0.89
2	0.100	0.050	0.001	−0.077	0.074	0.031	0.018	0.078	0.94
3	0.300	1	0.003	−0.037	0.034	0.019	0.017	0.020	0.95
4	0.300	0.050	0.001	−0.038	0.041	0.019	0.012	0.031	0.94
5	0.600	1	−0.001	−0.032	0.020	0.013	0.012	0.013	0.90
6	0.600	0.050	0.001	−0.027	0.022	0.013	0.010	0.016	0.94
Categorical									
7	0.100	1	−0.024	−0.204	0.052	0.076	0.067	0.088	0.60
8	0.100	0.050	−0.013	−0.160	0.189	0.074	0.062	0.089	0.85
9	0.300	1	−0.010	−0.104	0.052	0.033	0.031	0.038	0.87
10	0.300	0.050	−0.011	−0.075	0.046	0.032	0.028	0.036	0.92

Table S4: **FM** (4×4): Relative bias (RB, median and 2.5% and 97.5% quantiles), coefficient of variation (CV, median and 2.5% and 97.5% quantiles), and coverage probability of 95% CI of the population size (N) and the spatial scale parameter of the half-normal detection function (σ) across each scenario. Here '4×4' refers to the level to aggregation in the random effects (Section 3.2, main text).

Scenario	η	ϕ	RB			CV			Coverage prob.
			Median	2.5% Quantile	97.5% Quantile	Median	2.5% Quantile	97.5% Quantile	
N									
Continuous									
1	0.100	1	−0.009	−0.083	0.084	0.056	0.050	0.064	0.98
2	0.100	0.050	−0.057	−0.202	0.067	0.056	0.034	0.150	0.82
3	0.300	1	0.008	−0.051	0.071	0.033	0.031	0.035	0.95
4	0.300	0.050	−0.011	−0.092	0.060	0.034	0.028	0.051	0.93
5	0.600	1	0.008	−0.037	0.057	0.028	0.027	0.029	0.96
6	0.600	0.050	−0.0001	−0.053	0.050	0.028	0.026	0.032	0.99
Categorical									
7	0.100	1	−0.021	−0.184	0.299	0.137	0.115	0.169	0.97
8	0.100	0.050	−0.112	−0.352	0.125	0.137	0.120	0.161	0.84
9	0.300	1	0.004	−0.109	0.076	0.051	0.047	0.057	0.95
10	0.300	0.050	−0.115	−0.248	0.020	0.064	0.052	0.078	0.51
σ									
Continuous									
1	0.100	1	−0.013	−0.093	0.052	0.037	0.033	0.042	0.929
2	0.100	0.050	−0.005	−0.096	0.059	0.034	0.019	0.086	0.942
3	0.300	1	−0.005	−0.040	0.035	0.019	0.017	0.021	0.928
4	0.300	0.050	−0.001	−0.038	0.036	0.019	0.012	0.032	0.939
5	0.600	1	−0.001	−0.030	0.025	0.013	0.012	0.014	0.896
6	0.600	0.050	0.001	−0.024	0.022	0.013	0.010	0.016	0.960
Categorical									
7	0.100	1	−0.044	−0.196	0.162	0.085	0.073	0.101	0.864
8	0.100	0.050	−0.024	−0.172	0.185	0.075	0.063	0.088	0.837
9	0.300	1	−0.017	−0.096	0.042	0.034	0.031	0.037	0.850
10	0.300	0.050	−0.018	−0.079	0.039	0.032	0.028	0.036	0.909

Table S5: **FE**: Relative bias (RB, median and 2.5% and 97.5% quantiles), coefficient of variation (CV, median and 2.5% and 97.5% quantiles), and coverage probability of 95% CI of the population size (N) and the spatial scale parameter of the half-normal detection function (σ) across each scenario.

Scenario	η	ϕ	RB			CV			Coverage prob.
			Median	2.5% Quantile	97.5% Quantile	Median	2.5% Quantile	97.5% Quantile	
N									
Continuous									
1	0.100	1	0.017	−0.070	0.101	0.054	0.049	0.059	0.980
2	0.100	0.050	0.007	−0.103	0.152	0.057	0.035	0.123	0.950
3	0.300	1	0.010	−0.055	0.070	0.033	0.031	0.035	0.960
4	0.300	0.050	0.008	−0.067	0.083	0.035	0.028	0.050	0.920
5	0.600	1	0.007	−0.037	0.060	0.028	0.027	0.029	0.960
6	0.600	0.050	0.007	−0.047	0.047	0.028	0.026	0.033	0.980
Categorical									
7	0.100	1	0.033	−0.150	0.292	0.121	0.104	0.138	0.950
8	0.100	0.050	0.057	−0.129	0.323	0.113	0.100	0.127	0.950
9	0.300	1	0.020	−0.079	0.117	0.050	0.047	0.054	0.940
10	0.300	0.050	0.015	−0.085	0.128	0.062	0.055	0.067	0.930
σ									
Continuous									
1	0.100	1	0.0003	−0.067	0.045	0.026	0.023	0.030	0.940
2	0.100	0.050	0.001	−0.073	0.070	0.026	0.014	0.063	0.960
3	0.300	1	0.002	−0.021	0.027	0.014	0.012	0.015	0.960
4	0.300	0.050	0.001	−0.029	0.030	0.014	0.009	0.023	0.960
5	0.600	1	0.003	−0.021	0.021	0.010	0.009	0.010	0.910
6	0.600	0.050	−0.0005	−0.016	0.018	0.010	0.008	0.012	0.970
Categorical									
7	0.100	1	−0.008	−0.102	0.120	0.061	0.053	0.069	0.940
8	0.100	0.050	0.002	−0.090	0.122	0.055	0.048	0.063	0.950
9	0.300	1	0.003	−0.051	0.045	0.024	0.022	0.026	0.950
10	0.300	0.050	0.006	−0.037	0.042	0.023	0.021	0.027	0.990

Table S6: **SCR** and **FE**: Effective sample size (ESS) after burn-in, MCMC efficiency (=ESS/MCMC run time) and full MCMC run time of a single chain (in minutes). For comparison purposes, we report mean ESS and mean MCMC efficiency (=ESS/MCMC run time) averaged over each top-level parameters in the model and over each of the converged replicates. For both SCR and FE models, we ran three MCMC chains of 30,000 iterations (burn-in period 12,000).

Scenario	η	ϕ	SCR			FE		
			ESS	MCMC efficiency	MCMC run time	ESS	MCMC efficiency	MCMC run time
Continuous								
1	0.100	1	2277	1.224	17.260	10032	1.067	65.210
2	0.100	0.050	2369	1.312	16.520	9909	1.065	65.070
3	0.300	1	3608	1.853	18.050	12562	1.323	65.770
4	0.300	0.050	3691	1.922	17.790	12333	1.311	65.620
5	0.600	1	4133	2.096	18.280	13398	1.413	65.820
6	0.600	0.050	4215	2.145	18.210	13354	1.418	65.680
Categorical								
7	0.100	1	698	0.412	15.870	6160	0.876	48.910
8	0.100	0.050	1274	0.839	14.220	6362	0.901	49.140
9	0.300	1	2521	1.392	16.830	8453	1.176	50
10	0.300	0.050	3697	2.312	14.890	8187	1.153	49.410

Table S7: **RE**: Effective sample size (ESS) after burn-in, MCMC efficiency (=ESS/MCMC run time) and full MCMC run time of a single chain (in minutes). For comparison purposes, we report mean ESS and mean MCMC efficiency (=ESS/MCMC run time) averaged over each top-level parameters in the model and over each of the converged replicates. We ran three MCMC chains of 100,000 iterations (burn-in period 20,000, with or without aggregation). Scenarios without any converged replicates are indicated by '-'. Here '1×1' indicates that the model is fitted without aggregation and '4×4' refers to the level to aggregation in the random effects (Section 3.2, main text).

Scenario	η	ϕ	RE (1×1)			RE (4×4)		
			ESS	MCMC efficiency	MCMC run time	ESS	MCMC efficiency	MCMC run time
Continuous								
1	0.100	1	8976	0.557	112.140	5872	0.543	75.380
2	0.100	0.050	7525	0.486	108.690	5509	0.520	73.340
3	0.300	1	13420	0.813	115.280	9581	0.867	76.830
4	0.300	0.050	13671	0.847	112.710	9112	0.832	76.050
5	0.600	1	14221	0.855	115.110	11152	1.004	77.260
6	0.600	0.050	14775	0.901	114.360	11133	1.004	77.060
Categorical								
7	0.100	1	2897	0.185	109.560	2338	0.229	71.930
8	0.100	0.050	5166	0.360	100.490	2935	0.311	66.490
9	0.300	1	9875	0.610	112.260	6292	0.591	74.320
10	0.300	0.050	14092	0.961	102.290	4996	0.524	66.280

Table S8: **SARE**: Effective sample size (ESS) after burn-in, MCMC efficiency (=ESS/MCMC run time) and full MCMC run time of a single chain (in minutes). For comparison purposes, we report mean ESS and mean MCMC efficiency (=ESS/MCMC run time) averaged over each top-level parameters in the model and over each of the converged replicates. We ran three MCMC chains of 100,000 iterations (burn-in period 20,000, with or without aggregation). Scenarios without any converged replicates are indicated by '-'. Here '1×1' indicates that the model is fitted without aggregation and '4×4' refers to the level to aggregation in the random effects (Section 3.2, main text).

Scenario	η	ϕ	SARE (1×1)			SARE (4×4)		
			ESS	MCMC efficiency	MCMC run time	ESS	MCMC efficiency	MCMC run time
Continuous								
1	0.100	1	-	-	224.950	8803	1.028	60
2	0.100	0.050	-	-	221.370	6967	0.809	58.870
3	0.300	1	-	-	228.440	12234	1.361	62
4	0.300	0.050	-	-	229.610	10924	1.262	60.180
5	0.600	1	-	-	230.220	13749	1.564	62.060
6	0.600	0.050	-	-	231.900	12342	1.406	61.200
Categorical								
7	0.100	1	-	-	217.490	6634	0.774	57.070
8	0.100	0.050	-	-	214.990	2214	0.274	56.070
9	0.300	1	-	-	226.890	6108	0.699	60.540
10	0.300	0.050	-	-	221.840	4495	0.544	57.470

Table S9: **FM**: Effective sample size (ESS) after burn-in, MCMC efficiency (=ESS/MCMC run time) and full MCMC run time of a single chain (in minutes). For comparison purposes, we report mean ESS and mean MCMC efficiency (=ESS/MCMC run time) averaged over each top-level parameters in the model and over each of the converged replicates. We ran the MCMC for a. 60,000 iterations (burn-in period 12,000) when fitted without aggregation, b. 20,000 iterations (burn-in period 4,000) when fitted with aggregating random effects. Scenarios without any converged replicates are indicated by '-'. Here '1×1' and '4×4' refer to the level to aggregation in the random effects - '1×1' indicating that the model is fitted without aggregation and '4×4' indicating that we aggregated the random effects at 4×4 scale (Section 3.2, main text).

Scenario	η	ϕ	FM (1×1)			FM (4×4)		
			ESS	MCMC efficiency	MCMC run time	ESS	MCMC efficiency	MCMC run time
Continuous								
1	0.100	1	2865	0.072	283.140	1104	0.037	207.470
2	0.100	0.050	3258	0.086	260.920	1387	0.049	197.580
3	0.300	1	4111	0.095	292.790	1758	0.058	212.690
4	0.300	0.050	4312	0.106	281.680	2189	0.073	208.760
5	0.600	1	4822	0.114	294.450	1929	0.062	214.630
6	0.600	0.050	4820	0.119	289.410	2294	0.075	212.550
Categorical								
7	0.100	1	-	-	283.850	432	0.015	210.310
8	0.100	0.050	1561	0.059	223.690	967	0.036	188.820
9	0.300	1	3106	0.076	288.380	1269	0.042	210.900
10	0.300	0.050	4386	0.134	224.860	2585	0.095	189.170

S2 Simulations Study: Additional figures

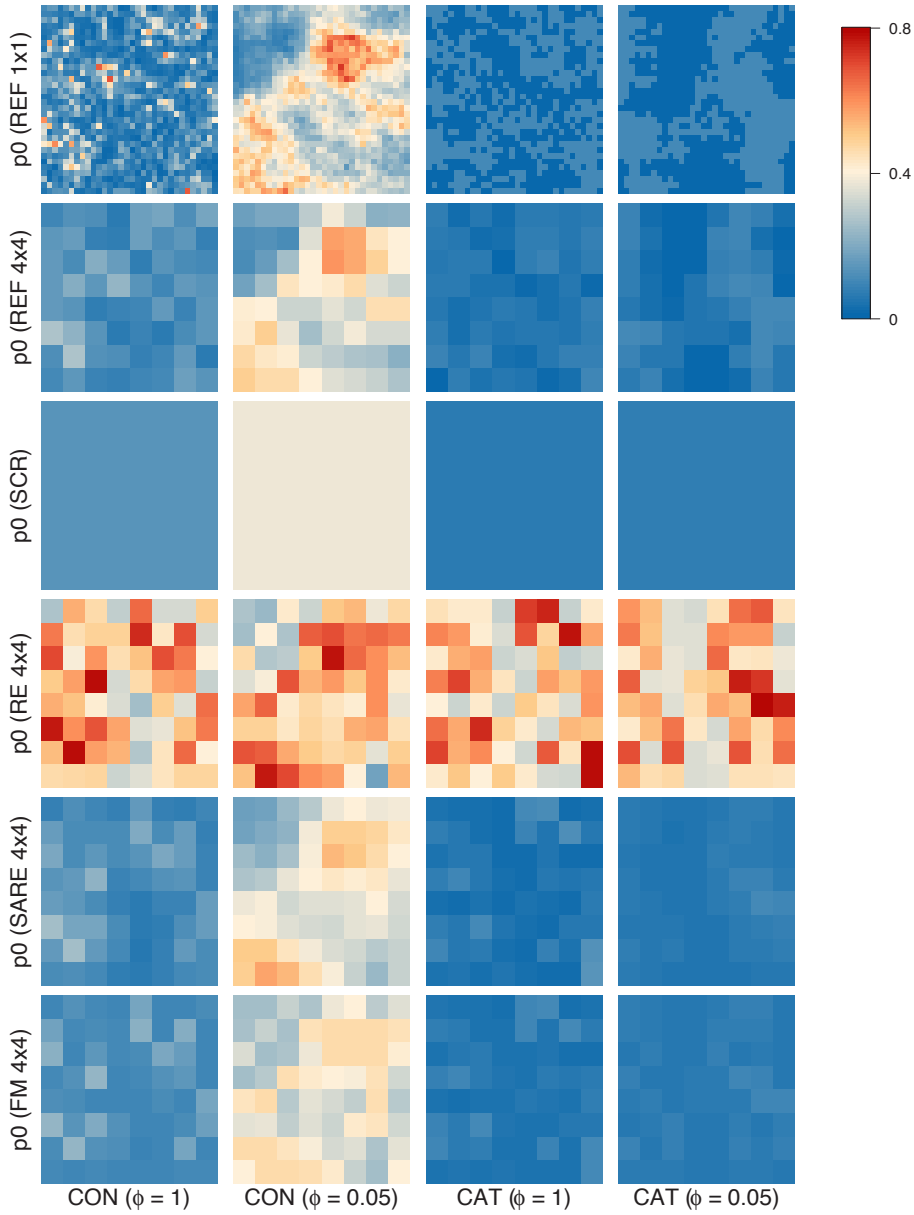

Figure S1: Illustration of baseline detection probability surfaces for simulation scenarios under average baseline detection probability $\eta = 0.1$. In rows: simulated baseline detection probability surface ('REF 1×1'), baseline detection probability surface after averaging the simulated values for each cluster of detectors at 4×4 scale ('REF 4×4'), predicted baseline detection probability surface from four models: SCR, RE (aggregation 4×4), SARE (aggregation 4×4), FM (aggregation 4×4). Labels on the x-axis refer to scenarios with continuous ("CON") and categorical ("CAT") detector-specific variation in detection probability. Second and fourth columns represent high autocorrelation among detectors (i.e., under $\phi = 0.05$), whereas first and the third column represent intermediate autocorrelation (i.e., under $\phi = 1$). Colors correspond to different values of baseline detection probability.

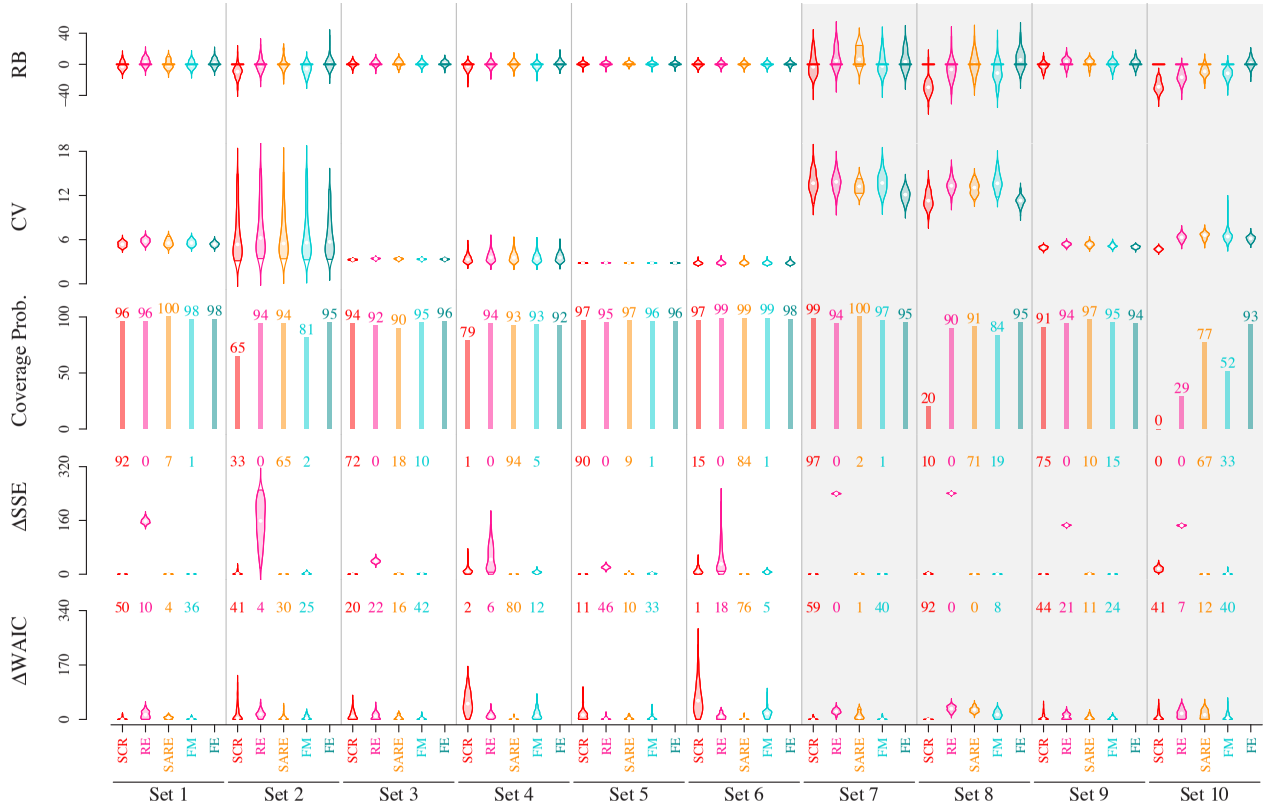

Figure S2: Posterior summaries of population size N derived using five models: (i) SCR, (ii) SARE (aggregation 4×4), (iii) RE (aggregation 4×4), (iv) FM (aggregation 4×4), (v) FE. Results compare relative bias (RB, in %), coefficient of variation (CV, in %), and coverage probability (in %) of 95% CI for different sets of simulation scenarios. Violins represent the distribution of RB/CV from 100 simulations. Set numbers on the x-axis refer to the serial number of the simulation scenario (as shown in the tables). Gray shaded background represents scenarios with categorical detector-specific variation, whereas white background represents continuous spatial variation. The figures were based on models that met convergence criteria (Section 3.3, main text).

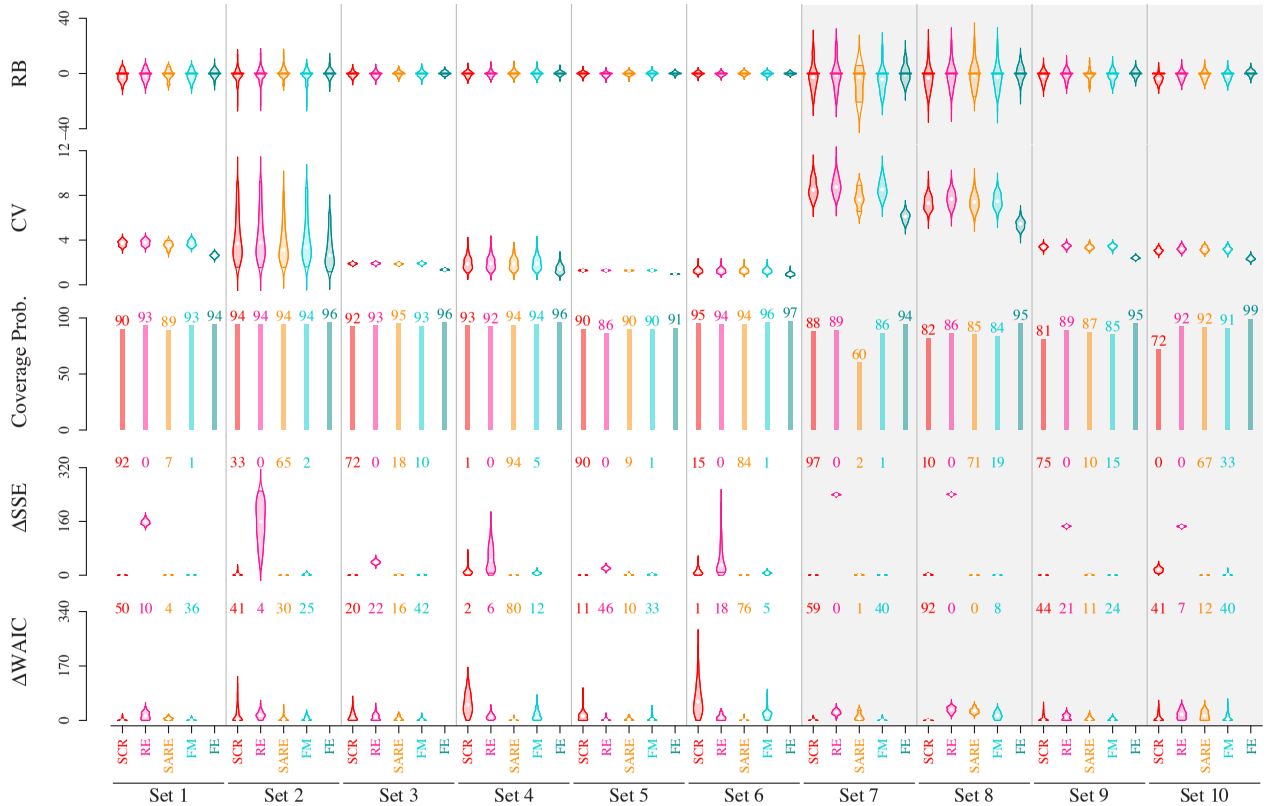

Figure S3: Posterior summaries of σ derived using five models: (i) SCR, (ii) SARE (aggregation 4×4), (iii) RE (aggregation 4×4), (iv) FM (aggregation 4×4), (v) FE. Results compare relative bias (RB, in %), coefficient of variation (CV, in %), and coverage probability (in %) of 95% CI for different sets of simulation scenarios. Violins represent the distribution of RB/CV from 100 simulations. Set numbers on the x-axis refer to the serial number of the simulation scenario (as shown in the tables). Gray shaded background represents scenarios with categorical detector-specific variation, whereas white background represents continuous spatial variation. The figures were based on models that met convergence criteria (Section 3.3, main text).

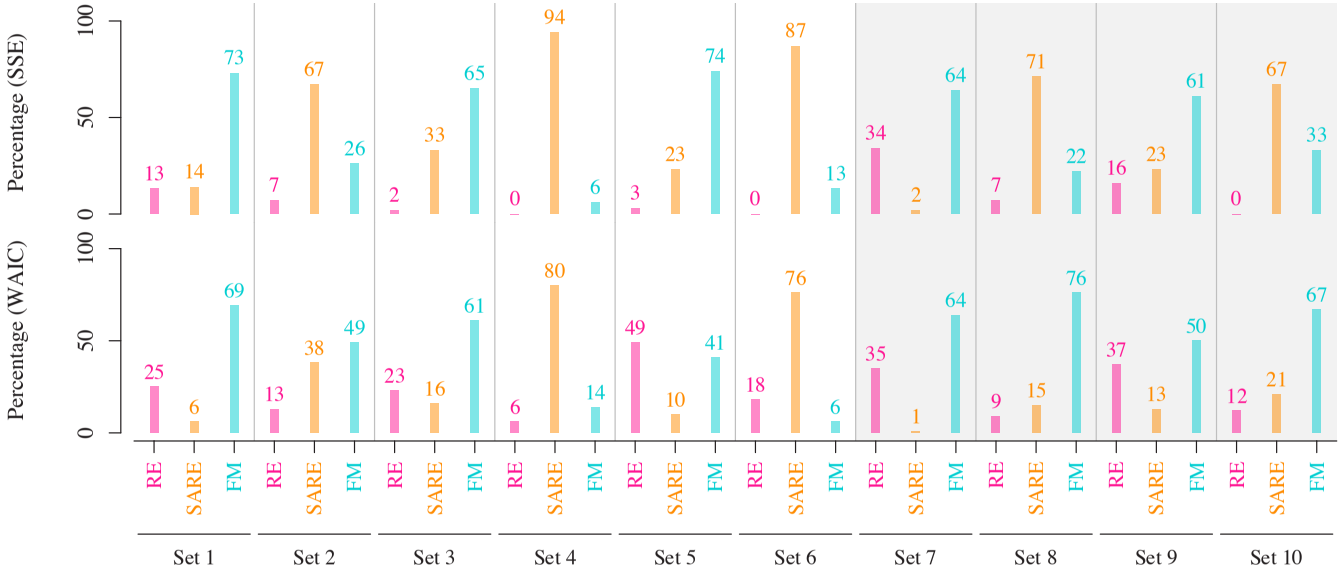

Figure S4: Barplot showing percentage of replicates where SSE of predicted baseline detection probability surface and WAIC from a fitted model is lowest among its competitors. Here we considered only the three SCR-GLMMs, namely RE, SARE, and FM. Set numbers on the x-axis refer to the serial number of the simulation scenario (as shown in the tables). Gray shaded background represents scenarios with categorical detector-specific variation, whereas white background represents continuous spatial variation. The figures were based on models that met convergence criteria and the MCMC chains were of different lengths for different models (Section 3.3, main text).

S3 Empirical example: Table of posterior estimates and effective sample size (ESS) of different models fitted to brown bear monitoring data

Table S10: Posterior estimates of the scale parameter σ under the five fitted models fitted to female brown bear (*Ursus arctos*) data from central Sweden. Mean, coefficient of variation (CV), 2.5%, 50% and 97.5% quantiles, $\hat{R}$, effective sample size (ESS), MCMC efficiency (=ESS/MCMC run time) and full MCMC run time of a single chain (in hours) of the spatial scale parameter of the half-normal detection function (σ; km) from each of the five models: **SCR, FE, RE, SARE** and **FM**, fitted to non-invasive genetic monitoring data of female brown bears from central Sweden, April - November 2020. The full MCMC run time of a single chain (in hours) and ΔWAIC values for each of the five models are shown in the last two columns.

Models	Mean	CV	2.5%	50%	97.5%	$\hat{R}$	ESS	MCMC efficiency	MCMC run time	ΔWAIC
SCR	5.66	0.014	5.52	5.66	5.82	1.000	7039	0.0552	10.05	896.02
RE	5.74	0.014	5.60	5.74	5.90	1.004	1297	0.0009	155.89	203.37
SARE	5.74	0.014	5.58	5.74	5.84	1.002	2035	0.0046	65.17	0.00
FM	5.70	0.014	5.56	5.90	5.86	1.003	7616	0.0055	66.57	505.56
FE	5.76	0.014	5.60	5.76	5.92	1.001	2833	0.0142	19.39	371.49

S4 Bear Empirical Example: Additional Figures

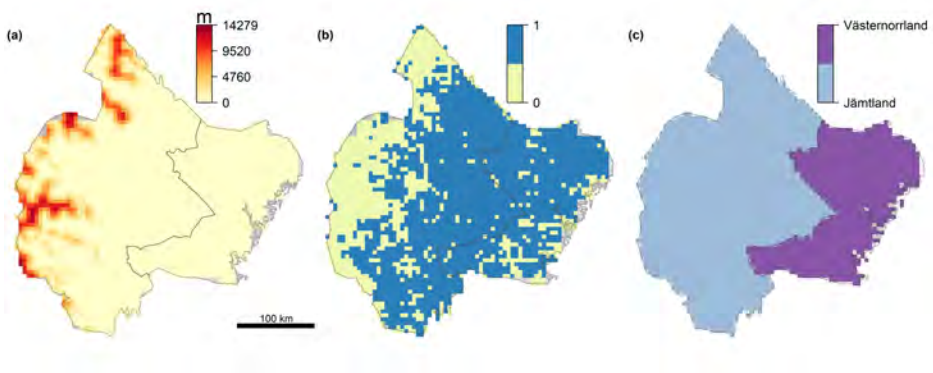

Figure S5: Maps of the three spatial covariates used to explain spatial heterogeneity in detection probability used in the **FE** model fitted to female brown bear (*Ursus arctos*) data from central Sweden: **(a)** Map of distance to the nearest road, **(b)** a proxy of opportunistic searching effort, i.e. presence/absence of at least one carnivore record other than the bear genetic detections and **(c)** a map of the two Sweden counties under study, Jämtland and Västernorrland.

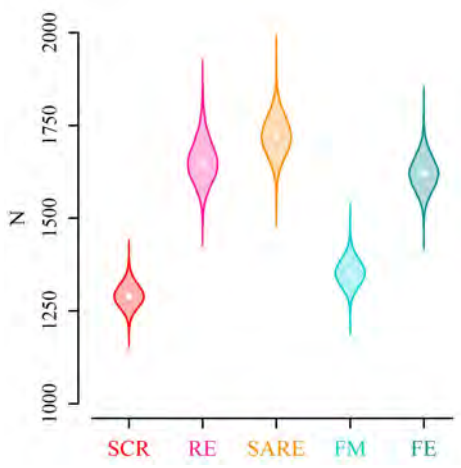

Figure S6: **Posterior density of population size N from the five models fitted to female brown bear (*Ursus arctos*) data in central Sweden April - November 2020.** The illustration shows the violin plot of posterior density of population size N from each of the five models: **SCR, RE, SARE, FM** and **FE**. For the models RE, SARE, and FM, the estimates are obtained after aggregating the random effects to 20 km resolution.

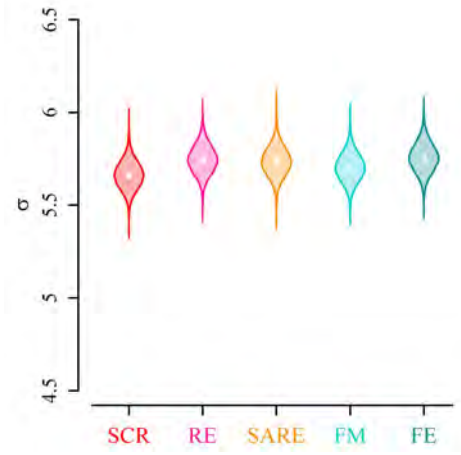

Figure S7: **Posterior density of the scale parameter σ from the five models fitted to female brown bear (*Ursus arctos*) data in central Sweden April - November 2020.** Violin plot of posterior density of the spatial scale parameter (σ; km) of the half-normal detection function from each of the five models: **SCR, RE, SARE, FM**. For the models RE, SARE, and FM, the estimates are obtained after aggregating the random effects to 20 km resolution.

Article III

Running Head: Wolverine density determinants in Scandinavia

Wolverine density distribution reflects past persecution and current management in Scandinavia

Ehsan Moqanaki[1,*], Cyril Milleret[1], Pierre Dupont[1], Henrik Brøseth[2] & Richard Bischof[1]

1. Faculty of Environmental Sciences and Natural Resource Management, Norwegian University of Life Sciences, P.O. Box 5003, 1432 Ås, Norway
2. Department of Terrestrial Ecology, Norwegian Institute for Nature Research, PB 5685 Torgarden, 7485 Trondheim, Norway

* Corresponding author – Email address: ehsan.moqanaki@gmail.com
https://orcid.org/0000-0001-7968-0210

Abstract

After centuries of intense persecution, several large carnivore species in Europe and North America have experienced a rebound. Today's spatial configuration of large carnivore populations has likely arisen from the interplay between their ecological traits and current environmental conditions, but also from their history of persecution and protection. Yet, due to the challenge of studying population-level phenomena, we are rarely able to disentangle and quantify the influence of past and present factors driving the spatial distribution and density of these controversial species. Using spatial capture-recapture models and a data set of 742 genetically identified wolverines *Gulo gulo* collected over ½ million km^2 across their entire range in Norway and Sweden, we identify landscape-level factors explaining the current population density of wolverines in the Scandinavian Peninsula. Distance from the relict range along the Swedish-Norwegian border, where the wolverine population survived a long history of persecution, remains a key determinant of wolverine density today. However, regional differences in management and

environmental conditions also played an important role in shaping spatial patterns in present-day wolverine density. Specifically, we found evidence of slower recolonization in areas that had set lower wolverine population goals in terms of the desired number of annual reproductions. Management of transboundary large carnivore populations at biologically relevant scales may be inhibited by administrative fragmentation. Yet, as our study shows, population-level monitoring is an achievable prerequisite for a comprehensive understanding of the distribution and density of large carnivores across an increasingly anthropogenic landscape.

Keywords: Abundance, Density, Distribution, Large carnivores, Noninvasive monitoring, Spatial capture-recapture, Transboundary wildlife, *Gulo gulo*

1 Introduction

Species distributions we observe today are the result of not only ecological traits and current local environmental conditions, but also land-use history, human activity, and management strategies (Donohue et al. 2000, Foster et al. 2003, Di Marco and Santini 2015). Emerging disturbance regimes, such as altered frequency and intensity of extreme weather and climate events (Ummenhofer and Meehl 2017), further impact species distributions. Identifying and disentangling the factors that lead to the distribution and dynamics of species is one of the most profound and long-standing research areas in ecology, with both fundamental and applied implications (Guisan and Zimmermann 2000, Elith and Leathwick 2009, Jetz et al. 2019).

Humans are the main transformers of Earth's ecosystems (Ellis 2011, Pereira et al. 2012, Waters et al. 2016), with a growing list of documented effects on wildlife (Yackulic et al. 2011, Tucker et al. 2018). Despite a broad overall consistency in wildlife responses to anthropogenic disturbances, there is considerable variability in scale, magnitude, and pattern of human impacts (Tablado and Jenni 2017, Gaynor et al. 2018, Tucker et al. 2018). A popular example is the case of large carnivore species that have undergone substantial range contractions due to intensive persecution by humans. While many species continue to struggle, some have in recent decades successfully recolonized part of their historic range, particularly in Western Europe and North America (Linnell et al. 2001, Zedrosser et al. 2011, Chapron et al. 2014, Ripple et al. 2014, Ingeman et al. 2022). Limited understanding of factors shaping the spatial configuration of carnivore populations poses a challenge to science and management, and the current knowledge gaps may hinder predictions of future responses in the face of increasing human pressure.

The fall and rise of wolverines *Gulo gulo* in Scandinavia is a prime example of recovery of an iconic large carnivore following intense persecution and range contraction. The wolverine was historically distributed throughout most of the Scandinavian Peninsula (Landa et al. 2000, Flagstad et al. 2004). During the nineteenth and twentieth centuries, intensive persecution of the wolverine reduced its range and population size drastically. By 1970, the population was functionally extinct in many areas with the exception of a narrow strip in the alpine region along the border between Sweden and Norway (Landa et al. 2000, Flagstad et al. 2004; Fig. 1). The situation was similarly grim in neighboring Finland, where wolverine observations were

rare beyond the borderland with Russia (Lansink et al. 2020; Fig. 1). The wolverine finally received legal protection in both Norway and Sweden by 1973, and later followed by Finland, and gradually recolonized many parts of its historical range in Fennoscandia (Flagstad et al. 2004, Aronsson and Persson 2017, Lansink et al. 2020). Today, the wolverine population is established across Norway and Sweden beyond the alpine refuge areas (Chapron et al. 2014, Gervasi et al. 2019, Bischof et al. 2020). The return of the wolverine has rekindled conflict with the sheep-farming industry and semidomesticated reindeer *Rangifer tarandus* husbandry (Flagstad et al. 2004, Hobbs et al. 2012, Persson et al. 2015, Aronsson and Persson 2017). The wolverine is listed on Appendix S2 of the Bern Convention for both countries and is therefore formally "strictly protected". However, because Norway is not a member of the European Union, it is not bound by the same set of regulations. Wolverines are therefore subject to persistent lethal control in Norway, while they are strictly protected in Sweden under the European Union's Habitats Directive 92/43 (annex IV; Habitats Directive 1992), and only recently were small hunting quotas (≈ 15) allowed for damage control purposes.

In a human-dominated world, understanding population-level drivers of species spatial distribution and particularly density is important to understand and predict the potential for species-environment interactions in a management context. What we know about landscape and environmental factors influencing wolverine distribution and density has been cobbled together from a small patchwork of studies, often with limited spatial extent in various parts of the global distribution range of the species (Fisher et al. 2022). In Scandinavia, population and landscape-level determinants of wolverine distribution and density are poorly known. Historical (Landa et al. 2000) and current (Chapron et al. 2014) range maps suggest that recolonization in this anthropogenic landscape has been facilitated by favorable legislation and improved cultural acceptance (Linnell et al. 2001, Flagstad et al. 2004, Aronsson and Persson 2017). However, there is evidence that biophysical constraints, such as climate, habitat, and terrain, have played a greater role in shaping the current spatial distribution of the wolverine at the continental scale (Cretois et al. 2021). Current management decisions use information that is largely based on data from the high-conflict alpine areas (Brøseth et al. 2010, Aronsson and Persson 2017), but would benefit from a better knowledge of the determinants of wolverine's spatial variation in density across its entire Scandinavian range. Until recently, this was out of reach, because of the

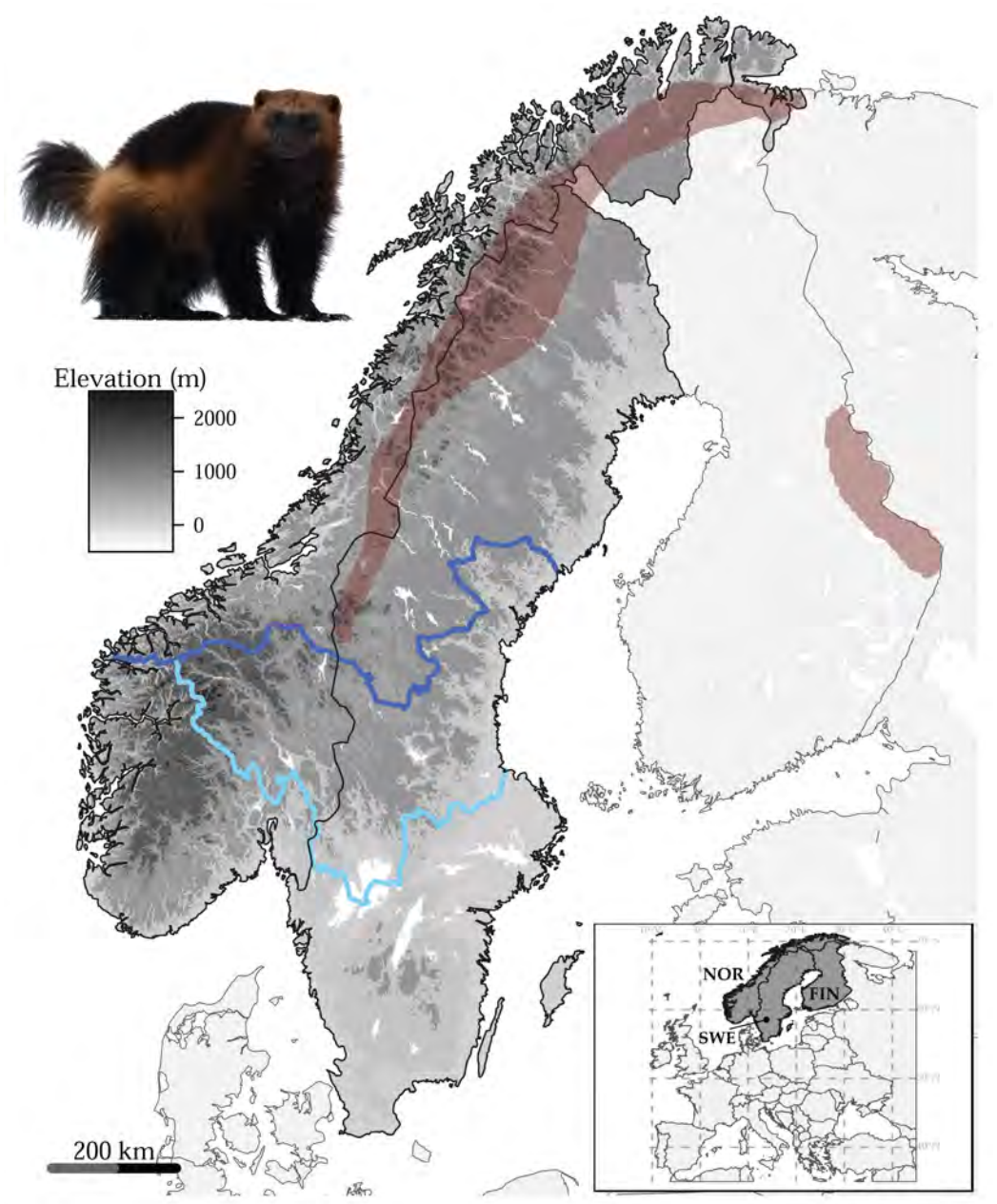

Figure 1: Approximate wolverine *Gulo gulo* distribution in the Scandinavian Peninsula (red polygon on the left) and Finland (red polygon on the right) in the 1970s, when the population range was at its lowest in modern times following intense human persecution (i.e., the relict range; Landa et al. 2000, Flagstad et al. 2004). Thick blue lines separate zones containing administrative units with shared population goals for the wolverine (i.e., large carnivore management regions in Norway and counties in Sweden; see Table 1). We merged the zones below the dark blue line into one southern zone in each country. Photo credit: Karel Bartik/www.shutterstock.com

rarity and elusive behavior of the species, the vast geographic expanse of the population, and spatially incomplete surveys (Flagstad et al. 2004, Gervasi et al. 2016, Aronsson and Persson 2017).

Here, we set out to quantify the extent to which current wolverine population density across the Scandinavian Peninsula is affected by past and present conditions. Importantly, we do so for the entire ½ million km^2 range of the species across Norway and Sweden. Three major challenges plague monitoring of elusive species, such as the wolverine, at ecologically relevant scales: (1) the collection of sufficiently detailed individual data from an entire population, (2) imperfect detection (i.e., not all individuals in the population are detected), and (3) a paucity of computationally efficient analytical tools to disentangle the effects of ecological drivers from both stochastic process noise and observation errors (Isaac et al. 2020, Cretois et al. 2021, van de Schoot et al. 2021). In this study, we tackled these challenges for the Scandinavian wolverine by analyzing a comprehensive capture-recapture data set of genetically identified wolverine individuals across the entire population in Norway and Sweden using recently developed efficient spatial capture-recapture (SCR) models (Bischof et al. 2020, Turek et al. 2021).

2 Methods

2.1 Noninvasive genetic sampling

We used wolverine noninvasive genetic sampling (NGS) data from the Scandinavian large carnivore monitoring database (Rovbase 3.0; `www.rovbase.no` and `www.rovbase.se`). This is one of the largest, long-term capture-recapture data of terrestrial wildlife globally (Smith et al. 2017, Tourani 2022). Wildlife authorities and volunteers conduct both structured searches and opportunistic sampling of putative wolverine scats and hair on snow between December and June each year throughout the species' range in Norway and Sweden. The structured search tracks and locations of noninvasive samples are GPS recorded (see Supporting Information). Further details on wolverine NGS is provided elsewhere (e.g., Brøseth et al. 2010, Gervasi et al. 2016, Bischof et al. 2020). Samples were processed and analyzed by two dedicated DNA labs using a number of control measures to minimize genotyping errors, as described elsewhere (Ekblom et al. 2018, Flagstad et al. 2019, Lansink et al. 2022). First, samples were analyzed with a Single

Nucleotide Polymorphism (SNP)-chip with 96 markers and, second, all individuals were analyzed with 19 microsatellite markers to determine species and identity of wolverine individuals, as well as their sex. We used NGS data collected between 1 December 2018 and 30 June 2019, which consisted of individual identity, sex, collection date, and coordinates associated with each wolverine sample. This sampling period represents the latest, most complete, semi-systematic wolverine NGS effort across the entire range of the wolverine population in Scandinavia to date (Flagstad et al. 2019, Bischof et al. 2020, Milleret et al. 2022). We minimized the probability of including juvenile ($\leq$ 10 months old) individuals in the analysis by using only NGS data collected from wolverine tracks on snow, before emergence of cubs of the year from natal dens (Gervasi et al. 2016). Nonetheless, our data could still include subadult wolverines (less than two years old) that may use space differently than adults. Especially subadult males are more likely to initiate long-distance movements (Vangen et al. 2001), which may introduce an unknown and unmodeled source of individual heterogeneity in our study (Gimenez et al. 2018). We detected a few individuals (n = 3 females and 21 males) that made long-distance movements of more than 40 km during the 2018/19 monitoring season, and those detections (3 female and 29 male detections) were removed from the analysis, as they likely constitute dispersal events instead of movement within the home range.

2.2 Analysis

SCR models offer a flexible framework to account for imperfect detection of individuals and provide spatially explicit estimates of abundance (i.e., density) and other population parameters (Efford 2004, Borchers and Efford 2008, Royle et al. 2014). The SCR modeling framework can support flexible sampling configurations and incorporate both individual- and detector-level covariates to account for sources of heterogeneity in detectability, and spatial covariates to account for variation in density (Royle et al. 2014). Although building spatially indexed hierarchical models, such as SCR, can be computationally challenging or even prohibitive for large spatial extents, recent developments have resulted in dramatic improvements (e.g., Milleret et al. 2019, Turek et al. 2021, Zhang et al. 2023). Here, we build on these recent developments to study the landscape-scale determinants of the Scandinavian wolverine density.

2.2.1 Spatial capture-recapture model

We built a single-season (i.e., demographically closed) SCR model in a Bayesian framework by expanding on our previous work (Bischof et al. 2020). Our SCR model contains two hierarchical levels: (1) The observation submodel accounts for imperfect and variable wolverine detectability during NGS; and (2) The ecological submodel describes wolverine density as the main ecological process of interest in this study. Our SCR model estimates the following parameters: (1) the baseline detection probability p_0: detection probability at a trap or hypothetical detector located at an animal's activity center s_i – a latent variable representing the expected location about which an individual uses space during the sampling period; (2) the spatial scale parameter of the detection function σ; (3) the number N of wolverine activity centers within the available habitat S (i.e., the detector grid and a buffer around it), which can be used to derive density D (see below); and (4) the effects (regression coefficients β) of spatial and individual covariates on the detection probability and density.

(1) The observation submodel: We used the conventional half-normal detection function (Borchers and Efford 2008, Royle et al. 2014) to model the probability p of detecting individual i at detector j as a decreasing function of the distance d between the detector and the individual's center of activity s_i: $p_{ij} = p_{0_{ij}}\, exp(-d_{ij}^2/2\sigma^2)$. The detection function is assumed to reflect individual space use and is therefore directly linked with the home range concept (Royle et al. 2014). Because we used a data-augmentation approach (Royle et al. 2007), the detection of an individual has to be made conditional on the individual's state z_i ($z_i = 1$ when individual i is member of the population N), which is governed by the inclusion probability ψ: $z_i \sim Bernoulli(\psi)$. The population size can be then derived by summing the z_i's: $N = \sum_{i=1}^{M} z_i$, where M is the chosen size of the data-augmented population (Royle et al. 2007) and represents the maximum number of wolverines in the habitat S (see *Ecological submodel*).

In our study, detectors are the centers of 5 572 10×10 km grid cells, covering a land area extending 100 km beyond the outermost wolverine NGS detections collected during the sampling period (Supporting Information). We used a partially aggregated binomial observation model (Milleret et al. 2018) to retain more information from the wolverine NGS data by dividing each main detector cell into 25 subdetector cells of 2×2 km. By retrieving the number of subdetector

cells with at least one noninvasive sample for each wolverine detected at each main detector cell, we generated individual spatial detection histories (Royle et al. 2014). Finally, we placed a 40-km buffer around the detector grid to define the habitat S. This value was chosen based on the average home-range radius of adult Scandinavian wolverines (Persson et al. 2010, Mattisson et al. 2011, Aronsson et al. 2022), so that the buffer is larger than three times the estimated σ of 10.3 km (95% Bayesian credible interval [CI] = 10.1 − 10.5 km) for male wolverines, as reported by Bischof et al. (2020). This buffer area allows detection of individuals even if their activity centers are located outside the detector grid (Efford 2004, 2011). The detector grid covered most of the contiguous Scandinavian Peninsula over Norway and Sweden (58° 08′ - 70° 42′ N, 5° 56′ - 32° 46′ E; Supporting Information), while parts of the buffer (41.6%) fell inside Finland and Russia. Thus, the available habitat was 633 200 km^2, after removing large lakes and other noncontiguous land areas, of which 88% (557 200 km^2) were in Norway and Sweden (Supporting Information).

Wolverine NGS was conducted by hundreds of field staff and volunteers across different jurisdictions in Norway and Sweden. We therefore expected spatial variability in detection probability of wolverine individuals (Efford et al. 2013, Moqanaki et al. 2021). Following Bischof et al. (2020), we considered a different baseline detection probability for each jurisdiction $p_{0_{County}}$ ($County = 1, 2, \ldots, 8$) to account for possible regional differences in monitoring regimes. Jurisdictions were defined based on carnivore management regions in Norway and counties in Sweden after Bischof et al. (2020), with slight modifications to match with our habitat extent (Supporting Information). We merged neighboring jurisdictions to ensure sufficient wolverine detections for estimating baseline detection probability in each unit (Bischof et al. 2020). In addition, we modeled the effect of three detector- and one individual-level covariates that may influence the probability of wolverine detection (Supporting Information):

$$logit(p_{0_{ij}}) = p_{0_{County_j}} + \beta_E \mathbf{Effort}_j + \beta_R \mathbf{Road}_j + \beta_S \mathbf{Snow}_j + \beta_P Previous_i \quad (1)$$

$\mathbf{Effort}_j$ is the length (m) of GPS search tracks within each detector grid cell j recorded during the structured NGS, $\mathbf{Road}_j$ is the logarithm of the average geographic distance (km) from each detector to the nearest road of any type, and $\mathbf{Snow}_j$ is the average percentage of snow-covered land in each detector grid cell during the sampling months (December 2018 - June

2019; Supporting Information). We also modeled individual variation linked with detection in the previous monitoring season $Previous_i$; a binary covariate which takes the value 1 if individual i was detected in the previous monitoring season and 0 otherwise. During NGS, investigators are believed to have the tendency to prioritize searching in locations where their searches were previously successful, which could positively influence the detection probability of those previously-detected wolverine individuals during the focal monitoring season (Gervasi et al. 2014, Milleret et al. 2022). Availability of the monitoring data from the previous year made it possible to account for this potential source of heterogeneity in wolverine detectability. This individual binary covariate $Previous_i$ is latent for augmented individuals and was modeled following a Bernoulli distribution: $Previous_i \sim Bernoulli(\pi)$, where π is the probability that an arbitrary individual from the population was detected in the previous year. All continuous spatial covariates were scaled before SCR model fitting. Further details on detection covariates, the rationale to include them, and their original source and spatial depiction are provided in the Supporting Information.

(2) The Ecological submodel describes the number and distribution of all wolverines present in the population (i.e., detected and nondetected). We used a data augmentation approach (Royle et al. 2007) to account for those wolverine individuals that were not detected during NGS, where the super-population size M (i.e., detected and augmented individuals) is chosen to be considerably larger than N. Following Bischof et al. (2020), and given the relatively high detectability of the target population during NGS (Milleret et al. 2022), we chose an augmentation factor of 0.8 to facilitate the analysis by Markov chain Monte Carlo (MCMC). Thus, M was large enough, such that the probability that M individuals were alive in S during NGS was negligible.

SCR estimates of abundance are spatially explicit, meaning that they are derived from the estimated location of all individual activity centers s_i with $z_i = 1$ across the available habitat S (Efford 2004, Borchers and Efford 2008, Royle et al. 2014). The collection of activity centers can be seen as the realization of a statistical point process (Illian et al. 2008). To study how wolverine density varies in Scandinavia in response to a number of environmental and history-related covariates (Table 1, Supporting Information), we used an inhomogeneous binomial point process

to model spatial variation in the distribution of individual activity centers with intensity function (Zhang et al. 2023): $\lambda(s) = e^{\beta \mathbf{X}(s)}$, where $\mathbf{X}(s)$ is a vector of spatial covariate values evaluated at location s, and β is a vector of associated regression coefficients. The intensity function λ conditions the placement of activity centers within each of the 20×20 km habitat grid cells s used in this analysis (Supporting Information). In this formulation, no intercept is needed as the number of activity centers is conditioned by data augmentation; thus, regression coefficients represent the relative effects of the different covariates on wolverine density (Zhang et al. 2023).

To disentangle the determinants of wolverine density within Scandinavia, we measured habitat characteristics at the scale of the home range of a wolverine (i.e., the second-order of habitat selection; Johnson 1980). We selected biotic and abiotic covariates following previous studies on wolverine distribution and habitat use and preferences (Fisher et al. 2022 and references therein; Table 1). Specifically, we selected covariates that may explain spatial variation in wolverine density in Scandinavia at broad scale (Table 1, Supporting Information): (1) Distance from the relict range (Landa et al. 2000, Flagstad et al. 2004; Fig. 1) to describe recolonization history; (2) Terrain Ruggedness Index (TRI), explaining general topographic complexity; (3) Average percentage of year-round snow-covered land as a measure of climate suitability (which was different from the snow covariate used as a detector-level covariate; Supporting Information); (4) Percentage of forest cover, representing land use and habitat productivity; (5) Moose *Alces alces* harvest density as a proxy of wild prey biomass availability, (6) Percentage of human settlement areas as a measure of human density and associated disturbances, and (7) Zonal management to account for regional differences in wolverine management plans and other large-scale environmental conditions.

The impact of current management was specifically included because of unique management goals for wolverines in different areas of Norway and Sweden (Ministry of the Environment 2003, Naturvårdsverket Ärendenr 2020). Briefly, we divided our habitat layer into northern and southern zones in each country (i.e., four zones; Table 1, Supporting Information) by aggregating jurisdictions with similar management goals for the number of wolverine annual reproduction and other environmental conditions (e.g., climate, prey availability and abundance, and human influence). We simplified the spatial variation in wolverine management by merging several counties or carnivore management regions, and partially included jurisdictions in the southern

part of each country without management goals (Table 1; Fig. 1), because these southern counties contained no NGS and wolverine detections in our data set (Supporting Information). Likewise, we merged the buffer area in neighboring Finland and Russia with the northern zones (Supporting Information). We then calculated the proportion overlap between each habitat cell and the resulting four zones to define four spatial covariates (Supporting Information). Because the four proportions sum to one, we did not use the first zone covariate to avoid identifiability issues (i.e., the northern zone in Sweden, zone 1.a in Table 1, was an implicit intercept). AC placement reflects environmental configuration throughout the home range, not just at one location. Thus, discrete changes in conditions (e.g., management) from one side of a border to another can lead to artificial behavior in the model when using cell-based covariate values. To achieve a more realistic scale of home range placement in the model, we averaged covariate values of the four management zones using a moving window (Table 1). This created gradual transitions between regions (Supporting Information). Because management goals and other zone-specific characteristics of the biotic and abiotic environment may also have affected the wolverine's ability to recolonize away from the relict range, we included an interaction term between the distance from the relict range and each of the four zones:

$$e^{\lambda(s)} = \sum_{r=2}^{4} \left\{ \beta_{R_r} \mathbf{R_r}(s) \; + \; \beta_{R_r X_1} \mathbf{X_1}(s) \mathbf{R_r}(s) \right\} \; + \; \sum_{c=1}^{6} \beta_{X_c} \mathbf{X_c}(s) \tag{2}$$

The spatial covariates $\mathbf{X}$ are the distance from the relict range $\mathbf{X}_1$, Terrain Ruggedness Index $\mathbf{X}_2$, the average percentage of year-round snow cover $\mathbf{X}_3$, the percentage of forest cover $\mathbf{X}_4$, the percentage of human settlement areas $\mathbf{X}_5$, and the moose harvest density $\mathbf{X}_6$. $\mathbf{R_2}$, $\mathbf{R_3}$, and $\mathbf{R_4}$ are the three zone covariates representing southern Sweden and northern and southern Norway (Table 1). In total, we estimated 12 regression coefficients β (Supporting Information).

We transformed all covariate raster layers from the original projection to the Universal Transverse Mercator (UTM zone 33N) and locally interpolated the raster values using the "bilinear" method of the `resample` function of the R package `raster` (Hijmans 2021) to match the 20 × 20 km habitat grid used in this analysis (Supporting Information). All continuous covariates were then standardized prior to their inclusion in the model to have a mean of zero and one unit standard deviation. Correlation among the covariates was generally low (Pearson's correlation coefficient $r \leq 0.62$). Further details regarding the rationale for including each

covariate, their sources, and their expected effects are provided in Table 1, and the Supporting Information provides their spatial depiction and mean and standard deviation of the values.

2.2.2 Implementation

We fitted SCR models with `NIMBLE` (version 0.12.2; de Valpine et al. 2022) in R (version 4.2.1; R Core Team 2022) for female and male wolverines separately, using the recent developments by Turek et al. (2021) and custom functions made available through the R package `nimbleSCR` (Bischof et al. 2021). We ran four MCMC chains, each with 200 000 iterations, discarded the initial 10 000 samples as burn-in, and thinned by a factor of 10 for creating the density maps. We assessed mixing of chains by inspecting traceplots, and we considered models as converged when the potential scale reduction value $\hat{R}$ was ≤ 1.10 for all parameters (Brooks and Gelman 1998). Data and R code for fitting the SCR model and the list of priors are provided in the Supporting Information.

To explore the relative importance of each covariate on density, we incorporated a Bayesian variable selection approach in `NIMBLE` using reversible jump MCMC with indicator variables (Green 1995, O'Hara and Sillanpää 2009). We incorporated an indicator variable w associated with each regression coefficient β (n = 12; Supporting Information). Thus, we modified equation (2) to include ($w = 1$) or exclude ($w = 0$) the effect of each coefficient in the presence of other covariate effects in a given posterior draw: $\lambda(s) = e^{\beta_1 w_1 \mathbf{X}_1(s) + \ldots + \beta_p w_p \mathbf{X}_p(s)}$. We constrained inclusion of the interaction coefficients to when the corresponding main effects were also included. For inference on the different coefficients, we discarded MCMC draws where $w = 0$.

We calculated the median and the 95% CI limits of the posterior distribution for all parameters, except for abundance, where we reported mean and 95% CI. To obtain total wolverine abundance, we combined N estimates of male and female wolverines by merging posterior MCMC samples from the sex-specific SCR models. In both total and sex-specific models, we summed the total number of predicted activity center locations of alive individuals ($z_i = 1$) within each habitat cell for each iteration of the MCMC chains; thus, we generated a cell-based posterior distribution of abundance that can be viewed also as density. Using this approach, we extracted abundance and density estimates and the associated uncertainty for different spatial units relevant for wolverine management at the country level, besides the total

Table 1: Description, rationale for inclusion, expected effects, and source and native spatial resolution of covariates of density used to model the density distribution of the wolverine *Gulo gulo* across Norway and Sweden between December 2018 and June 2019

Covariate	Description and Rationale	Effects	Resolution and Source
Relict ($\mathbf{X_1}$)	Distance (m) from the relict range represents the founding population and colonization history. The relict range describes roughly the area occupied by the Fennoscandian wolverine population at its lowest point in modern times (Landa et al. 2000, Flagstad et al. 2004, Chapron et al. 2014, Lansink et al. 2020).	–	Calculated using the wolverine's geographic distribution range in the 1970s as reported by Landa et al. (2000). All 20×20 km-habitat cells falling within the relict range area were assigned a value of 0. We then computed the Euclidean distance for all habitat cells to the nearest cell with a value of 0 using the `distance` function of the R package `raster` (Hijmans 2021).
Ruggedness ($\mathbf{X_2}$)	Terrain Ruggedness Index (TRI) is the mean of the absolute elevation differences between the value of a habitat cell and the value of its eight surrounding cells (Wilson et al. 2007). TRI represents topographic complexity, refuge availability, and level of human disturbances (May et al. 2008, 2012, Rauset et al. 2013, Poley et al. 2018)	+	Obtained through the `terrain` function of the R package `terra` (Hijmans et al. 2022) using an elevation layer (AWS Terrain Tiles and OT global datasets API) at about 256×256 m obtained via the `get_elev_raster` function of the R package `elevatr` (Hollister et al. 2021)
Snow ($\mathbf{X_3}$)	The average percentage of year-round snow cover across years 2008-2019, representing climate severity, denning suitability, and prey availability and vulnerability to predation (Copeland et al. 2010, May et al. 2012, Aronsson and Persson 2017, Lukacs et al. 2020, Mowat et al. 2020, Barrueto et al. 2022)	+	Calculated using monthly maps of the percentage of snow-covered land based on the MODIS/Terra Snow Cover Daily L3 Global 500m Grid data set (`www.neo.sci.gsfc.nasa.gov`)
Forest ($\mathbf{X_4}$)	Percentage of forest cover was a measure of land use, habitat productivity, greater wild prey availability, and cover (May et al. 2006, 2008, Inman et al. 2012, Scrafford et al. 2017, Cimatti et al. 2021)	+	Obtained using the ESA-CCI Land Cover project (categories 50, 60, 61, 62, 70, 71, 72, 80; `www.esa-landcover-cci.org`) at about 176×176 m
Moose ($\mathbf{X_5}$)	An index of moose *Alces alces* density using hunting bags, representing habitat productivity and a proxy for wild prey biomass (Van Dijk et al. 2008, Mattisson et al. 2016, van der Veen et al. 2020)	+	Calculated at 2×2 km resolution using the number of moose harvested/km^2 at the level of municipalities and hunting management units in Norway and Sweden, respectively (statistisk sentralbyrå 2021, Älgdata 2021a, and Älgdata 2021b). We used data from the previous hunting season (Sep-Oct 2017), as suggested by Ueno et al. (2014). Because of a lack of data from the buffer area in Finland and Russia, we replaced missing values with mean values of the 48 neighborhood cells using the `focal` function of the R package `raster` (Hijmans 2021)
Settlements ($\mathbf{X_6}$)	The percentage of ground surface covered by human settlements was a proxy for human population density and associated disturbances (May et al. 2006, Lukacs et al. 2020, Cretois et al. 2021, Barrueto et al. 2022)	–	Downloaded at about 57-m resolution from the World Settlement Footprint data set (WSF2015; Marconcini et al. 2020) and log transformed after adding a value of 1 to deal with 0 values
Zonal management ($\mathbf{R_1}, \ldots, \mathbf{R_4}$)	An aggregation of administrative units (i.e., large carnivore management regions in Norway and counties in Sweden) with shared population goals for the wolverine (Ministry of the Environment 2003, Naturvårdsverket Ärendenr 2020), representing regional variation in management strategies and other region-specific environmental conditions (Persson et al. 2009, Hobbs et al. 2012, Morehouse and Boyce 2016, Aronsson and Persson 2017, Kortello et al. 2019, Barrueto et al. 2020)	+/–	Counties in Sweden and carnivore management regions in Norway within (1) Northern zones with the management goal of 10 or more annual wolverine reproductions: (1.a) Norrbotten, Västerbotten, and Jämtland (Sweden), plus a small fraction of the buffer, and (1.b) Management region 8 (Finnmark and Troms), region 7 (Nordland) and region 6 (Trøndelag and Møre og Romsdal) in Norway; (2) Southern zones with the management goal of less than 10 annual wolverine reproductions: (2.a) Västernorrland, Dalarna, Gävleborg, and Värmland, plus a small part of the neighboring counties with no management goals: Västmanland, Västra Götaland, and Örebro (Sweden), and (2.b) Management region 5 (Hedmark) and region 3 (Oppland), plus a small part of the neighboring counties with no management goals: Sogn og Fjordane, Hordaland, Rogaland, Vest-Agder, Aust-Agder, Telemark, Buskerud, and Vestfold (Norway)

estimates for the entire population in Norway and Sweden.

We constructed two types of sex-specific density maps: (1) a realized density map based on the posterior location of activity centers as described above, and (2) an expected density map based on the estimated intensity of the density point process per habitat cell of 20×20 km and the estimate of population size: $\mathbf{D_{exp}}(s) = N\lambda(s)/\sum_{s=1}^{S} \lambda(s)$. "Realized" density maps show density based on the average model-estimated activity center locations of individuals, as opposed to "expected" density maps, which show predicted density based on the regression model underlying the intensity surface. To present uncertainty, we calculated and mapped the standard deviation of the per cell posterior of density (Miller et al. 2013). We used all MCMC samples to construct the density maps, regardless of the indicator variable values.

3 Results

3.1 Noninvasive genetic sampling

During the sampling period between 1 December 2018 and 30 June 2019, 283 282 km of GPS search tracks were recorded within our designated detector grid (Supporting Information) across Norway (34%) and Sweden (66%). The final NGS data set consisted of 2 444 (1 350 male and 1 094 female) detections from 742 (335 males and 407 females) genetically identified wolverine individuals across the entire population on the Scandinavian Peninsula (Supporting Information). The number of detections (i.e., recaptures) per identified individual ranged from 1 to 13 for both sexes (mean = 3.0 males and 2.1 females).

3.2 Density predictors

The variation in wolverine density across Scandinavia was explained by distance from the relict range in different zones, human settlement areas, moose density proxy, year-round snow, terrain ruggedness, and forest cover (Fig. 2). The magnitude of the effects and uncertainty around them varied moderately between the sexes (Fig. 2). For both females and males, the effects of being in southern Norway, distance from the relict range in northern Sweden, and percentage of human settlements received the most support based on the inclusion probability (≥ 0.99; Fig. 2). In addition, for female wolverines, the effects of being in northern Norway and

distance from the relict range in southern Norway, and, for males, the effect of moose density proxy received inclusion probabilities of ≥ 0.99 (Fig. 2). The most supported SCR models for each sex are reported in the Supporting Information.

Among the covariates considered, percentage of human settlement areas had the largest negative effects on both female and male wolverine densities (median and 95% CI β_{X_5} = –1.61, –2.66 to –0.79 [female] and –2.27, –3.41 to –1.33 [male]; Fig. 2). Likewise, distance from the relict range negatively affected the density of both sexes, with significantly stronger effects in southern Norway ($\beta_{R_4X_1}$ = –1.35, –1.99 to –0.70 [female] and –1.07, –1.87 to –0.26 [male]), compared to the effect of distance from the relict range in northern Sweden (Fig. 3). Based on our results, we predicted that areas located 30 km away from the relict range, as-the-crow-flies, would have on average about two-third lower expected wolverine densities in the southern zones of Norway and Sweden compared to the northern zones (Fig. 3). Moose density was positively associated with both female and male wolverine densities (β_{X_6} = 0.19, 0.02 to 0.35 [female] and 0.46, 0.31 to 0.63 [male]; Fig. 2). The effects of forest cover (β_{X_4} = 0.32, 0.12 to 0.52) and terrain ruggedness on density was significantly positive for female wolverines only (β_{X_2} = 0.42, 0.25 to 0.59), while the effect of year-round snow cover was positive for males only (β_{X_3} = 0.35, 0.11 to 0.56; Fig. 2).

3.3 Detection predictors

The effects of detection covariates varied slightly between male and female wolverines (Supporting Information). Baseline detection probability p_0 was comparable between sexes (median and 95% CI p_0 = 0.02, 0.01 to 0.02 for both males and females), but varied moderately among the eight carnivore management regions and counties in Norway and Sweden, respectively (Supporting Information). Both female and male wolverine detection probabilities increased with search effort (β_E = 0.62, 0.53 to 0.71 [female] and 0.51, 0.44 to 0.59 [male]). Further, for female wolverines, searching farther away from the nearest road increased their detectability (β_R = 0.19, 0.07 to 0.31). Higher percentage of snow cover during the sampling months decreased detectability of males (β_S = –0.22, –0.37 to –0.08). The individual-level covariate representing wolverine detection in the previous sampling year positively influenced male wolverine detectability only (β_P = 0.61, 0.44 to 0.77), suggesting sex-specific detection bias during NGS. The spatial scale

parameter was greater for males (σ_m = 8 km, 7.6 - 8.2) than for females (σ_f = 6 km, 5.6 - 6.4). More details are provided in the Supporting Information.

3.4 Sex-specific and total estimates of abundance and density

We estimated the abundance of the Scandinavian wolverine population within our detector grid (Supporting Information) during the 2018/19 monitoring season at 408 (95% CI = 397 - 420) males and 667 (95% CI = 640 - 697) females. The wolverine population in Sweden was estimated to be between 640 and 692 individuals, while in Norway we estimated between 397 and 425 wolverines (Fig S5). Overall, we predicted higher wolverine densities for both males and females closer to the relict range, but the pattern was more pronounced for females (Fig. 4).

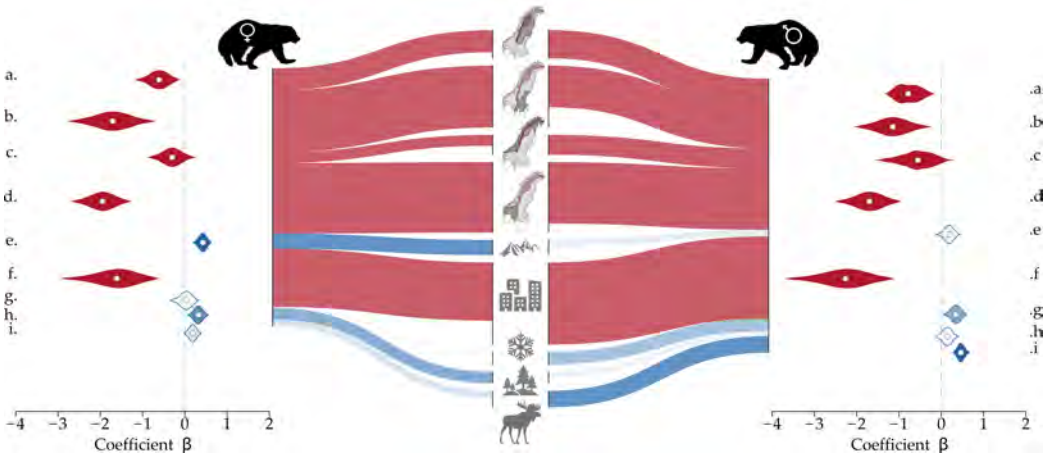

Figure 2: The effect of environmental covariates on density of female (left) and male (right) wolverines *Gulo gulo* in the Scandinavian Peninsula between December 2018 and June 2019. The covariates of density are (from top to bottom): Distance from the relict range in (a) northern Sweden, (b) southern Sweden, (c) northern Norway, and (d) southern Norway; (e) Terrain Ruggedness Index; (f) Human settlement index; (g) Year-round snow cover; (h) Forest cover; and (i) Moose *Alces alces* harvest density (see Table 1). All continuous covariates were standardized prior to their inclusion in the models. Zone-specific intercepts are not shown (see Supporting Information). The violins show median (white dots) and 95% Bayesian credible interval limits of regression coefficients β estimates, where effect sizes are on exponential scale. Line widths represent the magnitude of the median effect (i.e., the thicker, the larger the strength of the covariate effects). Line and violin colors show direction of the effects (blue = positive and red = negative effects), and the opacity level indicates the inclusion probability (0 [transparent] to 1 [opaque]; Supporting Information). For the four zone-specific effects of distance from the relict range (a-d), inclusion probabilities are based on the inclusion probability of the distance effect in northern Sweden (a).

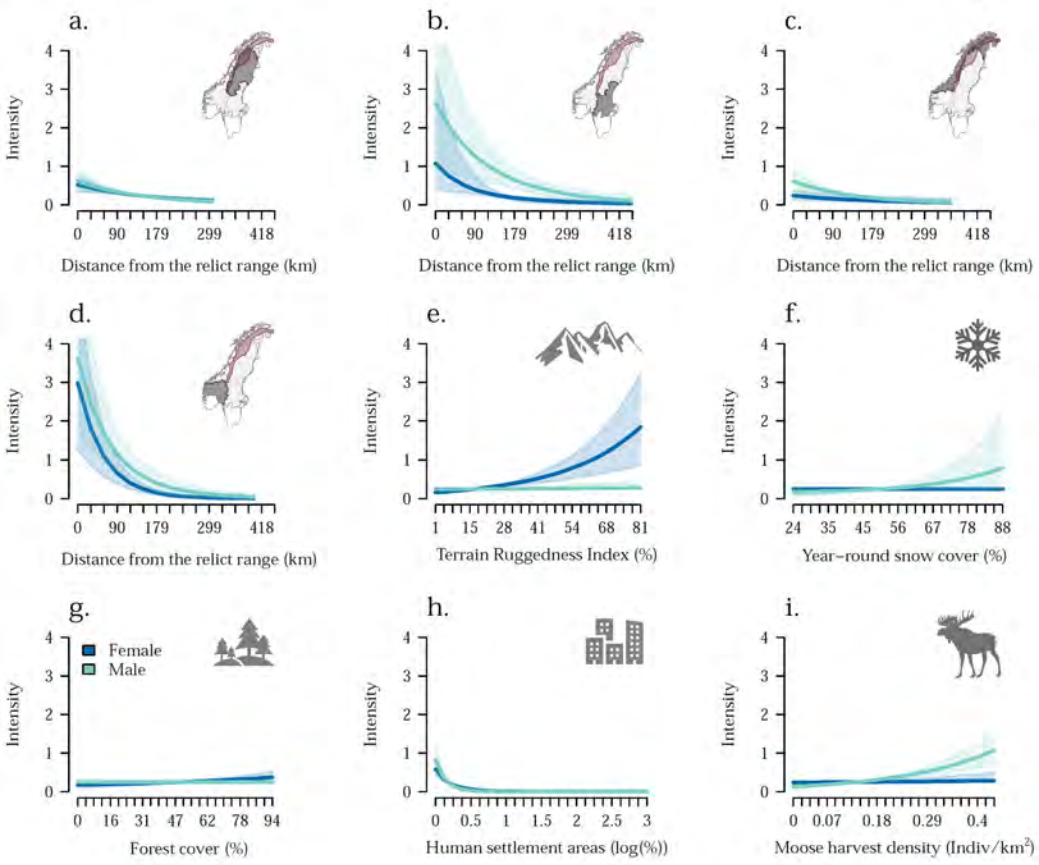

Figure 3: Expected intensity of the density point process for female (blue) and male (green) wolverines *Gulo gulo* in Norway and Sweden as a function of environmental covariates included in this study. Mean response and 95% Bayesian credible interval limits are represented by thick lines and transparent polygons, respectively. Predictions in plots a-d are for the range of values of distance from the relict range (km) that was available in the given zone: a. northern Sweden; b. southern Sweden; c. northern Norway; and d. southern Norway. The red polygons on the small maps a-d indicate the relict range (Fig. 1), and the dark gray polygons are different zones with contrasting management goals and environmental conditions for the wolverine across the available habitat (see the Supporting Information). The intensity of the point process reflects the relative distribution of individual activity centers. For example, twice as many individuals are expected to have their activity centers located in a cell with an intensity of 2 compared to 1.

4 Discussion

The present spatial configuration of wolverine density across the Scandinavian Peninsula reflects the species' recovery from past range-contraction and population decline, modulated by current management and environmental conditions. The importance of the relict range along

the Swedish-Norwegian border highlights the need for coordinated monitoring and management of this transboundary population of wolverines. Monitoring is already coordinated to some extent (Gervasi et al. 2016, 2019, Bischof et al. 2020), but fully coordinated management is made difficult by existing differences in national and regional population goals and legal obligations, which are also tied to differences in the intensity of conflict.

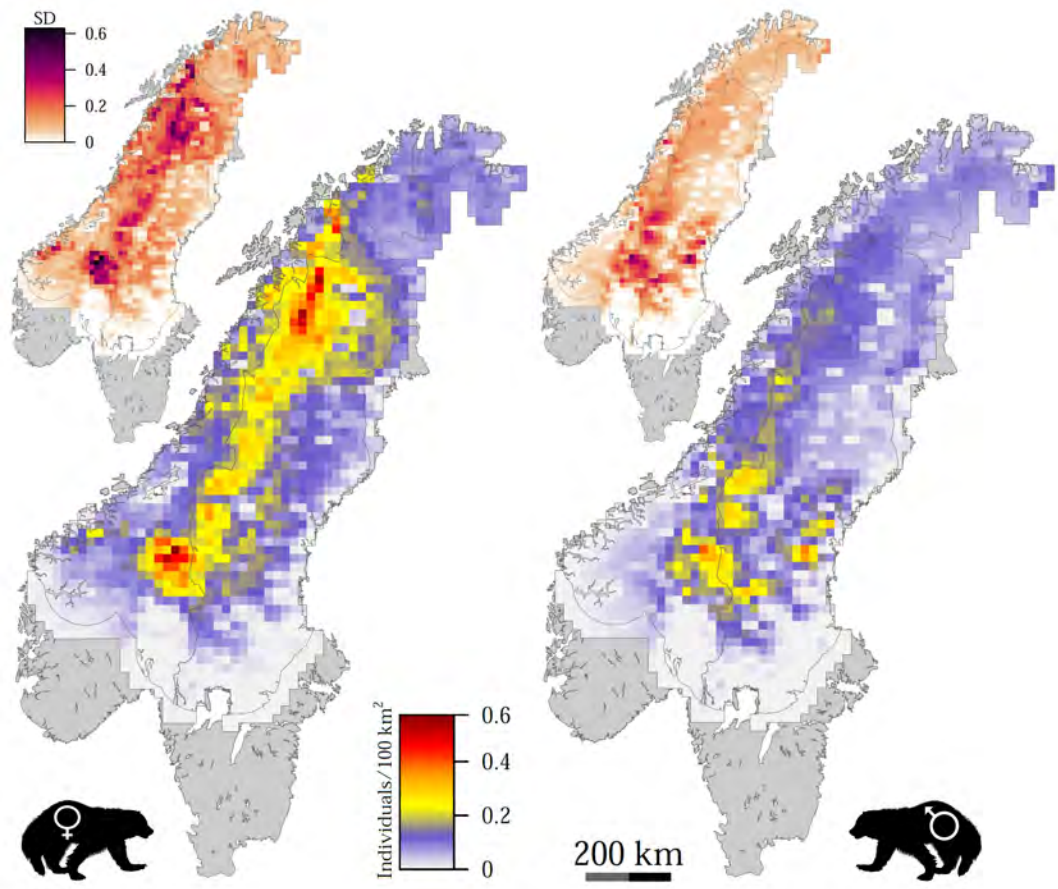

Figure 4: Expected density surfaces of female (left) and male (right) wolverines *Gulo gulo* in Norway and Sweden as a function of environmental covariates included in spatial capture-recapture analysis (Table 1). The main maps show the average expected density surfaces for each sex (individuals per 100 km^2) and smaller inset maps show the cell-based standard deviation of predictions.

The ghosts of the past

A key driver of current wolverine density distribution for both sexes in Norway and Sweden appears to be distance from the relict range (Fig. 1 and Supporting Information), where Scandinavian wolverines survived human persecution before their legal protection in the 1970s (Landa et al. 2000, Flagstad et al. 2004). We also found that zonal management is one of the main drivers of wolverine density in Scandinavia (Fig. 3). The density of both male and female wolverines declines with increasing distance from the relict range, and the rate of decline further varies among zones with contrasting management goals regarding wolverine annual reproduction (Figs. 2-3). Regional differences in the effect of distance from the relict range is likely a sign that the current recolonization of wolverines is both a function of past and current management practices and environmental conditions. Together, these factors explained much of the spatial variation in current density of wolverines in the Scandinavian Peninsula (Fig. 4). Whether the relict range represents a highly suitable habitat for the Scandinavian wolverine (i.e., historical and current core) or the species was pushed into the alpine refuge areas during the peak of the persecution is not fully understood (Flagstad et al. 2004, Kerley et al. 2012, Zigouris et al. 2013). Nonetheless, wolverine recolonization in Scandinavia matches the general pattern of return of other large carnivore species in Western Europe and North America (Linnell et al. 2001, Chapron et al. 2014). Successful recovery of these species is partially attributed to changing public attitudes towards large carnivores and effective law enforcement, which, in turn have lowered the risk of direct killing by humans (Zedrosser et al. 2011, Ingeman et al. 2022). Likewise, increasing tolerance towards wolverines by Scandinavian farmers and herders has in part been achieved through intensive zonal management of wolverines and compensation schemes (Persson et al. 2015, Aronsson and Persson 2017, Strand et al. 2019). Balancing the landscape-level requirements of a viable wolverine (meta-)population and human interests will therefore remain crucial for successful management.

The ability of wolverines to travel long distances has probably contributed to their successful recolonization in part of their historical range in Scandinavia. Male wolverines are more likely to disperse, whereas females usually stay close to their natal range and show high home-range fidelity (Inman et al. 2012, Packila et al. 2017, Aronsson and Persson 2018). We found that spatial covariates tested in our study had qualitatively similar effects on the density of female

and male wolverines (Fig. 2). We note that male and female Scandinavian wolverines have a comparable level of human-induced mortality (Bischof et al. 2020, Milleret et al. 2022). Additionally, long-distance dispersal events that lead to successful colonization of unoccupied habitat are not common (Flagstad et al. 2004, Packila et al. 2017). Even if male wolverines on average disperse farther, they may not always successfully establish significantly farther than females. Nonetheless, we observed pockets of higher expected male wolverine density farther from the relict range compared to the expected female density, which remained the highest in and near the relict range (Fig. 4). This pattern was reflected in the sex-specific estimates of the effect of distance from the relict range in the southern zones of Sweden and Norway (Fig. 2).

We estimated, on average, substantially lower wolverine densities in the southern zones of Norway and Sweden compared to the northern zones (Fig. 3). The southern zones generally do not cover semidomesticated reindeer husbandry areas and calving grounds, but the southern zone in Norway includes areas with free-ranging domestic sheep. The current management strategy in both countries allows more wolverine annual reproduction in the northern zones (Ministry of the Environment 2003, Naturvårdsverket Ärendenr 2020), and the legal removal of wolverines is proportionally more intense in the south, especially in southwestern Norway to protect the free-ranging sheep (Strand et al. 2019). Consequently, no wolverines are currently tolerated in southwestern Norway. There are also mismatches between the management goals, their implementation, and regional tolerance of the wolverine in Scandinavia (Aronsson and Persson 2017, Gervasi et al. 2019) that are not entirely reflected by the four zones we considered. Thus, it is likely that the combined effect of the higher cost of dispersal from the relict range and the current management plans regarding wolverine recolonization, together with region-specific environmental characteristics, have resulted in slower wolverine expansion and lower densities in the southern parts of the Scandinavian Peninsula.

Population-level drivers of variation in density

Wildlife distributions and densities are continuously being shaped by multiple factors at different spatio-temporal scales. Abiotic factors, such as temperature and precipitation, play a key role in shaping species distributions at broad scales (Benton 2009). There is also increasing evidence that biotic factors are important determinants of species distributions at both local

and large spatial extents, particularly when accounting for interacting drivers (Van der Putten et al. 2010, Wisz et al. 2013). We found that current environmental features that describe landscape heterogeneity and productivity can explain variation in the Scandinavian wolverine density at the landscape level. Although the relative importance of some of these covariates varied between sexes (Fig. 2), anthropogenic factors had a consistently negative impact on both male and female wolverine density. Studies from the Nearctic range of the wolverine have also shown that drivers associated with anthropogenic disturbances can be more important than the traditionally held drivers of wolverine density, such as topographic ruggedness and snow cover (Fisher et al. 2013, Heim et al. 2017, Chow-Fraser et al. 2022). Besides quantifying the driving factors of density for the entire population of the Scandinavian wolverines, our study advances the previous findings (Fisher et al. 2022 and references in Table 1) by highlighting the role of past persecution history and current management practices in modulating natural recolonization across a human-dominated landscape.

Human-caused mortality and anthropogenic fragmentation of habitat are limiting wolverine distribution and density globally (May et al. 2006, Persson et al. 2009, Fisher et al. 2013, Mowat et al. 2020, Lukacs et al. 2020, Lansink et al. 2022, Barrueto et al. 2022). Within the Scandinavian large carnivore guild, wolverines are believed to be the most sensitive to habitat fragmentation (May et al. 2008). We included the percentage of human settlement areas as a measure of human pressure on the natural environment (Marconcini et al. 2020), which represents human population density and the associated disturbances. The negative impact of human settlements on wolverine density appeared to be substantial (Fig. 2), and we observed drastic declines in the expected density of both male and female wolverines with increasing human settlements (Fig. 3). In Norway and Sweden, the majority of large towns with the highest concentration of permanent human settlements and high traffic-volume roads are located in the southern parts. Likewise, the farthest distance from the relict range and zones with lower annual wolverine reproduction goals are also in the south (Figs. 3 and Supporting Information). Thus, the combined effect of all these anthropogenic factors, as well as the zero tolerance towards wolverines in southwestern Norway, have probably limited the wolverine density distribution in the southern parts of the Scandinavian Peninsula. Nonetheless, the south represents the wolverine population's expansion front and the observed latitudinal pattern may

be also explained with the observation that wildlife population dynamics can differ considerably from the core areas (Swenson et al. 1998, Burton et al. 2010, Angert et al. 2020). With increasing human-made barriers to wolverine movement and dispersal (Aronsson and Persson 2018, Sawaya et al. 2019, Lansink et al. 2022), we expect the resulting population fragmentation will also play a major role in shaping the spatial distribution and dynamics of the Scandinavian wolverine population in the future.

As a measure of wild prey biomass availability, we included moose harvest density in our models (Table 1, Supporting Information). We estimated significantly higher wolverine densities in areas with higher moose harvest density, and this positive effect was more pronounced for males (Fig. 3). Wolverines are generally facultative scavengers and in many areas of Fennoscandia, they depend on slaughter remains from hunting and carcasses of prey killed by other top predators, including the Eurasian lynx *Lynx lynx*, wolf *Canis lupus*, and brown bear *Ursus arctos*, as well as animals dead from natural causes and roadkills (Van Dijk et al. 2008, Mattisson et al. 2011, Koskela et al. 2013, Aronsson et al. 2022). Moose occurs throughout the wolverine range in Scandinavia and moose carrion is an important food source for wolverines in many areas (Van Dijk et al. 2008, Mattisson et al. 2016, Aronsson et al. 2022), especially for breeding females (Koskela et al. 2013) and during winter (October - April) that overlaps with our study period. There is, however, considerable spatial and temporal variation in wolverine diet in Scandinavia, with reindeer as the most important prey for wolverines in some areas (Mattisson et al. 2016). Unfortunately, we were unable to find comprehensive and reliable data on the density of wild or semidomesticated reindeer across the entire Scandinavian Peninsula to be considered for our study.

The positive effects of terrain ruggedness and the percentage of forest cover on wolverine density were significant for females only, whereas the average percentage of year-round snow appeared to only impact male density (Fig. 2). Until recently, Scandinavian wolverines were not considered to be a forest-dwelling species, as they appeared to select open and rugged terrain at higher elevations with snow, away from human activity (May et al. 2008, 2012, Rauset et al. 2013). Spring snow cover in particular is believed to be important for reproducing females, because it determines denning suitability and offspring survival (Copeland et al. 2010, Mowat et al. 2020, Barrueto et al. 2022). However, in recent years, the Scandinavian wolverine

population has expanded considerably into the boreal forest and has now colonized areas without persistent spring snow cover (Aronsson and Persson 2017). We chose the average year-round snow cover during the past decade not to specifically account for denning suitability for the wolverine, but as a measure of climatic niche suitability that may have shaped the wolverine's density distribution today (Table 1). Terrain ruggedness and forest cover probably correlate with the degree of past persecution due to accessibility and history of land protection (Joppa and Pfaff 2009, Kerley et al. 2012) and the significance of these covariates for female wolverines may then reflect their affinity for high-quality habitat compared to males (May et al. 2008, 2012, Rauset et al. 2013, Aronsson and Persson 2018).

Wolverines in the past, present, and future

Scandinavian wolverines have recovered from the brink of extinction and are now occupying a considerable portion of their historic range (Flagstad et al. 2004, Chapron et al. 2014, Aronsson and Persson 2017, Gervasi et al. 2019, Bischof et al. 2020). The effects of past impacts are, nonetheless, still clearly visible today, modulated, but not masked, by current environmental conditions and management regimes. The wolverine density in Scandinavia is shaped by human interests, while interacting with the history of local extinction. Wolverines are also impacted by other environmental covariates, several of which are directly or indirectly influenced by humans (e.g., prey base, land-use, and climate conditions). In an increasingly human-dominated landscape, the impact of humans on wolverines is likely to be even greater in the coming decades, further defining the state of the Scandinavian wolverine population. Despite the expansion of wolverines (Chapron et al. 2014, Gervasi et al. 2019), an increasing human impact, if neglected, may therefore eventually again limit wolverines to the relict range that served as a refuge in the past.

Data Availability Statement

Wolverine detections used in this study are available through the database Rovbase 3.0 at `www.rovbase.no` or `www.rovbase.se`. Data and R scripts of the spatial capture-recapture analysis is available at: `https://github.com/eMoqanaki/WolverineDensitySCR`.

Author contributions

Ehsan Moqanaki: Conceptualization (equal); Formal analysis (lead); Investigation (lead); Methodology (lead); Validation (lead); Visualization (lead); Writing – original draft (lead); Writing – review and editing (lead). **Cyril Milleret:** Formal analysis (supporting); Methodology (supporting); Validation (supporting); Writing – review and editing (supporting). **Pierre Dupont:** Formal analysis (supporting); Methodology (supporting); Validation (supporting); Visualization (supporting); Writing – review and editing (supporting). **Henrik Brøseth:** Data curation (lead); Investigation (supporting); Validation (supporting); Writing – review and editing (supporting). **Richard Bischof:** Conceptualization (equal); Formal analysis (supporting); Funding acquisition (lead); Investigation (supporting); Methodology (supporting); Project administration (lead); Supervision (lead); Validation (supporting); Writing – original draft (supporting); Writing – review and editing (supporting).

Competing interests

We declare we have no interests which might be perceived as posing a conflict or bias.

Funding

This study was funded by the Research Council of Norway through project WildMap (NFR 286886), the Swedish Environmental Protection Agency (Naturvårdsverket), and the Norwegian Environment Agency (Miljødirektoratet). E.M. was supported by a PhD scholarship from the Norwegian University of Life Sciences.

Acknowledgments

We thank all contributors to the Scandinavian large carnivore monitoring database Rovbase 3.0. M. Tourani helped with the implementation of the variable selection approach and provided feedback on the figures. J. Kindberg provided access to the moose harvest data used in this study. We appreciate the comments by the Subject Editor, N. Yoccoz, and J. Fisher, S. Dey, and S. Schowanek. J. Mattisson provided the numbers of wolverines that were legally hunted in Sweden by 2022.

References

Angert, A. L., Bontrager, M. G., and Ågren, J. (2020). What do we really know about adaptation at range edges? *Annual Review of Ecology, Evolution, and Systematics*, 51:341–361.

Aronsson, M. and Persson, J. (2017). Mismatch between goals and the scale of actions constrains adaptive carnivore management: the case of the wolverine in sweden. *Animal Conservation*, 20(3):261–269.

Aronsson, M. and Persson, J. (2018). Female breeding dispersal in wolverines, a solitary carnivore with high territorial fidelity. *European Journal of Wildlife Research*, 64(1):1–10.

Aronsson, M., Persson, J., Zimmermann, B., Märtz, J., Wabakken, P., Heeres, R., and Nordli, K. (2022). *Järven i Inre Skandinaviens skogslandskap–områdesbruk, födoval och reproduktion*. SLU Grimsö forskningsstation Institutionen för ekologi Sveriges lantbruksuniversitet.

Barrueto, M., Forshner, A., Whittington, J., Clevenger, A. P., and Musiani, M. (2022). Protection status, human disturbance, snow cover and trapping drive density of a declining wolverine population in the [canadian rocky mountains]. *Scientific Reports*, 12(1):1–15.

Barrueto, M., Sawaya, M. A., and Clevenger, A. P. (2020). Low wolverine (*Gulo gulo*) density in a national park complex of the Canadian Rocky Mountains. *Canadian Journal of Zoology*, 98(5):287–298.

Benton, M. J. (2009). The red queen and the court jester: species diversity and the role of biotic and abiotic factors through time. *Science*, 323(5915):728–732.

Bischof, R., Milleret, C., Dupont, P., Chipperfield, J., Tourani, M., Ordiz, A., de Valpine, P., Turek, D., Royle, J. A., Gimenez, O., et al. (2020). Estimating and forecasting spatial population dynamics of apex predators using transnational genetic monitoring. *Proceedings of the National Academy of Sciences*, 117(48):30531–30538.

Bischof, R., Turek, D., Milleret, C., Ergon, T., Dupont, P., Dey, S., Zhang, W., and de Valpine, P. (2021). *nimbleSCR: Spatial Capture-Recapture (SCR) Methods Using 'nimble'*.

Borchers, D. L. and Efford, M. G. (2008). Spatially explicit maximum likelihood methods for capture-recapture studies. *Biometrics*, 64(2):377–385.

Brooks, S. P. and Gelman, A. (1998). General methods for monitoring convergence of iterative simulations. *Journal of Computational and Graphical Statistics*, 7(4):434–455.

Brøseth, H., Flagstad, Ø., Wärdig, C., Johansson, M., and Ellegren, H. (2010). Large-scale noninvasive genetic monitoring of wolverines using scats reveals density dependent adult survival. *Biological Conservation*, 143(1):113–120.

Burton, O. J., Phillips, B. L., and Travis, J. M. (2010). Trade-offs and the evolution of life-histories during range expansion. *Ecology Letters*, 13(10):1210–1220.

Chapron, G., Kaczensky, P., Linnell, J. D., Von Arx, M., Huber, D., Andrén, H., López-Bao, J. V., Adamec, M., Álvares, F., Anders, O., et al. (2014). Recovery of large carnivores in europe's modern human-dominated landscapes. *Science*, 346(6216):1517–1519.

Chow-Fraser, G., Heim, N., Paczkowski, J., Volpe, J. P., and Fisher, J. T. (2022). Landscape change shifts competitive dynamics between declining at-risk wolverines and range-expanding coyotes, compelling a new conservation focus. *Biological Conservation*, 266:109435.

Cimatti, M., Ranc, N., Benítez-López, A., Maiorano, L., Boitani, L., Cagnacci, F., Čengić, M., Ciucci, P., Huijbregts, M. A., Krofel, M., et al. (2021). Large carnivore expansion in Europe is associated with human population density and land cover changes. *Diversity and Distributions*, 27(4):602–617.

Copeland, J., McKelvey, K., Aubry, K., Landa, A., Persson, J., Inman, R., Krebs, J., Lofroth, E., Golden, H., Squires, J., et al. (2010). The bioclimatic envelope of the wolverine (*Gulo gulo*): do climatic constraints limit its geographic distribution? *Canadian Journal of Zoology*, 88(3):233–246.

Cretois, B., Linnell, J. D., Van Moorter, B., Kaczensky, P., Nilsen, E. B., Parada, J., and Rød, J. K. (2021). Coexistence of large mammals and humans is possible in europe's anthropogenic landscapes. *iScience*, 24(9):103083.

de Valpine, P., Paciorek, C., Turek, D., Michaud, N., Anderson-Bergman, C., Obermeyer, F., Wehrhahn Cortes, C., Rodrìguez, A., Temple Lang, D., and S, P. (2022). *NIMBLE User Manual*. R package manual version 0.12.2.

Di Marco, M. and Santini, L. (2015). Human pressures predict species' geographic range size better than biological traits. *Global Change Biology*, 21(6):2169–2178.

Donohue, K., Foster, D. R., and Motzkin, G. (2000). Effects of the past and the present on species distribution: land-use history and demography of wintergreen. *Journal of Ecology*, 88(2):303–316.

Efford, M. (2004). Density estimation in live-trapping studies. *Oikos*, 106(3):598–610.

Efford, M. G. (2011). Estimation of population density by spatially explicit capture–recapture analysis of data from area searches. *Ecology*, 92(12):2202–2207.

Efford, M. G., Borchers, D. L., and Mowat, G. (2013). Varying effort in capture-recapture studies. *Methods in Ecology and Evolution*, 4(7):629–636.

Ekblom, R., Brechlin, B., Persson, J., Smeds, L., Johansson, M., Magnusson, J., Flagstad, Ø., and Ellegren, H. (2018). Genome sequencing and conservation genomics in the Scandinavian wolverine population. *Conservation Biology*, 32(6):1301–1312.

Elith, J. and Leathwick, J. R. (2009). Species distribution models: ecological explanation and prediction across space and time. *Annual Review of Ecology, Evolution, and Systematics*, 40:677–697.

Ellis, E. C. (2011). Anthropogenic transformation of the terrestrial biosphere. *Philosophical Transactions of the Royal Society A: Mathematical, Physical and Engineering Sciences*, 369(1938):1010–1035.

Fisher, J. T., Bradbury, S., Anholt, B., Nolan, L., Roy, L., Volpe, J., and Wheatley, M. (2013). Wolverines (*Gulo gulo luscus*) on the Rocky Mountain slopes: natural heterogeneity and landscape alteration as predictors of distribution. *Canadian Journal of Zoology*, 91(10):706–716.

Fisher, J. T., Murray, S., Barrueto, M., Carroll, K., Clevenger, A. P., Hausleitner, D., Harrower, W., Heim, N., Heinemeyer, K., Jacob, A. L., et al. (2022). Wolverines (*Gulo gulo*) in a changing landscape and warming climate: A decadal synthesis of global conservation ecology research. *Global Ecology and Conservation*, page e02019.

649 Flagstad, Ø., Hedmark, E., Landa, A., Brøseth, H., Persson, J., Andersen, R., Segerström, P.,
650 and Ellegren, H. (2004). Colonization history and noninvasive monitoring of a reestablished
651 wolverine population. *Conservation Biology*, 18(3):676–688.

652 Flagstad, Ø., Kleven, O., Erlandsen, S. E., Brandsegg, H., Spets, M. H., Spets, M. H., Eriksen,
653 L. B., Andersskog, I. P. Ø., Johansson, M., Ekblom, R., Ellegren, H., and Brøseth, H. (2019).
654 DNA-based monitoring of the Scandinavian wolverine population 2019: Nina report 1762.
655 Technical report, Norwegian Institute for Nature Research (NINA).

656 Foster, D., Swanson, F., Aber, J., Burke, I., Brokaw, N., Tilman, D., and Knapp, A. (2003).
657 The importance of land-use legacies to ecology and conservation. *BioScience*, 53(1):77–88.

658 Gaynor, K. M., Hojnowski, C. E., Carter, N. H., and Brashares, J. S. (2018). The influence of
659 human disturbance on wildlife nocturnality. *Science*, 360(6394):1232–1235.

660 Gervasi, V., Brøseth, H., Gimenez, O., Nilsen, E. B., and Linnell, J. D. (2014). The risks of
661 learning: confounding detection and demographic trend when using count-based indices for
662 population monitoring. *Ecology and Evolution*, 4(24):4637–4648.

663 Gervasi, V., Brøseth, H., Gimenez, O., Nilsen, E. B., Odden, J., Flagstad, Ø., and Linnell,
664 J. D. (2016). Sharing data improves monitoring of trans-boundary populations: the case of
665 wolverines in central scandinavia. *Wildlife Biology*, 22(3):95–106.

666 Gervasi, V., Linnell, J. D., Brøseth, H., and Gimenez, O. (2019). Failure to coordinate
667 management in transboundary populations hinders the achievement of national management
668 goals: The case of wolverines in Scandinavia. *Journal of Applied Ecology*, 56(8):1905–1915.

669 Gimenez, O., Cam, E., and Gaillard, J.-M. (2018). Individual heterogeneity and capture–
670 recapture models: what, why and how? *Oikos*, 127(5):664–686.

671 Green, P. J. (1995). Reversible jump markov chain monte carlo computation and bayesian
672 model determination. *Biometrika*, 82(4):711–732.

673 Guisan, A. and Zimmermann, N. E. (2000). Predictive habitat distribution models in ecology.
674 *Ecological Modelling*, 135(2-3):147–186.

Habitats Directive (1992). Council directive 92/43/eec of 21 may 1992 on the conservation of natural habitats and of wild fauna and flora. *Official Journal of the European Union*, 206:7–50.

Heim, N., Fisher, J. T., Clevenger, A., Paczkowski, J., and Volpe, J. (2017). Cumulative effects of climate and landscape change drive spatial distribution of Rocky Mountain wolverine (*Gulo gulo* l.). *Ecology and Evolution*, 7(21):8903–8914.

Hijmans, R. J. (2021). *raster: Geographic Data Analysis and Modeling*. R package version 3.4-13.

Hijmans, R. J., Bivand, R., van Etten, J., Forner, K., Ooms, J., and Pebesma, E. (2022). *Package 'terra': Spatial Data Analysis*. R package version 1.5-21.

Hobbs, N. T., Andren, H., Persson, J., Aronsson, M., and Chapron, G. (2012). Native predators reduce harvest of reindeer by Sámi pastoralists. *Ecological Applications*, 22(5):1640–1654.

Hollister, J., Shah, T., Robitaille, A. L., Beck, M. W., and Johnson, M. (2021). *elevatr: Access Elevation Data from Various APIs*. R package version 0.4.1.

Illian, J., Penttinen, A., Stoyan, H., and Stoyan, D. (2008). *Statistical analysis and modelling of spatial point patterns*, volume 70. John Wiley & Sons.

Ingeman, K. E., Zhao, L. Z., Wolf, C., Williams, D. R., Ritger, A. L., Ripple, W. J., Kopecky, K. L., Dillon, E. M., DiFiore, B. P., Curtis, J. S., et al. (2022). Glimmers of hope in large carnivore recoveries. *Scientific Reports*, 12(1):1–13.

Inman, R. M., Packila, M. L., Inman, K. H., Mccue, A. J., White, G. C., Persson, J., Aber, B. C., Orme, M. L., Alt, K. L., Cain, S. L., et al. (2012). Spatial ecology of wolverines at the southern periphery of distribution. *The Journal of Wildlife Management*, 76(4):778–792.

Isaac, N. J., Jarzyna, M. A., Keil, P., Dambly, L. I., Boersch-Supan, P. H., Browning, E., Freeman, S. N., Golding, N., Guillera-Arroita, G., Henrys, P. A., et al. (2020). Data integration for large-scale models of species distributions. *Trends in Ecology & Evolution*, 35(1):56–67.

Jetz, W., McGeoch, M. A., Guralnick, R., Ferrier, S., Beck, J., Costello, M. J., Fernandez, M., Geller, G. N., Keil, P., Merow, C., et al. (2019). Essential biodiversity variables for mapping and monitoring species populations. *Nature Ecology & Evolution*, 3(4):539–551.

Johnson, D. H. (1980). The comparison of usage and availability measurements for evaluating resource preference. *Ecology*, 61(1):65–71.

Joppa, L. N. and Pfaff, A. (2009). High and far: biases in the location of protected areas. *PLoS ONE*, 4(12):e8273.

Kerley, G. I., Kowalczyk, R., and Cromsigt, J. P. (2012). Conservation implications of the refugee species concept and the European bison: king of the forest or refugee in a marginal habitat? *Ecography*, 35(6):519–529.

Kortello, A., Hausleitner, D., and Mowat, G. (2019). Mechanisms influencing the winter distribution of wolverine *Gulo gulo luscus* in the southern Columbia Mountains, Canada. *Wildlife Biology*, 2019(1):1–13.

Koskela, A., Aspi, J., Hyvärinen, M., et al. (2013). Effect of reproductive status on the diet composition of wolverines (*Gulo gulo*) in boreal forests of eastern Finland. In *Annales Zoologici Fennici*, volume 50, pages 100–106. BioOne.

Landa, A., Lindén, M., Kojola, I., et al. (2000). *Action plan for the conservation of wolverines in Europe (Gulo gulo)*. Number 18-115. Council of Europe.

Lansink, G., Kleven, O., Ekblom, R., Spong, G., Kopatz, A., Mattisson, J., Persson, J., Kojola, I., Holmala, K., Ollila, T., et al. (2022). Potential for increased connectivity between differentiated wolverine populations. *Biological Conservation*, 272:109601.

Lansink, G. M., Esparza-Salas, R., Joensuu, M., Koskela, A., Bujnáková, D., Kleven, O., Flagstad, Ø., Ollila, T., Kojola, I., Aspi, J., et al. (2020). Population genetics of the wolverine in Finland: the road to recovery? *Conservation Genetics*, 21(3):481–499.

Linnell, J. D., Swenson, J. E., and Anderson, R. (2001). Predators and people: conservation of large carnivores is possible at high human densities if management policy is favourable. *Animal Conservation*, 4(4):345–349.

727 Lukacs, P. M., Evans Mack, D., Inman, R., Gude, J. A., Ivan, J. S., Lanka, R. P., Lewis,
728 J. C., Long, R. A., Sallabanks, R., Walker, Z., et al. (2020). Wolverine occupancy, spatial
729 distribution, and monitoring design. *The Journal of Wildlife Management*, 84(5):841–851.

730 Marconcini, M., Metz-Marconcini, A., Üreyen, S., Palacios-Lopez, D., Hanke, W., Bachofer, F.,
731 Zeidler, J., Esch, T., Gorelick, N., Kakarla, A., et al. (2020). Outlining where humans live,
732 the world settlement footprint 2015. *Scientific Data*, 7(1):1–14.

733 Mattisson, J., Persson, J., Andren, H., and Segerström, P. (2011). Temporal and spatial
734 interactions between an obligate predator, the Erasian lynx (*Lynx lynx*), and a facultative
735 scavenger, the wolverine (*Gulo gulo*). *Canadian Journal of Zoology*, 89(2):79–89.

736 Mattisson, J., Rauset, G. R., Odden, J., Andrén, H., Linnell, J. D., and Persson, J. (2016).
737 Predation or scavenging? prey body condition influences decision-making in a facultative
738 predator, the wolverine. *Ecosphere*, 7(8):e01407.

739 May, R., Gorini, L., Van Dijk, J., Brøseth, H., Linnell, J., and Landa, A. (2012). Habitat
740 characteristics associated with wolverine den sites in Norwegian multiple-use landscapes.
741 *Journal of Zoology*, 287(3):195–204.

742 May, R., Landa, A., van Dijk, J., Linnell, J. D., and Andersen, R. (2006). Impact of infrastructure
743 on habitat selection of wolverines *Gulo gulo*. *Wildlife Biology*, 12(3):285–295.

744 May, R., Van Dijk, J., Wabakken, P., Swenson, J. E., Linnell, J. D., Zimmermann, B., Odden,
745 J., Pedersen, H. C., Andersen, R., and Landa, A. (2008). Habitat differentiation within the
746 large-carnivore community of Norway's multiple-use landscapes. *Journal of Applied Ecology*,
747 45(5):1382–1391.

748 Miller, D. L., Burt, M. L., Rexstad, E. A., and Thomas, L. (2013). Spatial models for distance
749 sampling data: recent developments and future directions. *Methods in Ecology and Evolution*,
750 4(11):1001–1010.

751 Milleret, C., Dupont, P., Bonenfant, C., Brøseth, H., Flagstad, Ø., Sutherland, C., and Bischof,
752 R. (2019). A local evaluation of the individual state-space to scale up Bayesian spatial
753 capture–recapture. *Ecology and Evolution*, 9(1):352–363.

Milleret, C., Dupont, P., Brøseth, H., Kindberg, J., Royle, J. A., and Bischof, R. (2018). Using partial aggregation in spatial capture recapture. *Methods in Ecology and Evolution*, 9(8):1896–1907.

Milleret, C., Dupont, P., Moqanaki, E., Brøseth, H., Flagstad, Ø., Kleven, O., Kindberg, J., and Bischof, R. (2022). *Estimates of wolverine density, abundance, and population dynamics in Scandinavia, 2014–2022*. The Faculty of Environmental Sciences and Natural Resource Management (MINA), Norwegian University of Life Sciences.

Ministry of the Environment (2003). Rovvilt i norsk natur [Carnivores in Norwegian nature]. *Stortingsmelding 15 (2003–2004)*.

Moqanaki, E. M., Milleret, C., Tourani, M., Dupont, P., and Bischof, R. (2021). Consequences of ignoring variable and spatially autocorrelated detection probability in spatial capture-recapture. *Landscape Ecology*, 36(10):2879–2895.

Morehouse, A. T. and Boyce, M. S. (2016). Grizzly bears without borders: Spatially explicit capture–recapture in southwestern Alberta. *The Journal of Wildlife Management*, 80(7):1152–1166.

Mowat, G., Clevenger, A. P., Kortello, A. D., Hausleitner, D., Barrueto, M., Smit, L., Lamb, C., DorsEy, B., and Ott, P. K. (2020). The sustainability of wolverine trapping mortality in southern Canada. *The Journal of Wildlife Management*, 84(2):213–226.

Naturvårdsverket Ärendenr (2020). Fastställande av miniminivåer för järv gällande rovdjursförvaltningsområden och län. *NV-01525-18*.

O'Hara, R. B. and Sillanpää, M. J. (2009). A review of bayesian variable selection methods: what, how and which. *Bayesian Analysis*, 4(1):85–117.

Packila, M. L., Riley, M. D., Spence, R. S., and Inman, R. M. (2017). Long-distance wolverine dispersal from Wyoming to historic range in Colorado. *Northwest Science*, 91(4):399–407.

Pereira, H. M., Navarro, L. M., and Martins, I. S. (2012). Global biodiversity change: the bad, the good, and the unknown. *Annual Review of Environment and Resources*, 37:25–50.

780 Persson, J., Ericsson, G., and Segerström, P. (2009). Human caused mortality in the endangered
781 Scandinavian wolverine population. *Biological Conservation*, 142(2):325–331.

782 Persson, J., Rauset, G. R., and Chapron, G. (2015). Paying for an endangered predator leads
783 to population recovery. *Conservation Letters*, 8(5):345–350.

784 Persson, J., Wedholm, P., and Segerström, P. (2010). Space use and territoriality of wolverines
785 (*Gulo gulo*) in northern Scandinavia. *European Journal of Wildlife Research*, 56(1):49–57.

786 Poley, L. G., Magoun, A. J., Robards, M. D., and Klimstra, R. L. (2018). Distribution and
787 occupancy of wolverines on tundra, northwestern Alaska. *The Journal of Wildlife Management*,
788 82(5):991–1002.

789 R Core Team (2022). *R: A Language and Environment for Statistical Computing*. R Foundation
790 for Statistical Computing, Vienna, Austria.

791 Rauset, G. R., Mattisson, J., Andrén, H., Chapron, G., and Persson, J. (2013). When species'
792 ranges meet: assessing differences in habitat selection between sympatric large carnivores.
793 *Oecologia*, 172(3):701–711.

794 Ripple, W. J., Estes, J. A., Beschta, R. L., Wilmers, C. C., Ritchie, E. G., Hebblewhite, M.,
795 Berger, J., Elmhagen, B., Letnic, M., Nelson, M. P., et al. (2014). Status and ecological
796 effects of the world's largest carnivores. *Science*, 343(6167):1241484.

797 Royle, J. A., Chandler, R. B., Sollmann, R., and Gardner, B. (2014). *Spatial Capture-Recapture*.
798 Academic Press, Waltham.

799 Royle, J. A., Dorazio, R. M., and Link, W. A. (2007). Analysis of multinomial models with
800 unknown index using data augmentation. *Journal of Computational and Graphical Statistics*,
801 16(1):67–85.

802 Sawaya, M. A., Clevenger, A. P., and Schwartz, M. K. (2019). Demographic fragmentation
803 of a protected wolverine population bisected by a major transportation corridor. *Biological*
804 *Conservation*, 236:616–625.

Scrafford, M. A., Avgar, T., Abercrombie, B., Tigner, J., and Boyce, M. S. (2017). Wolverine habitat selection in response to anthropogenic disturbance in the western Canadian boreal forest. *Forest Ecology and Management*, 395:27–36.

Smith, J. E., Lehmann, K. D., Montgomery, T. M., Strauss, E. D., and Holekamp, K. E. (2017). Insights from long-term field studies of mammalian carnivores. *Journal of Mammalogy*, 98(3):631–641.

statistisk sentralbyrå (2021). Moose hunting. Accessed: 2021-11-04.

Strand, G.-H., Hansen, I., de Boon, A., and Sandström, C. (2019). Carnivore management zones and their impact on sheep farming in Norway. *Environmental Management*, 64(5):537–552.

Swenson, J. E., Sandegren, F., and SO-Derberg, A. (1998). Geographic expansion of an increasing brown bear population: evidence for presaturation dispersal. *Journal of Animal Ecology*, 67(5):819–826.

Tablado, Z. and Jenni, L. (2017). Determinants of uncertainty in wildlife responses to human disturbance. *Biological Reviews*, 92(1):216–233.

Tourani, M. (2022). A review of spatial capture–recapture: Ecological insights, limitations, and prospects. *Ecology and Evolution*, 12(1):e8468.

Tucker, M. A., Böhning-Gaese, K., Fagan, W. F., Fryxell, J. M., Van Moorter, B., Alberts, S. C., Ali, A. H., Allen, A. M., Attias, N., Avgar, T., et al. (2018). Moving in the anthropocene: Global reductions in terrestrial mammalian movements. *Science*, 359(6374):466–469.

Turek, D., Milleret, C., Ergon, T., Brøseth, H., Dupont, P., Bischof, R., and De Valpine, P. (2021). Efficient estimation of large-scale spatial capture–recapture models. *Ecosphere*, 12(2):e03385.

Ueno, M., Solberg, E. J., Iijima, H., Rolandsen, C. M., and Gangsei, L. E. (2014). Performance of hunting statistics as spatiotemporal density indices of moose (*Alces alces*) in norway. *Ecosphere*, 5(2):1–20.

Ummenhofer, C. C. and Meehl, G. A. (2017). Extreme weather and climate events with ecological relevance: a review. *Philosophical Transactions of the Royal Society B: Biological Sciences*, 372(1723):20160135.

van de Schoot, R., Depaoli, S., King, R., Kramer, B., Märtens, K., Tadesse, M. G., Vannucci, M., Gelman, A., Veen, D., Willemsen, J., et al. (2021). Bayesian statistics and modelling. *Nature Reviews Methods Primers*, 1(1):1–26.

Van der Putten, W. H., Macel, M., and Visser, M. E. (2010). Predicting species distribution and abundance responses to climate change: why it is essential to include biotic interactions across trophic levels. *Philosophical Transactions of the Royal Society B: Biological Sciences*, 365(1549):2025–2034.

van der Veen, B., Mattisson, J., Zimmermann, B., Odden, J., and Persson, J. (2020). Refrigeration or anti-theft? food-caching behavior of wolverines (gulo gulo) in scandinavia. *Behavioral Ecology and Sociobiology*, 74(5):1–13.

Van Dijk, J., Gustavsen, L., Mysterud, A., May, R., Flagstad, Ø., Brøseth, H., Andersen, R., Andersen, R., Steen, H., and Landa, A. (2008). Diet shift of a facultative scavenger, the wolverine, following recolonization of wolves. *Journal of Animal Ecology*, 77(6):1183–1190.

Vangen, K. M., Persson, J., Landa, A., Andersen, R., and Segerström, P. (2001). Characteristics of dispersal in wolverines. *Canadian Journal of Zoology*, 79(9):1641–1649.

Waters, C. N., Zalasiewicz, J., Summerhayes, C., Barnosky, A. D., Poirier, C., Gałuszka, A., Cearreta, A., Edgeworth, M., Ellis, E. C., Ellis, M., et al. (2016). The anthropocene is functionally and stratigraphically distinct from the holocene. *Science*, 351(6269):aad2622.

Wilson, M. F., O'Connell, B., Brown, C., Guinan, J. C., and Grehan, A. J. (2007). Multiscale terrain analysis of multibeam bathymetry data for habitat mapping on the continental slope. *Marine Geodesy*, 30(1-2):3–35.

Wisz, M. S., Pottier, J., Kissling, W. D., Pellissier, L., Lenoir, J., Damgaard, C. F., Dormann, C. F., Forchhammer, M. C., Grytnes, J.-A., Guisan, A., et al. (2013). The role of biotic interactions in shaping distributions and realised assemblages of species: implications for species distribution modelling. *Biological Reviews*, 88(1):15–30.

Yackulic, C. B., Sanderson, E. W., and Uriarte, M. (2011). Anthropogenic and environmental drivers of modern range loss in large mammals. *Proceedings of the National Academy of Sciences*, 108(10):4024–4029.

Zedrosser, A., Steyaert, S. M., Gossow, H., and Swenson, J. E. (2011). Brown bear conservation and the ghost of persecution past. *Biological Conservation*, 144(9):2163–2170.

Zhang, W., Chipperfield, J. D., Illian, J. B., Dupont, P., Milleret, C., de Valpine, P., and Bischof, R. (2023). A flexible and efficient Bayesian implementation of point process models for spatial capture–recapture data. *Ecology*, 104(1):e3887.

Zigouris, J., Schaefer, J. A., Fortin, C., and Kyle, C. J. (2013). Phylogeography and post-glacial recolonization in wolverines (*Gulo gulo*) from across their circumpolar distribution. *PLoS ONE*, 8(12):e83837.

Älgdata (2021a). Statistik för älgdata. Accessed: 2021-11-04.

Älgdata, L. (2021b). Länsstyrelsernas karttjänst för beslutade älgförvaltningsområden och älgjaktsområden. Accessed: 2021-11-04.

Supplementary Information

Moqanaki E, Milleret C, Dupont P, Brøseth H, Bischof R. Wolverine density distribution reflects past persecution and current management in Scandinavia.

Contents

List of Figures

List of Tables

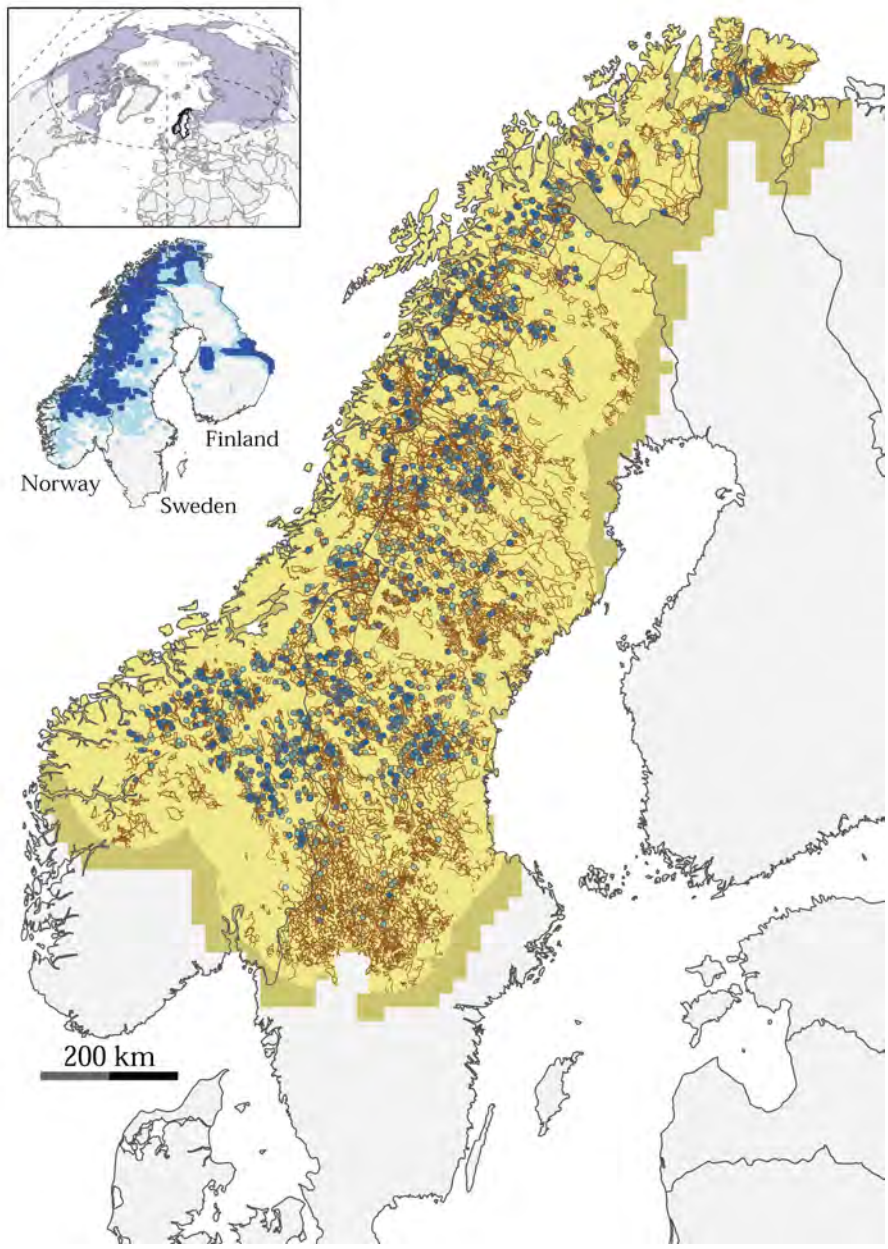

Figure S1: Distribution of confirmed wolverine *Gulo gulo* noninvasive DNA samples (males: light blue circles, females: dark blue) collected along GPS search tracks (brown lines) and opportunistically by management authorities and volunteers across Norway and Sweden between 1 December 2018 and 30 June 2019. The colored polygons show the spatial extent included in the analysis (light yellow) and the 40-km buffer around the detector grid (dark yellow). The upper inset map shows the location of the Scandinavian Peninsula (thick black lines) in relation to the global distribution of the wolverine (purple polygon), after Abramov (2016). The lower inset map indicates areas of permanent (dark blue) and sporadic wolverine occurrences (light blue), redrawn from Chapron et al. (2014).

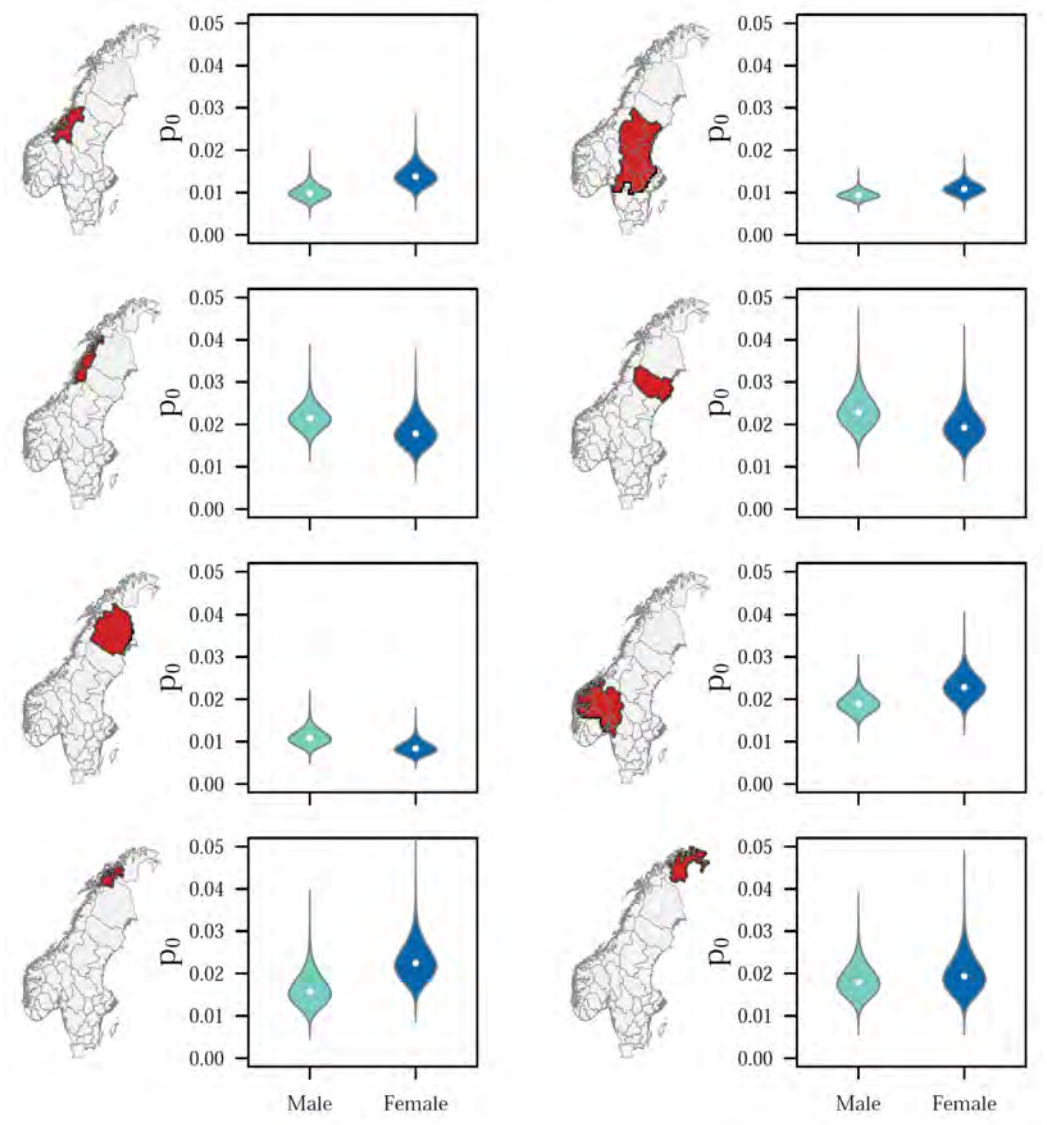

Figure S2: Baseline detection probability p_0 of the Scandinavian wolverine *Gulo gulo* during the noninvasive DNA sampling between 1 December 2018 and 30 June 2019, estimated by the sex-specific single-season spatial capture-recapture models used in this study. Violins represent median (white dots) and 95% Bayesian credible interval limits for females (blue) and males (green). Results are separated into panels based on five carnivore management regions in Norway and three group of counties in Sweden (red polygons) following Bischof et al. (2020), with slight modifications to match the habitat extent. Note that p_0 is a theoretical value of detection probability, where a detector coincides with the location of an individual's activity center and it is not to be confused with detectability – i.e, the overall probability of detecting an individual.

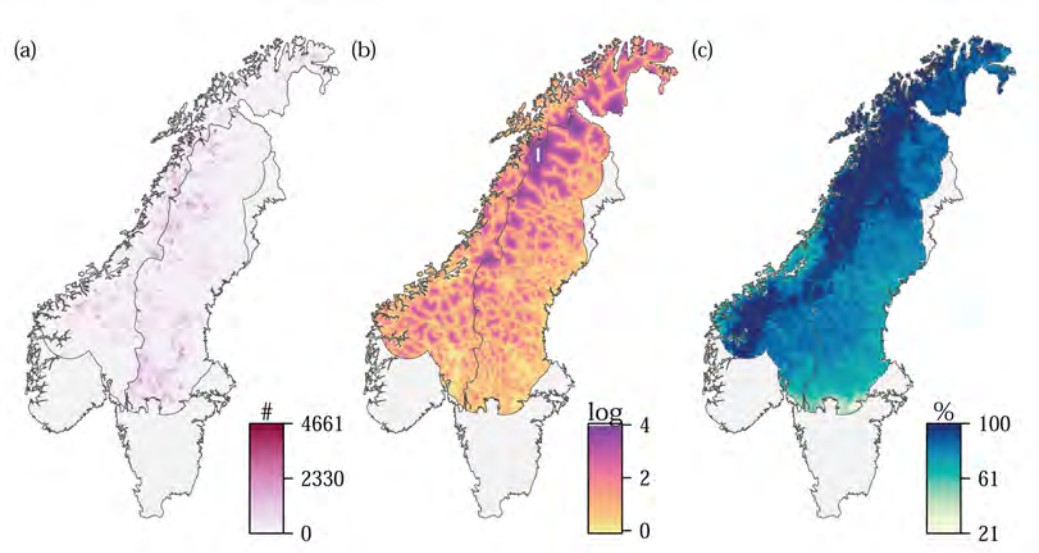

Figure S3: Spatial covariates used to explain spatial variation in wolverine *Gulo gulo* detection probability in the Scandinavian Peninsula. From left to right: (a) Number of track points per 500 m of GPS search tracks as a measure of sampling effort; (b) Average distance (km) to the nearest road on logarithmic scale, representing site accessibility during the sampling; and (c) Average percentage of snow-covered land during the sampling months, December 2018 - June 2019, as a measure of snow-tracking conditions. All covariates were resampled to detector resolution at 10×10 km and standardized prior to analysis. See Table S1 for details.

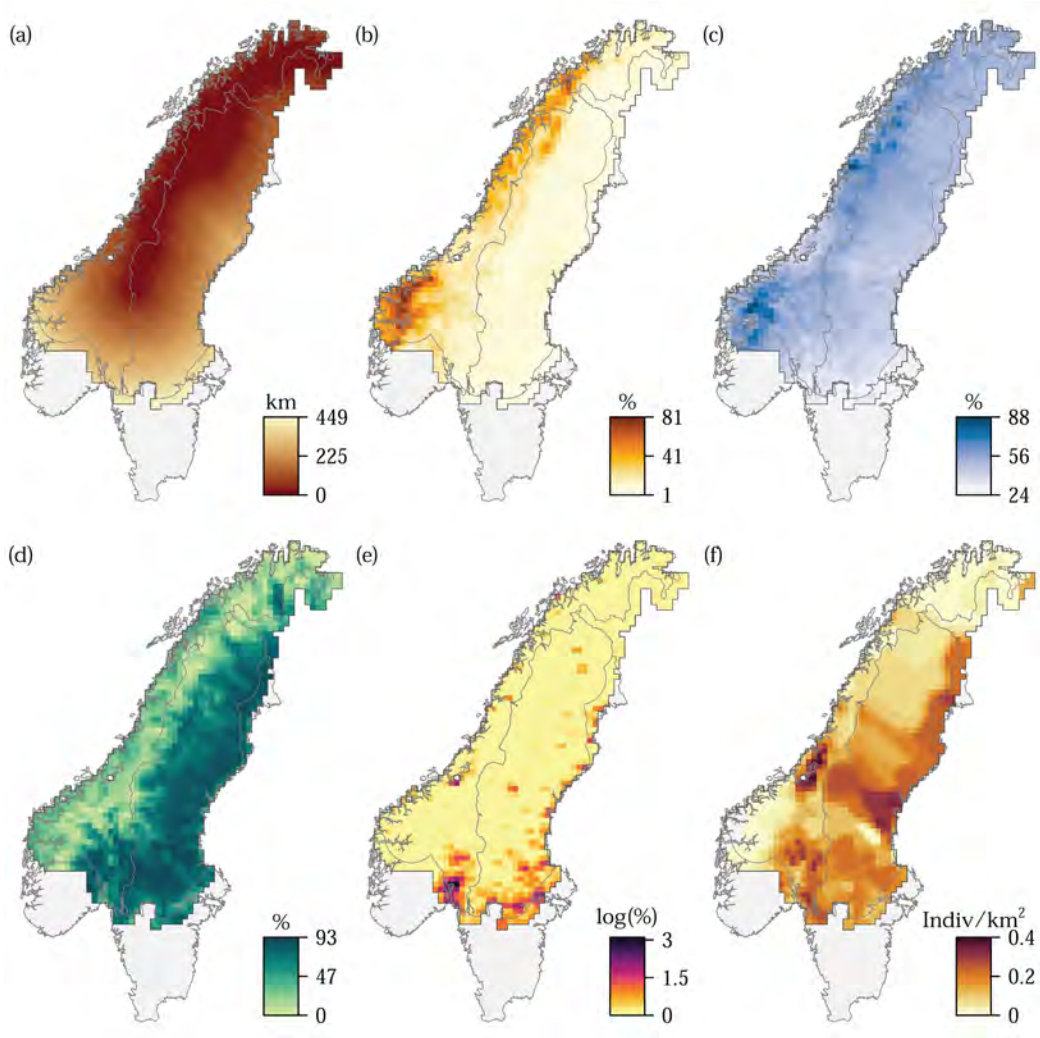

Figure S4: Spatial covariates used to explain spatial variation in wolverine *Gulo gulo* density in the Scandinavian Peninsula during the 2018/19 monitoring season. From top, left to right: (a) Distance from the relic range; (b) Terrain Ruggedness Index, TRI; (c) Percentage of year-round snow-covered land; (d) Percentage of forest cover; (e) Percentage of human settlement areas on logarithmic scale; and (f) Moose *Alces alces* harvest density. All covariates were resampled to habitat resolution at 20×20 km and standardized prior to analysis. See Table 1 in the main text for details.

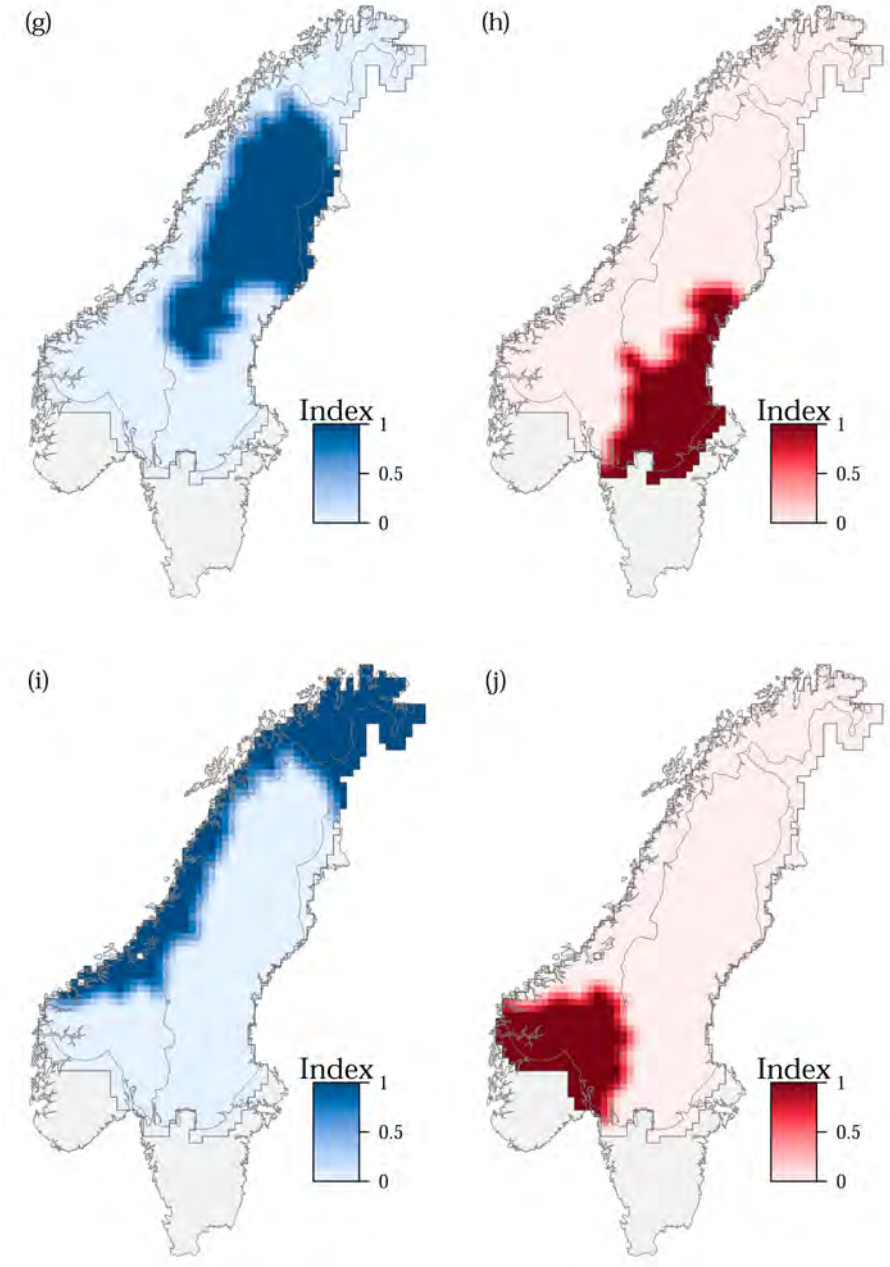

Figure S4: (continued) Spatial covariates used to explain spatial variation in wolverine *Gulo gulo* density in the Scandinavian Peninsula during the 2018/19 monitoring season. We described two zones in each country, representing the variation in wolverine annual reproduction goals in the country's management plans and other region-specific environmental conditions: Northern zones in (g) Sweden and (i) Norway, where jurisdictions have management goal of 10 or more annual wolverine reproductions; Southern zones in (h) Sweden and (j) Norway, where jurisdictions have management goal of less than 10 annual wolverine reproductions, including parts of jurisdictions without management goals. The buffer area in neighboring Finland and Russia were also merged into the corresponding northern zones. See Table 1 and Figure 1 in the main text for details.

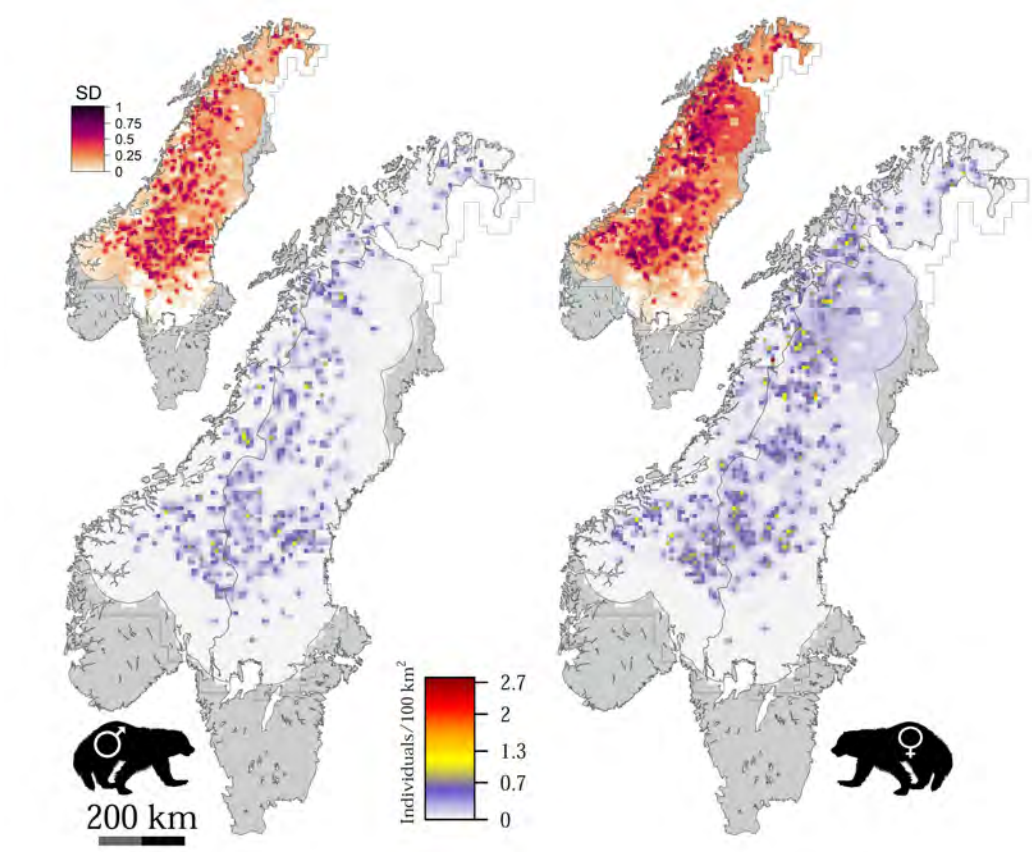

Figure S5: Realized density surfaces of male (left) and female (right) wolverines *Gulo gulo* in the Scandinavian Peninsula between December 2018 and June 2019, as estimated by sex-specific spatial capture-recapture models used in this study. The main maps show the average realized density surfaces for each sex (individuals per 100 km^2) based on the posterior location of individual activity centers in each 10 × 10-km habitat cell and inclusion parameter. Smaller inset maps show the associated cell-based standard deviation. See the main text for details.

Table S1: Description, rationale for inclusion, expected effects, and source and native spatial resolution of covariates of baseline detection probability p_0 used to model the density distribution of the wolverine *Gulo gulo* across Norway and Sweden between December 2018 and June 2019.

Covariate	Description and Rationale	Effects	Resolution and Source
Effort	Length (m) of GPS search tracks recorded by investigators within each detector grid cell during the monitoring period, representing the sampling effort	+	Search tracks were recorded by wildlife authorities during the structured sampling effort. We simplified the tracks by retaining one point per 500 m of tracks using the `gSimplify` function of the R package `rgeos` (Bivand et al. 2019). We then calculated the total number of points at 10×10-km detector cells.
Road	The average distance (km) from each detector to the nearest road as a measure of site accessibility	–	5×5 arcminute resolution ($\approx 8 \times 8$ km at the equator) from the global road data set (GRIP) provided by Meijer et al. (2018), converted in km and log-transformed after adding a value of 1 to deal with 0 values
Snow	The average percentage of snow cover during sampling months between December 2018 and June 2019 in each detector grid cell, representing snow-tracking conditions	+	Calculated using monthly maps of the percentage of snow-covered land based on the MODIS/Terra Snow Cover Daily L3 Global 500 m Grid data set (`www.neo.sci.gsfc.nasa.gov`)
Jurisdiction	Carnivore management regions in Norway and aggregation of counties in Sweden (n = 8) as an index of variation in monitoring regimes and effort across the study landscape	+/–	Bischof et al. (2020)
Previous	Individual covariate indicating whether the focal individual was previously detected or not, representing a potential source of detection bias	+	Wolverine detection data from the previous monitoring season between December 2017 and June 2018 (Milleret et al. 2022)

Table S2: Mean and standard deviation (SD) of the spatial covariates of wolverine *Gulo gulo* density and detection probability used in this study prior to their standardization. Covariates of density and detection probability were prepared at 20×20 and 10×10 km spatial resolutions, respectively. Note that the snow covariate of density was different from the one used to model detection probability. See Figs. S3, S4a, and S4b for spatial depiction of the covariates, and Tables 1 and S1 for details.

Covariate	Unit	Mean	SD
Density			
Relict	Meters	135 274.3	119 377
Ruggedness	Percentage	16.8	14.1
Snow	Percentage	50.6	8.6
Forest	Percentage	50.3	27.5
Moose	Individuals/km^2	0.1	0.1
Settlements	Percentage (log-transformed)	0.2	0.3
Detection			
Effort	Number of track points per 500 meters of search tracks	253.2	345.3
Road	Kilometers (log-transformed)	1.5	0.9
Snow	Percentage	84.6	12.1

Table S3: Description and prior distribution for the focal parameters estimated by the spatial capture-recapture model for the Scandinavian wolverine *Gulo gulo* used in this study

Parameter		Description	Prior
Detection process	σ	Scale parameter of the half-normal detection function	Uniform(0,4)
	p_{0_c}	Baseline detection probability at each jurisdiction	Uniform(0,1)
	β_E	Effect of sampling effort on detection probability	Uniform(-5,5)
	β_R	Effect of distance to the nearest road on detection probability	Uniform(-5,5)
	β_S	Effect of the average snow cover during the sampling months on detection probability	Uniform(-5,5)
	β_P	Effect of previous detection as an individual-level covariate on detection probability	Uniform(-5,5)
Spatial process	β_{R_2}	Effect of management region 2 (southern Sweden) on activity center locations	Uniform(-5,5)
	β_{R_3}	Effect of management region 3 (northern Norway) on activity center locations	Uniform(-5,5)
	β_{R_4}	Effect of management region 4 (southern Norway) on activity center locations	Uniform(-5,5)
	β_{X_1}	Effect of distance from the relic range in northern Sweden on activity center locations	Uniform(-5,5)
	$\beta_{R_2X_1}$	The difference between the effect of distance from the relic range in southern Sweden and northern Sweden on activity center locations	Uniform(-5,5)
	$\beta_{R_3X_1}$	The difference between the effect of distance from the relic range in northern Norway and northern Sweden on activity center locations	Uniform(-5,5)
	$\beta_{R_4X_1}$	The difference between the effect of distance from the relic range in southern Norway and northern Sweden on activity center locations	Uniform(-5,5)
	β_{X_2}	Effect of Terrain Ruggedness Index on activity center locations	Uniform(-5,5)
	β_{X_3}	Effect of the average year-round snow cover on activity center locations	Uniform(-5,5)
	β_{X_4}	Effect of the percentage of forest cover on activity center locations	Uniform(-5,5)
	β_{X_5}	Effect of the percentage of human settlement areas on activity center locations	Uniform(-5,5)
	β_{X_6}	Effect of moose harvest density on activity center locations	Uniform(-5,5)
Demographic process	ψ	Inclusion probability	Uniform(0,1)
	π	Probability of being detected in the previous sampling year	Uniform(0,1)
Variable selection	ω	Inclusion probability of regression coefficients β	Beta(2,8)

Table S4: Alternative description of the relationship between the density of female and male wolverines *Gulo gulo* and determinants thereof. Shown are covariate combinations with the highest (top 5) probabilities of joint inclusion in any given Markov chain Monte Carlo (MCMC) iteration. Inclusion probability (reported here as percentages, %) was determined using an indicator variable approach with reversible jump MCMC method. '×' implies the interaction term between distance from the relic range and a given zone (i.e., Sweden North, Sweden South, Norway North, and Norway South). See Table 1 in the main text for the description of the covariates.

Rank	Model	%
Female		
1	Norway North + Sweden North × Relict + Sweden South × Relict + Norway North × Relict + Snow + Forest + Settlements	30.2
2	Norway North + Sweden North × Relict + Sweden South × Relict + Norway North × Relict + TRI + Snow + Forest + Settlements + Moose	14.0
3	Norway North + Sweden North × Relict + Sweden South × Relict + Norway North × Relict + Norway South × Relict + Snow + Forest + Settlements	11.6
4	Sweden North × Relict + Sweden South × Relict + Norway North × Relict + Snow + Forest + Settlements	10.9
5	Sweden North × Relict + Sweden South × Relict + Norway North × Relict + TRI + Snow + Forest + Settlements + Moose	5.3
Male		
1	Sweden South + Norway South + Sweden North × Relict + Norway North × Relict + Snow + Forest + Moose	31.9
2	Sweden South + Sweden North × Relict + Snow + Forest + Moose	26.0
3	Sweden South + Sweden North × Relict + Norway North × Relict + Snow + Forest + Moose	8.7
4	Sweden South + Norway South + Sweden North × Relict + Norway North × Relict + TRI + Snow + Forest + Moose	7.7
5	Sweden South + Norway South + Sweden North × Relict + Snow + Forest + Moose	4.8

Table S5: The effects (median and 95% Bayesian credible interval limits, CI) of spatial and individual-level covariates of female and male wolverine *Gulo gulo* density and detection probability in the Scandinavian Peninsula between December 2018 and June 2019. To quantify the relative importance of the covariates of density, we used an indicator variable approach and report the probability of inclusion. For reporting the effects of the covariates of density, regression coefficients β, we discarded Markov chain Monte Carlo (MCMC) draws, out of a total of 760 000 MCMC samples, where indicator variable was estimated to be zero – i.e., when the covariate was proposed to be excluded from the sex-specific model. We constrained inclusion of the interaction coefficients (shown by '×') to when the corresponding zone-specific effects were also included – i.e., their inclusion probability cannot exceed that of the additive effect of the given zone. Coefficients with a '*' are relative to the intercept effect of distance from the relict range ("Relict" in the zone Sweden North). Significant effects (i.e., where 95% CI does not overlap zero) are shown in bold. See Table 1 in the main text and Table S1 for the description of the covariates.

Covariate		Female	Inclusion Prob.	Male	Inclusion Prob.
Density	Sweden South	0.08 (–0.52 - 0.63)	0.34	**1.24 (0.68 - 1.79)**	1
	Norway North	–0.73 (–1.16 - 0.07)	0.99	–0.25 (–0.69 - 0.33)	0.09
	Norway South	0.18 (–0.37 - 0.71)	0.99	**0.94 (0.38 - 1.49)**	1
	Relict	**–0.61 (–1.05 - –0.21)**	1	**–0.78 (–1.23 - –0.28)**	1
	Relict × Sweden South*	**–1.23 (–2.08 - –0.40)**	0.30	–0.53 (–1.27 - 0.24)	0.14
	Relict × Norway North*	0.51 (–0.12 - 1.09)	0.21	0.30 (–0.65 - 1.10)	0.01
	Relict × Norway South*	**–1.35 (–1.99 - –0.70)**	0.99	**–1.07 (–1.87 - –0.26)**	0.62
	Ruggedness	**0.42 (0.25 - 0.59)**	1	0.18 (–0.06 - 0.38)	0.07
	Snow	0.03 (–0.27 - 0.27)	0.03	**0.35 (0.11 - 0.56)**	0.53
	Forest	**0.32 (0.12 - 0.52)**	0.72	0.14 (–0.08 - 0.35)	0.04
	Moose	**0.19 (0.02 - 0.35)**	0.17	**0.46 (0.31 - 0.63)**	1
	Settlements	**–1.61 (–2.66 - –0.79)**	1	**–2.27 (–3.41 - –1.33)**	1
Detection	Effort	**0.62 (0.53 - 0.71)**		**0.51 (0.44 - 0.59**)	
	Road	**0.19 (0.07 - 0.31)**		0.05 (–0.05 - 0.15)	
	Snow	–0.12 (–0.29 - 0.05)		**–0.22** (**–0.37** - **–0.08**)	
	Previous	0.12 (–0.06 - 0.30)		**0.61 (0.44 - 0.77)**	

1 Sources of heterogeneity in detectability

Increasing search effort for wolverine DNA (Table S1) increased the probability of detecting both female and male wolverines (Table S5). Contrary to our expectations (Table S5), the effect of distance from roads, a measure of site accessibility during noninvasive genetic sampling (NGS), was positive for females, while increasing snow-covered land during the sampling months reduced the probability of detecting males (Table S5). During NGS, many search tracks have to be surveyed using snowmobiles or by skiing away from the road network. There is also evidence that females avoid linear infrastructure more than males (May et al. 2006, 2012, Rauset et al. 2013), which may explain in part the need to search for their DNA farther away from roads. Likewise, while higher snow cover decreased male wolverine detectability, a detection in the previous year appeared to increase their chance to be detected in the following year (Table S5), suggesting a source of sampling bias during NGS (Gervasi et al. 2014, Bischof et al. 2020). Good conditions for snow tracking are determined locally in the field, and other factors, such as terrain ruggedness and availability and capacity of volunteers, may have also affected the performance of NGS, whereas the spatial covariates of baseline detection probability we included in the analysis explain the spatial variability in detection at the detector level (10×10 km). Also, it seems that the addition of data from the Norrbotten County in northern Sweden has a considerable influence on the estimated effect of the spatial covariates on baseline detection probability (Milleret et al. 2022). Thus, although we accounted for the main known spatial and individual-level factors affecting wolverine detectability, additional unexplained heterogeneity in detectability likely remains (Moqanaki et al. 2021, Dey et al. 2023).

2 References

Abramov, A. (2016). *Gulo gulo*. the iucn red list of threatened species, 2016: e. t9561a45198537.

Bischof, R., Milleret, C., Dupont, P., Chipperfield, J., Tourani, M., Ordiz, A., de Valpine, P., Turek, D., Royle, J. A., Gimenez, O., et al. (2020). Estimating and forecasting spatial population dynamics of apex predators using transnational genetic monitoring. *Proceedings of the National Academy of Sciences*, 117(48):30531–30538.

Bivand, R., Rundel, C., Pebesma, E., Stuetz, R., Hufthammer, K., Giraudoux, P., et al. (2019). rgeos: interface to geometry engine—open source ('geos'). 2019. *URL http://CRAN. R-project. org/package= rgeos. R package version 0.3-14.[p 388]*.

Chapron, G., Kaczensky, P., Linnell, J. D., Von Arx, M., Huber, D., Andrén, H., López-Bao, J. V., Adamec, M., Álvares, F., Anders, O., et al. (2014). Recovery of large carnivores in europe's modern human-dominated landscapes. *Science*, 346(6216):1517–1519.

Dey, S., Moqanaki, E., Milleret, C., Dupont, P., Tourani, M., and Bischof, R. (2023). Modelling spatially autocorrelated detection probabilities in spatial capture-recapture using random effects. *Ecological Modelling*, 479:110324.

Gervasi, V., Brøseth, H., Gimenez, O., Nilsen, E. B., and Linnell, J. D. (2014). The risks of learning: confounding detection and demographic trend when using count-based indices for population monitoring. *Ecology and Evolution*, 4(24):4637–4648.

May, R., Gorini, L., Van Dijk, J., Brøseth, H., Linnell, J., and Landa, A. (2012). Habitat characteristics associated with wolverine den sites in Norwegian multiple-use landscapes. *Journal of Zoology*, 287(3):195–204.

May, R., Landa, A., van Dijk, J., Linnell, J. D., and Andersen, R. (2006). Impact of infrastructure on habitat selection of wolverines *Gulo gulo*. *Wildlife Biology*, 12(3):285–295.

Meijer, J. R., Huijbregts, M. A., Schotten, K. C., and Schipper, A. M. (2018). Global patterns of current and future road infrastructure. *Environmental Research Letters*, 13(6):064006.

Milleret, C., Dupont, P., Moqanaki, E., Brøseth, H., Flagstad, Ø., Kleven, O., Kindberg, J., and Bischof, R. (2022). *Estimates of wolverine density, abundance, and population dynamics*

in Scandinavia, 2014–2022. The Faculty of Environmental Sciences and Natural Resource Management (MINA), Norwegian University of Life Sciences.

Moqanaki, E. M., Milleret, C., Tourani, M., Dupont, P., and Bischof, R. (2021). Consequences of ignoring variable and spatially autocorrelated detection probability in spatial capture-recapture. *Landscape Ecology*, 36(10):2879–2895.

Rauset, G. R., Mattisson, J., Andrén, H., Chapron, G., and Persson, J. (2013). When species' ranges meet: assessing differences in habitat selection between sympatric large carnivores. *Oecologia*, 172(3):701–711.

Article IV

Running Head: Scandinavian wolverine density dynamics

Environmental variability across space and time drives recolonization pattern of a historically persecuted large carnivore population

Ehsan Moqanaki[1,*], Cyril Milleret[1], Pierre Dupont[1], Soumen Dey[1], Jenny Mattisson[2], Henrik Brøseth[2], Malin Aronsson[3], Jens Persson[3], Petter Wabakken[4], Øystein Flagstad[2] & Richard Bischof[1]

1. Faculty of Environmental Sciences and Natural Resource Management, Norwegian University of Life Sciences, P.O. Box 5003, 1432 Ås, Norway
2. Norwegian Institute for Nature Research, PB 5685 Torgarden, 7485 Trondheim, Norway
3. Grimsö Wildlife Research Station, Department of Ecology, Swedish University of Agricultural Sciences, SE-730 91 Riddarhyttan, Sweden
4. Faculty of Applied Ecology, Agricultural Sciences and Biotechnology, Inland Norway, University of Applied Sciences, Campus Evenstad, NO-2480 Koppang, Norway

* Corresponding author – Email address: ehsan.moqanaki@gmail.com
https://orcid.org/0000-0001-7968-0210

Abstract

The spatial distribution of wildlife populations is not static. Intrinsic and extrinsic factors lead to spatiotemporal variation in population density and range. Yet, spatial dynamics in density and their drivers are rarely documented, due in part to the inherent difficulty of studying long-term population-level phenomena in situ at ecologically meaningful scales. We studied the spatiotemporal dynamics in population density of a recolonizing large carnivore, the wolverine *Gulo gulo*, across the Scandinavian Peninsula over nine years (2014 - 2022). We fitted open-population spatial capture-recapture models to noninvasively collected genetic data across the entire ≈600 000-km^2 range of the wolverine in Norway and Sweden to construct annual density surfaces. This approach allowed us to model changes in wolverine density and its sex-specific responses to landscape-level environmental determinants over time as the population continues to expand. The Scandinavian wolverine population is still in flux, as it recovers from centuries of persecution and severe range contraction. Our results revealed that as wolverines successfully recolonized many parts of their historical range in Scandinavia, the relationship between density and its spatial determinants, such as distance to the relict range, forest cover, and prey availability, has changed over time. We also found that temporal dynamics in the environmental effects (distance to the relict range, proportion of reindeer *Rangifer tarandus* areas, and free-ranging sheep *Ovis aries* numbers) differ between male and female wolverines. Our findings show that wildlife density surfaces and their determinants can be both vary across time.

Keywords: Density, Distribution, Large carnivores, Noninvasive monitoring, Population dynamics, Spatial capture-recapture, Transboundary wildlife populations, Wolverine

1 Introduction

Many wildlife populations have historically been persecuted by humans. Despite the widespread loss of wilderness, effective management and conservation measures have reversed the extinction trajectory for several wild species (Hoffmann et al. 2015, Bolam et al. 2021). Such successes have even been achieved in altered ecosystems, where natural habitats have transformed to a new state to meet human interests (Balmford 2012, Chapron et al. 2014). However, this means that recovering wildlife populations need to cope with new, drastically altered environments within their historical ranges. In the Anthropocene, land-use history and management interests are dominant forces that are transforming ecosystems and altering fundamental patterns of landscape heterogeneity (Yackulic et al. 2011, Newbold et al. 2016). Understanding how environmental factors determine the distribution and density of wildlife is a primary goal of ecology, and crucial to the adaptive management of recovering wildlife populations on today's human-dominated landscapes.

Recovery is often poorly defined for many wildlife populations. This is in part because of a long history of human-induced changes to populations and their habitats, as well as shifting baselines of population status (Lotze et al. 2011, Roman et al. 2015). In addition, different methodologies are used to reconstruct historical reference points for species persisting on human-altered landscapes. The uncertainty in wildlife population trajectory makes comparisons and impact assessments difficult and inhibits reliable inferences of population status. For some species, recovery starts from a relict range, where the species survived persecution, because either the relict range represented a core habitat of high suitability for the species or the last remnant population was pushed into a sub-optimal habitat with lower human pressure (i.e., habitat refuge; Kerley et al. 2012, Monsarrat et al. 2019). Recovery can also follow successful restoration attempts, where a small, but viable, population is established after reintroduction in suitable habitats (Seddon et al. 2014, Resende et al. 2020). Different factors contribute to the successful recovery and expansion of wildlife into currently unoccupied habitats. Biotic and abiotic environmental characteristics vary spatially and temporally and this variability influences species and ecological processes. Thus, each case of recovery has its own attributes and different lessons can be learned from studying them.

Population density estimation offers a significant advance in our ability to quantify and study species' spatial distribution and, thus, range limits (Royle et al. 2018). Reliable estimates of current population density and its determinants can also help in establishing baselines for forecasting the population status in the future under different scenarios. However, estimates of density are often of limited use for informing management, because (i) these estimates are usually derived from a portion of the population only and may not represent the status of the entire population and its responses to different environmental factors; (ii) they are often limited to a short temporal snapshot of the population, ignoring the fact that habitat-density relationships may change over time; and (iii) such estimates are rarely linked to fitness or demography (e.g., reproduction, sex ratio), limiting the understanding of the response to environmental factors or management actions. The current distribution and density of a wildlife population are the result of both historical and present-day factors that are constantly shaping that population (Sibly and Hone 2002, Monsarrat et al. 2019). Considering the temporal variation in drivers of population density can give us a more complete picture and improve our ability to forecast population responses to future changes in the environment and human intervention. This, in turn, requires long-term monitoring data at the population level and a spatially-explicit analytical framework that can handle the associated large computation demands (Chandler and Clark 2014, Hughes et al. 2017, Royle et al. 2018).

The Scandinavian wolverine *Gulo gulo* population has recolonized many parts of its historical range in Norway and Sweden after a long period of intense persecution (Landa et al. 2000, Flagstad et al. 2004, Chapron et al. 2014, Aronsson and Persson 2017). Once almost functionally extinct, a combination of protective measures, higher tolerance of wolverines by humans, and a surviving relict population along the alpine border with Norway and Sweden has contributed to the recovery of the wolverine in Scandinavia (Flagstad et al. 2004, Persson et al. 2015, Gervasi et al. 2019, Moqanaki et al. 2022). Like other members of the Scandinavian large carnivore guild, the wolverine is still intensely managed in many areas, especially in Norway, to control population size and expansion, and mitigate conflicts (Bischof et al. 2012, 2020, Hobbs et al. 2012, Aronsson and Persson 2017, Gervasi et al. 2019). Despite the transboundary nature of the wolverine population, management goals, laws, and regulations vary not only between Norway and Sweden, but also at the regional level within each country, partly as a result of

differences in the level of conflict (Gervasi et al. 2016, Aronsson and Persson 2017, Strand et al. 2019). On a national level, both countries aim for viable wolverine populations, but management differs substantially due to different livestock husbandry practices, conflict levels, and regulatory contexts. In Norway, increasing conflicts with sheep *Ovis aries*-farming industry and semidomesticated reindeer *Rangifer tarandus* husbandry have resulted in the abolishment of core conservation areas and introducing large annual hunting quota (Flagstad et al. 2004, Bischof et al. 2012, Hobbs et al. 2012, Tveraa et al. 2014, Strand et al. 2019). In contrast, EU member Sweden (Habitats Directive 1992), strictly protects wolverines throughout the country, and lethal control has until very recently only been permitted in areas with high levels of predation on semidomesticated reindeer (Persson et al. 2015, Aronsson and Persson 2017). Successful management of this conflict-prone large carnivore requires up-to-date information on the spatiotemporal impact of the factors shaping the spatial configuration of the population and its trajectory.

To identify the landscape-level effects of environmental conditions and changes in wolverine population density, we used a comprehensive data set of genetically identified wolverine individuals collected across their entire range in Norway and Sweden over nine years. We fitted open-population spatial capture-recapture (OPSCR) models (Gardner et al. 2010, Ergon and Gardner 2014, Bischof et al. 2016a, 2020) to quantify changes in the drivers of wolverine density, while controlling for imperfect and spatially and temporally variable sampling effort. We hypothesized that the relative contributions of wolverine density determinants have changed over the years, as the wolverine population continues to reclaim parts of its former range. There is evidence that today's wolverine density reflects in part the location of the relict range along the Norwegian-Swedish border, where the population survived human persecution by the 1970s and presumably started to recolonize its historical range (Flagstad et al. 2004, Gervasi et al. 2019, Moqanaki et al. 2022). Therefore, we hypothesized that a combination of historical and present-day environmental covariates has driven the wolverine density in Scandinavia over the past decade, and that the effects of these covariates have changed through time. Specifically, (i) the effect of distance from the relict range would be stronger in the first years, and, as the wolverine population expanded, the negative impact of distance from the relict range would become weaker. (ii) Traditionally, the wolverine is not considered a forest-dwelling species in

Scandinavia. Recently, however, the species has expanded into the boreal forest (i.e., taiga) and is now occupying areas that were not considered prime habitat during the last century (May et al. 2006, 2008b, Rauset et al. 2013, Aronsson and Persson 2017). We hypothesized that by successfully establishing themselves in the boreal forest, the positive effect of the forest on the wolverine density would become stronger over time.

2 Methods

2.1 Noninvasive genetic monitoring

We used noninvasive genetic sampling (NGS) data of the wolverine in Norway and Sweden collected between 2013/14 and 2021/22 from the Scandinavian large carnivore monitoring database (Rovbase 3.0; `www.rovbase.no` and `www.rovbase.se`). This is a comprehensive multinational database containing mostly structured annual sampling, but also opportunistically collected records of large carnivores by different means (e.g., noninvasive DNA samples, dead recoveries, public observations, livestock predation) over the past two decades (Brøseth et al. 2010, Gervasi et al. 2016). We used wolverine NGS data with coordinates, detection date, and individual and sex identification (i.e., genotypes) to construct spatially referenced individual detection histories for nine consecutive monitoring seasons (Royle et al. 2014).

Field staff of management authorities in Norway (The Norwegian Nature Inspectorate, SNO) and Sweden (County Administrative Boards) conduct extensive searches for carnivore signs and DNA across both countries at the level of carnivore management regions in Norway and counties in Sweden annually. In this study, we used the data collected between December 1 and June 30 as the sampling period in each year to retain most of the data (i.e., December 2013 – June 2014 to December 2021 – June 2022). We did not include samples that were suspected to be from wolverine cubs in spring (i.e., individuals born during the sampling season), based on the information collected from active natal dens (Landa et al. 1998b, Gervasi et al. 2016). Therefore, all individuals in our data set were at least 10 months old (i.e., born in February and detected the earliest in December). Collection of noninvasive DNA samples and protocols to process the samples in DNA labs are described in detail elsewhere (e.g., Flagstad et al. 2004, 2021, Brøseth et al. 2010, Gervasi et al. 2016, Ekblom et al. 2018).

Investigators searched for putative wolverine DNA material (e.g., scat, hair, secretion) mostly on snow and recorded their search effort by handheld GPS. These data contained detailed records of the spatial configuration and intensity of effort during the structured NGS. In addition to these structured searches, authorities and volunteers (e.g., hunters) also provided opportunistically collected DNA samples for analysis, but no direct measure of their search effort existed. Samples were then processed for DNA extraction and genotyping to identify species, individuals, and sex using a suite of nuclear DNA markers. The protocol has evolved through the sampling years, but the process ensures high-quality DNA data by using as many wolverine-specific markers as possible and controlling for genotyping errors using standard procedures (Ekblom et al. 2018, Flagstad et al. 2021). The genotypes from each sample were then used to identify wolverine individuals and their sex, which can be regarded as a genetic detection of that individual.

We defined the surveyed area as the entire contiguous land area in Norway and Sweden extending 100 km beyond the outermost wolverine DNA detections in our data set – i.e., noninvasive DNA samples and dead recoveries obtained during the nine-year sampling period for both sexes combined (58° 23′ - 71° 10′ N, 4° 45′ - 31° 03′ E; Fig. B1). To allow detection of individuals with activity centers located outside the detector grid (Efford 2004, 2011; see below), we placed a 60-km buffer around the designated 605 717-km^2 surveyed area to define the habitat (Fig. B1). We chose this buffer based on the average home-range radius of adult Scandinavian wolverines (Persson et al. 2010, Mattisson et al. 2011). This amounts to a buffer that is more than five times larger than the average estimated spatial scale parameter (σ, which accommodates individual variation in detection; see below) for male wolverines from this population (Bischof et al. 2020).

2.2 Open-population spatial capture-recapture analysis

Spatial capture-recapture (SCR) is an extension of capture-recapture models (Efford 2004, Borchers and Efford 2008, Royle et al. 2014, 2018). Conventional capture-recapture models use the information contained in a detection history of individuals from the target population (i.e., detections and nondetections) to estimate abundance and other ecological parameters, while accounting for imperfect detection – i.e., the fact that not all individuals from the target population are detected during sampling (Pollock et al. 1990, Royle et al. 2014). SCR models

include an additional spatial component, which exploits the spatial information contained in the detections. From the pattern of multiple individual detections and nondetections, SCR models estimate the relationship between individual detection probability and the distance from the center of their home range (Borchers and Efford 2008, Royle et al. 2014). SCR models estimate the latent activity centers of all individuals potentially available for detection, including those alive individuals that were never detected during sampling. Thus, SCR provides a spatially explicit estimate of abundance (i.e., density) in the study area.

A conventional SCR model can be used to estimate density, the effect of spatial and individual covariates on detection probability, and the effect of spatial covariates on density for a given point in time, with the assumption that the target population is demographically closed during sampling (i.e., no births, mortality, immigration or emigration). When data are collected over multiple years and the interest lies in understanding population changes, OPSCR models can be used to simultaneously estimate density and vital rates (e.g., recruitment and survival; Gardner et al. 2010, Ergon and Gardner 2014, Bischof et al. 2016a, Chandler et al. 2018). Thus, OPSCR models provide not only estimates of annual density and its determinants, but also estimates of the demographic parameters needed to predict changes in population dynamics and forecast the impact of management actions (Bischof et al. 2020). OPSCR models can also quantify temporal changes in the effect of spatial determinants of density, although such models are not widely used yet (Tourani 2022). In this study, we developed an OPSCR model for estimating temporal patterns in large-scale determinants of wolverine density in Scandinavia. We fitted separate OPSCR models in the Bayesian framework to the nine-year wolverine data time series for each sex, because of female-male differences in morphology, physiology, behavior, and ecology (Pasitschniak-Arts and Larivière 1995, Fisher et al. 2022). Our OPSCR model was composed of three sub-models for (1) density, (2) demography, and (3) detection.

2.2.1 Density submodel

This component of the OPSCR model describes the distribution of individual activity centers during each sampling year t. We used an inhomogeneous binomial point process with spatial intensity: $\lambda(s_t) = e^{\beta_t \mathbf{X}_t(s_t)}$ (Zhang et al. 2023), where s_t is a vector of spatial coordinates of activity centers, $\mathbf{X}_t$ is a vector of spatial covariate values evaluated at location s_t, and β_t is a

vector of associated regression coefficients for the monitoring season t. The intensity function λ conditions the placement of activity centers within each of the 20×20 km habitat grid cells s_t used in this analysis (1 809 cells in total) as a function of the covariates included. In this formulation, the number of activity centers is conditioned by data augmentation (Royle et al. 2007; see below), and the regression coefficients β_t represent the relative effects of the different covariates on wolverine density during the monitoring season t (Zhang et al. 2023). Thus, each spatial covariate is associated with a regression coefficient β_t that describes the relationship between wolverine density and the given covariate for each year of the sampling. To explore the temporal trends in the relative effects of the covariates on wolverine density (i.e., changes in regression coefficients), we modeled β_t as a linear function of time: $\beta_t = \beta_0 + \beta_1 \times Time_t$, where β_0 and β_1 are the intercept and slope, respectively, and $Time_t$ is a vector representing the monitoring period from the first monitoring season $t = 0$ to the last year $t = 8$. Thus, in this formulation, β_0 corresponds to the first monitoring season in December 2013 - June 2014.

Our OPSCR model did not include a movement model between years (Efford and Schofield 2022), because we were specifically interested in potential changes in the association between the environmental covariates and the overall distribution of wolverines in Scandinavia. This can be compared to the second-order of habitat selection (i.e., placement of home range; Johnson 1980). Although the selection of habitat by the wolverines could be restricted by their activity centers in the previous year, modeling interannual movement makes specific assumptions (Ergon and Gardner 2014, Efford and Schofield 2022) that may affect the interpretation of habitat-density relationships, given our study objectives. We, therefore, chose to model the location of individual activity centers independently from their locations in the previous years.

Considering the body of literature about the determinants of wolverine distribution, habitat selection, and density in Scandinavia and globally (Fisher et al. 2022 and references therein; Table C1), we selected eight spatial covariates that may have influenced population-level density of wolverine in Scandinavia (Table C1 and Fig. C1): (i) Distance from the relict range as a measure of recolonization history; (ii) Forest cover to describe land use, habitat productivity, prey availability, and shelter; (iii) Moose *Alces alces* harvest density as a proxy of moose density and carrion availability to describe food availability; (iv) Reindeer areas as a proxy of prey availability and risk of human-caused mortality; (v) Number of free-ranging sheep and

lambs as an alternative prey source for the wolverine and the risk of human-caused mortality; (vi) Terrain ruggedness as a measure of topographic heterogeneity, human disturbances, and refuge availability; (vii) Year-round snow cover to describe climate suitability and a proxy of vulnerability of prey to predation; and (viii) Human settlements index that describes human population density and associated disturbances.

Details on how the spatial covariates were obtained and prepared for the OPSCR analysis are provided in Table C1. We transformed all covariate raster layers from their original projections to the Universal Transverse Mercator (UTM zone 33N) and locally interpolated the raster values using the "bilinear" method of the `resample` function of the R package `raster` (Hijmans 2021) to match the 20×20 km habitat grid used in the OPSCR analysis (Fig. C1). We standardized all continuous covariates prior to their inclusion in the analysis to have a mean of zero and one unit standard deviation. Correlation among the covariates of wolverine density was generally low (Pearson's correlation coefficient $r < 0.7$; Fig. C2).

2.2.2 Demographic submodel

To model individual state transitions between years, we used a multistate formulation (Lebreton and Pradel 2002), where each individual life history is represented by a succession of up to three discrete states z_{it}: (a) "unborn": if the individual i has not been recruited in the population in a given year t; (b) "alive" if the individual is alive; and (c) "dead": if the individual has died. In this formulation, individuals can only be designated as either "unborn" ($z_{i,1} = 1$) or "alive" ($z_{i,1} = 2$) during the first year $t = 1$: $z_{i,1} \sim Categorical(1 - \gamma_1, \gamma_1, 0, 0)$, where γ_1 is the probability of being "alive" in the first year. During subsequent years, $t \geq 2$, $z_{i,t}$ is conditional on the state of individual i at $t - 1$. In our OPSCR model, (a) if $z_{i,t-1} = 1$, the "unborn" individual i can either transition to state 2 to be "alive" with probability γ_t (i.e., recruitment), or remain "unborn" with probability $1 - \gamma_t$, so that $z_{i,1} \sim Categorical(1 - \gamma_1, \gamma_t, 0, 0)$; (b) if $z_{i,t-1} = 2$, individual i can survive and remain "alive" with probability ϕ (i.e., survival), so it remains as $z_{i,t} = 2$. If the individual does not survive and dies, regardless of the cause of the death, it transitions to $z_{i,t-1} = 3$, with probability $1 - \phi$, so that $z_{i,t} \sim Categorical(0, \phi, 1 - \phi)$. All individuals with $z_{i,t-1} = 3$ remain in the state 3, the absorbing state, with probability 1.

To account for those alive individuals that were not detected during NGS, but were available

for inclusion in the population at a given year, we used a data augmentation approach (Royle et al. 2007). In this approach, the super-population size M consists of both detected and augmented individuals and is, therefore, chosen to be considerably larger than the total number of individuals ever alive in the population over the study period. Previous analyses of this population have shown relatively high detectability of wolverine individuals during NGS (Bischof et al. 2020, Milleret et al. 2022). Therefore, we set M to be large enough, while still facilitating the analysis by Markov chain Monte Carlo (MCMC) sampling. We then defined year-specific abundance by summing up the indicator variable for alive individuals: $N_t = \sum_{i=1}^{M} I(z_{i,t} = 2)$.

2.2.3 Observation submodel

In Scandinavia, noninvasive DNA material from alive wolverines is collected following two main processes. First, management authorities collect genetic samples and record the corresponding search effort during official searches ("structured sampling"). Second, DNA material can be voluntarily collected by the public (e.g., hunters), or by the authorities in an opportunistic manner, which means that search effort is not directly available ("unstructured sampling"). However, the available data do not allow for an unambiguous distinction of samples collected in a structured manner from those collected during unstructured monitoring. Following Milleret et al. (2022), we assigned samples to the structured sampling, if (i) the associated metadata confirmed it was collected by authorities in Norway or Sweden, and (ii) it was located within 500 m from a GPS search track that was recorded on the same day the sample was collected. We assigned all remaining wolverine DNA samples to the unstructured sampling.

We assumed a double-observation process to model structured and unstructured sampling separately. We used the conventional half-normal function to model detection probability (Royle et al. 2014), where the probability p of detecting individual i at detector j and time t decreases with distance d_{ijt} between the detector and the activity center s_{it}: $p_{1_{ijt}} = p_{0_{1_{ijt}}} \exp(-d_{ijt}^2/2\sigma_t^2)$ for structured sampling and $p_{2_{ijt}} = p_{0_{2_{ijt}}} \exp(-d_{ijt}^2/2\sigma_t^2)$ for unstructured sampling. Here, σ is the spatial scale parameter of the detection function, and p_{0_1} and p_{0_2} are the baseline detection probabilities for structured and unstructured sampling, respectively. We assumed that detections of wolverines as part of structured and unstructured searches could occur throughout most of the Scandinavian Peninsula (Fig. B1). We defined the search area as a grid of 10×10 km

cells extending 100 km beyond the outermost wolverine genetic detections collected during the nine-year period (Fig. B1). Multiple detections of the same individual were partially aggregated into 2×2 km sub-grids, allowing for up to 25 independent genetic encounters within one of the main detectors (Milleret et al. 2018). Encounter frequency Y of an individual at each main detector was assumed to follow a binomial distribution with a maximum sample size K of 100 for both the structured $Y_{1_{ijt}} \sim Binomial(K_j, p_{1_{ijt}} \times I(z_{it} = 2))$ and the unstructured sampling processes $Y_{2_{ijt}} \sim Binomial(K_j, p_{2_{ijt}} \times I(z_{it} = 2))$. Here, $I(z_{it} = 2)$ is an indicator function used to condition detection on the individual being alive. One exception was Norrbotten County in northern Sweden, which was comprehensively searched for wolverine DNA only during 2016/17, 2017/18, and 2018/19 monitoring seasons (Figs. B1 and B2). Therefore, we discarded the small number of opportunistic DNA samples collected in the remaining years and set baseline detection probability to zero ($p_{0_{1_{ijt}}} = 0$ and $p_{0_{2_{ijt}}} = 0$) for all j detectors located in Norrbotten County in the remaining six years.

Spatial and temporal variations in the probability to detect a wolverine sample during structured and unstructured sampling were assumed to be driven by different processes. For the structured sampling, we considered a different baseline detection probability for each jurisdiction $p_{0_{1_{County}}}$ ($County = 1, 2, \ldots, 8$) to account for possible regional differences in monitoring regimes (i.e., five carnivore management areas in Norway and three aggregated counties in Sweden; Bischof et al. 2020). Counties with very few wolverine DNA samples were merged with neighboring counties to ensure sufficient wolverine detections for estimating jurisdiction-specific baseline detection probability. In addition, we modeled the effects of two detector-level and one individual-level covariate that may influence the probability of wolverine detection (Bischof et al. 2020, Milleret et al. 2022). The detection-specific spatio-temporal covariates were: (i) Length of GPS search tracks in each sampling year to describe variation in search effort; and (ii) Snow cover during NGS months in each year to describe snow-tracking conditions. The snow-related detector-level covariate was different from that of the density covariate; the detection-related covariate was a spatio-temporal covariate describing the snow conditions during the sampling each year (Fig. C3), contrary to the density-related covariate that was a spatial covariate representing the average percentage of land covered with snow between 2008 and 2021 (Table C1). Further, we included one individual and temporal level covariate of detection to quantify

the effect of probability of being detected on subsequent occasions for alive wolverine individuals (Milleret et al. 2022). There is evidence that investigators may prefer to sample or search more intensively areas with a positive wolverine detection in the previous year (Gervasi et al. 2014). Thus, detection in the previous monitoring season may influence the probability of being detected during the focal sampling year (Bischof et al. 2020). This binary covariate indicates whether each detected wolverine individual was also genetically detected in the previous sampling year.

To model varying effort during unstructured sampling, we considered the following detector- and individual-specific covariates: (i) a binary spatio-temporal covariate describing the availability of a detector to be searched for wolverine DNA (see below); (ii) Snow cover during the sampling months in each year; (iii) Distance from the nearest road of any type as a measure of site accessibility for investigators; (iv) variation between Norway and Sweden as country-specific baseline detection probabilities; and (v) individual and temporal variation in detection linked with a previous detection. To create the binary spatio-temporal covariate as a proxy of opportunistic search effort, we used all observation records available from the Skandobs database (`www.skandobs.se` and `www.skandobs.no`) – a web application that allows the public to anonymously register their observations of wildlife (e.g., sightings, tracks, scats) in Scandinavia. We restricted this information to the wolverine NGS period in each year, excluding the wolverine NGS data used in the analysis (extraction date: 2022-06-09; Fig. C4). Although most of the Skandobs observations are not verified, they offer the best available proxy for spatio-temporal variation in the opportunistic search efforts for the wolverine DNA (Milleret et al. 2022). We assumed that an area that was opportunistically searched for any given carnivore species could have been potentially searched for wolverine DNA as well. We transformed all covariate layers to UTM zone 33N and locally interpolated the raster values to match the 10×10 km detector grid. We standardized all continuous covariates to have a mean of zero and one unit standard deviation prior to their inclusion in the analysis.

2.3 Model fitting

We fitted separate OPSCR models for male and female wolverines using MCMC with NIMBLE version 0.13.0 (de Valpine et al. 2017, 2022) and nimbleSCR version 0.2.1 (Bischof et al. 2022, Turek et al. 2021) in R 4.2.2 (R Core Team 2022). We ran three chains of 150 000

MCMC iterations for each model, including a 50 000-iterations burn-in period (i.e., 300 000 MCMC samples in total). We considered MCMC chains from each model run as converged when the Gelman-Rubin diagnostics ($\hat{R}$, Brooks and Gelman 1998) was less than or equal to 1.1 for all parameters and by visually inspecting the mixing of MCMC chains using trace plots.

We used the mean and associated 95% Bayesian credible interval limits (CI) to summarize posterior distributions of abundance for each sex. For the rest of the parameters, we report median and 95% CI. We obtained combined (female and male) parameter estimates by merging posterior samples from the sex-specific models. To obtain an estimate of abundance for a given habitat cell, we summed the number of predicted individual activity center locations of live individuals that fell within that cell for each iteration of the MCMC chains and generated a posterior distribution of abundance for that cell (i.e., "realized" density). In this fashion, we could also extract abundance estimates and the associated uncertainty around it for any spatial units of interest.

We constructed two types of annual sex-specific density maps: (i) a map of "expected" density based on the estimated intensity of the density point process and the estimated wolverine abundance, and (ii) a map of "realized" density based on the estimated locations of activity centers. The "expected" density in habitat cell s and time t was calculated as $N_t \lambda_{s_t} / \sum_{s=1}^{S} \lambda_{s_t}$ for each iteration of the MCMC. We then derived the mean and standard deviation of the expected density surface across iterations in each cell. The "realized" density maps were constructed by summing the number of individuals with their activity center in each habitat cell for each iteration of the MCMC, before calculating the mean and standard deviation across iterations in each cell.

3 Results

3.1 Noninvasive genetic monitoring

Within our designated study area across Norway and Sweden, management authorities annually conducted between 197 673 and 316 839 km of structured searches for wolverine DNA during the primary monitoring period (Fig. B2). Structured and unstructured sampling efforts and genetic analyses led to a total of 8 418 and 10 327 successfully genotyped female and male

wolverine samples, respectively, belonging to 1 360 female (median = 481, range = 337 - 529 individuals annually) and 1 190 male wolverines (median = 425, range = 274 - 471 individuals annually) over nine monitoring seasons. The annual number of detections (i.e., recaptures) per identified individual ranged from 1 to 11 for females and 1 to 12 for males (Fig. B1). On average, 58.9% (range = 54 - 65.3%) and 56.3% (range = 51.1 - 62.3%) of female and male wolverine individuals were detected during the structured sampling, respectively, and the rest by unstructured sampling.

3.2 Density determinants

A key driver of the wolverine density dynamics for both sexes in Scandinavia appeared to be the distance from the relict range along the alpine border between Norway and Sweden (Fig. 1). Over the nine years of the study, wolverine density consistently declined with increasing distance from the relict range for both sexes (median and 95% CI $\beta_{relict_{2014}} = -1.06$, -1.28 - -0.92 to $\beta_{relict_{2022}} = -0.81$, -0.95 - -0.67 [females], and from $\beta_{relict_{2014}} = -0.9$, -1.1 - -0.7 to $\beta_{relict_{2022}} = -0.86$, -1.05 - -0.68 [males]), but this effect was diminishing over time for females only (median and 95% CI $\beta_{1_{relict}} = 0.03$, 0.002 - 0.07 [female] and 0.01, -0.04 - 0.04 [male]; Figs. 1 and 2). At the same time, forest cover had an increasingly positive impact on wolverine densities for both sexes (median and 95% CI $\beta_{1_{forest}} = 0.03$, 0.001 - 0.05 [female] and 0.02, 0.001 - 0.06 [male]), changing from 0.11 (95% CI $\beta_{forest_{2014}} = 0$ - 0.27) to 0.37 (95% CI $\beta_{forest_{2022}} = 0.26$ - 0.48) for females, and from 0.19 (95% CI $\beta_{forest_{2014}} = 0.05$ - 0.33) to 0.39 (95% CI $\beta_{forest_{2022}} =$ 0.26 - 0.54) for males (Figs. 1 and 2).

Among the prey-related covariates, the impact of the moose density proxy was increasingly positive across the monitoring years for both sexes (median and 95% CI $\beta_{1_{moose}} = 0.04$, 0.02 - 0.07 [female] and 0.02, 0.001 - 0.04 [male]; Figs. 1 and 2), from 0.07 (95% CI $\beta_{moose_{2014}} = -0.04$ - 0.19) [female] and 0.33 (95% CI $\beta_{moose_{2014}} = 0.23$ - 0.44) [male] up to 0.43 (95% CI $\beta_{moose_{2022}} =$ 0.34 - 0.52) [female] and 0.51 (95% CI $\beta_{moose_{2022}} = 0.41$ - 0.6) [male]. In contrast, reindeer areas had an increasingly negative impact on male wolverines only (median and 95% CI $\beta_{1_{reindeer}} =$ 0, -0.02 - 0.03 [female], -0.03, -0.06 - -0.003; Figs. 1 and 2), changing from -0.01 (95% $\beta_{reindeer_{2014}} = -0.2$ - 0.11) [female] and -0.09 (95% $\beta_{reindeer_{2014}} = -0.25$ - 0.07) [male] to -0.02 (95% $\beta_{reindeer_{2022}} = -0.13$ - 0.09) [female] and -0.33 (95% $\beta_{reindeer_{2022}} = -0.44$ - -0.21) [male].

The impact of numbers of free-ranging sheep and lambs on male and female wolverine densities changed from positive to negative (median and 95% CI $\beta_{sheep_{2014}} = 0.09$, 0 - 0.19 to $\beta_{sheep_{2022}} = -0.07$, -0.16 - 0.02 [females], and from $\beta_{sheep_{2014}} = 0.05$, -0.04 - 0.15 to $\beta_{sheep_{2022}} = -0.01$, -0.12 - 0.08 [males]), but the negative trend was only significant for females (median and 95% CI $\beta_{1_{sheep}} = -0.02$, -0.04 - -0.002 [female], -0.01, -0.03 - 0.01 [male]; Figs. 1 and 2).

Terrain ruggedness had an overall positive impact for female density only (median and 95% CI $\beta_{TRI_{2014}} = 0.1$, -0.03 - 0.21 to $\beta_{TRI_{2022}} = 0.11$, -0.01 - 0.22 [females], and from $\beta_{TRI_{2014}} = -0.05$, -0.2 - 0.09 to $\beta_{TRI_{2022}} = 0.06$, -0.1 - 0.19 [males]), but with no significant trend for either sex over the years (median and 95% CI $\beta_{1_{TRI}} = 0.001$, -0.02 - 0.03 [female] and 0.01, -0.02 - 0.04 [male]; Figs. 1 and 2). The average year-round snow cover had an overall positive impact on the density of both sexes (median and 95% CI $\beta_{snow_{2014}} = 0.25$, 0.08 - 0.45 to $\beta_{snow_{2022}} = 0.34$, 0.2 - 0.49 [females], and from $\beta_{snow_{2014}} = 0.53$, 0.33 - 0.73 to $\beta_{snow_{2022}} = 0.3$, 0.15 - 0.52 [males]), but we observed no significant trend in its impact for either sex (median and 95% CI $\beta_{1_{snow}} = 0.01$, -0.03 - 0.05 [female] and -0.03, -0.07 - 0.02 [male]; Figs. 1 and 2).

The human settlements index had a substantial negative impact on both sexes, which remained significant over the monitoring years (median and 95% CI $\beta_{settlements_{2014}} = -2.53$, -3.63 - -1.52 to $\beta_{settlements_{2022}} = -2.14$, -2.88 - -1.53 [females], and from $\beta_{settlements_{2014}} = -3.24$, -4.27 - -1.97 to $\beta_{settlements_{2022}} = -2.66$, -3.46 - -1.95 [males]), with no apparent temporal trends (median and 95% CI $\beta_{1_{settlements}} = 0.06$, -0.15 - 0.23 [female] and 0.08, -0.16 - 0.25 [male]; Figs. 1 and 2).

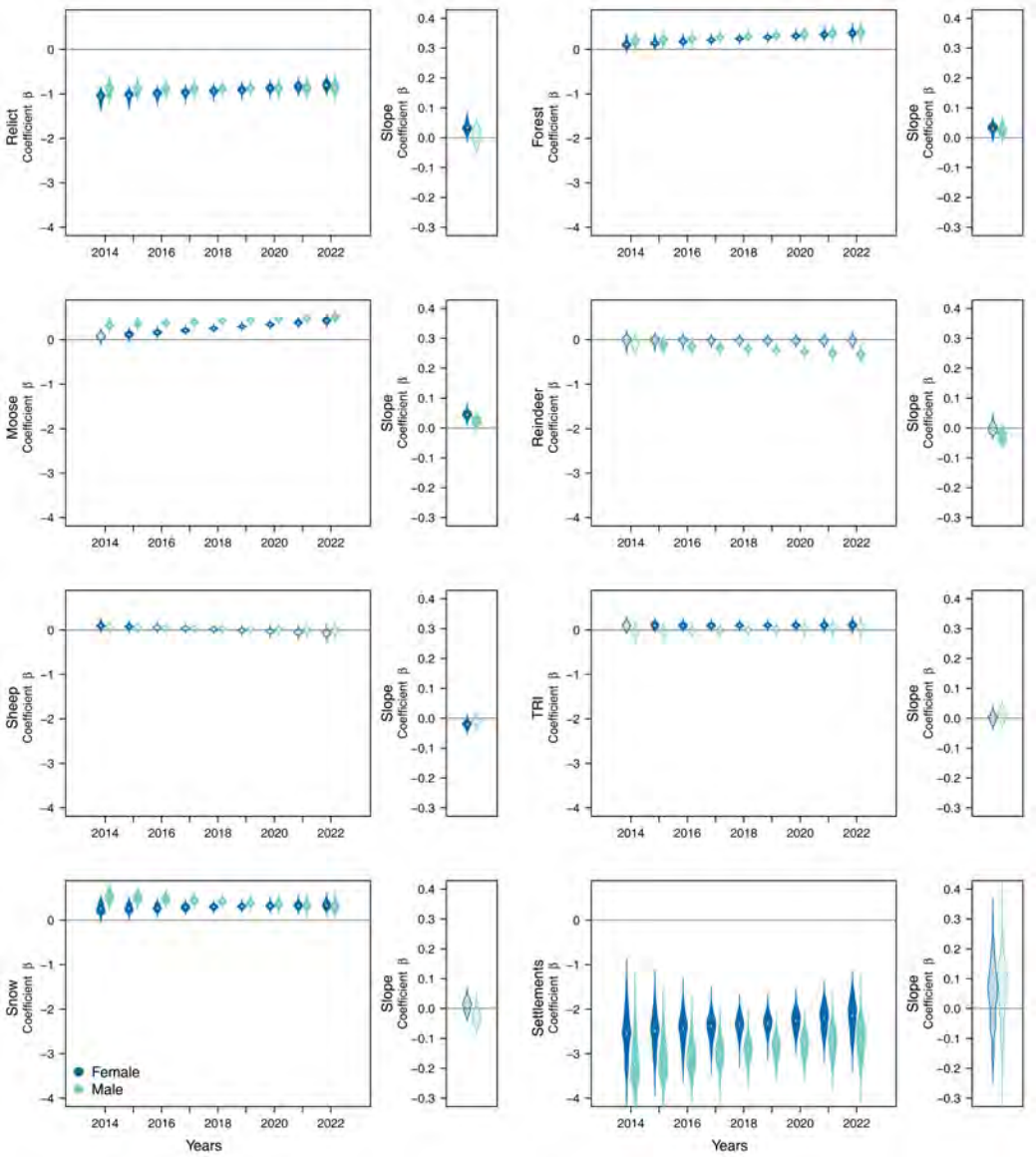

Figure 1: The effects of spatial covariates on female (blue) and male (green) wolverine *Gulo gulo* densities across their entire range in the Scandinavian Peninsula between 2013/14 and 2021/22 (i.e., nine monitoring seasons). The violin plots show median (white dots) and 95% Bayesian credible interval limits CI of regression coefficient β estimates to describe (i) annual regression coefficients (large boxes); and (ii) Slope: temporal changes in regression coefficients β (small boxes). The effect sizes are on exponential scale, and violins in which the 90% CI of the posteriors overlapped zero (i.e., no significant effects) are shown in transparent colors.

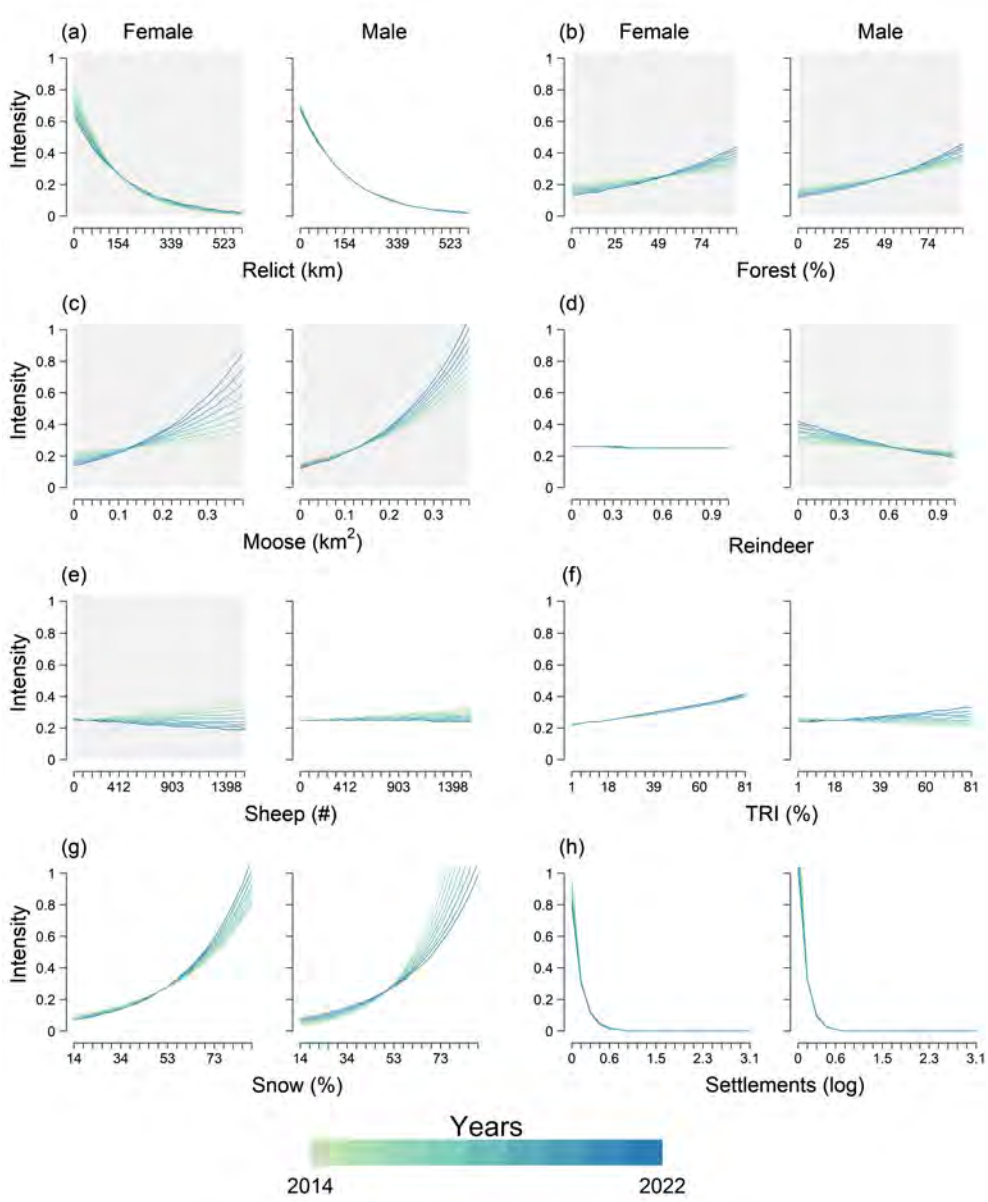

Figure 2: Intensity of the density point process for female and male wolverines *Gulo gulo* in the Scandinavia Peninsula between 2013/14 and 2021/22 (i.e., nine monitoring seasons), as a function of environmental covariates (Table C1): (a) Distance from the relic range; (b) Forest cover; (c) Moose *Alces alces* density proxy; (d) Proportion of reindeer *Rangifer tarandus* areas; (e) Numbers of free-ranging sheep *Ovis aries* and lambs; (f) Terrain Ruggedness Index, TRI; (g) Year-round snow cover; and (h) Human settlements index. Median predicted responses in each sampling year are represented by colored lines, where darker colors show more recent years. Gray background boxes mark predictions in which open-population spatial capture-recapture models estimated significant temporal changes in the effect of the covariates of wolverine density (see Fig. 1). The intensity of the point process reflects the relative distribution of individual activity centers, so that, for example, twice as many individuals are expected to have their activity center located in a place with an intensity of 0.8 compared to 0.4.

3.3 Detection determinants

The estimated annual baseline detection probabilities of male and female wolverines were qualitatively comparable during the nine-year sampling period, regardless of the two different sampling designs (i.e., structured and unstructured; Fig. D1). Median estimates across the eight management regions during the structured sampling was 0.01 (95% CI $p_{0_1} = 0 - 0.02$) for both sexes (Fig. D1). The overall estimated baseline detection probabilities during the unstructured sampling appeared to be slightly higher for both sexes in Norway than Sweden (median and 95% CI $p_{0_2} = 0.006, 0.003 - 0.009$ [Norway] and $0.004, 0.002 - 0.007$ [Sweden] for both female and males; Fig D1), which might be influenced by the exclusion of six years of wolverine data from the Norrbotten County in Sweden.

For the structured sampling, sampling effort, measured by the length of recorded search tracks, had an overall strong positive effect on the detection probability of both wolverine sexes (median and 95% CI $\beta_{effort_{structured}} = 0.46,\ 0.35 - 0.63$ [female] and $0.45,\ 0.37 - 0.55$ [male]; Fig. D2). The impact of snow cover during the sampling months on the structured sampling varied between years for each sex, but overall we did not detect a significant association between this covariate and wolverine detectability (median and 95% CI $\beta_{snow_{structured}} = 0.05,\ -0.23 - 0.39$ [female] and $0.07,\ -0.29 - 0.41$ [male]; Fig. D2). The pattern was qualitatively similar for the effect of snow cover during the unstructured sampling (median and 95% CI $\beta_{snow_{unstructured}} = 0.16,\ -0.2 - 0.67$ [female] and $0.12,\ -0.21 - 0.52$ [male]; Fig. D2). Likewise, we did not observe a consistent pattern in the impact of distance from the nearest road on wolverine detectability during the unstructured sampling (median and 95% CI $\beta_{road_{unstructured}} = -0.01,\ -0.3$ - 0.22 [female] and $-0.004,\ -0.25$ - 0.18 [male]; Fig. D2). The binary covariate representing a proxy of opportunistic search effort had an overall significant positive impact on the detectability of both sexes over years (median and 95% CI $\beta_{search_{unstructured}} = 0.76$, 0.24 - 1.31 [female] and 0.65, 0.25 - 1.03 [male]; Fig. D2).

The detection-level covariate explaining individual variation in wolverine detectability over the duration of the study (i.e., detection during the previous season) had a positive impact on both female and male wolverine detectability over most of the years during both structured and unstructured sampling, although the effect for males appeared to be slightly stronger (Fig. D2).

3.4 Abundance estimates and density surfaces

Our estimates of male and female wolverine abundance suggested an increasing trend over the nine-year monitoring period (Fig. D3), changing from 625 (95% CI N_{2014} = 565 - 689) females and 413 (95% CI N_{2014} = 368 - 465) males in the first year to 769 (95% CI N_{2022} = 704 - 824) females and 466 (95% CI N_{2022} = 433 - 501) males during the last monitoring season. The wolverine population was also estimated to be highly skewed towards females (F: M = 1.5 to 1.7 during the nine years; Fig. D3).

3.5 Other parameters

We estimated the median spatial scale parameter of the half-normal detection function σ during the monitoring period as 6.3 km (95% CI = 5.6 - 6.9) for female wolverines and 8.2 km (95% CI = 7.7 - 8.8) for males (Fig. D2). Recruitment probability was comparable between the sexes over the years (median and 95% CI = 0.1, 0.004 - 0.16 for females and males), but survival probability was higher for females (median and 95% CI = 0.80, 0.67 - 0.97 [female] and 0.68, 0.59 - 0.8 [male]; Fig. D4).

4 Discussion

A population in flux

Our study revealed evidence that the spatial configuration of the Scandinavian wolverine population, as well as the effect of some spatial determinants, has changed during the nine-year study period (Figs. 1 and 2). We found support for our main hypotheses that the wolverine population has expanded from the relict range towards the boreal forest. We also discovered that areas with more human settlements were consistently and negatively associated with wolverine density over the monitoring period (Fig. 1). To our knowledge, population-level determinants of density and temporal changes in their effects have rarely been quantified at such a large spatial extent (Tourani 2022). Given the comparatively short monitoring period for tracking dynamics of a large carnivore population (Smith et al. 2017, Fisher et al. 2022), our findings are particularly important as they reflect rapid changes in the spatial configuration of the

Scandinavian wolverine population. We specifically showed that although the shrinkage of the Scandinavian wolverine population possibly ended about half a century ago (Landa et al. 2000, Flagstad et al. 2004), the population is still in flux and a combination of natural and anthropogenic factors keep shaping population density. We also found support for sex-specific responses of the Scandinavian wolverine to the environmental determinants of density and differences in the temporal dynamics of their effects (Figs. 2 and 3).

Recovery from the relict range

The Scandinavian wolverine population probably started expanding from the relict range next to the Norwegian-Swedish border, after the management was changed from legal persecution to protection in 1968 and 1973, respectively (Landa et al. 2000, Flagstad et al. 2004). Currently, wolverines have successfully recolonized many areas across their historical range, pushing the expansion frontline significantly farther away from the relict range (Chapron et al. 2014, Gervasi et al. 2019, Bischof et al. 2020, Moqanaki et al. 2022). The fact that distance from the relict range still plays an important, but diminishing, role in driving the density of the wolverine for females (Figs. 1 and D1) reflects this ongoing population expansion. Wolverines are still managed in many areas by legal removal to control their population size and expansion (Aronsson and Persson 2017, Gervasi et al. 2019). Particularly in the southwest of Norway, no wolverines are currently tolerated (Strand et al. 2019), which together with the removal in southern reindeer areas, has probably limited recolonization in southern Sweden as well. Without such active interventions, we would expect the wolverine to have recolonized almost its entire historical range in the Scandinavian Peninsula by now. As long as the wolverine is not tolerated in some areas, proximity to the relict range – as the long-term core area of reproduction – will likely play an important role in shaping the population density and dynamics also in the future.

Moving into the forest

The Scandinavian wolverine was not considered a forest-dwelling species for a long time (May et al. 2006, 2008b), although wolverines inhabit the taiga further east in Russia and in North America (Glass et al. 2022). However, the Scandinavian population has successfully expanded into the boreal forest in recent decades (Aronsson and Persson 2017, Gervasi et al.

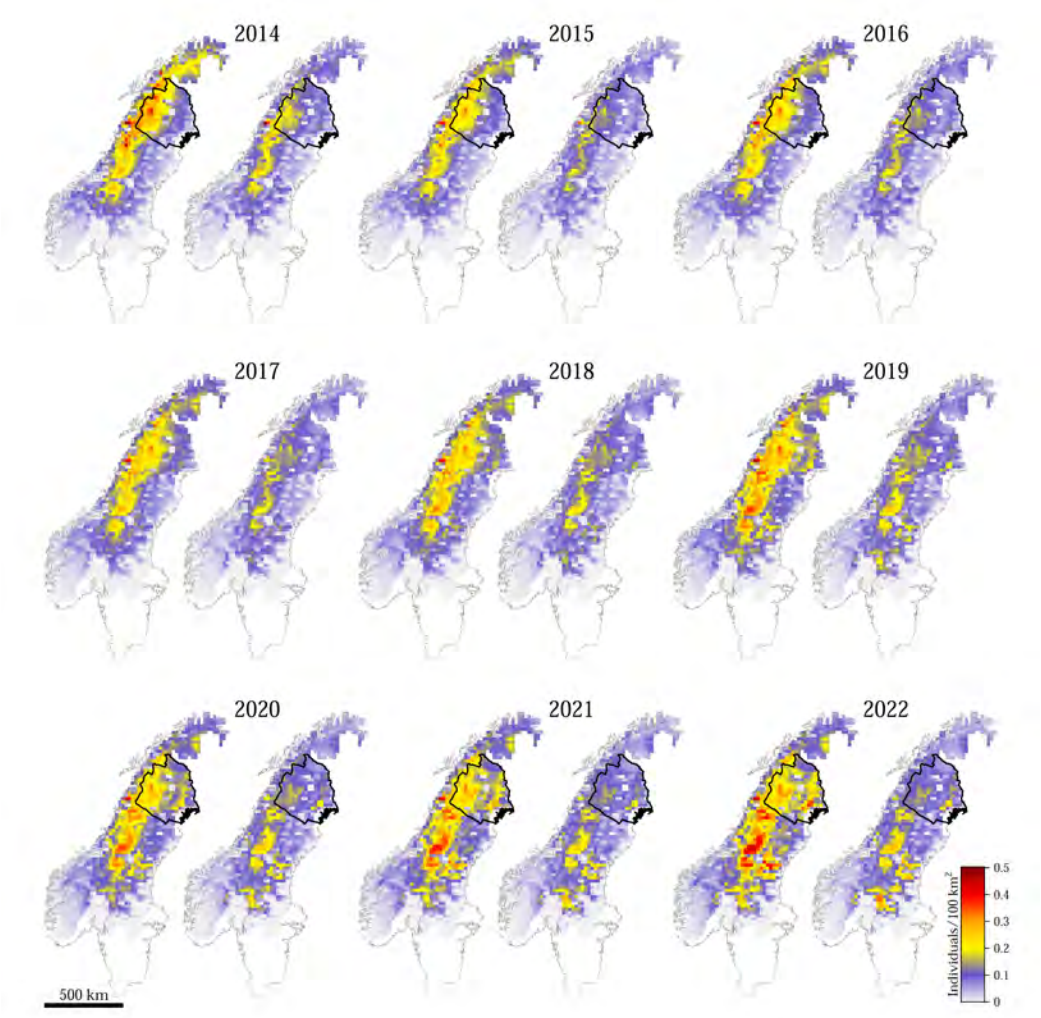

Figure 3: Expected density (individuals per 100 km^2) of female (left) and male (right) wolverine *Gulo gulo* in the Scandinavian Peninsula between December 2013 - June 2014 and December 2021 - June 2022 (i.e., nine monitoring seasons), as a function of environmental covariates included in this study. No comprehensive noninvasive genetic sampling was conducted in Norrbotten County in Sweden (polygons outlined in black) from 2013/14 to 2015/16 and from 2019/20 to 2021/22, which means that the results are solely based on the model prediction. The white area in each map represents areas that were not included in the analysis.

2019). Our results suggest that the positive influence of forest cover on the wolverine population is increasing over years (Fig. 2). The relationship of the wolverine with forest landscapes is studied in different areas in Scandinavia (e.g., May et al. 2008b, Rauset et al. 2013), but so far this has been done through telemetry of a few instrumented individuals from the population and with a bias towards northern alpine areas (Aronsson and Persson 2017, Aronsson et al. 2022).

The historical range maps of the wolverine distribution in Scandinavia suggest that the species was once present in both the alpine areas above the treeline and in the boreal forest, before the peak of their persecution in the mid-nineteenth and early twentieth centuries (Landa et al. 2000, Flagstad et al. 2004). The relict range along the Norwegian-Swedish border constitutes mostly rugged alpine areas with comparatively lower human density, but often with the boreal forest nearby (Haglund 1966, May et al. 2006, 2008b). Our understanding of the wolverine's habitat selection and preference is subsequently influenced by the relict range being the starting point of their modern expansion. This might also be the case for the current belief in the importance of spring snow for the wolverine (Brodie and Post 2010, Copeland et al. 2010, May et al. 2012), although the relevance of different measurements may vary spatially and temporally (Reinking et al. 2022). It is unclear whether Scandinavian wolverines prefer the rugged alpine areas to the low-elevation boreal forests. We revealed a positive effect of the proportion of forest, terrain ruggedness, and year-round snow cover on wolverine density but the magnitude of their impact differed slightly between sexes and varied over the course of the nine-year monitoring period (Fig. 2). Although GPS tracking provides a wealth of knowledge about fine-scale habitat selection of the tagged individuals, our study allowed us to reveal population-level determinants of wolverine density using noninvasive monitoring methods.

Large-scale impact of prey and management

We observed contrasting responses of wolverine densities to large-scale prey covariates (Fig. 2). Although higher male and female wolverine densities were associated with higher values of the moose density proxy and this association was becoming stronger over the past decade, the effects of the reindeer and free-ranging sheep proxies were either becoming negative or were insignificant (Figs. 2 and D1). These covariates probably interact with other environmental covariates, including the current zonal management plan that aims at controlling wolverine density in high conflict areas and restricting the expansion in southern Norway, to address the conflict with reindeer husbandry and sheep farming (Flagstad et al. 2004, May et al. 2008a, Aronsson and Persson 2017, Strand et al. 2019, Moqanaki et al. 2022).

Moose carrion, either carcasses left by other large carnivores (e.g., wolves *Canis lupus* and, to a lesser extent, bears *Ursus arctos*) or from natural and human-induced mortality (e.g., roadkill,

hunting baits, and slaughter remains), is an important food source for the wolverine in many areas, especially during winter (Van Dijk et al. 2008, Mattisson et al. 2011, 2016, Gomo et al. 2020, Aronsson et al. 2022). In addition, this covariate roughly reflects the forest productivity in Scandinavia. Thus, we expected the moose-related covariate to be important for wolverine density at the landscape scale. Free-ranging sheep and lambs are also only available to the wolverine in summer in Norway, with higher numbers in the southern areas (Fig. C1). This area is also where intense removal of wolverines occurs as a response to sheep predation (Flagstad et al. 2004, May et al. 2008a, Strand et al. 2019). Thus, this covariate not only represents seasonal sheep availability, but also a higher risk of human-induced mortality (Persson et al. 2009, 2015, Bischof et al. 2012, Hobbs et al. 2012, Rauset et al. 2016).

The semidomesticated reindeer is the most important food for the Scandinavian wolverine within reindeer grazing areas, which cover the majority of our study landscape (Landa et al. 1997, Hobbs et al. 2012, Tveraa et al. 2014, Mattisson et al. 2016; Fig. C1). Thus, we were expecting the reindeer proxy to be positively associated with wolverine density. However, we were not able to retain a reliable Scandinavian-wide data set for reindeer numbers with comparable resolution between Norway and Sweden. Instead, we used areas the semidomesticated reindeer are allowed to graze, plus the geographic range of the wild reindeer, as a proxy of reindeer presence (Table C1). However, the reindeer covariate did not reflect the spatial variation in reindeer availability across the study landscape (Fig. C1). This covariate had also a considerable negative correlation with distance from the relict range (Fig. C2), which probably masked some of the effects of the recolonization covariate. A further improvement of this study would be to develop and include a reliable spatial covariate for reindeer density in Scandinavia in the future, but it requires closer collaboration and further trust-building between authorities and Sámi reindeer herders in both countries.

Sex-specific responses to density determinants

Our findings suggest slightly different associations of, and trends in, male and female wolverine densities with the environmental determinants over the monitoring period (Fig. 2). Male and female behavioral differences with respect to their environment are documented (e.g., Landa et al. 1998a, May et al. 2006, Aronsson and Persson 2018, Kortello et al. 2019, Barrueto

et al. 2022), which may also reflect their responses to landscape-level determinants of density. For example, wolverines, like many solitary large carnivores, show intrasexual territoriality and males maintain larger home ranges that overlap with several females (Whitman et al. 1986, Landa et al. 1998a, Bischof et al. 2016b, Fisher et al. 2022). Long-distance dispersal is also more common in males, whereas females show stronger fidelity to their natal range (Vangen et al. 2001). Such different space-use strategies can result in variation in the relative importance of the environmental covariates of density for each sex. We expect these differences to scale up to population-level responses of wolverine sexes to their spatio-temporal determinants of density as we observed in this study (Fig. 2).

Density surface modeling to study population ecology

We attempted to untangle the changing impacts of historical and present-day environmental covariates in explaining trends in population density of the recovering Scandinavian wolverine population during the past decade (Fig. 3). We acknowledge that the reality is likely to be more complicated, when we consider that both the focal species' density surface and the environment are dynamic, some of the environmental covariates are probably interacting with each other, and the response of wolverine density to the change can be nonlinear. Therefore, it is important to note that the temporal trends in spatial covariate effects we observed (Fig. 2) can either reflect a difference in spatial covariate effects over time due to changes in the wolverine data (i.e., variation in population configuration across space), the effect of the covariates on wolverine density has changed during the nine-year study period (i.e., our hypotheses), or a combination of both. OPSCR analysis with a properly specified movement model (Efford and Schofield 2022) may help to disentangle some of these confounding factors. Such a model would allow us to differentiate between association with covariates to model density as a result of population expansion and active selection for a given covariate, depending on what is available within the movement range of the individual.

Implications for monitoring and management

Insights from our study can contribute to analyses of long-term, large-scale monitoring data of wildlife using OPSCR models. For the Scandinavian wolverine population, future research

on spatio-temporal determinants of population density should consider intra- and interspecific interactions, in addition to the abiotic and biotic covariates we considered. Particularly, exploitation competition with co-occurring large carnivores over resources (wolves, lynx *Lynx lynx*, and bears), are known drivers of wolverine resource partitioning and is, therefore, an important area of research in the future (Van Dijk et al. 2008, Mattisson et al. 2011, Rauset et al. 2013, Khalil et al. 2014, Scrafford et al. 2017). There is also evidence of negative density dependence (Sæther et al. 2005, Brøseth et al. 2010) and compensatory immigration (Gervasi et al. 2019) in wolverine population dynamics in Scandinavia. Further understanding of how vital rates interact with population density to shape the Scandinavian wolverine population is a crucial component of informed management. Accounting for spatially variable vital rates in the future (Milleret et al. 2023) could allow us to quantify potential density-dependent effects on the survival and recruitment of wolverines and further increase our understanding of the population-level determinants of density for Scandinavian wolverines and facilitate population forecasts.

5 Conclusions

The wolverine in Scandinavia has been long associated with pristine wilderness, which is juxtaposed with the near absence of impact-free areas in modern-day Scandinavia (May et al. 2008b, 2012, Watson et al. 2016). The recovery of the Scandinavian wolverine population highlights the fact that even such an elusive and quintessential symbol of wilderness can live and recover in an increasingly human-altered environment (Linnell et al. 2000, 2001, Chapron et al. 2014, Cretois et al. 2021). However, the population expansion poses new challenges for society and managers, as wolverines are recolonizing areas with free-ranging sheep and reindeer husbandry, where they have been absent for decades. Since wolverine recovery has occurred in a heterogeneous landscape shared by two countries with different national and regional management goals, legislation, and obligations, a diversity of management strategies that involve methods to mitigate conflict with farmers and herders, and increase tolerance towards the wolverine is essential for the long-term survival of the population. Our findings reiterate the importance of the collection of long-term and coordinated monitoring data and adaptive management of recovering wildlife populations on transboundary landscapes (Bischof

et al. 2016b, 2020, Gervasi et al. 2016, 2019).

Data Availability Statement

Wolverine detections used in this study are available through the database Rovbase 3.0 at www.rovbase.no or www.rovbase.se. Data and R scripts of the open-population spatial capture-recapture analysis will be deposited upon acceptance at: https://github.com/eMoqanaki.

Authors' contributions

R.B., E.M., C.M., and P.D. conceived and designed the study; H.B. gave access to the genetic data; J.M., H.B., M.A., J.P., P.W., and Ø.F. provided context on wolverine ecology, monitoring, and management in Scandinavia; E.M. led the analysis with contributions from C.M., P.D., R.B., S.D., J.M., and H.B.; E.M. wrote the first draft and all co-authors discussed and contributed to the manuscript; all authors gave final approval for publication.

Competing interests

We declare we have no interests which might be perceived as posing a conflict or bias.

Funding

This study was funded by the Research Council of Norway through the project WildMap (NFR 286886), the Norwegian Environment Agency (Miljødirektoratet), and the Swedish Environmental Protection Agency (Naturvårdsverket). J.M., H.B., and Ø.F. were supported by the NINA basic funding, financed by The Research Council of Norway (project no. 160022/F40).

Acknowledgments

We thank all contributors to the Scandinavian large carnivore monitoring database Rovbase 3.0. J. Kindberg gave access to the moose harvest data used in this study.

References

Aronsson, M. and Persson, J. (2017). Mismatch between goals and the scale of actions constrains adaptive carnivore management: the case of the wolverine in Sweden. *Animal Conservation*, 20(3):261–269.

Aronsson, M. and Persson, J. (2018). Female breeding dispersal in wolverines, a solitary carnivore with high territorial fidelity. *European Journal of Wildlife Research*, 64(1):1–10.

Aronsson, M., Persson, J., Zimmermann, B., Märtz, J., Wabakken, P., Heeres, R., and Nordli, K. (2022). *Järven i Inre Skandinaviens skogslandskap–områdesbruk, födoval och reproduktion.* SLU Grimsö forskningsstation Institutionen för ekologi Sveriges lantbruksuniversitet.

Balmford, A. (2012). *Wild hope: on the front lines of conservation success.* University of Chicago Press.

Barrueto, M., Forshner, A., Whittington, J., Clevenger, A. P., and Musiani, M. (2022). Protection status, human disturbance, snow cover and trapping drive density of a declining wolverine population in the Canadian Rocky Mountains. *Scientific Reports*, 12(1):1–15.

Bischof, R., Brøseth, H., and Gimenez, O. (2016a). Wildlife in a politically divided world: insularism inflates estimates of brown bear abundance. *Conservation Letters*, 9(2):122–130.

Bischof, R., Gregersen, E. R., Brøseth, H., Ellegren, H., and Flagstad, Ø. (2016b). Noninvasive genetic sampling reveals intrasex territoriality in wolverines. *Ecology and Evolution*, 6(5):1527–1536.

Bischof, R., Milleret, C., Dupont, P., Chipperfield, J., Tourani, M., Ordiz, A., de Valpine, P., Turek, D., Royle, J. A., Gimenez, O., et al. (2020). Estimating and forecasting spatial population dynamics of apex predators using transnational genetic monitoring. *Proceedings of the National Academy of Sciences*, 117(48):30531–30538.

Bischof, R., Nilsen, E. B., Brøseth, H., Männil, P., Ozoliņš, J., and Linnell, J. D. (2012). Implementation uncertainty when using recreational hunting to manage carnivores. *Journal of Applied Ecology*, 49(4):824–832.

689 Bischof, R., Turek, D., Milleret, C., Ergon, T., Dupont, P., Dey, S., Zhang, W., and de Valpine,
690 P. (2022). *nimbleSCR: Spatial Capture-Recapture (SCR) Methods Using 'nimble'*.

691 Bolam, F. C., Mair, L., Angelico, M., Brooks, T. M., Burgman, M., Hermes, C., Hoffmann, M.,
692 Martin, R. W., McGowan, P. J., Rodrigues, A. S., et al. (2021). How many bird and mammal
693 extinctions has recent conservation action prevented? *Conservation Letters*, 14(1):e12762.

694 Borchers, D. L. and Efford, M. G. (2008). Spatially explicit maximum likelihood methods for
695 capture-recapture studies. *Biometrics*, 64(2):377–385.

696 Brodie, J. F. and Post, E. (2010). Nonlinear responses of wolverine populations to declining
697 winter snowpack. *Population Ecology*, 52:279–287.

698 Brooks, S. P. and Gelman, A. (1998). General methods for monitoring convergence of iterative
699 simulations. *Journal of Computational and Graphical Statistics*, 7(4):434–455.

700 Brøseth, H., Flagstad, Ø., Wärdig, C., Johansson, M., and Ellegren, H. (2010). Large-scale
701 noninvasive genetic monitoring of wolverines using scats reveals density dependent adult
702 survival. *Biological Conservation*, 143(1):113–120.

703 Chandler, R. B. and Clark, J. D. (2014). Spatially explicit integrated population models.
704 *Methods in Ecology and Evolution*, 5(12):1351–1360.

705 Chandler, R. B., Engebretsen, K., Cherry, M. J., Garrison, E. P., and Miller, K. V. (2018).
706 Estimating recruitment from capture–recapture data by modelling spatio-temporal variation
707 in birth and age-specific survival rates. *Methods in Ecology and Evolution*, 9(10):2115–2130.

708 Chapron, G., Kaczensky, P., Linnell, J. D., Von Arx, M., Huber, D., Andrén, H., López-Bao,
709 J. V., Adamec, M., Álvares, F., Anders, O., et al. (2014). Recovery of large carnivores in
710 Europe's modern human-dominated landscapes. *Science*, 346(6216):1517–1519.

711 Copeland, J., McKelvey, K., Aubry, K., Landa, A., Persson, J., Inman, R., Krebs, J., Lofroth,
712 E., Golden, H., Squires, J., et al. (2010). The bioclimatic envelope of the wolverine (*Gulo*
713 *gulo*): do climatic constraints limit its geographic distribution? *Canadian Journal of Zoology*,
714 88(3):233–246.

715 Cretois, B., Linnell, J. D., Van Moorter, B., Kaczensky, P., Nilsen, E. B., Parada, J., and Rød,
716 J. K. (2021). Coexistence of large mammals and humans is possible in europe's anthropogenic
717 landscapes. *iScience*, 24(9):103083.

718 de Valpine, P., Paciorek, C., Turek, D., Michaud, N., Anderson-Bergman, C., Obermeyer, F.,
719 Wehrhahn Cortes, C., Rodrìguez, A., Temple Lang, D., and S., P. (2022). *NIMBLE User*
720 *Manual*. R package manual version 0.13.0.

721 de Valpine, P., Turek, D., Paciorek, C. J., Anderson-Bergman, C., Lang, D. T., and Bodik, R.
722 (2017). Programming with models: writing statistical algorithms for general model structures
723 with NIMBLE. *Journal of Computational and Graphical Statistics*, 26(2):403–413.

724 Efford, M. (2004). Density estimation in live-trapping studies. *Oikos*, 106(3):598–610.

725 Efford, M. G. (2011). Estimation of population density by spatially explicit capture–recapture
726 analysis of data from area searches. *Ecology*, 92(12):2202–2207.

727 Efford, M. G. and Schofield, M. R. (2022). A review of movement models in open population
728 capture–recapture. *Methods in Ecology and Evolution*, 13(10):2106–2118.

729 Ekblom, R., Brechlin, B., Persson, J., Smeds, L., Johansson, M., Magnusson, J., Flagstad, Ø.,
730 and Ellegren, H. (2018). Genome sequencing and conservation genomics in the Scandinavian
731 wolverine population. *Conservation Biology*, 32(6):1301–1312.

732 Ergon, T. and Gardner, B. (2014). Separating mortality and emigration: modelling space use,
733 dispersal and survival with robust-design spatial capture–recapture data. *Methods in Ecology*
734 *and Evolution*, 5(12):1327–1336.

735 Fisher, J. T., Murray, S., Barrueto, M., Carroll, K., Clevenger, A. P., Hausleitner, D., Harrower,
736 W., Heim, N., Heinemeyer, K., Jacob, A. L., et al. (2022). Wolverines (*Gulo gulo*) in a
737 changing landscape and warming climate: A decadal synthesis of global conservation ecology
738 research. *Global Ecology and Conservation*, page e02019.

739 Flagstad, Ø., Hedmark, E., Landa, A., Brøseth, H., Persson, J., Andersen, R., Segerström, P.,
740 and Ellegren, H. (2004). Colonization history and noninvasive monitoring of a reestablished
741 wolverine population. *Conservation Biology*, 18(3):676–688.

Flagstad, Ø., Kleven, O., Brandsegg, H., Spets, M. H., Eriksen, L. B., Andersskog, I. P. Ø., Johansson, M., Ekblom, R., Ellegren, H., and Brøseth, H. (2021). DNA-basert overvåking av den skandinaviske jervebestanden 2020. Technical report, Norsk institutt for naturforskning (NINA).

Gardner, B., Reppucci, J., Lucherini, M., and Royle, J. A. (2010). Spatially explicit inference for open populations: estimating demographic parameters from camera-trap studies. *Ecology*, 91(11):3376–3383.

Gervasi, V., Brøseth, H., Gimenez, O., Nilsen, E. B., and Linnell, J. D. (2014). The risks of learning: confounding detection and demographic trend when using count-based indices for population monitoring. *Ecology and Evolution*, 4(24):4637–4648.

Gervasi, V., Brøseth, H., Gimenez, O., Nilsen, E. B., Odden, J., Flagstad, Ø., and Linnell, J. D. (2016). Sharing data improves monitoring of trans-boundary populations: the case of wolverines in central Scandinavia. *Wildlife Biology*, 22(3):95–106.

Gervasi, V., Linnell, J. D., Brøseth, H., and Gimenez, O. (2019). Failure to coordinate management in transboundary populations hinders the achievement of national management goals: the case of wolverines in Scandinavia. *Journal of Applied Ecology*, 56(8):1905–1915.

Glass, T. W., Magoun, A. J., Robards, M. D., and Kielland, K. (2022). Wolverines (*Gulo gulo*) in the Arctic: Revisiting distribution and identifying research and conservation priorities amid rapid environmental change. *Polar Biology*, 45(9):1465–1482.

Gomo, G., Rød-Eriksen, L., Andreassen, H. P., Mattisson, J., Odden, M., Devineau, O., and Eide, N. E. (2020). Scavenger community structure along an environmental gradient from boreal forest to alpine tundra in Scandinavia. *Ecology and Evolution*, 10(23):12860–12869.

Habitats Directive (1992). Council directive 92/43/eec of 21 may 1992 on the conservation of natural habitats and of wild fauna and flora. *Official Journal of the European Union*, 206:7–50.

Haglund, B. (1966). *De stora rovdjurens vintervanor*. Swedish Sportsmen's Association = Svenska Jägareförbundet.

Hijmans, R. J. (2021). *raster: Geographic Data Analysis and Modeling*. R package version 3.4-13.

Hobbs, N. T., Andren, H., Persson, J., Aronsson, M., and Chapron, G. (2012). Native predators reduce harvest of reindeer by Sámi pastoralists. *Ecological Applications*, 22(5):1640–1654.

Hoffmann, M., Duckworth, J., Holmes, K., Mallon, D. P., Rodrigues, A. S., and Stuart, S. N. (2015). The difference conservation makes to extinction risk of the world's ungulates. *Conservation Biology*, 29(5):1303–1313.

Hughes, B. B., Beas-Luna, R., Barner, A. K., Brewitt, K., Brumbaugh, D. R., Cerny-Chipman, E. B., Close, S. L., Coblentz, K. E., De Nesnera, K. L., Drobnitch, S. T., et al. (2017). Long-term studies contribute disproportionately to ecology and policy. *BioScience*, 67(3):271–281.

Johnson, D. H. (1980). The comparison of usage and availability measurements for evaluating resource preference. *Ecology*, 61(1):65–71.

Kerley, G. I., Kowalczyk, R., and Cromsigt, J. P. (2012). Conservation implications of the refugee species concept and the European bison: king of the forest or refugee in a marginal habitat? *Ecography*, 35(6):519–529.

Khalil, H., Pasanen-Mortensen, M., and Elmhagen, B. (2014). The relationship between wolverine and larger predators, lynx and wolf, in a historical ecosystem context. *Oecologia*, 175(2):625–637.

Kortello, A., Hausleitner, D., and Mowat, G. (2019). Mechanisms influencing the winter distribution of wolverine *Gulo gulo luscus* in the southern Columbia Mountains, Canada. *Wildlife Biology*, 2019(1):1–13.

Landa, A., Lindén, M., Kojola, I., et al. (2000). *Action plan for the conservation of wolverines in Europe (Gulo gulo)*. Council of Europe.

Landa, A., Strand, O., Linnell, J. D., and Skogland, T. (1998a). Home-range sizes and altitude selection for arctic foxes and wolverines in an alpine environment. *Canadian Journal of Zoology*, 76(3):448–457.

795 Landa, A., Strand, O., Swenson, J. E., and Skogland, T. (1997). Wolverines and their prey in
796 southern Norway. *Canadian Journal of Zoology*, 75(8):1292–1299.

797 Landa, A., Tufto, J., Franzén, R., Bø, T., Lindén, M., and Swenson, J. E. (1998b). Active
798 wolverine *Gulo gulo* dens as a minimum population estimator in Scandinavia. *Wildlife Biology*,
799 4(3):159–168.

800 Lebreton, J.-D. and Pradel, R. (2002). Multistate recapture models: modelling incomplete
801 individual histories. *Journal of Applied Statistics*, 29(1-4):353–369.

802 Linnell, J. D., Swenson, J. E., and Andersen, R. (2000). Conservation of biodiversity in
803 Scandinavian boreal forests: large carnivores as flagships, umbrellas, indicators, or keystones?
804 *Biodiversity & Conservation*, 9:857–868.

805 Linnell, J. D., Swenson, J. E., and Anderson, R. (2001). Predators and people: conservation
806 of large carnivores is possible at high human densities if management policy is favourable.
807 *Animal Conservation*, 4(4):345–349.

808 Lotze, H. K., Coll, M., Magera, A. M., Ward-Paige, C., and Airoldi, L. (2011). Recovery of
809 marine animal populations and ecosystems. *Trends in Ecology & Evolution*, 26(11):595–605.

810 Mattisson, J., Persson, J., Andren, H., and Segerström, P. (2011). Temporal and spatial
811 interactions between an obligate predator, the Erasian lynx (*Lynx lynx*), and a facultative
812 scavenger, the wolverine (*Gulo gulo*). *Canadian Journal of Zoology*, 89(2):79–89.

813 Mattisson, J., Rauset, G. R., Odden, J., Andrén, H., Linnell, J. D., and Persson, J. (2016).
814 Predation or scavenging? prey body condition influences decision-making in a facultative
815 predator, the wolverine. *Ecosphere*, 7(8):e01407.

816 May, R., Gorini, L., Van Dijk, J., Brøseth, H., Linnell, J., and Landa, A. (2012). Habitat
817 characteristics associated with wolverine den sites in Norwegian multiple-use landscapes.
818 *Journal of Zoology*, 287(3):195–204.

819 May, R., Landa, A., van Dijk, J., Linnell, J. D., and Andersen, R. (2006). Impact of infrastructure
820 on habitat selection of wolverines *Gulo gulo*. *Wildlife Biology*, 12(3):285–295.

May, R., van Dijk, J., Forland, J. M., Andersen, R., and Landa, A. (2008a). Behavioural patterns in ewe–lamb pairs and vulnerability to predation by wolverines. *Applied Animal Behaviour Science*, 112(1-2):58–67.

May, R., Van Dijk, J., Wabakken, P., Swenson, J. E., Linnell, J. D., Zimmermann, B., Odden, J., Pedersen, H. C., Andersen, R., and Landa, A. (2008b). Habitat differentiation within the large-carnivore community of Norway's multiple-use landscapes. *Journal of Applied Ecology*, 45(5):1382–1391.

Milleret, C., Dey, S., Dupont, P., Brøseth, H., Turek, D., de Valpine, P., and Bischof, R. (2023). Estimating spatially variable and density-dependent survival using open-population spatial capture–recapture models. *Ecology*, 104(2):e3934.

Milleret, C., Dupont, P., Brøseth, H., Kindberg, J., Royle, J. A., and Bischof, R. (2018). Using partial aggregation in spatial capture recapture. *Methods in Ecology and Evolution*, 9(8):1896–1907.

Milleret, C., Dupont, P., Moqanaki, E., Brøseth, H., Flagstad, Ø., Kleven, O., Kindberg, J., and Bischof, R. (2022). *Estimates of wolverine density, abundance, and population dynamics in Scandinavia, 2014–2022*. The Faculty of Environmental Sciences and Natural Resource Management (MINA), Norwegian University of Life Sciences.

Monsarrat, S., Jarvie, S., and Svenning, J.-C. (2019). Anthropocene refugia: integrating history and predictive modelling to assess the space available for biodiversity in a human-dominated world. *Philosophical Transactions of the Royal Society B*, 374(1788):20190219.

Moqanaki, E., Milleret, C., Dupont, P., Brøseth, H., and Bischof, R. (2022). Wolverine density distribution reflects past persecution and current management in Scandinavia. *bioRxiv*.

Newbold, T., Hudson, L. N., Arnell, A. P., Contu, S., De Palma, A., Ferrier, S., Hill, S. L., Hoskins, A. J., Lysenko, I., Phillips, H. R., et al. (2016). Has land use pushed terrestrial biodiversity beyond the planetary boundary? a global assessment. *Science*, 353(6296):288–291.

Pasitschniak-Arts, M. and Larivière, S. (1995). *Gulo gulo*. *Mammalian Species*, (499):1–10.

Persson, J., Ericsson, G., and Segerström, P. (2009). Human caused mortality in the endangered Scandinavian wolverine population. *Biological Conservation*, 142(2):325–331.

Persson, J., Rauset, G. R., and Chapron, G. (2015). Paying for an endangered predator leads to population recovery. *Conservation Letters*, 8(5):345–350.

Persson, J., Wedholm, P., and Segerström, P. (2010). Space use and territoriality of wolverines (*Gulo gulo*) in northern Scandinavia. *European Journal of Wildlife Research*, 56(1):49–57.

Pollock, K. H., Nichols, J. D., Brownie, C., and Hines, J. E. (1990). Statistical inference for capture-recapture experiments. *Wildlife Monographs*, pages 3–97.

R Core Team (2022). *R: A Language and Environment for Statistical Computing*. R Foundation for Statistical Computing, Vienna, Austria.

Rauset, G. R., Andrén, H., Swenson, J. E., Samelius, G., Segerström, P., Zedrosser, A., and Persson, J. (2016). National parks in northern Sweden as refuges for illegal killing of large carnivores. *Conservation Letters*, 9(5):334–341.

Rauset, G. R., Mattisson, J., Andrén, H., Chapron, G., and Persson, J. (2013). When species' ranges meet: assessing differences in habitat selection between sympatric large carnivores. *Oecologia*, 172(3):701–711.

Reinking, A. K., Højlund Pedersen, S., Elder, K., Boelman, N. T., Glass, T. W., Oates, B. A., Bergen, S., Roberts, S., Prugh, L. R., Brinkman, T. J., et al. (2022). Collaborative wildlife–snow science: Integrating wildlife and snow expertise to improve research and management. *Ecosphere*, 13(6):e4094.

Resende, P., Viana-Junior, A., Young, R., De Azevedo, C., et al. (2020). A global review of animal translocation programs. *Animal Biodiversity and Conservation*, 43(2):221–232.

Roman, J., Dunphy-Daly, M. M., Johnston, D. W., and Read, A. J. (2015). Lifting baselines to address the consequences of conservation success. *Trends in Ecology & Evolution*, 30(6):299–302.

Royle, J. A., Chandler, R. B., Sollmann, R., and Gardner, B. (2014). *Spatial Capture-Recapture*. Academic Press, Waltham.

Royle, J. A., Dorazio, R. M., and Link, W. A. (2007). Analysis of multinomial models with unknown index using data augmentation. *Journal of Computational and Graphical Statistics*, 16(1):67–85.

Royle, J. A., Fuller, A. K., and Sutherland, C. (2018). Unifying population and landscape ecology with spatial capture–recapture. *Ecography*, 41(3):444–456.

Sæther, B.-E., Engen, S., Persson, J., Brøseth, H., Landa, A., and Willebrand, T. (2005). Management strategies for the wolverine in Scandinavia. *The Journal of Wildlife Management*, 69(3):1001–1014.

Scrafford, M. A., Avgar, T., Abercrombie, B., Tigner, J., and Boyce, M. S. (2017). Wolverine habitat selection in response to anthropogenic disturbance in the western Canadian boreal forest. *Forest Ecology and Management*, 395:27–36.

Seddon, P. J., Griffiths, C. J., Soorae, P. S., and Armstrong, D. P. (2014). Reversing defaunation: restoring species in a changing world. *Science*, 345(6195):406–412.

Sibly, R. M. and Hone, J. (2002). Population growth rate and its determinants: an overview. *Philosophical Transactions of the Royal Society of London. Series B: Biological Sciences*, 357(1425):1153–1170.

Smith, J. E., Lehmann, K. D., Montgomery, T. M., Strauss, E. D., and Holekamp, K. E. (2017). Insights from long-term field studies of mammalian carnivores. *Journal of Mammalogy*, 98(3):631–641.

Strand, G.-H., Hansen, I., de Boon, A., and Sandström, C. (2019). Carnivore management zones and their impact on sheep farming in Norway. *Environmental Management*, 64(5):537–552.

Tourani, M. (2022). A review of spatial capture–recapture: Ecological insights, limitations, and prospects. *Ecology and Evolution*, 12(1):e8468.

Turek, D., Milleret, C., Ergon, T., Brøseth, H., Dupont, P., Bischof, R., and De Valpine, P. (2021). Efficient estimation of large-scale spatial capture–recapture models. *Ecosphere*, 12(2):e03385.

900 Tveraa, T., Stien, A., Brøseth, H., and Yoccoz, N. G. (2014). The role of predation and
901 food limitation on claims for compensation, reindeer demography and population dynamics.
902 *Journal of Applied Ecology*, 51(5):1264–1272.

903 Van Dijk, J., Gustavsen, L., Mysterud, A., May, R., Flagstad, Ø., Brøseth, H., Andersen, R.,
904 Andersen, R., Steen, H., and Landa, A. (2008). Diet shift of a facultative scavenger, the
905 wolverine, following recolonization of wolves. *Journal of Animal Ecology*, 77(6):1183–1190.

906 Vangen, K. M., Persson, J., Landa, A., Andersen, R., and Segerström, P. (2001). Characteristics
907 of dispersal in wolverines. *Canadian Journal of Zoology*, 79(9):1641–1649.

908 Watson, J. E., Shanahan, D. F., Di Marco, M., Allan, J., Laurance, W. F., Sanderson, E. W.,
909 Mackey, B., and Venter, O. (2016). Catastrophic declines in wilderness areas undermine
910 global environment targets. *Current Biology*, 26(21):2929–2934.

911 Whitman, J. S., Ballard, W. B., and Gardner, C. L. (1986). Home range and habitat use by
912 wolverines in southcentral Alaska. *The Journal of Wildlife Management*, pages 460–463.

913 Yackulic, C. B., Sanderson, E. W., and Uriarte, M. (2011). Anthropogenic and environmental
914 drivers of modern range loss in large mammals. *Proceedings of the National Academy of*
915 *Sciences*, 108(10):4024–4029.

916 Zhang, W., Chipperfield, J. D., Illian, J. B., Dupont, P., Milleret, C., de Valpine, P., and Bischof,
917 R. (2023). A flexible and efficient Bayesian implementation of point process models for spatial
918 capture–recapture data. *Ecology*, 104(1):e3887.

Supplementary Information

Moqanaki E, Milleret C, Dupont P, Dey S, Mattisson J, Brøseth H, Aronsson M, Persson J, Wabakken P, Flagstad Ø, and Bischof R. Environmental variability across space and time drives recolonization pattern of a historically persecuted large carnivore population.

Appendix A: Data and R scripts

Appendix B: Annual wolverine genetic detections and search effort

Appendix C: Covariates of wolverine density and detectability

Appendix D: Sex-specific estimates by open-population spatial capture-recapture models

Appendix E: Annual wolverine density surfaces

1 APPENDIX A

Data and R scripts of the open-population spatial capture-recapture analysis will be deposited upon acceptance at: https://github.com/eMoqanaki

2 APPENDIX B

Map of the study landscape in the Scandinavian Peninsula, including the sampling grid and a 60-km habitat buffer around it, where annual noninvasive genetic sampling of the wolverine *Gulo gulo* was conducted at the population level in Norway and Sweden:

- Figure B1: Number of independent genetic detections of female and male wolverines assigned to detectors considered in this study
- Figure B2: GPS-recorded search effort by management authorities during the structured noninvasive genetic sampling of the wolverine between 2013/2014 and 2021/2022

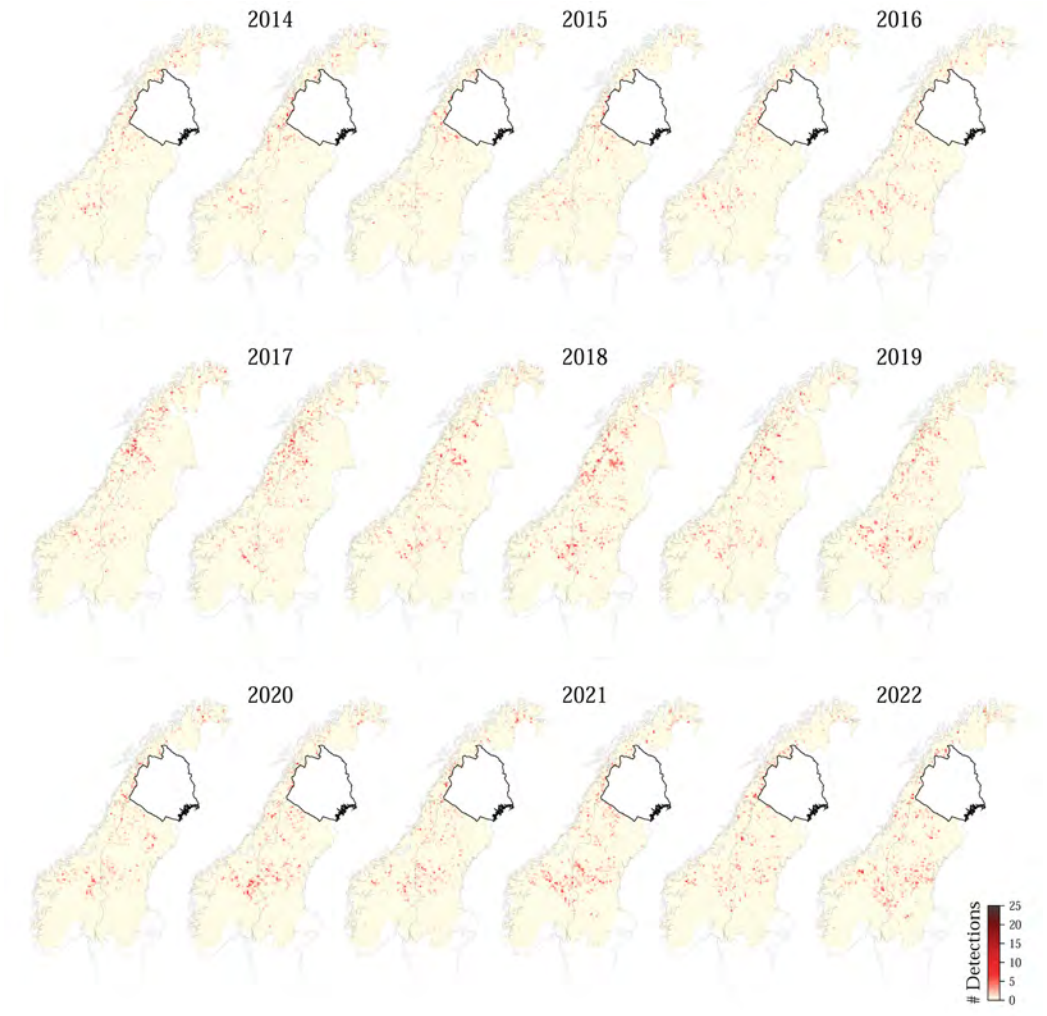

Figure B1: Number of genetic detections of female and male wolverines *Gulo gulo* assigned to each 10×10-km detector cell across the entire species range in Norway and Sweden. The colored polygon shows the detector grid and the white polygon around it is a buffer of 60 km. We used noninvasive genetic samples of wolverines collected between December 1 and June 30 each year from 2013/14 until 2021/22 (i.e., nine monitoring seasons), with unambiguous individual and sex identity, collection date, and location. A partial aggregation approach was followed to assign multiple genetic detections of the same individual to, first, 2×2-km subgrids, which then allowed up to 25 independent genetic detections of each individual within each of 10×10-km main detectors. Norrbotten County in northern Sweden was comprehensively searched for wolverine noninvasive DNA in three monitoring seasons only, and the county was not included in the remaining six years (blank polygon). See the main text for details.

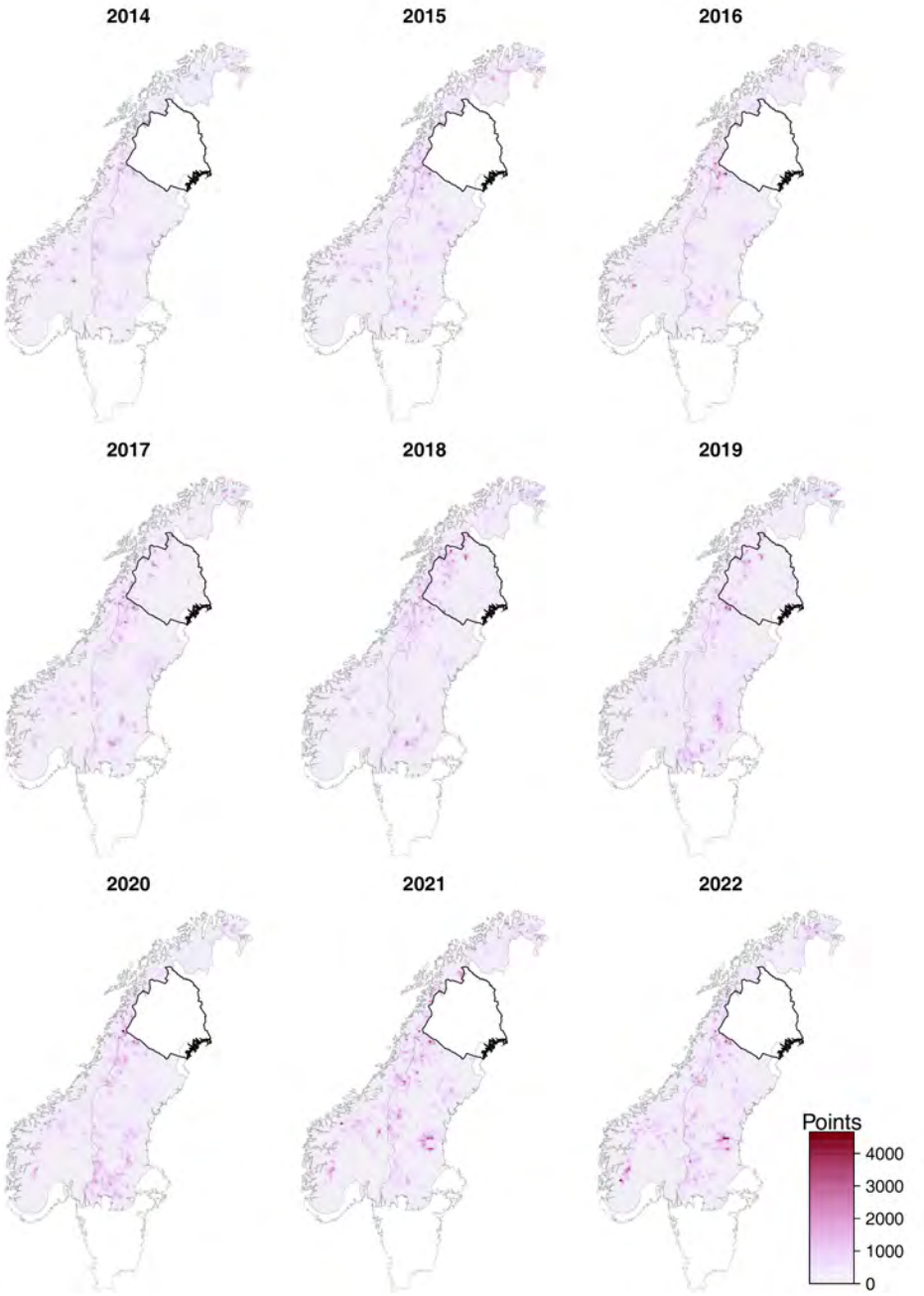

Figure B2: Search effort during the structured noninvasive genetic sampling of the wolverines *Gulo gulo* in Norway and Sweden collected between December 1 and June 30 each year from 2013/14 until 2021/22 (i.e., nine monitoring seasons). GPS-recorded search tracks within each main detector of 10×10 km were simplified to one point per 500 m of tracks and the number of points per detector cell was used as a measure of varying effort to quantify wolverine detectability. Norrbotten County in northern Sweden was comprehensively searched for wolverine noninvasive DNA in three monitoring seasons only, and the county was not included in the remaining six years (blank polygon).

3 APPENDIX C

Description and spatial depiction of covariates of density and detection probability used to model temporal variation in the determinants of wolverine *Gulo gulo* density in the Scandinavian Peninsula in this study:

- Figure C1: Spatial covariates of wolverine density
- Figure C2: Correlation plot of the spatial covariates of density
- Figure C3: The snow covariate used to model wolverine detectability
- Figure C4: The covariate used to model wolverine detectability during unstructured sampling
- Table C1: Details about the spatial covariates of wolverine density

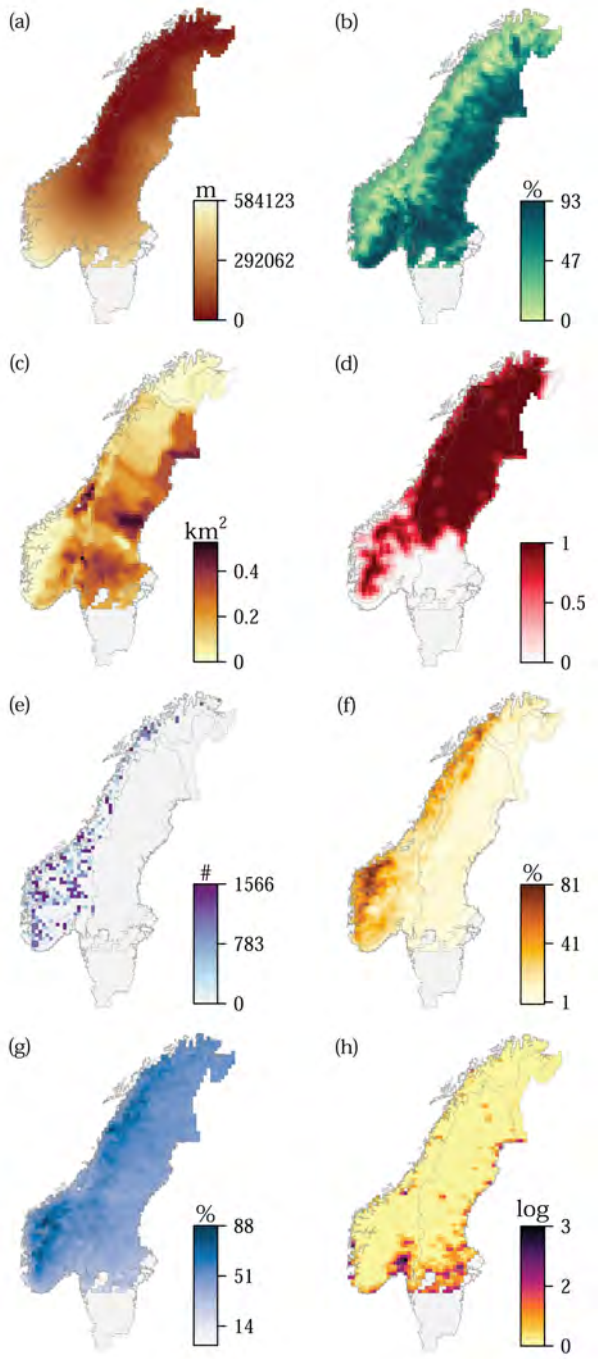

Figure C1: Spatial covariates used to explain spatiotemporal variation in wolverine *Gulo gulo* density in the Scandinavian Peninsula during nine monitoring seasons between 2013/14 and 2021/22: (a) Distance from the relict range; (b) Forest percentage; (c) Moose *Alces alces* density proxy; (d) Proportion of reindeer *Rangifer tarandus* areas; (e) Number of free-ranging sheep *Ovis aries* and lambs; (f) Terrain Ruggedness Index, TRI; (g) Year-round snow cover; and (f) Human settlements index. All covariates were resampled to the habitat resolution at 20×20 km and standardized prior to analysis. See Table C1 for details.

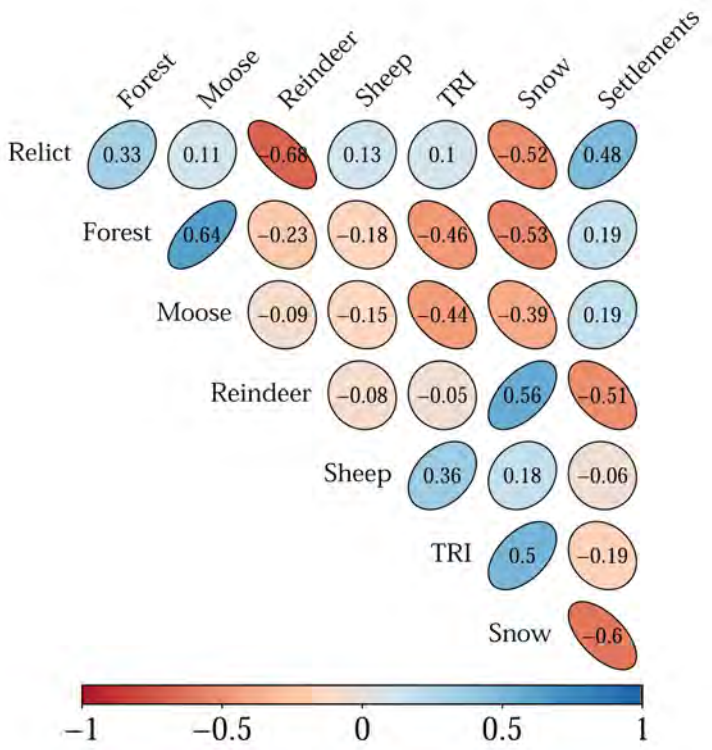

Figure C2: Correlation matrix of spatial covariates (n = 8; Fig. C1) used in the sex-specific open-population spatial capture-recapture models for quantifying variation in density of wolverine *Gulo gulo* in the Scandinavian Peninsula during nine monitoring seasons between 2013/14 and 2021/22. Blue color indicates a positive correlation, whereas red color represents a negative correlation. Darker shades of blue and red indicate high collinearity among the covariates of wolverine density. The size and orientation of the convexes denote the extent and direction of the correlation between the covariates, respectively, with those facing left signifying a negative correlation. Table C1 describes the covariates of wolverine density across the designated study landscape in Norway and Sweden.

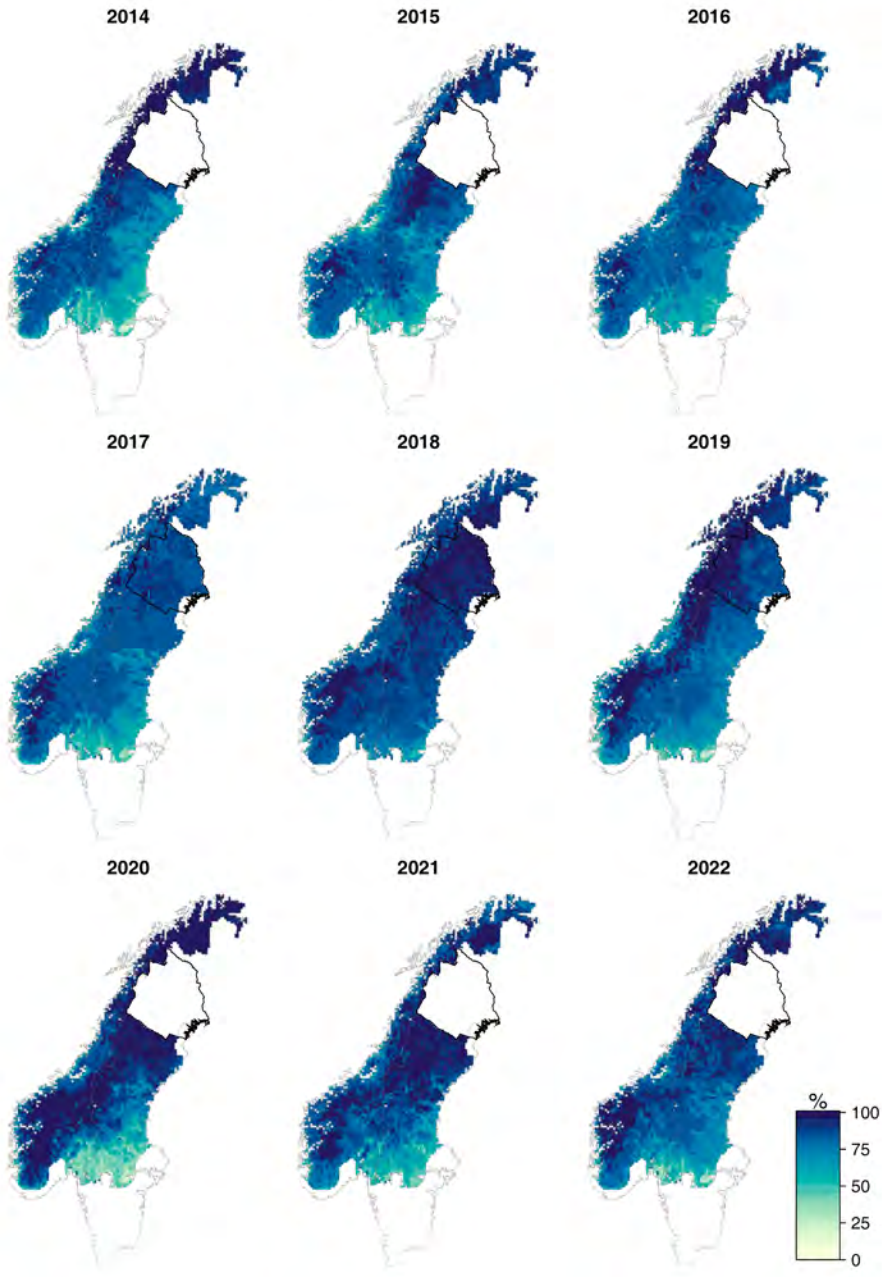

Figure C3: The average percentage of snow-covered land from December 1 to June 30 each year between 2013/14 and 2021/22 as a spatial covariate of wolverine *Gulo gulo* detectability. The covariate was resampled to the main detector resolution at 10 × 10 km and standardized prior to analysis. Norrbotten County in northern Sweden was comprehensively searched for wolverine noninvasive DNA in three monitoring seasons only, and the county was not included in the remaining six years (blank polygon).

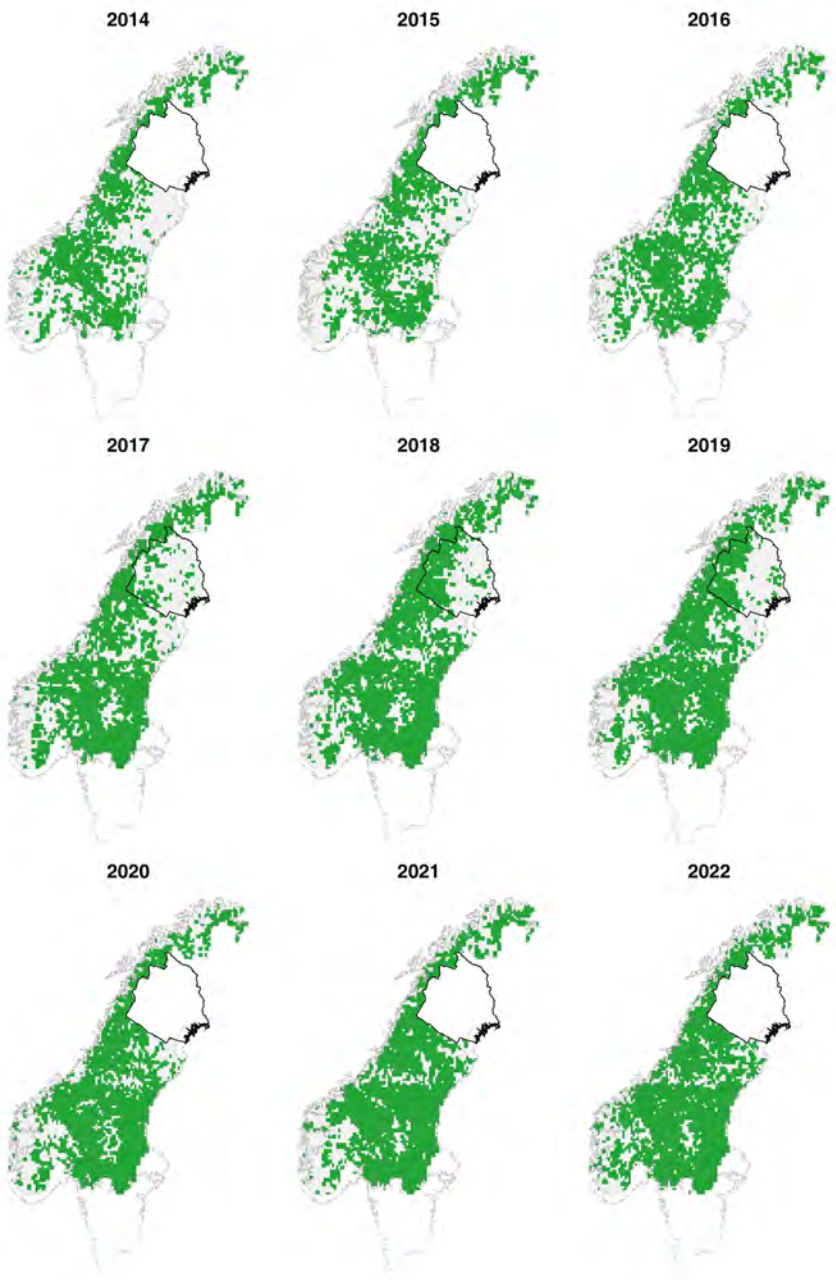

Figure C4: Covariate used to account for spatiotemporal variation in the unstructured sampling of the wolverine *Gulo gulo* in the Scandinavian Peninsula from December 1 to June 30 each year between 2013/14 and 2021/22. Green 10 × 10-km cells represent areas with at least one carnivore record from the website Rovbase (rovbase.no or rovbase.se), excluding the wolverine samples used in this study, or observation records from Skandobs (skandobs.no and skandobs.se) during the nine-year monitoring seasons. Norrbotten County in northern Sweden was comprehensively searched for wolverine noninvasive DNA in three monitoring seasons only, and the county was not included in the remaining six years (blank polygon).

Table C1: Description, the rationale for inclusion, expected effects, and source and native spatial resolution of spatial covariates of density used to model trends in the density distribution of the wolverine *Gulo gulo* in the Scandinavian Peninsula between 2013/14 and 2021/22 (i.e., nine monitoring seasons)

Covariate	Description and Rationale	Effects	Resolution and Source
Relict	Distance (m) from the relict range represents the founding population and recolonization history. The relict range describes roughly the area occupied by the Fennoscandian wolverine population at its lowest point in modern times (Landa et al. 2000, Flagstad et al. 2004, Chapron et al. 2014, Lansink et al. 2020, Moqanaki et al. 2022).	–	Calculated using the wolverine's geographic distribution range in the 1970s as reported by Landa et al. (2000) and shapefiles by Chapron et al. (2014). All 20×20 km habitat cells falling within the relict range area were assigned a value of 0. We then computed the Euclidean distance for all habitat cells to the nearest cell with a value of 0 using the `distance` function of the R package `raster` (Hijmans 2021).
Forest	Percentage of forest habitat was a measure of land use, habitat productivity, greater wild prey availability, and cover (May et al. 2006, 2008, Inman et al. 2012, Scrafford et al. 2017, Cimatti et al. 2021)	+	The average forest proportion between 1992 and 2015 was obtained using the ESA-CCI Land Cover project (categories 50, 60, 61, 62, 70, 71, 72, 80; `www.esa-landcover-cci.org`) at about 176×176 m
Moose	An index of moose *Alces alces* density using hunting bags, representing habitat productivity and a proxy for moose carrion availability (Van Dijk et al. 2008, Ueno et al. 2014, Mattisson et al. 2016, van der Veen et al. 2020, Aronsson et al. 2022)	+	Calculated at 2×2 km resolution using the averaged numbers of moose harvested/km^2 at the level of municipalities and hunting management units in Norway and Sweden, respectively, from 2012 to 2020 (statistisk sentralbyrå 2021, Älgdata 2021a,b). Because of a lack of data from the buffer area in Finland and Russia, we replaced missing values with mean values of the 48 neighborhood cells using the `focal` function of the R package `raster` (Hijmans 2021)
Reindeer	Proportion of the general areas of occurrence for wild and semidomesticated reindeer *Rangifer tarandus*, representing a proxy of reindeer availability and greater risk of human-induced mortality (Van Dijk et al. 2008, Persson et al. 2009, 2015, Andrén et al. 2011, Hobbs et al. 2012, Mattisson et al. 2016, Aronsson and Persson 2017)	+/–	Calculated at 20×20 km using polygons of the geographic range of the wild reindeer in Norway (Miljødirektoratet 2022) and polygons of the districts of the semidomesticated reindeer in both countries (Norway: Kilden - Reindrift, `www.nibio.no`; Sweden: Länsstyrelserna 2000 - 2008, `www.sweco.se`). We created "soft" edges, where the cell-based covariate values gradually increased from 0 (no reindeer area) to 1 (reindeer area), to account for the edge effect and for practical reasons (Moqanaki et al. 2022). The reindeer districts do not necessarily represent the year-round presence of the reindeer, but include the different seasonal grazing areas in which the reindeer's seasonal migration occurs. Missing values in the buffer area were replaced with mean values of the neighborhood cells as described above.
Sheep	The average number of free-ranging domestic sheep *Ovis aries* and lambs in Norway, representing sheep availability as prey and greater risk of human-induced mortality (Landa et al. 1997, 1999, Van Dijk et al. 2008, Mabille et al. 2015, Strand et al. 2019)	+/–	Calculated at 20×20 km using polygons of numbers of sheep and lamb released in unfenced grazing areas in the Norwegian mountains and forests in 2021 (NIBIO 2022).
Ruggedness	Terrain Ruggedness Index (TRI) is the mean of the absolute elevation differences between the value of a habitat cell and the value of its eight surrounding cells (Wilson et al. 2007). TRI represents topographic complexity, availability of cover, and level of human disturbances (May et al. 2008, 2012, Rauset et al. 2013, Poley et al. 2018)	+	Obtained through the `terrain` function of the R package `terra` (Hijmans et al. 2022) using an elevation layer (AWS Terrain Tiles and OT global datasets API) at about 256×256 m obtained via the `get_elev_raster` function of the R package `elevatr` (Hollister et al. 2021)
Snow	The average percentage of year-round snow cover across years 2008 - 2021, representing climate severity, denning suitability, and prey vulnerability to predation (Copeland et al. 2010, May et al. 2012, Aronsson and Persson 2017, Lukacs et al. 2020, Mowat et al. 2020, Barrueto et al. 2022)	+	Calculated using monthly maps of the percentage of snow-covered land based on the MODIS/Terra Snow Cover Daily L3 Global 500m Grid data set (`www.neo.sci.gsfc.nasa.gov`)
Settlements	The percentage of the ground surface covered by human settlements was a proxy of human population density and associated disturbances (May et al. 2006, Lukacs et al. 2020, Cretois et al. 2021, Barrueto et al. 2022)	–	Downloaded at about 57-m resolution from the World Settlement Footprint data set (WSF2015; Marconcini et al. 2020) and log-transformed after adding a value of 1 to deal with 0 values

References

Andrén, H., Persson, J., Mattisson, J., and Danell, A. C. (2011). Modelling the combined effect of an obligate predator and a facultative predator on a common prey: lynx *Lynx lynx* and wolverine *Gulo gulo* predation on reindeer *Rangifer tarandus*. *Wildlife Biology*, 17(1):33–43.

Aronsson, M. and Persson, J. (2017). Mismatch between goals and the scale of actions constrains adaptive carnivore management: the case of the wolverine in Sweden. *Animal Conservation*, 20(3):261–269.

Aronsson, M., Persson, J., Zimmermann, B., Märtz, J., Wabakken, P., Heeres, R., and Nordli, K. (2022). *Järven i Inre Skandinaviens skogslandskap–områdesbruk, födoval och reproduktion*. SLU Grimsö forskningsstation Institutionen för ekologi Sveriges lantbruksuniversitet.

Barrueto, M., Forshner, A., Whittington, J., Clevenger, A. P., and Musiani, M. (2022). Protection status, human disturbance, snow cover and trapping drive density of a declining wolverine population in the Canadian Rocky Mountains. *Scientific Reports*, 12(1):1–15.

Chapron, G., Kaczensky, P., Linnell, J. D., Von Arx, M., Huber, D., Andrén, H., López-Bao, J. V., Adamec, M., Álvares, F., Anders, O., et al. (2014). Recovery of large carnivores in Europe's modern human-dominated landscapes. *Science*, 346(6216):1517–1519.

Cimatti, M., Ranc, N., Benítez-López, A., Maiorano, L., Boitani, L., Cagnacci, F., Čengić, M., Ciucci, P., Huijbregts, M. A., Krofel, M., et al. (2021). Large carnivore expansion in Europe is associated with human population density and land cover changes. *Diversity and Distributions*, 27(4):602–617.

Copeland, J., McKelvey, K., Aubry, K., Landa, A., Persson, J., Inman, R., Krebs, J., Lofroth, E., Golden, H., Squires, J., et al. (2010). The bioclimatic envelope of the wolverine (*Gulo gulo*): do climatic constraints limit its geographic distribution? *Canadian Journal of Zoology*, 88(3):233–246.

Cretois, B., Linnell, J. D., Van Moorter, B., Kaczensky, P., Nilsen, E. B., Parada, J., and Rød, J. K. (2021). Coexistence of large mammals and humans is possible in Europe's anthropogenic landscapes. *iScience*, 24(9):103083.

Flagstad, Ø., Hedmark, E., Landa, A., Brøseth, H., Persson, J., Andersen, R., Segerström, P., and Ellegren, H. (2004). Colonization history and noninvasive monitoring of a reestablished wolverine population. *Conservation Biology*, 18(3):676–688.

Hijmans, R. J. (2021). *raster: Geographic Data Analysis and Modeling*. R package version 3.4-13.

Hijmans, R. J., Bivand, R., van Etten, J., Forner, K., Ooms, J., and Pebesma, E. (2022). *Package 'terra': Spatial Data Analysis*. R package version 1.5-21.

Hobbs, N. T., Andren, H., Persson, J., Aronsson, M., and Chapron, G. (2012). Native predators reduce harvest of reindeer by Sámi pastoralists. *Ecological Applications*, 22(5):1640–1654.

Hollister, J., Shah, T., Robitaille, A. L., Beck, M. W., and Johnson, M. (2021). *elevatr: Access Elevation Data from Various APIs*. R package version 0.4.1.

Inman, R. M., Packila, M. L., Inman, K. H., Mccue, A. J., White, G. C., Persson, J., Aber, B. C., Orme, M. L., Alt, K. L., Cain, S. L., et al. (2012). Spatial ecology of wolverines at the southern periphery of distribution. *The Journal of Wildlife Management*, 76(4):778–792.

Landa, A., Gudvangen, K., Swenson, J., and Røskaft, E. (1999). Factors associated with wolverine *Gulo gulo* predation on domestic sheep. *Journal of Applied Ecology*, 36(6):963–973.

Landa, A., Lindén, M., Kojola, I., et al. (2000). *Action plan for the conservation of wolverines in Europe (Gulo gulo)*. Council of Europe.

Landa, A., Strand, O., Swenson, J. E., and Skogland, T. (1997). Wolverines and their prey in southern Norway. *Canadian Journal of Zoology*, 75(8):1292–1299.

Lansink, G. M., Esparza-Salas, R., Joensuu, M., Koskela, A., Bujnáková, D., Kleven, O., Flagstad, Ø., Ollila, T., Kojola, I., Aspi, J., et al. (2020). Population genetics of the wolverine in Finland: the road to recovery? *Conservation Genetics*, 21(3):481–499.

Lukacs, P. M., Evans Mack, D., Inman, R., Gude, J. A., Ivan, J. S., Lanka, R. P., Lewis, J. C., Long, R. A., Sallabanks, R., Walker, Z., et al. (2020). Wolverine occupancy, spatial distribution, and monitoring design. *The Journal of Wildlife Management*, 84(5):841–851.

Mabille, G., Stien, A., Tveraa, T., Mysterud, A., Brøseth, H., and Linnell, J. D. (2015). Sheep farming and large carnivores: What are the factors influencing claimed losses? *Ecosphere*, 6(5):1–17.

Marconcini, M., Metz-Marconcini, A., Üreyen, S., Palacios-Lopez, D., Hanke, W., Bachofer, F., Zeidler, J., Esch, T., Gorelick, N., Kakarla, A., et al. (2020). Outlining where humans live, the World Settlement Footprint 2015. *Scientific Data*, 7(1):1–14.

Mattisson, J., Rauset, G. R., Odden, J., Andrén, H., Linnell, J. D., and Persson, J. (2016). Predation or scavenging? prey body condition influences decision-making in a facultative predator, the wolverine. *Ecosphere*, 7(8):e01407.

May, R., Gorini, L., Van Dijk, J., Brøseth, H., Linnell, J., and Landa, A. (2012). Habitat characteristics associated with wolverine den sites in Norwegian multiple-use landscapes. *Journal of Zoology*, 287(3):195–204.

May, R., Landa, A., van Dijk, J., Linnell, J. D., and Andersen, R. (2006). Impact of infrastructure on habitat selection of wolverines *Gulo gulo*. *Wildlife Biology*, 12(3):285–295.

May, R., Van Dijk, J., Wabakken, P., Swenson, J. E., Linnell, J. D., Zimmermann, B., Odden, J., Pedersen, H. C., Andersen, R., and Landa, A. (2008). Habitat differentiation within the large-carnivore community of Norway's multiple-use landscapes. *Journal of Applied Ecology*, 45(5):1382–1391.

Miljødirektoratet (2022). Villreinområder: Datasett. Accessed: 2022-09-16.

Moqanaki, E., Milleret, C., Dupont, P., Brøseth, H., and Bischof, R. (2022). Wolverine density distribution reflects past persecution and current management in Scandinavia. *bioRxiv*.

Mowat, G., Clevenger, A. P., Kortello, A. D., Hausleitner, D., Barrueto, M., Smit, L., Lamb, C., DorsEy, B., and Ott, P. K. (2020). The sustainability of wolverine trapping mortality in southern Canada. *The Journal of Wildlife Management*, 84(2):213–226.

NIBIO (2022). Sau lam slept i utmarka. Accessed: 2022-09-16.

Persson, J., Ericsson, G., and Segerström, P. (2009). Human caused mortality in the endangered Scandinavian wolverine population. *Biological Conservation*, 142(2):325–331.

Persson, J., Rauset, G. R., and Chapron, G. (2015). Paying for an endangered predator leads to population recovery. *Conservation Letters*, 8(5):345–350.

Poley, L. G., Magoun, A. J., Robards, M. D., and Klimstra, R. L. (2018). Distribution and occupancy of wolverines on tundra, northwestern Alaska. *The Journal of Wildlife Management*, 82(5):991–1002.

Rauset, G. R., Mattisson, J., Andrén, H., Chapron, G., and Persson, J. (2013). When species' ranges meet: assessing differences in habitat selection between sympatric large carnivores. *Oecologia*, 172(3):701–711.

Scrafford, M. A., Avgar, T., Abercrombie, B., Tigner, J., and Boyce, M. S. (2017). Wolverine habitat selection in response to anthropogenic disturbance in the western Canadian boreal forest. *Forest Ecology and Management*, 395:27–36.

statistisk sentralbyrå (2021). Moose hunting. Accessed: 2021-11-04.

Strand, G.-H., Hansen, I., de Boon, A., and Sandström, C. (2019). Carnivore management zones and their impact on sheep farming in Norway. *Environmental Management*, 64(5):537–552.

Ueno, M., Solberg, E. J., Iijima, H., Rolandsen, C. M., and Gangsei, L. E. (2014). Performance of hunting statistics as spatiotemporal density indices of moose (*Alces alces*) in norway. *Ecosphere*, 5(2):1–20.

van der Veen, B., Mattisson, J., Zimmermann, B., Odden, J., and Persson, J. (2020). Refrigeration or anti-theft? food-caching behavior of wolverines (*Gulo gulo*) in Scandinavia. *Behavioral Ecology and Sociobiology*, 74(5):1–13.

Van Dijk, J., Gustavsen, L., Mysterud, A., May, R., Flagstad, Ø., Brøseth, H., Andersen, R., Andersen, R., Steen, H., and Landa, A. (2008). Diet shift of a facultative scavenger, the wolverine, following recolonization of wolves. *Journal of Animal Ecology*, 77(6):1183–1190.

Wilson, M. F., O'Connell, B., Brown, C., Guinan, J. C., and Grehan, A. J. (2007). Multiscale terrain analysis of multibeam bathymetry data for habitat mapping on the continental slope. *Marine Geodesy*, 30(1-2):3–35.

Älgdata (2021a). Statistik för älgdata. Accessed: 2021-11-04.

Älgdata, L. (2021b). Länsstyrelsernas karttjänst för beslutade älgförvaltningsområden och älgjaktsområden. Accessed: 2021-11-04.

4 APPENDIX D

Sex-specific estimates by the open-population spatial capture-recapture models used in this study:

- Figure D1: Baseline detection probability of the wolverine across different management regions during the annual structured and unstructured sampling efforts
- Figure D2: Effects of covariates of wolverine detectability during the annual structured and unstructured sampling and sex-specific estimates of the spatial scale parameter
- Figure D3: Female and male annual abundance estimates
- Figure D4: Annual estimates of recruitment and survival probability

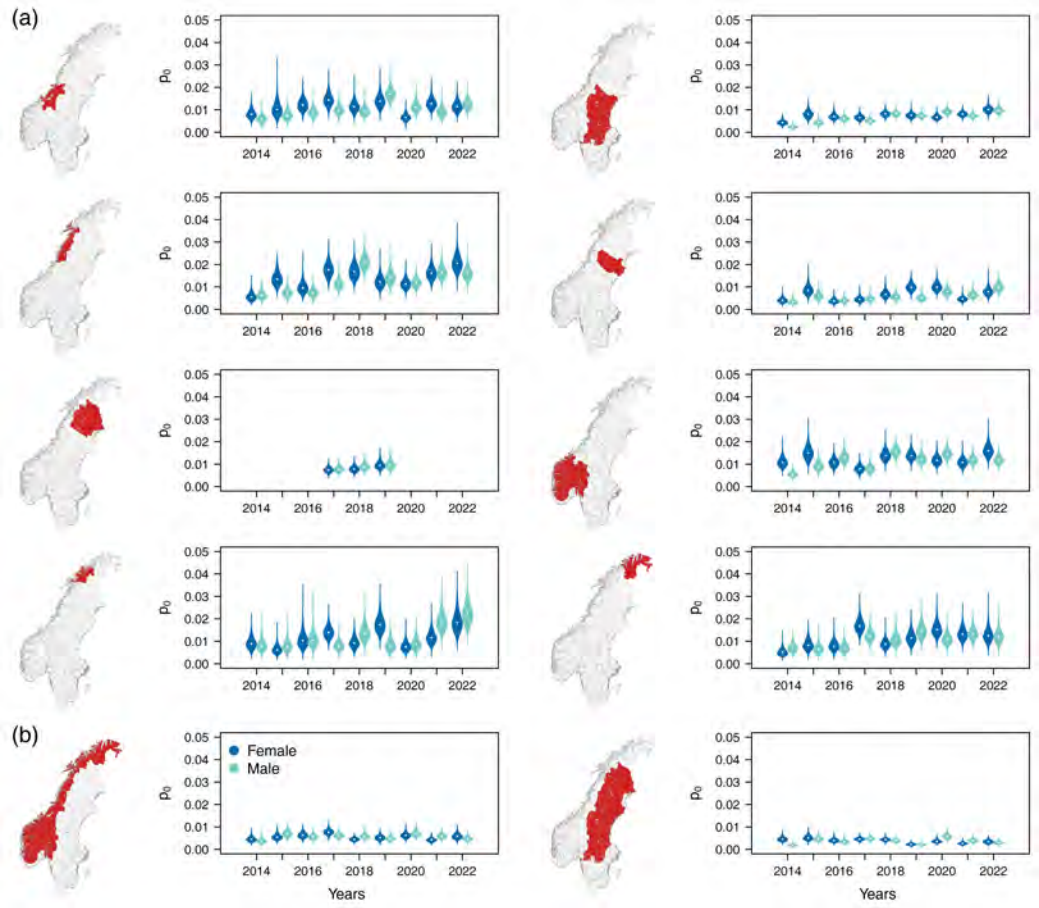

Figure D1: Baseline detection probability p_0 of the Scandinavian wolverine *Gulo gulo* during noninvasive genetic sampling between December 1 and June 30 of each monitoring season (2013/14 - 2021/22), estimated by the sex-specific open-population spatial capture-recapture models used in this study. Violins represent the median (white dots) and 95% Bayesian credible interval of the year-specific estimates for females (blue) and males (green). Results are separated into panels based on (a) Structured sampling effort, where management authorities conducted DNA searches and recorded their search tracks at five carnivore management regions in Norway and three aggregations of counties in Sweden (red polygons); and (b) Unstructured sampling effort, where authorities and volunteers opportunistically collected wolverine DNA samples in each country (red polygons in the bottom row). p_0 is a theoretical value of detection probability, where a detector coincides with the location of an individual's activity center and it is not to be confused with detectability – i.e, the overall probability of detecting an individual. See the main text for details.

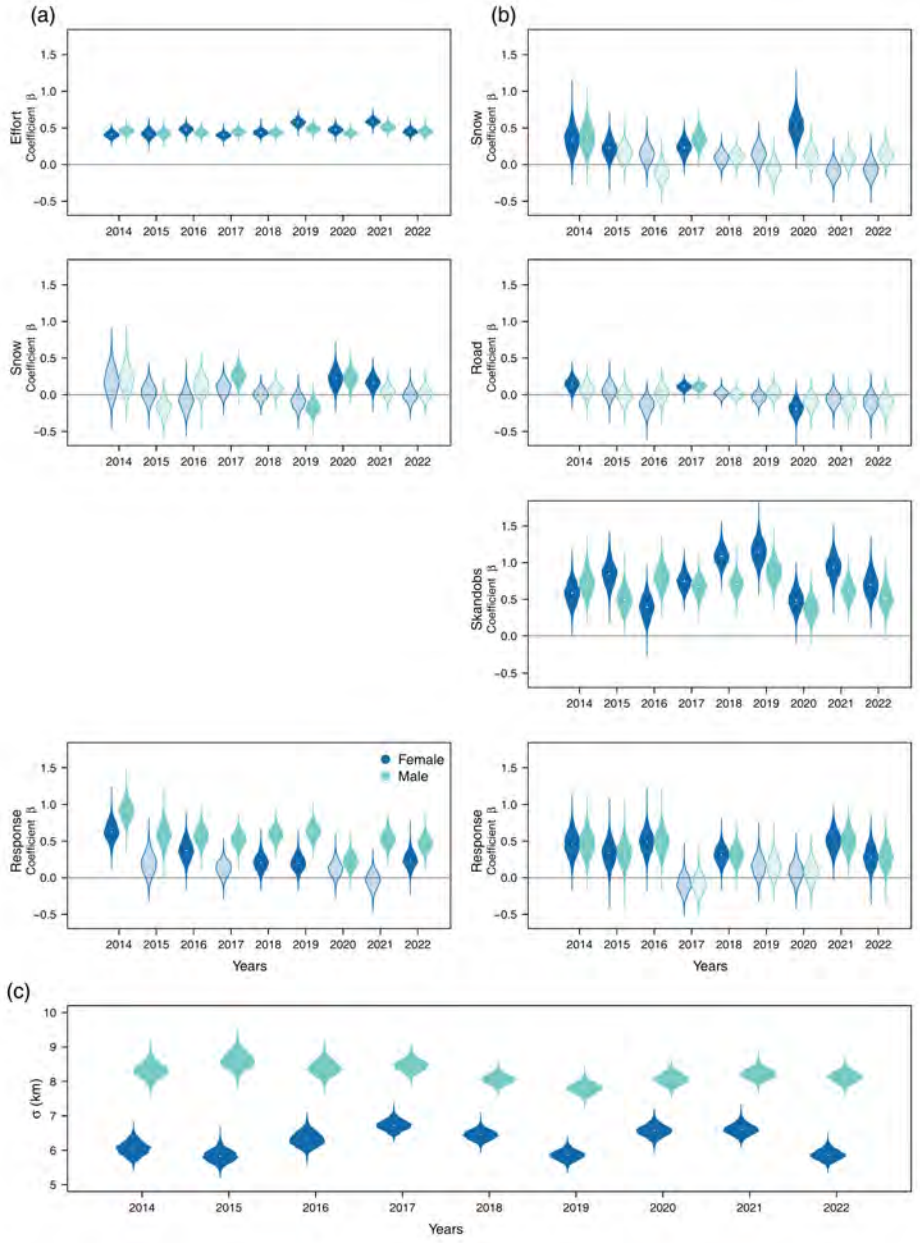

Figure D2: The effects (median and 95% Bayesian credible interval limits, CI) of spatial (top three rows) and individual (fourth row) covariates on female (blue) and male (green) wolverine *Gulo gulo* baseline detection probability p_0 during (a) left-column panel: structured and (b) right-column panel: unstructured sampling. (c) The estimated spatial scale parameter of the half-normal detection function σ across Scandinavia during nine monitoring seasons, 2013/14 - 2021/22. (a,b) The violin plots show regression coefficient β estimates to describe the relationship between wolverine baseline detection probability and the given covariate for each sampling year during (a) structured and (b) unstructured sampling. The effect sizes are on exponential scale, and the white dots in the violins show median values. Violins in which the 90% CI of the posteriors overlapped zero (i.e., no significant effects) are shown in transparent colors. Descriptions of the covariates are given in the main text.

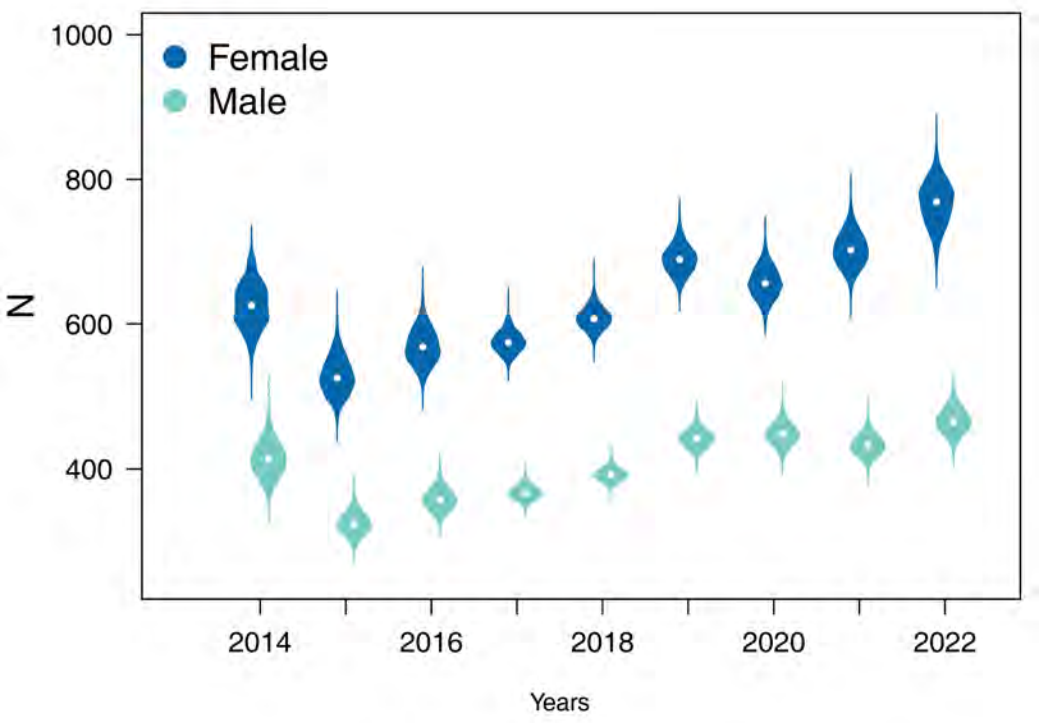

Figure D3: Annual abundance N estimates of female (blue) and male (green) wolverines *Gulo gulo* across their entire range in the Scandinavian Peninsula during nine monitoring seasons from 2013/14 to 2021/22. The violins show median (white dots) and 95% Bayesian credible interval limits. The designated study landscape from which the estimates were extracted is shown in Figure B1.

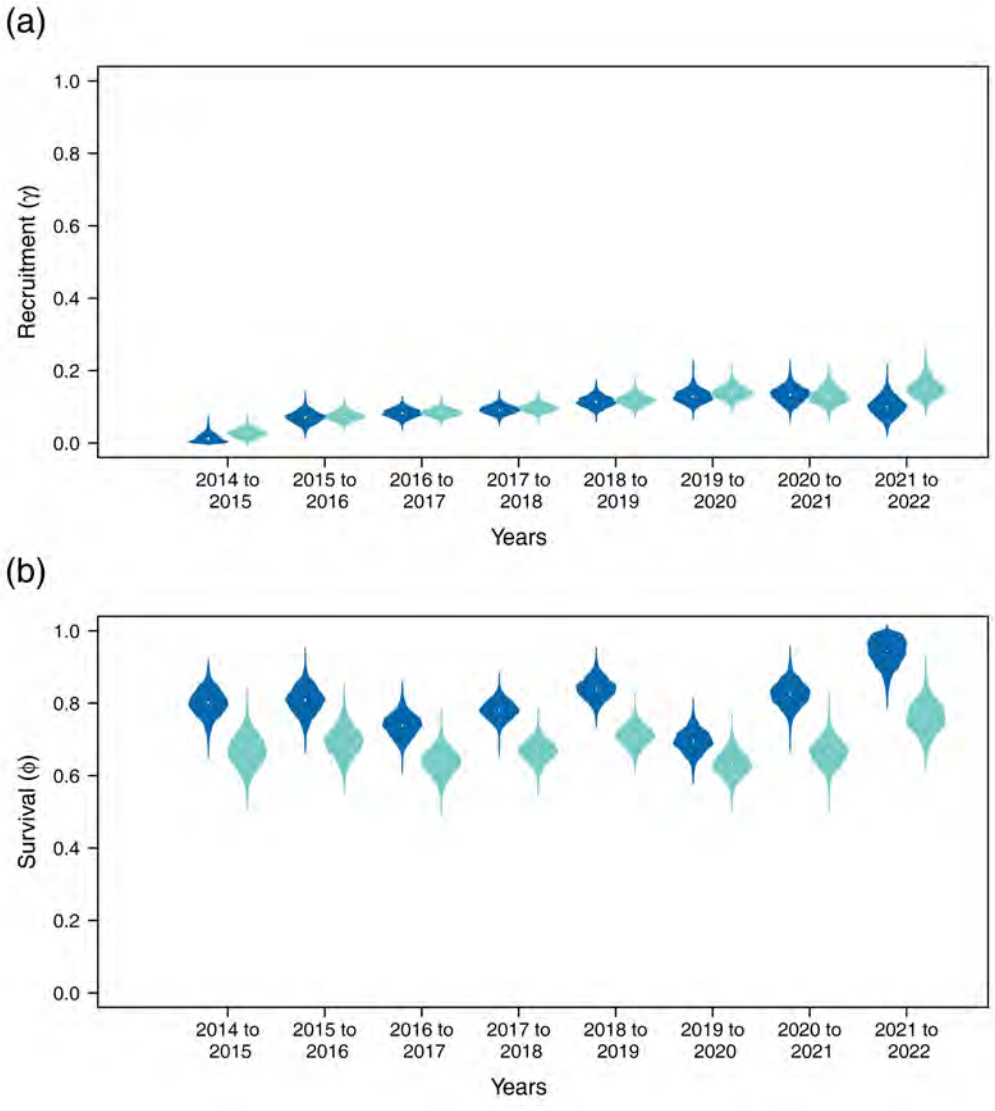

Figure D4: (a) Annual recruitment and (b) survival probability for female (blue) and male (green) wolverines *Gulo gulo* across their entire range in the Scandinavian Peninsula during nine monitoring seasons from 2013/14 - 2021/22. The violins show median (white dots) and 95% Bayesian credible interval limits of the estimates.

5 APPENDIX E

Wolverine *Gulo gulo* density surfaces (10×10 km) between 2013/14 and 2021/22 as estimates by the open-population spatial capture-recapture models used in this study:

- Figure E1: Female and male "realized" density surfaces
- Figure E2: The cell-based standard deviation of the "realized" density estimates for females and males
- Figure E3: The cell-based standard deviation of "expected" density estimates for females and males

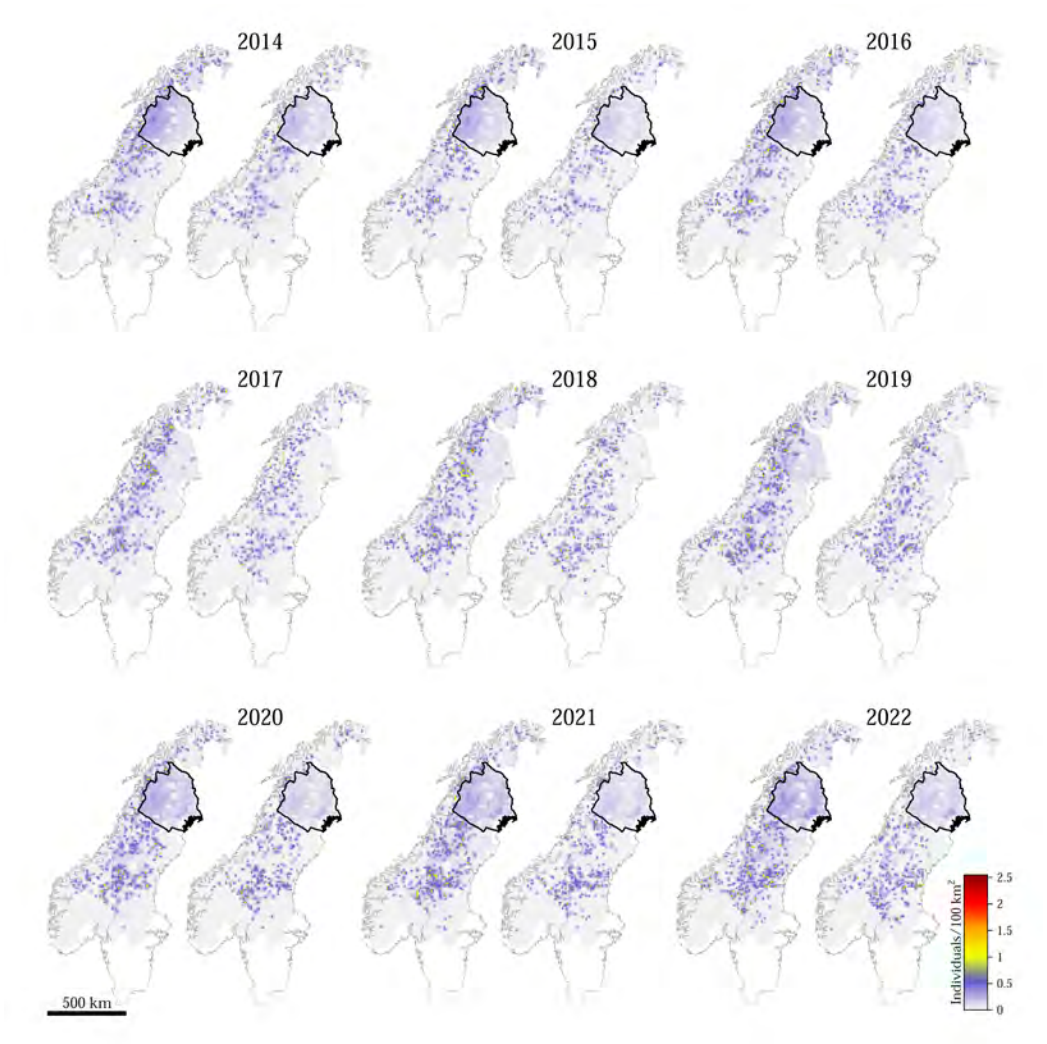

Figure E1: Annual realized density (individuals per 100 km^2) surfaces of female (left) and male (right) wolverines *Gulo gulo* in the Scandinavian Peninsula each year between December 2013 - June 2014 and December 2021 - June 2022 (i.e., nine monitoring seasons), as estimated by sex-specific open-population spatial capture-recapture models used in this study. The density surfaces are created based on the average posterior location of "alive" individual activity centers in each 10×10-km habitat cell and inclusion parameter. No comprehensive noninvasive genetic sampling was conducted in Norrbotten County in Sweden from 2013/14 - 2015/16 and from 2019/20 - 2021/22 (polygons outlined in thick black), which means that the results are solely based on the model prediction. See the main text for details.

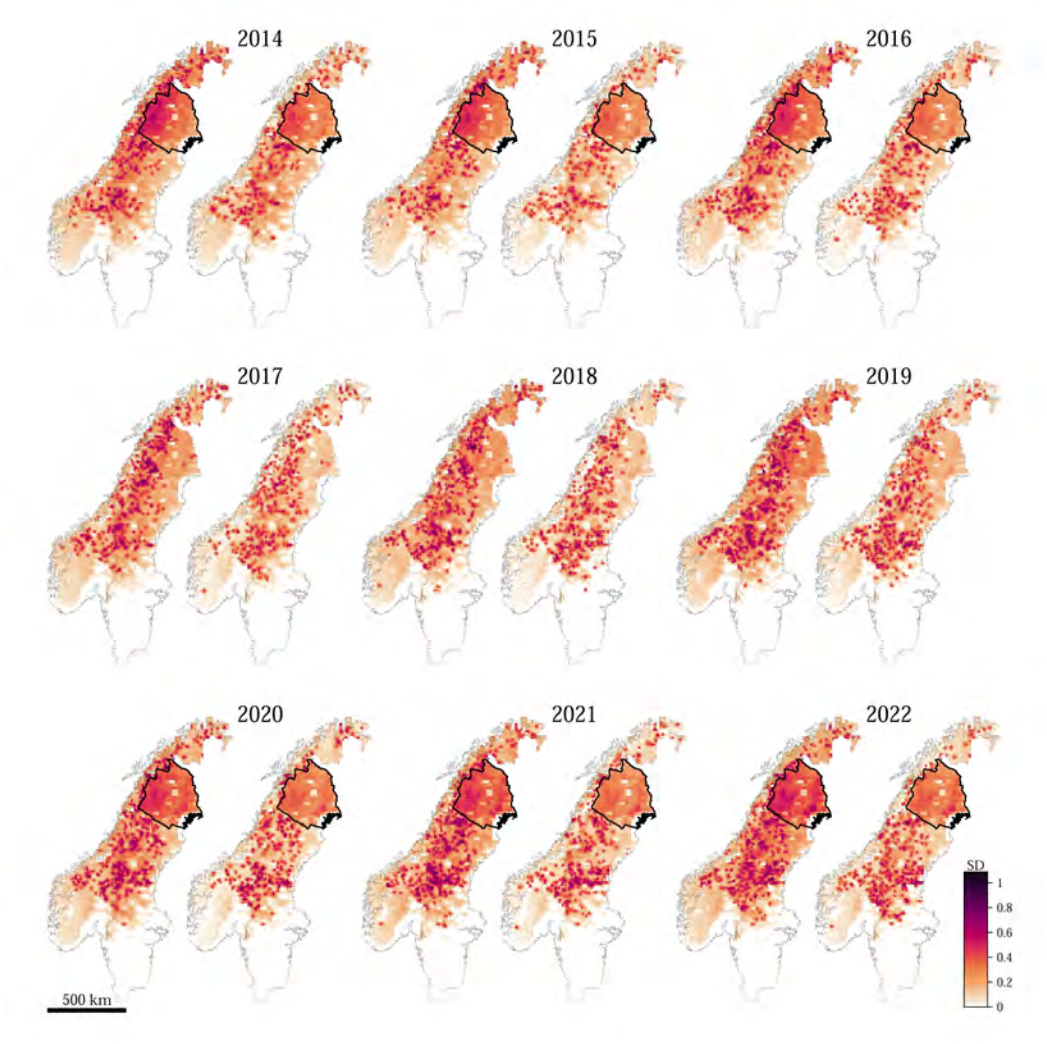

Figure E2: The cell-based standard deviation of realized density surfaces of female (left) and male (right) wolverines *Gulo gulo* in the Scandinavian Peninsula each year between December 2013 - June 2014 and December 2021 - June 2022 (i.e., nine monitoring seasons), as estimated by sex-specific open-population spatial capture-recapture models. No comprehensive noninvasive genetic sampling was conducted in Norrbotten County in Sweden from 2013/14 - 2015/16 and from 2019/20 - 2021/22 (polygons outlined in thick black), which means that the results are solely based on the model prediction.

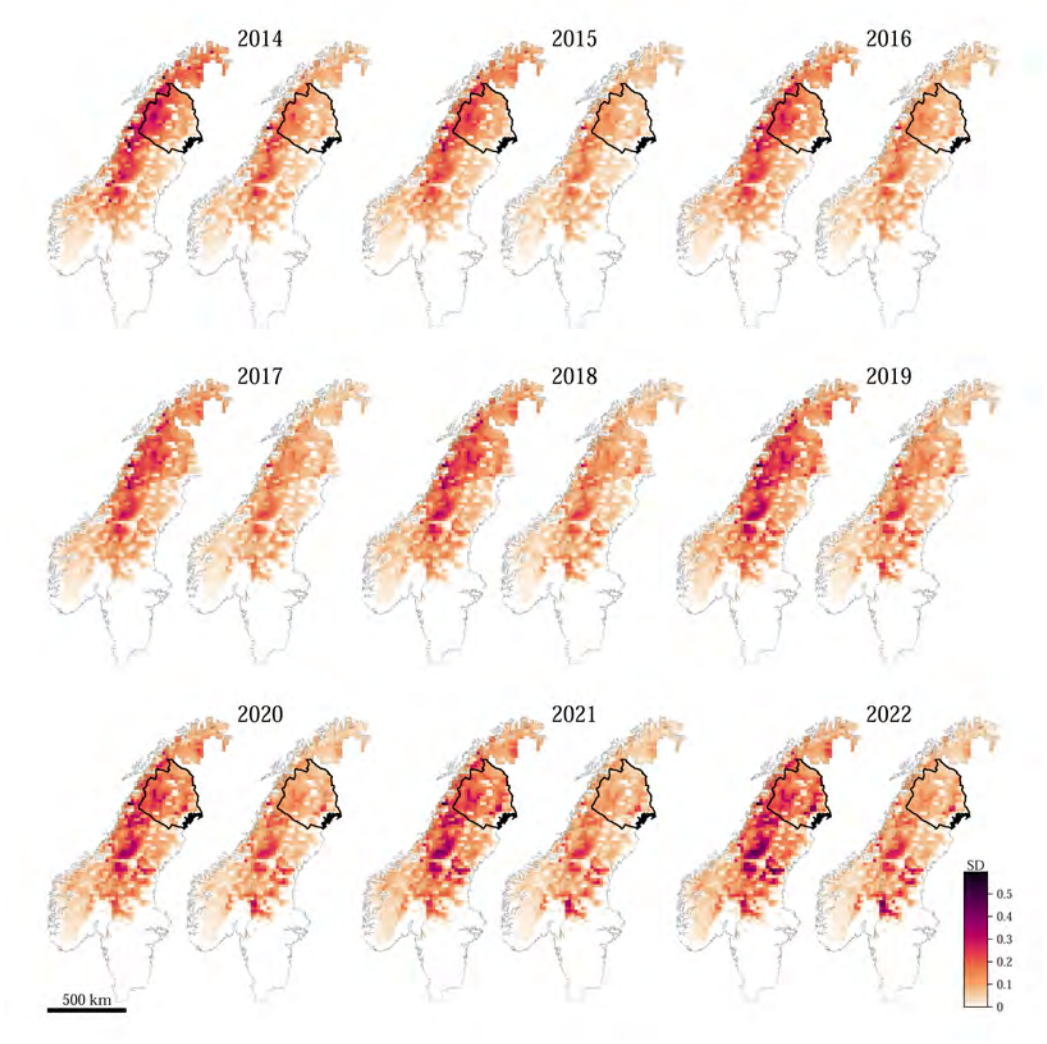

Figure E3: The cell-based standard deviation of expected density surfaces of female (left) and male (right) wolverines *Gulo gulo* in the Scandinavian Peninsula each year between December 2013 - June 2014 and December 2021 - June 2022 (i.e., nine monitoring seasons). No comprehensive noninvasive genetic sampling was conducted in Norrbotten County in Sweden from 2013/14 - 2015/16 and from 2019/20 - 2021/22 (polygons outlined in thick black), which means that the results are solely based on the model prediction. See the main text for details.

ISBN: 978-82-575-2064-9
ISSN: 1894-6402

Norwegian University
of Life Sciences

Postboks 5003
NO-1432 Ås, Norway
+47 67 23 00 00
www.nmbu.no

116738 / ANDVORDGRAFISK.NO